Springer Series in
Computational
Mathematics

37

Sergej Rjasanow
Wolfgang Wagner

Stochastic Numerics for the Boltzmann Equation

With 98 Figures

Springer

Sergej Rjasanow
Fachrichtung 6.1 – Mathematik
Universität des Saarlandes
Postfach 151150
66041 Saarbrücken
Germany
email: rjasanow@num.uni-sb.de

Wolfgang Wagner
Weierstrass Institute
for Applied Analysis and Stochastics
Mohrenstr. 39
10117 Berlin
Germany
e-mail: wagner@wias-berlin.de

Library of Congress Control Number: 2005922826

Mathematics Subject Classification (2000): 65C05, 65C20, 65C35, 60K35, 82C22, 82C40, 82C80

ISSN 0179-3632
ISBN-10 3-540-25268-1 Springer Berlin Heidelberg New York
ISBN-13 978-3-540-25268-9 Springer Berlin Heidelberg New York

Springer is a part of Springer Science+Business Media
springeronline.com

Cover design: *design&production*, Heidelberg
Typeset by the authors using a Springer LaTeX macro package
Printed on acid-free paper 46/3142sz-5 4 3 2 1 0

Preface

Stochastic numerical methods play an important role in large scale computations in the applied sciences. Such algorithms are convenient, since inherent stochastic components of complex phenomena can easily be incorporated. However, even if the real phenomenon is described by a deterministic equation, the high dimensionality often makes deterministic numerical methods intractable.

A stochastic procedure, called direct simulation Monte Carlo (DSMC) method, has been developed in the physics and engineering community since the sixties. This method turned out to be a powerful tool for numerical studies of complex rarefied gas flows. It was successfully applied to problems ranging from aerospace engineering to material processing and nanotechnology. In many situations, DSMC can be considered as a stochastic algorithm for solving some macroscopic kinetic equation. An important example is the classical Boltzmann equation, which describes the time evolution of large systems of gas molecules in the rarefied regime, when the mean free path (distance between subsequent collisions of molecules) is not negligible compared to the characteristic length scale of the problem. This means that either the mean free path is big (space-shuttle design, vacuum technology), or the characteristic length is small (micro-device engineering). As the dimensionality of this nonlinear integro-differential equation is high (time, position, velocity), its numerical treatment is a typical application field of Monte Carlo algorithms.

Intensive mathematical research on stochastic algorithms for the Boltzmann equation started in the eighties, when techniques for studying the convergence of interacting particle systems became available. Since that time much progress has been made in the justification and further development of these numerical methods.

The purpose of this book is twofold. The first goal is to give a mathematical description of various classical DSMC procedures, using the theory of Markov processes (in particular, stochastic interacting particle systems) as a unifying framework. The second goal is a systematic treatment of an extension of DSMC, called stochastic weighted particle method (SWPM). This

method has been developed by the authors during the last decade. SWPM includes several new features, which are introduced for the purpose of variance reduction (rare event simulation). Rigorous results concerning the approximation of solutions to the Boltzmann equation by particle systems are given, covering both DSMC and SWPM. Thorough numerical experiments are performed, illustrating the behavior of systematic and statistical error as well as the performance of the methods.

We restricted our considerations to monoatomic gases. In this case the introduction of weights is a completely artificial approach motivated by numerical purposes. This is the point we wanted to emphasize. In other situations, like gas flows with several types of molecules of different concentrations, weighted particles occur in a natural way. SWPM contains more degrees of freedom than we have implemented and tested so far. Thus, there is some hope that there will be further applications. Both DSMC and SWPM can be applied to more general kinetic equations. Interesting examples are related to rarefied granular gases (inelastic Boltzmann equation) and to ideal quantum gases (Uehling-Uhlenbeck-Boltzmann equation). In both cases there are non-Maxwellian equilibrium distributions. Other types of molecules (internal degrees of freedom, electrical charge) and many other interactions (chemical reactions, coagulation, fragmentation) can be treated.

The structure of the book is reflected in the table of contents. Chapter 1 recalls basic facts from kinetic theory, mainly about the Boltzmann equation. Chapter 2 is concerned with Markov processes related to Boltzmann type equations. A relatively general class of piecewise-deterministic processes is described. The transition to the corresponding macroscopic equation is sketched heuristically. Chapter 3 describes the stochastic algorithms related to the Boltzmann equation. This is the largest part of the book. All components of the procedures are discussed in detail and a rigorous convergence theorem is given. Chapter 4 contains results of numerical experiments. First, the spatially homogeneous Boltzmann equation is considered. Then, a spatially one-dimensional test problem is studied. Finally, results are obtained for a specific spatially two-dimensional test configuration. Some auxiliary results are collected in two appendixes.

The chapters are relatively independent of each other. Necessary notations and formulas are usually repeated at the beginning of a chapter, instead of cross-referring to other chapters. A list of main notations is given at the end of this Preface. Symbols from that list will be used throughout the book. We mostly avoided citing literature in the main text. Instead, each of the first three chapters is completed by a section including bibliographic remarks. An extensive (but naturally not exhaustive) list of references is given at the end of the book.

The idea to write this book came up in 1999, when we had completed several papers related to DSMC and SWPM. Our naive hope was to finish it rather quickly. In May 2001 this Preface contained only one remark – "seven months left to deadline". On the one hand, the long delay of three years was

sometimes annoying, but, on the other hand, we mostly enjoyed the intensive work on a very interesting subject. We would like to thank our colleagues from the kinetics community for many useful discussions and suggestions. We are grateful to our home institutions, the University of Saarland in Saarbrücken and the Weierstrass Institute for Applied Analysis and Stochastics in Berlin, for providing an encouraging scientific environment. Finally, we are glad to acknowledge support by the Mathematical Research Institute Oberwolfach (RiP program) during an early stage of the project, and a research grant from the German Research Foundation (DFG).

Saarbrücken and Berlin *Sergej Rjasanow*
December 2004 *Wolfgang Wagner*

List of notations

$\mathbb{R}^3$	Euclidean space
$(.,.)$	scalar product in $\mathbb{R}^3$
$\|.\|$	norm in $\mathbb{R}^3$
$\mathcal{S}^2$	unit sphere in $\mathbb{R}^3$
D	open subset of $\mathbb{R}^3$
∂D	boundary of D
$n(x)$	unit inward normal vector at $x \in \partial D$
$\sigma(dx)$	uniform surface measure (area) on ∂D
$\delta(x)$	Dirac's delta-function
I	identity matrix
$\operatorname{tr} C$	trace of a matrix C
vv^{T}	matrix with elements $v_i v_j$ for $v \in \mathbb{R}^3$
∇_x	gradient with respect to $x \in \mathbb{R}^3$
$\operatorname{div} b(x)$	divergence of a vector function b on $\mathbb{R}^3$
$\mathbb{E}\,\xi$	expectation of a random variable ξ
$\operatorname{Var} \xi$	variance of a random variable ξ
$\mathcal{B}(X)$	Borel sets of a metric space X
$\mathcal{M}(X)$	finite Borel measures on X

$$M_{V,T}(v) = \frac{1}{(2\pi\, T)^{3/2}} \exp\left(-\frac{|v-V|^2}{2\,T}\right)$$
Maxwell distribution, with $v, V \in \mathbb{R}^3$ and $T > 0$

$$\mathbb{R}^3_{in}(x) = \left\{v \in \mathbb{R}^3 \,:\, \big(v, n(x)\big) > 0\right\}$$
velocities leading a particle from $x \in \partial D$ inside D

$$\mathbb{R}^3_{out}(x) = \left\{v \in \mathbb{R}^3 \,:\, \big(v, n(x)\big) < 0\right\}$$
velocities leading a particle from $x \in \partial D$ outside D

$$\delta_{i,j} = \begin{cases} 1\,, & \text{if} \quad i = j \\ 0\,, & \text{otherwise} \end{cases}$$
Kronecker's symbol

$$\delta_x(A) = \begin{cases} 1\,, & \text{if} \quad x \in A \\ 0\,, & \text{otherwise} \end{cases}$$

Dirac measure, with $x \in X$ and $A \in \mathcal{B}(X)$

$$\chi_A(x) = \begin{cases} 1\,, & \text{if} \quad x \in A \\ 0\,, & \text{otherwise} \end{cases}$$

indicator function of a set A, with $x \in X$ and $A \subset X$

$$||\varphi||_\infty = \sup_{x \in X} |\varphi(x)|$$

for any measurable function φ on X

$$\langle \varphi, \nu \rangle = \int_X \varphi(x)\, \nu(dx)$$

for any $\nu \in \mathcal{M}(X)$ and φ such that $||\varphi||_\infty < \infty$

Contents

1 Kinetic theory 1
1.1 The Boltzmann equation 1
1.2 Collision transformations 2
1.3 Collision kernels 8
1.4 Boundary conditions 11
1.5 Physical properties of gas flows 12
1.5.1 Physical quantities and units 12
1.5.2 Macroscopic flow properties 13
1.5.3 Molecular flow properties 14
1.5.4 Measurements 15
1.5.5 Air at standard conditions 15
1.6 Properties of the collision integral 16
1.7 Moment equations 21
1.8 Criterion of local equilibrium 24
1.9 Scaling transformations 28
1.10 Comments and bibliographic remarks 30

2 Related Markov processes 33
2.1 Boltzmann type piecewise-deterministic Markov processes 33
2.1.1 Free flow and state space 33
2.1.2 Construction of sample paths 34
2.1.3 Jump behavior 35
2.1.4 Extended generator 39
2.2 Heuristic derivation of the limiting equation 41
2.2.1 Equation for measures 41
2.2.2 Equation for densities 43
2.2.3 Boundary conditions 46
2.3 Special cases and bibliographic remarks 47
2.3.1 Boltzmann equation and boundary conditions 47
2.3.2 Boltzmann type processes 48
2.3.3 History 55

3 Stochastic weighted particle method 65
3.1 The DSMC framework 67
3.1.1 Generating the initial state 67
3.1.2 Decoupling of free flow and collisions 68
3.1.3 Limiting equations 69
3.1.4 Calculation of functionals 69
3.2 Free flow part 71
3.2.1 Modeling of boundary conditions 71
3.2.2 Modeling of inflow 74
3.3 Collision part 78
3.3.1 Cell structure 78
3.3.2 Fictitious collisions 80
3.3.3 Majorant condition 81
3.3.4 Global upper bound for the relative velocity norm 83
3.3.5 Shells in the velocity space 85
3.3.6 Temperature time counter 89
3.4 Controlling the number of particles 97
3.4.1 Collision processes with reduction 97
3.4.2 Convergence theorem 99
3.4.3 Proof of the convergence theorem 103
3.4.4 Construction of reduction measures 119
3.5 Comments and bibliographic remarks 132
3.5.1 Some Monte Carlo history 132
3.5.2 Time counting procedures 132
3.5.3 Convergence and variance reduction 134
3.5.4 Nanbu's method 136
3.5.5 Approximation order 140
3.5.6 Further references 145

4 Numerical experiments 147
4.1 Maxwellian initial state 149
4.1.1 Uniform approximation of the velocity space 150
4.1.2 Stability of moments 150
4.1.3 Tail functionals 151
4.1.4 Hard sphere model 156
4.2 Relaxation of a mixture of two Maxwellians 157
4.2.1 Convergence of DSMC 159
4.2.2 Convergence of SWPM 161
4.2.3 Tail functionals 164
4.2.4 Hard sphere model 169
4.3 BKW solution of the Boltzmann equation 171
4.3.1 Convergence of moments 172
4.3.2 Tail functionals 175
4.4 Eternal solution of the Boltzmann equation 178
4.4.1 Power functionals 180

4.4.2 Tail functionals . . . 181
4.5 A spatially one-dimensional example . . . 181
4.5.1 Properties of the shock wave problem . . . 182
4.5.2 Mott-Smith model . . . 185
4.5.3 DSMC calculations . . . 189
4.5.4 Comparison with the Mott-Smith model . . . 191
4.5.5 Histograms . . . 194
4.5.6 Bibliographic remarks . . . 197
4.6 A spatially two-dimensional example . . . 198
4.6.1 Explicit formulas in the collisionless case . . . 200
4.6.2 Case with collisions . . . 206
4.6.3 Influence of a hot wall . . . 207
4.6.4 Bibliographic remarks . . . 210

A Auxiliary results . . . 211
A.1 Properties of the Maxwell distribution . . . 211
A.2 Exact relaxation of moments . . . 213
A.3 Properties of the BKW solution . . . 217
A.4 Convergence of random measures . . . 220
A.5 Existence of solutions . . . 223

B Modeling of distributions . . . 229
B.1 General techniques . . . 229
B.1.1 Acceptance-rejection method . . . 229
B.1.2 Transformation method . . . 230
B.1.3 Composition method . . . 231
B.2 Uniform distribution on the unit sphere . . . 231
B.3 Directed distribution on the unit sphere . . . 232
B.4 Maxwell distribution . . . 234
B.5 Directed half-space Maxwell distribution . . . 236
B.6 Initial distribution of the BKW solution . . . 239
B.7 Initial distribution of the eternal solution . . . 241

References . . . 243

Index . . . 255

1

Kinetic theory

1.1 The Boltzmann equation

Kinetic theory describes a gas as a system of many particles (molecules) moving around according to the laws of classical mechanics. Particles interact, changing their velocities through binary collisions. The gas is assumed to be sufficiently dilute so that interactions involving more than two particles can be neglected. In the simplest case all particles are assumed to be identical and no effects of chemistry or electrical charge are considered.

Since the number of gas molecules is huge (10^{19} per cm^3 at standard conditions), it would be impossible to study the individual behavior of each of them. Instead a statistical description is used, i.e., some function

$$f(t,x,v)\,, \qquad t \geq 0\,, \quad x \in \mathbb{R}^3\,, \quad v \in \mathbb{R}^3\,, \tag{1.1}$$

is introduced that represents the average number of gas particles at time t having a position close to x and a velocity close to v. The basis for this statistical theory was provided in the second half of the 19th century. James Clerk Maxwell (1831-1879) found the distribution function of the gas molecule velocities in thermal equilibrium. Ludwig Boltzmann (1844-1906) studied the problem if a gas starting from any initial state reaches the **Maxwell distribution**

$$f_{\mathrm{eq}}(v) = \varrho \left[\frac{m}{2\pi\, k\, T}\right]^{\frac{3}{2}} \exp\left(-\frac{m\,|v-V|^2}{2\,k\,T}\right), \qquad v \in \mathbb{R}^3\,, \tag{1.2}$$

where ϱ, V, T are the density (number of molecules per unit volume), the stream velocity and the absolute temperature of the gas, m is the mass of a molecule and k is Boltzmann's constant. In 1872 he established the equation

$$\frac{\partial}{\partial t} f(t,x,v) + (v, \nabla_x)\, f(t,x,v) = \tag{1.3}$$
$$\int_{\mathbb{R}^3} dw \int_0^\infty r\, dr \int_0^{2\pi} d\varphi\, |v-w| \Big[f(t,x,v')\, f(t,x,w') - f(t,x,v)\, f(t,x,w) \Big]$$

describing the time evolution of the distribution function (1.1). The **collision transformation**

$$v, w, r, \varphi \quad \longrightarrow \quad v', w' \tag{1.4}$$

is determined by the interaction potential governing collisions and by the relative position of the molecules. This position is uniformly spread over the plane perpendicular to $v - w$ and expressed via polar coordinates. The left-hand side of equation (1.3) corresponds to the free streaming of the particles, while the right-hand side corresponds to the binary collisions that may either increase (gain term) or decrease (loss term) the number of particles with given position and velocity. The (perhaps slightly confusing) fact that the gain term contains the post-collision velocities instead of the pre-collision velocities (leading to v, w) is due to symmetry of the interaction law. The conservation properties for momentum and energy

$$v' + w' = v + w\,, \qquad |v'|^2 + |w'|^2 = |v|^2 + |w|^2 \tag{1.5}$$

imply that the function (1.2) satisfies equation (1.3).

1.2 Collision transformations

Even in the simple case of hard sphere interaction (particles collide like billiard balls) an explicit expression of the collision transformation (1.4) would be rather complicated. Therefore other forms are commonly used.

Assuming a spherically symmetric interaction law and using the centered velocities

$$\tilde{v} = v - \frac{v+w}{2} = \frac{v-w}{2}\,, \qquad \tilde{w} = w - \frac{v+w}{2} = \frac{w-v}{2}$$

a collision can be illustrated as shown in Fig. 1.1. The relative position of the colliding particles projected onto the plane perpendicular to their relative velocity is parametrized in polar coordinates r, φ. The **impact parameter** r is the distance of closest approach of the two (point) particles had they continued their motion without interaction. Due to symmetry the angle φ does not influence the collision transformation. The out-going velocities $\tilde{v}', \tilde{w}'$ depend on the in-going velocities v, w and on the **scattering angle** $\theta \in [0, \pi]$, which is determined by the parameter r and the interaction law. The value $r = 0$ corresponds to a central collision (scattering angle $\theta = \pi$), while $r \to \infty$ corresponds to grazing collisions (scattering angle $\theta \to 0$). Using the unit vector e' depending on θ and φ (considered as spherical coordinates), i.e.

$$e'_1 = \cos\theta\,, \quad e'_2 = \sin\theta\,\cos\varphi\,, \quad e'_3 = \sin\theta\,\sin\varphi\,,$$

one obtains $\tilde{v}' = c\,e'$, which implies $\tilde{w}' = -c\,e'$ and $c = \frac{|v'-w'|}{2} = \frac{|v-w|}{2}$, according to the conservation properties (1.5). Thus, the out-going velocities are represented in the form

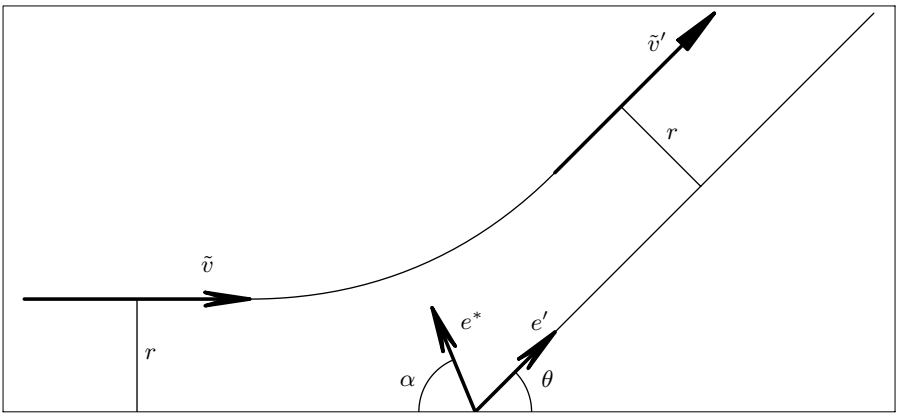

Fig. 1.1. Schematic of a collision

$$v' = v'(v, w, e'(\theta, \varphi))\,, \qquad w' = w'(v, w, e'(\theta, \varphi))\,,$$

where

$$\begin{aligned} v'(v, w, e) &= \frac{v+w}{2} + e\,\frac{|v-w|}{2}\,, \\ w'(v, w, e) &= \frac{v+w}{2} - e\,\frac{|v-w|}{2}\,, \qquad e \in \mathcal{S}^2\,. \end{aligned} \tag{1.6}$$

In this way the collision transformation (1.4) has been expressed as the superposition of the mappings

$$v, w, r, \varphi \quad \longrightarrow \quad v, w, \theta(v, w, r), \varphi$$

and

$$v, w, \theta, \varphi \quad \longrightarrow \quad v, w, e'(\theta, \varphi)$$

and (1.6).

Next the substitution of variables $r \to \theta(v, w, r)$ is used at the right-hand side of equation (1.3) leading to the form

$$\begin{aligned} \int_{\mathbb{R}^3} dw \int_0^\pi d\theta \int_0^{2\pi} d\varphi\, |v-w| \times \\ b(|v-w|, \theta)\Big[f(t, x, v')\, f(t, x, w') - f(t, x, v)\, f(t, x, w)\Big], \end{aligned} \tag{1.7}$$

where

$$b(|v-w|,\theta)\,d\theta = r\,dr\,, \qquad r = r(v,w,\theta)\,. \tag{1.8}$$

The function b is called **differential cross section** and is determined by the interaction law. In the case of spherically symmetric interactions it depends only on the relative speed and on the scattering angle. Switching in (1.7) from spherical coordinates to integration over the surface of the unit sphere, one obtains the common form of the **collision integral** in the Boltzmann equation

$$\int_{\mathbb{R}^3} dw \int_{\mathcal{S}^2} de\, B(v,w,e)\Big[f(t,x,v')\,f(t,x,w') - f(t,x,v)\,f(t,x,w)\Big], \tag{1.9}$$

where

$$B(v,w,e) = |v-w|\,\frac{b(|v-w|,\theta)}{\sin\theta}\,, \qquad \theta = \arccos\frac{(v-w,e)}{|v-w|}\,. \tag{1.10}$$

The function B is called **collision kernel**.

Remark 1.1. The forms (1.7) or (1.9) of the collision integral suggest that the direction vector, which determines the output of a collision (1.6), is distributed according to b or B, respectively. In the original form (1.3) there is a stream of particles with uniformly smeared positions (in the plane perpendicular to $v-w$) providing another view on the source of stochasticity.

There is an alternative to the collision transformation (1.6). Using the unit vector $e^* = e^*(\alpha,\varphi)$ depending on the angles (cf. Fig. 1.1)

$$\alpha = \frac{\pi-\theta}{2} \in [0,\pi/2] \tag{1.11}$$

and φ (considered as spherical coordinates), i.e.

$$e_1^* = \cos\alpha\,, \quad e_2^* = \sin\alpha\,\cos\varphi\,, \quad e_3^* = \sin\alpha\,\sin\varphi\,,$$

one obtains $\tilde v' = \tilde v + c\,e^*$, which implies $\tilde w' = \tilde w - c\,e^*$ and $c = (e^*, w-v)$, according to the conservation properties (1.5). Thus, the out-going velocities are represented in the form

$$v' = v^*(v,w,e^*(\alpha,\varphi))\,, \qquad w' = w^*(v,w,e^*(\alpha,\varphi))\,,$$

where

$$\begin{aligned} v^*(v,w,e) &= v + e\,(e,w-v)\,, \\ w^*(v,w,e) &= w + e\,(e,v-w)\,, \qquad e\in\mathcal{S}^2\,. \end{aligned} \tag{1.12}$$

The collision transformation (1.4) has been expressed as the superposition of the mappings

$$v,w,r,\varphi \quad\longrightarrow\quad v,w,\alpha(v,w,r),\varphi$$

and

$$v, w, \alpha, \varphi \quad \longrightarrow \quad v, w, e^*(\alpha, \varphi)$$

and (1.12).

The substitution of variables $r \to \alpha(v, w, r)$ at the right-hand side of equation (1.3) leads to the form

$$\int_{\mathbb{R}^3} dw \int_0^{\frac{\pi}{2}} d\alpha \int_0^{2\pi} d\varphi \, |v - w| \times \tag{1.13}$$
$$b^*(|v - w|, \alpha) \Big[f(t, x, v^*) \, f(t, x, w^*) - f(t, x, v) \, f(t, x, w) \Big],$$

where

$$b^*(|v - w|, \alpha) \, d\alpha = r \, dr \,, \qquad r = r(v, w, \alpha) \,. \tag{1.14}$$

Switching in (1.13) from spherical coordinates to integration over the surface of the unit sphere, one obtains

$$\int_{\mathbb{R}^3} dw \int_{\mathcal{S}^2_+(w-v)} de \, B^*(v, w, e) \Big[f(t, x, v^*) \, f(t, x, w^*) - f(t, x, v) \, f(t, x, w) \Big], \tag{1.15}$$

where

$$B^*(v, w, e) = |v - w| \, \frac{b^*(|v - w|, \alpha)}{\sin \alpha} \,, \qquad \alpha = \arccos \frac{(w - v, e)}{|w - v|} \tag{1.16}$$

and (for $u \in \mathbb{R}^3$)

$$\mathcal{S}^2_+(u) = \{ e \in \mathcal{S}^2 : (e, u) > 0 \} \,, \quad \mathcal{S}^2_-(u) = \{ e \in \mathcal{S}^2 : (e, u) < 0 \} \,. \tag{1.17}$$

Thus, there are two different forms (1.9) and (1.15) of the collision integral in the Boltzmann equation, corresponding to the collision transformations (1.6) and (1.12).

Theorem 1.2. *The collision kernels appearing in (1.9) and (1.15) are related to each other via*

$$B^*(v, w, e) = 4 \, (e, u) \, B(v, w, 2 \, e \, (e, u) - u) \tag{1.18}$$

and

$$B(v, w, e) = \frac{1}{2 \sqrt{2 \, (1 + (e, u))}} \, B^* \left(v, w, \frac{e + u}{\sqrt{2 \, (1 + (e, u))}} \right), \tag{1.19}$$

where

$$u = u(v, w) = \frac{w - v}{|w - v|} \,, \qquad v \neq w \,.$$

Note that

$$|2\,e\,(e,u)-u|^2=1 \qquad \text{and} \qquad |e+u|^2=2\,(1+(e,u))=2\,(e+u,u)\,.$$

We prepare the proof by the following lemma.

Lemma 1.3. *Let Φ be an appropriate test function and $u\in\mathcal{S}^2$. Then (cf. (1.17))*

$$\begin{aligned}\int_{\mathcal{S}^2}\Phi(e+u)\,de &= 4\int_{\mathcal{S}^2_+(u)}(e,u)\,\Phi(2\,e\,(e,u))\,de \qquad (1.20)\\ &= 4\int_{\mathcal{S}^2_-(u)}|(e,u)|\,\Phi(2\,e\,(e,u))\,de = 2\int_{\mathcal{S}^2}|(e,u)|\,\Phi(2\,e\,(e,u))\,de\,.\end{aligned}$$

Proof. Introducing spherical coordinates $\varphi_1\in[0,\pi]$, $\varphi_2\in[0,2\pi]$ such that

$$e_1=\cos\varphi_1\,,\quad e_2=\sin\varphi_1\,\cos\varphi_2\,,\quad e_3=\sin\varphi_1\,\sin\varphi_2$$

and $u=(1,0,0)$, one obtains

$$\begin{aligned}&\int_{\mathcal{S}^2}\Phi(e+u)\,de = \qquad (1.21)\\ &\int_0^\pi d\varphi_1\int_0^{2\pi}d\varphi_2\,\sin\varphi_1\,\Phi(1+\cos\varphi_1,\sin\varphi_1\,\cos\varphi_2,\sin\varphi_1\,\sin\varphi_2)\,.\end{aligned}$$

On the other hand, using the elementary properties

$$\sin 2\alpha=2\sin\alpha\,\cos\alpha\,,\qquad 1+\cos 2\alpha=2\cos^2\alpha\,,$$

one obtains

$$\begin{aligned}&\int_{\mathcal{S}^2_+(u)}(e,u)\,\Phi(2\,e\,(e,u))\,de=\int_0^{\frac{\pi}{2}}d\varphi_1\int_0^{2\pi}d\varphi_2\,\sin\varphi_1\,\cos\varphi_1\times\\ &\quad\Phi\left(2\,\cos^2\varphi_1,2\,\cos\varphi_1\,\sin\varphi_1\,\cos\varphi_2,2\,\cos\varphi_1\,\sin\varphi_1\,\sin\varphi_2\right)\\ &=\int_0^{\frac{\pi}{2}}d\varphi_1\int_0^{2\pi}d\varphi_2\,\frac{1}{2}\,\sin 2\varphi_1\,\times \qquad (1.22)\\ &\quad\Phi\left(1+\cos 2\varphi_1,\sin 2\varphi_1\,\cos\varphi_2,\sin 2\varphi_1\,\sin\varphi_2\right)\\ &=\frac{1}{4}\int_0^{\pi}d\varphi_1\int_0^{2\pi}d\varphi_2\,\sin\varphi_1\,\Phi\left(1+\cos\varphi_1,\sin\varphi_1\,\cos\varphi_2,\sin\varphi_1\,\sin\varphi_2\right).\end{aligned}$$

Comparing (1.21) and (1.22) gives (1.20). ∎

Proof of Theorem 1.2. Using Lemma 1.3 with

$$\Phi(z)=B(v,w,z-u)\left[f\Big(v+\frac{|v-w|}{2}\,z\Big)\,f\Big(w-\frac{|v-w|}{2}\,z\Big)-f(v)\,f(w)\right]$$

and taking into account that (cf. (1.6))

$$v'(v,w,e) = v + \frac{|v-w|}{2}\,[e+u]\,, \qquad w'(v,w,e) = w - \frac{|v-w|}{2}\,[e+u]\,,$$

one obtains

$$\begin{aligned}
&\int_{\mathcal{S}^2} B(v,w,e)\Big[f(v')\,f(w') - f(v)\,f(w)\Big]de = \\
&\qquad \int_{\mathcal{S}^2} \Phi(e+u)\,de = 4\int_{\mathcal{S}^2_+(u)} (e,u)\,\Phi(2\,e\,(e,u))\,de \\
&= 4\int_{\mathcal{S}^2_+(u)} (e,u)\,B(v,w,2\,e\,(e,u)-u)\,\times \\
&\qquad \Big[f\Big(v + \frac{|v-w|}{2}\,2\,e\,(e,u)\Big)\,f\Big(w - \frac{|v-w|}{2}\,2\,e\,(e,u)\Big) - f(v)\,f(w)\Big] \\
&= 4\int_{\mathcal{S}^2_+(u)} (e,u)\,B(v,w,2\,e\,(e,u)-u)\,\times \\
&\qquad \Big[f(v+e\,(e,w-v))\,f(w-e\,(e,w-v)) - f(v)\,f(w)\Big] \\
&= \int_{\mathcal{S}^2_+(u)} B^*(v,w,e)\Big[f(v^*)\,f(w^*) - f(v)\,f(w)\Big]de\,,
\end{aligned}$$

where B^* is given in (1.18). Denoting

$$2\,e\,(e,u) - u = \tilde{e} \tag{1.23}$$

one obtains

$$(e,u) = \sqrt{\frac{1+(\tilde{e},u)}{2}}$$

and

$$e = \frac{\tilde{e}+u}{\sqrt{2\,(1+(\tilde{e},u))}}\,. \tag{1.24}$$

Consequently (1.18) implies (1.19). ∎

Formulas (1.23) and (1.24) show the transformations between the vectors $e^* = e^*(\alpha,\varphi)$ and $e' = e'(\theta,\varphi)$. One obtains (cf. (1.6), (1.12))

$$\begin{aligned}
&v'(v,w,2\,e^*\,(e^*,u)-u) = \frac{v+w}{2} - \frac{w-v}{2} + e^*\,(e^*,w-v) = v^*(v,w,e^*)\,, \\
&w'(v,w,2\,e^*\,(e^*,u)-u) = w^*(v,w,e^*)
\end{aligned}$$

and

$$v^*(v,w,(e'+u)/\sqrt{2\,(1+(e',u))} = v + \frac{e'+u}{2\,(1+(e',u))}\,(e'+u, w-v)$$
$$= v + \frac{e'+u}{2\,(1+(e',u))}\,[(e',u)+1]\,|v-w| = v + \frac{e'+u}{2}\,|v-w|$$
$$= v + e'\,\frac{|v-w|}{2} + \frac{w-v}{2} = v'(v,w,e')\,,$$
$$w^*(v,w,(e'+u)/\sqrt{2\,(1+(e',u))} = w'(v,w,e')\,.$$

Remark 1.4. From (1.18), (1.16) and (1.10) one obtains

$$|v-w|\,\frac{b^*(|v-w|,\alpha)}{\sin\alpha} = 4\,(e^*(\alpha,\varphi),u)\,B(v,w,e'(\theta,\varphi))$$
$$= 4\,\cos\alpha\,|v-w|\,\frac{b(|v-w|,\theta)}{\sin\theta}$$

so that (cf. (1.11))

$$b^*(|v-w|,\alpha) = 2\,\sin 2\alpha\,\frac{b(|v-w|,\theta)}{\sin\theta} = 2\,b(|v-w|,\pi-2\alpha) \tag{1.25}$$

and

$$b(|v-w|,\theta) = \frac{1}{2}\,b^*(|v-w|,(\pi-\theta)/2)\,. \tag{1.26}$$

Note that (1.8) and (1.14) imply

$$b(|v-w|,\theta)\,d\theta = b^*(|v-w|,\alpha)\,d\alpha$$

and (1.25), (1.26) follow from (1.11).

1.3 Collision kernels

The differential cross section (1.8) is a quantity measurable by physical experiments. It represents the relative number of particles in a uniform incoming stream scattered into a certain area of directions. Therefore the Boltzmann equation with the collision integral (1.7) or (1.9) can be used even if the specific form of the collision transformation (1.4) is unknown. However, for some interaction laws the differential cross section and the corresponding collision kernel can be calculated explicitly.

Example 1.5. In the case of **hard sphere molecules** with diameter d the basic relationship between the impact parameter r and the scattering angle θ is

$$\sin\frac{\pi-\theta}{2} = \frac{r}{d}\,, \qquad r\in[0,d]\,. \tag{1.27}$$

The impact parameter $r = d$ corresponds to grazing collisions (scattering angle $\theta = 0$). One obtains

$$r\,dr = d\,\sin\frac{\pi-\theta}{2}\,\frac{d}{2}\,\cos\frac{\pi-\theta}{2}\,d\theta = \frac{d^2}{4}\,\sin\theta\,d\theta$$

so that (cf. (1.8))

$$b(|v-w|,\theta) = \frac{d^2}{4}\,\sin\theta \tag{1.28}$$

and (cf. (1.10))

$$B(v,w,e) = \frac{d^2}{4}\,|v-w|\,, \qquad e \in \mathcal{S}^2\,. \tag{1.29}$$

Analogously one obtains from (1.27) and (1.11)

$$r\,dr = d^2\,\sin\alpha\,\cos\alpha\,d\alpha$$

so that (cf. (1.14))

$$b^*(|v-w|,\alpha) = d^2\,\sin\alpha\,\cos\alpha$$

and

$$B^*(v,w,e) = |v-w|\,d^2\,\cos\alpha = d^2\,\big(w-v,e\big)\,, \qquad e \in \mathcal{S}^2_+(w-v)\,, \tag{1.30}$$

according to (1.16), (1.17). ■

Since the derivation of the Boltzmann equation assumes binary interactions between molecules, an assumption of a finite **interaction distance** d (the maximal distance at which particles influence each other) is usually made. Using (1.8) one obtains

$$\int_0^{2\pi}\int_0^{\pi} b(|v-w|,\theta)\,d\theta\,d\varphi = 2\pi\int_0^d r\,dr = \pi\,d^2\,. \tag{1.31}$$

The integral (1.31) over the differential cross section is called **total cross section**. It represents an area in the plane perpendicular to $v-w$, crossed by those particles influencing a given one. The total cross section (1.31) is independent of the specific interaction law. Note that (cf. (1.10))

$$\int_{\mathcal{S}^2} B(v,w,e)\,de = \pi\,d^2\,|v-w|\,.$$

Example 1.6. Let the particles be mass points interacting with central forces determined as gradients of some potential. The simplest case is an inverse power potential

$$\mathcal{U}(|x-y|) = \frac{C}{|x-y|^\alpha}\,, \qquad C>0\,, \quad \alpha>0\,,$$

where x, y are the positions of the particles. In this case the corresponding differential cross-section has the representation

$$b(|v-w|,\theta) = |v-w|^{-\frac{4}{\alpha}}\,\tilde{b}_\alpha(\theta) \tag{1.32}$$

and the collision kernel (1.10) takes the form

$$B(v,w,e) = |v-w|^{1-\frac{4}{\alpha}}\,\frac{\tilde{b}_\alpha(\theta)}{\sin\theta}\,. \tag{1.33}$$

Interaction laws with $\alpha<4$, where the collision kernel decreases with increasing relative velocity, are called **soft interactions**. Interactions with $\alpha>4$, where the collision kernel increases with increasing relative velocity, are called **hard interactions**. The "hardest" interaction with $\alpha\to\infty$ would correspond to hard sphere molecules. Here the differential cross section is independent of the relative velocity. ■

The analytic formulas (1.32), (1.33) hold for infinite range potentials ($d=\infty$) so that

$$\int_0^\pi \tilde{b}_\alpha(\theta)\,d\theta = \infty\,.$$

The differential cross section has a singularity at $\theta=0$. Therefore often some "angular cut-off" is used, ignoring scattering angles less than a certain value. This corresponds to an "impact parameter cut-off" with some interaction distance $d(|v-w|)$ depending on the relative velocity. Thus, the total cross section takes the form $\pi\,d(|v-w|)^2$ (cf. (1.31)).

Example 1.7. In the special case $\alpha=4$ the collision kernel (1.33) takes the form

$$B(v,w,e) = \frac{\tilde{b}_4(\theta)}{\sin\theta} \tag{1.34}$$

and does not depend on the relative velocity. Particles with this kind of interaction are called **Maxwell molecules**. This interaction law forms the border line which separates soft and hard interactions. Particles are called **pseudo-Maxwell molecules** if the function $\tilde{b}_4$ is replaced by some integrable function (in particular, if an angular cut-off is used).

Example 1.8. The collision kernel of the **variable hard sphere model** is given by

$$B(v,w,e) = C_\beta\,|v-w|^\beta\,,$$

with some parameter β and a constant $C_\beta>0$. The special case $\beta=1$ and $C_1=d^2/4$ corresponds to the hard sphere model (1.29). The case $\beta=0$ corresponds to pseudo-Maxwell molecules with constant collision kernel (1.34).

1.4 Boundary conditions

The Boltzmann equation (1.3) is subject to an initial condition

$$f(0,x,v) = f_0(x,v)\,, \qquad x \in D\,, \quad v \in \mathbb{R}^3\,, \tag{1.35}$$

and to conditions at the boundary of the domain D containing the gas. The boundary conditions prescribe the relation between values of the solution

$$f(t,x,v)\,, \qquad t \geq 0\,, \quad x \in \partial D\,,$$

for $v \in \mathbb{R}^3_{in}(x)$ and $v \in \mathbb{R}^3_{out}(x)$ and correspond to a certain behavior of particles at the boundary.

One example is the **inflow** boundary condition

$$f(t,x,v) = f_{in}(t,x,v)\,, \qquad v \in \mathbb{R}^3_{in}(x)\,, \tag{1.36}$$

where f_{in} is a given non-negative integrable function, e.g. some half-space Maxwellian. Here the values of the solution f for in-going velocities do not depend on the values of f for out-going velocities.

A second example is the boundary condition of **specular reflection**

$$f(t,x,v) = f(t,x,v - 2\big(v,n(x)\big)n(x))\,, \qquad v \in \mathbb{R}^3_{in}(x)\,. \tag{1.37}$$

Since $v - 2\big(v,n(x)\big)n(x) \in \mathbb{R}^3_{out}(x)$, the values of the solution f for in-going velocities are completely determined by the values of f for out-going velocities. Condition (1.37) is usually inadequate for real surfaces but perfect for artificial boundaries due to spatial symmetry of the flow.

A further example is the boundary condition of **diffuse reflection**

$$f(t,x,v) = M_b(t,x,v) \int\limits_{\mathbb{R}^3_{out}(x)} f(t,x,w)\,\big|\big(w,n(x)\big)\big|\,dw\,, \qquad v \in \mathbb{R}^3_{in}(x)\,, \tag{1.38}$$

where (cf. (1.2))

$$M_b(t,x,v) = \frac{1}{2\pi\,(k\,T_b(t,x)/m)^2}\,\exp\left(-\frac{m\,|v - V_b(t,x)|^2}{2k\,T_b(t,x)}\right) \tag{1.39}$$

is a Maxwell distribution at the boundary, m is the mass of a molecule and k is Boltzmann's constant. The temperature of the wall (boundary) at time t and position x is denoted by $T_b(t,x)$. The velocity of the wall $V_b(t,x)$ is assumed to satisfy

$$\big(n(x), V_b(t,x)\big) = 0\,.$$

The normalization of the function (1.39) (cf. Lemma A.2)

$$\int\limits_{\mathbb{R}^3_{in}(x)} M_b(t,x,v)\,\big(v,n(x)\big)\,dv = 1$$

implies that the total in-going and out-going **fluxes** are equal, i.e.

$$\int\limits_{\mathbb{R}^3_{in}(x)} f(t,x,v)\,\big(v,n(x)\big)\,dv = \int\limits_{\mathbb{R}^3_{out}(x)} f(t,x,w)\,\big|\big(w,n(x)\big)\big|\,dw\,. \qquad (1.40)$$

In condition (1.38) the values of the solution f for in-going velocities depend on the values of f for out-going velocities only through the total out-going flux.

1.5 Physical properties of gas flows

This section might be useful for mathematicians who often are lacking the quantitative physical information.

1.5.1 Physical quantities and units

Basic and derived units

length	m	meter
time	s	second
mass	kg	kilogram
temperature	K	Kelvin
force	N=kg m s^{-2}	Newton
energy	J=N m	Joule
pressure/stress	Pa=N m^{-2}	Pascal

Constants

N_A	6.0221 10^{23}	Avogadro's number
k	1.38066 10^{-23} J K^{-1}	Boltzmann's constant

Additional units

length	$A^o = 10^{-10}$ m	Angstrom	atomic sizes
mass	amu=1.66054 10^{-27} kg	atomic mass unit	N_A amu= 1 g
temperature	0^oC = 273 K	degree Celcius	100^oC = 373 K
	32^oF = 273 K	degree Fahrenheit	212^oF = 373 K
energy	erg=10^{-7} J	erg	
	eV=1.602 -19 J	electron volt	theory of atoms
	cal=4.19 J	calorie	theory of heat
pressure	bar=10^5 Pa	bar	
	atm=101325 Pa	atmosphere	
	torr=133.322 Pa	torr	mm of mercury

1.5.2 Macroscopic flow properties

The solution f of the Boltzmann equation (1.3) has the physical dimension "number per volume and velocity cube" $[\mathrm{m}^{-3}\,\mathrm{m}^{-3}\,\mathrm{s}^3]$. Considering the right-hand side of the equation in the form (1.7) or (1.9) one notes that the differential cross section b has the dimension "area" $[\mathrm{m}^2]$, while the collision kernel B has the dimension "velocity times area" $[\mathrm{m\,s}^{-1}\,\mathrm{m}^2]$.

Macroscopic properties of the gas are calculated as functionals of f. The **number density**

$$\varrho(t,x) = \int_{\mathbb{R}^3} f(t,x,v)\,dv \tag{1.41}$$

has the dimension "number per volume" $[\mathrm{m}^{-3}]$. The dimensionless quantity

$$\int_D \varrho(t,x)\,dx = \int_D \int_{\mathbb{R}^3} f(t,x,v)\,dv\,dx$$

represents the number of particles in the domain D at time t. The components of the bulk or **stream velocity**

$$V_i(t,x) = \frac{1}{\varrho(t,x)} \int_{\mathbb{R}^3} v_i\, f(t,x,v)\,dv\,, \qquad i = 1,2,3\,, \tag{1.42}$$

have the dimension $[\mathrm{m\,s}^{-1}]$. The components of the **pressure tensor**

$$P_{i,j}(t,x) = m \int_{\mathbb{R}^3} [v_i - V_i(t,x)]\,[v_j - V_j(t,x)]\, f(t,x,v)\,dv\,, \qquad i,j = 1,2,3\,, \tag{1.43}$$

and the **scalar pressure**

$$p(t,x) = \frac{1}{3}\sum_{i=1}^{3} P_{i,i}(t,x) = \frac{m}{3}\int_{\mathbb{R}^3} |v - V(t,x)|^2\, f(t,x,v)\,dv \tag{1.44}$$

have the dimension [kg $\mathrm{m}^2\,\mathrm{s}^{-2}\,\mathrm{m}^{-3}$=Pa]. Having in mind the **ideal gas law**

$$p = \varrho\, k\, T \tag{1.45}$$

the **temperature** is defined as

$$T(t,x) = \frac{1}{k\,\varrho(t,x)}\, p(t,x) \tag{1.46}$$

with the dimension [K N^{-1} m^{-1} m^3 N m^{-2}=K]. Note that the definitions (1.41), (1.42) and (1.46) are consistent with the notations used in the Maxwell distribution (1.2). In particular, one obtains

$$\frac{m}{3\,k\,\varrho}\int_{\mathbb{R}^3}|v-V|^2\,f_{eq}(v)\,dv = T\,.$$

The fluxes (1.40) have the dimension "number per area and time" [$\mathrm{m}^{-2}\ \mathrm{s}^{-1}$]. The components of the **heat flux vector**

$$q_i(t,x) = \frac{m}{2}\int_{\mathbb{R}^3}[v_i - V_i(t,x)]\,|v-V(t,x)|^2\,f(t,x,v)\,dv\,, \qquad i=1,2,3\,, \tag{1.47}$$

have the dimension [$\mathrm{kg\ m^3\ s^{-3}\ m^{-3}} = \mathrm{J\ m^{-2}\ s^{-1}}$] representing the transport of energy (heat) through some area per unit of time.

Further quantities of interest are the **speed of sound**

$$v_{\mathrm{sound}}(t,x) = \sqrt{\frac{\gamma\,k\,T(t,x)}{m}} \tag{1.48}$$

and the **Mach number**

$$\mathrm{Mach}(t,x) = \frac{|V(t,x)|}{v_{\mathrm{sound}}(t,x)} \tag{1.49}$$

which measures the bulk velocity in multiples of the speed of sound. The **specific heat ratio** γ used in (1.48) is related to the number β of degrees of freedom of the gas molecules as $\gamma = (\beta+2)/\beta$. Monatomic gases (like helium) have only three translational degrees of freedom so that $\gamma = 5/3$. Diatomic molecules (like oxygen or nitrogen) have, in addition, two rotational degrees of freedom so that $\gamma = 7/5$.

1.5.3 Molecular flow properties

The **mean molecule velocity** (in equilibrium)

$$\bar v = \frac{1}{\varrho}\int_{\mathbb{R}^3}|v|\,f_{\mathrm{eq}}(v)\,dv = \sqrt{\frac{8kT}{\pi m}} \tag{1.50}$$

is calculated using the Maxwell distribution (1.2) with $V = 0$. The **mean free path** L is the average distance travelled by a molecule between collisions. Heuristically it is derived as follows. Let d be the interaction distance (e.g. the diameter in the hard sphere case). Then the interaction area is $\pi\,d^2$ and the average number of collisions during time t is $\pi\,d^2\,\sqrt{2}\,\bar v\,t\,\varrho$. The factor $\sqrt{2}$ takes into account the relative velocity of the colliding particles. The mean free path is obtained as

$$L = \frac{\text{path length}}{\text{number of collisions}} = \frac{\bar v\,t}{\pi\,d^2\,\sqrt{2}\,\bar v\,t\,\varrho} = \frac{1}{\sqrt{2}\,\pi\,d^2\,\varrho}\,. \tag{1.51}$$

To calculate the mean free path one needs the molecule diameter and the density (or pressure and temperature) of the gas.

1.5.4 Measurements

The following data are taken from the U.S. Standard Atmosphere tables (1962, idealized year-round mean; first two lines: 1976).

Height (km)	Density ($\mathrm{g\,cm^{-3}}$)	Particle density ($\mathrm{cm^{-3}}$)	Collision frequency ($\mathrm{s^{-1}}$)	Mean free path (cm)	Kinetic temperature (Kelvin)	Pressure (torr)
0		2.55 +19			288	7.60 +2
5		1.53 +19			256	4.06 +2
10	4.14 -4	8.60 +18	2.06 +9	1.96 -5	223	1.99 +2
20	8.89 -5	1.85 +18	4.35 +8	9.14 -5	217	4.14 +1
30	1.84 -5	3.83 +17	9.22 +7	4.41 -4	227	8.98 +0
40	4.00 -6	8.31 +16	2.10 +7	2.03 -3	250	2.15 +0
50	1.03 -6	2.14 +16	5.62 +6	7.91 -3	271	5.98 -1
60	3.06 -7	6.36 +15	1.63 +6	2.66 -2	256	1.68 -1
70	8.75 -8	1.82 +15	4.32 +5	9.28 -2	220	4.14 -2
80	1.99 -8	4.16 +14	8.94 +4	4.07 -1	181	7.78 -3
90	3.17 -9	6.59 +13	1.42 +4	2.56 +0	181	1.23 -3
100	4.97 -10	1.04 +13	2.41 +3	1.63 +1	210	2.26 -4
110	9.83 -11	2.07 +12	5.36 +2	8.15 +1	257	5.52 -5
120	2.44 -11	5.23 +11	1.59 +2	3.23 +2	351	1.89 -5

These data show good agreement with the theoretical predictions mentioned above. The product 'mean free path' times 'particle density' has roughly the constant value $16.9 * 10^{13}\,\mathrm{cm^{-2}}$. Using (1.51) one obtains

$$d^2 = \frac{1}{\sqrt{2}\,\pi\,L\,\varrho} \sim \frac{1}{1.41 * 3.14 * 1.69 * 10^{14}\,\mathrm{cm^{-2}}} = 0.134 * 10^{-14}\,\mathrm{cm^2}$$

so that

$$d \sim 0.37 * 10^{-9}\,\mathrm{m} = 3.7\,\mathrm{A}^o\,.$$

The ratio 'mass density' divided by 'particle density' has roughly the constant value

$$48 * 10^{-27}\,\mathrm{kg} \sim 29\,\mathrm{amu}\,.$$

1.5.5 Air at standard conditions

The average molecular mass for dry air (78% N_2, 21% O_2) is 29 amu (oxygen atom 16 amu, nitrogen atom 14 amu). For air at standard conditions ($T = 0^o$C, $p = 1$ atm) one obtains from (1.50) the mean molecule velocity

$$\bar{v} = \left(\frac{8}{\pi}\frac{1.38 * 10^{-23}\ \mathrm{J/K}\ 273\,\mathrm{K}}{29 * 1.66\ 10^{-27}\ \mathrm{kg}}\right)^{\frac{1}{2}} \sim 446\,\mathrm{m/s}\,.$$

Assuming $d = 3.7\,\mathrm{A}^o$ and using (1.45), one obtains from (1.51) the mean free path

$$L = \frac{1.38 * 10^{-23}\,\mathrm{J/K}\ 273\,\mathrm{K}}{\sqrt{2}\,\pi * 13.7 * 10^{-20}\,\mathrm{m}^2\ 1.01 * 10^5\,\mathrm{N/m}^2} \sim 61\,\mathrm{nm}\,.$$

Correspondingly, a molecule suffers about $7 * 10^9$ collisions per second. The ratio between mean free path and diameter is $L/d \sim 165$. The relative volume occupied by gas molecules is

$$\frac{\pi}{6}\,\frac{d^3\,p}{k\,T} = \frac{\pi}{6}\,\frac{(0.37)^3 * 10^{-27}\,\mathrm{m}^3\ 1.01 * 10^5\,\mathrm{N/m}^2}{1.38 * 10^{-23}\,\mathrm{J/K}\ 273\,\mathrm{K}} \sim 0.0007\,.$$

The speed of sound (1.48) is

$$\left(\frac{1.4 * 1.38 * 10^{-23}\,\mathrm{J/K}\ 273\,\mathrm{K}}{29 * 1.66\ 10^{-27}\ \mathrm{kg}}\right)^{\frac{1}{2}} \sim 331\,\mathrm{m/s}\,.$$

1.6 Properties of the collision integral

To study the collision integral (1.9), we introduce the notation

$$Q(f,g)(v) = \frac{1}{2}\int_{\mathbb{R}^3} dw \int_{\mathcal{S}^2} de\, B(v,w,e) \times \Big[f(v')\,g(w') + g(v')\,f(w') - f(v)\,g(w) - g(v)\,f(w)\Big],$$

where f, g are appropriate functions on $\mathbb{R}^3$ and v', w' are defined in (1.6).

Theorem 1.9. *All strictly positive integrable solutions g of the equation*

$$Q(g,g) = 0 \tag{1.52}$$

are Maxwell distributions, i.e.

$$g(v) = \varrho\, M_{V,T}(v)\,, \qquad \forall v \in \mathbb{R}^3\,, \tag{1.53}$$

for some $\varrho, T > 0$ and $V \in \mathbb{R}^3$.

The proof is prepared by several lemmas.

Lemma 1.10. *Let v', w' be defined by the collision transformation (1.6). Then*

$$\int_{\mathbb{R}^3}\int_{\mathbb{R}^3}\int_{\mathcal{S}^2} \Phi(|v-w|, (v-w,e), v, w, v', w')\,de\,dw\,dv = \int_{\mathbb{R}^3}\int_{\mathbb{R}^3}\int_{\mathcal{S}^2} \Phi(|v-w|, (v-w,e), v', w', v, w)\,de\,dw\,dv\,, \tag{1.54}$$

for any appropriate test function Φ.

Proof. The integral at the left-hand side of (1.54) transforms under the substitution

$$v = U + \frac{1}{2}\,u\,, \quad w = U - \frac{1}{2}\,u\,, \qquad dw\,dv = du\,dU\,,$$

into

$$\int_{\mathcal{S}^2}\int_{\mathbb{R}^3}\int_{\mathbb{R}^3} \Phi\left(|u|, (u,e), U + \frac{u}{2}, U - \frac{u}{2}, U + e\,\frac{|u|}{2}, U - e\,\frac{|u|}{2}\right) du\,dU\,de\,.$$

Using spherical coordinates

$$u = r\,\tilde{e}\,, \quad r \in [0,\infty)\,, \quad \tilde{e} \in \mathcal{S}^2\,, \qquad du = r^2 dr\,d\tilde{e}\,,$$

this integral takes the form

$$\int_{\mathcal{S}^2}\int_{\mathbb{R}^3}\int_{\mathcal{S}^2}\int_0^\infty \Phi\left(r, r(\tilde{e}, e), U + \frac{r\,\tilde{e}}{2}, U - \frac{r\,\tilde{e}}{2}, U + \frac{r\,e}{2}, U - \frac{r\,e}{2}\right) \times r^2 dr\,d\tilde{e}\,dU\,de\,.$$

Combining r and e as spherical coordinates into a new variable

$$\tilde{u} = r\,e\,, \quad r \in [0,\infty)\,, \quad e \in \mathcal{S}^2\,, \qquad d\tilde{u} = r^2 dr\,de\,,$$

one obtains

$$\int_{\mathcal{S}^2}\int_{\mathbb{R}^3}\int_{\mathbb{R}^3} \Phi\left(|\tilde{u}|, (\tilde{e}, \tilde{u}), U + \frac{|\tilde{u}|\,\tilde{e}}{2}, U - \frac{|\tilde{u}|\,\tilde{e}}{2}, U + \frac{\tilde{u}}{2}, U - \frac{\tilde{u}}{2}\right) d\tilde{u}\,dU\,d\tilde{e}\,.$$

Using the substitution

$$U = \frac{v+w}{2}\,, \quad \tilde{u} = v - w\,, \qquad d\tilde{u}\,dU = dw\,dv\,,$$

and removing the tilde sign of the variable $\tilde{e}$ one obtains (1.54). ∎

Lemma 1.11. *Let v', w' be defined by the collision transformation (1.6). Then*

$$\begin{aligned}
&\int_{\mathbb{R}^3} \varphi(v)\,Q(f,g)(v)\,dv = \\
&\quad \frac{1}{2}\int_{\mathbb{R}^3}\int_{\mathbb{R}^3}\int_{\mathcal{S}^2} B(v,w,e)\Big[f(v)\,g(w) + g(v)\,f(w)\Big]\Big[\varphi(v') - \varphi(v)\Big]de\,dw\,dv \\
&= \frac{1}{4}\int_{\mathbb{R}^3}\int_{\mathbb{R}^3}\int_{\mathcal{S}^2} B(v,w,e) \times \\
&\qquad \Big[f(v)\,g(w) + g(v)\,f(w)\Big]\Big[\varphi(v') + \varphi(w') - \varphi(v) - \varphi(w)\Big]de\,dw\,dv \\
&= \frac{1}{8}\int_{\mathbb{R}^3}\int_{\mathbb{R}^3}\int_{\mathcal{S}^2} B(v,w,e)\Big[\varphi(v') + \varphi(w') - \varphi(v) - \varphi(w)\Big] \times \\
&\qquad \Big[f(v)\,g(w) + g(v)\,f(w) - f(v')\,g(w') - g(v')\,f(w')\Big]de\,dw\,dv\,,
\end{aligned}$$

for any appropriate functions φ, f and g.

Proof. Note that B depends on its arguments via $|v-w|$ and $(v-w,e)$, according to (1.10). Thus, Lemma 1.10 implies the first part of the assertion. Changing the variables v and w, using the substitution $e=-\tilde{e}$, $de=d\tilde{e}$ and removing the tilde sign over $\tilde{e}$ leads to

$$\int_{\mathbb{R}^3}\varphi(v)\,Q(f,g)(v)\,dv=\frac{1}{2}\int_{\mathbb{R}^3}\int_{\mathbb{R}^3}\int_{\mathcal{S}^2}B(w,v,-e)\times \\ \Big[f(v)\,g(w)+g(v)\,f(w)\Big]\Big[\varphi(v'(w,v,-e))-\varphi(w)\Big]de\,dv\,dw\,. \tag{1.55}$$

Using the first part of the assertion, (1.55) and the property

$$B(w,v,-e)=B(v,w,e)\,,$$

one obtains the second part of the assertion, and one more application of Lemma 1.10 gives the third part. ∎

A function $\psi:\mathbb{R}^3\to\mathbb{R}$ is called **collision invariant** if

$$\psi(v')+\psi(w')=\psi(v)+\psi(w)\,,\qquad \forall\, v,w\in\mathbb{R}^3\,,\quad e\in\mathcal{S}^2\,. \tag{1.56}$$

It follows from conservation of mass, momentum and energy during collisions that the functions

$$\psi_0(v)=1\,,\quad \psi_j(v)=v_j\,,\ j=1,2,3\,,\quad \psi_4(v)=|v|^2 \tag{1.57}$$

are collision invariants. Note that Lemma 1.11 implies

$$\int_{\mathbb{R}^3}\psi(v)\,Q(g,g)(v)\,dv=0\,, \tag{1.58}$$

for any collision invariant ψ, independently of the particular choice of the function g.

Lemma 1.12. *A continuous function $\psi:\mathbb{R}^3\to\mathbb{R}$ is a collision invariant if and only if it is a linear combination of the basic collision invariants (1.57), i.e.*

$$\psi(v)=a+(b,v)+c\,|v|^2\,,\qquad \textit{for some}\quad a,c\in\mathbb{R}\,,\ b\in\mathbb{R}^3\,.$$

Proof of Theorem 1.9. Assuming that the function g is strictly positive one can use $\log g$ as a test function. It follows from Lemma 1.11 that

$$\int_{\mathbb{R}^3}\log g(v)\,Q(g,g)(v)\,dv= \\ -\frac{1}{4}\int\limits_{\mathbb{R}^3}\int\limits_{\mathbb{R}^3}\int\limits_{\mathcal{S}^2}B(v,w,e)\,g(v)\,g(w)\left[\frac{g(v')\,g(w')}{g(v)\,g(w)}-1\right]\log\frac{g(v')\,g(w')}{g(v)\,g(w)}dw\,dv\,de\,. \tag{1.59}$$

Since the expression $(z-1)\log z$ is always non-negative and vanishes only if $z=1$, one obtains from (1.59) Boltzmann's inequality

$$\int_{\mathbb{R}^3} \log g(v)\, Q(g,g)(v)\, dv \le 0 \tag{1.60}$$

and concludes that

$$\int_{\mathbb{R}^3} \log g(v)\, Q(g,g)(v)\, dv = 0 \tag{1.61}$$

if and only if

$$g(v')\, g(w') = g(v)\, g(w)\,, \qquad \forall\, v, w \in \mathbb{R}^3\,, \quad e \in \mathcal{S}^2\,,$$

i.e., if the function $\log g$ is a collision invariant (cf. (1.56)). Thus, according to Lemma 1.12, property (1.61) is fulfilled if and only if the function g is of the form

$$g(v) = \exp\left(a + (b, v) + c\,|v|^2\right), \qquad \text{for some} \quad a, c \in \mathbb{R}\,,\ b \in \mathbb{R}^3\,.$$

Note that c must be negative so that g is integrable over the velocity space. Thus, the function g takes the form (1.53). ∎

Let $f(t,v)$ be a solution of the **spatially homogeneous Boltzmann equation**

$$\frac{\partial}{\partial t} f(t,v) = Q(f,f)(t,v)\,. \tag{1.62}$$

Note that (1.58) implies

$$\frac{d}{dt} \int_{\mathbb{R}^3} \psi_j(v)\, f(t,v)\, dv = 0\,, \tag{1.63}$$

for the basic collision invariants (1.57). The functional

$$H[f](t) = \int_{\mathbb{R}^3} \log f(t,v)\, f(t,v)\, dv \tag{1.64}$$

is called **H-functional**. Using (1.62) and (1.63) (with $j = 0$) one obtains the equation

$$\frac{d}{dt}\, H[f](t) = \int_{\mathbb{R}^3} \log f(t,v)\, Q(f,f)(t,v)\, dv\,.$$

Thus, according to (1.60), the H-functional is a monotonically decreasing function in time, unless f has the form (1.53) with constant parameters ϱ, V and T. In this case the H-functional has a constant value

$$H[f](t) = \varrho \left(\log \frac{\varrho}{(2\pi\, T)^{3/2}} - \frac{3}{2} \right), \qquad t \ge 0\,. \tag{1.65}$$

Example 1.13. Let us consider the initial value problem for the spatially homogeneous Boltzmann equation (1.62) with initial condition

$$f(0,v) = \alpha\, M_{V,T_1}(v) + (1-\alpha)\, M_{V,T_2}(v) \qquad \text{for some} \quad \alpha \in [0,1]\,.$$

The asymptotic distribution function is

$$\lim_{t\to\infty} f(t,v) = M_{V,T}(v) \qquad \text{with} \qquad T = \alpha\, T_1 + (1-\alpha)\, T_2\,.$$

According to (1.65), the asymptotic value of the H-functional is

$$H[M_{V,T}] = -\frac{3}{2}\Big[\log(2\pi T) + 1\Big].$$

Fig. 1.2 shows the time evolution of the H-functional (1.64) for the hard sphere model

$$B(v,w,e) = \frac{1}{4\pi}\,|v-w|$$

and for the parameters

$$\alpha = 0.25\,, \quad V = (0,0,0)\,, \quad T_1 = 0.1\,, \quad T_2 = 0.3\,, \quad T = 0.25\,.$$

The solid line in this figure represents the H-functional, while the dotted line shows its asymptotic value $3/2\,[\log(2/\pi) - 1] \sim -2.1774$.

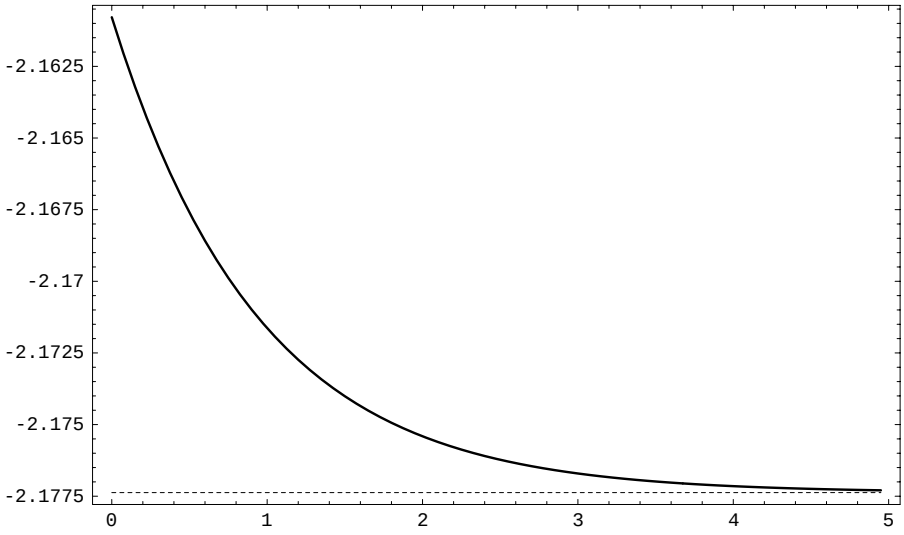

Fig. 1.2. Time evolution of the H-functional

1.7 Moment equations

Here we use the property (1.58) of the collision integral. Multiplying the Boltzmann equation (1.3) by one of the basic collision invariants (1.57), integrating the result with respect to v over the velocity space and changing the order of integration and differentiation, one obtains the equations

$$\frac{\partial}{\partial t}\int_{\mathbb{R}^3}\psi_j(v)f(t,x,v)\,dv+\sum_{i=1}^{3}\frac{\partial}{\partial x_i}\int_{\mathbb{R}^3}v_i\,\psi_j(v)f(t,x,v)\,dv=0\,,\qquad j=0,1,2,3,4\,. \tag{1.66}$$

Using the definition (1.41) of the number density and the notations

$$l_i(t,x)=\int_{\mathbb{R}^3}v_i\,f(t,x,v)\,dv\,,\qquad i=1,2,3\,,$$

$$L_{i,j}(t,x)=\int_{\mathbb{R}^3}v_i\,v_j\,f(t,x,v)\,dv\,,\qquad i,j=1,2,3\,,$$

and

$$r_i(t,x)=\int_{\mathbb{R}^3}v_i\,|v|^2\,f(t,x,v)\,dv\,,\qquad i=1,2,3\,,$$

we rewrite equations (1.66) in terms of moments of the distribution function

$$\begin{aligned}
&\frac{\partial}{\partial t}\,\varrho(t,x)+\sum_{i=1}^{3}\frac{\partial}{\partial x_i}\,l_i(t,x)=0\,,\\
&\frac{\partial}{\partial t}\,l_j(t,x)+\sum_{i=1}^{3}\frac{\partial}{\partial x_i}\,L_{i,j}(t,x)=0\,,\qquad j=1,2,3\,,\\
&\frac{\partial}{\partial t}\sum_{i=1}^{3}L_{i,i}(t,x)+\sum_{i=1}^{3}\frac{\partial}{\partial x_i}\,r_i(t,x)=0\,.
\end{aligned} \tag{1.67}$$

Recalling the definitions (1.42)-(1.44), (1.46) and (1.47), one obtains

$$\begin{aligned}
V_i(t,x)&=\frac{1}{\varrho(t,x)}\,l_i(t,x)\,,\\
P_{i,j}(t,x)&=m\Big[L_{i,j}(t,x)-\varrho(t,x)\,V_i(t,x)\,V_j(t,x)\Big],\\
\varrho(t,x)\,k\,T(t,x)&=\frac{m}{3}\left[\sum_{i=1}^{3}L_{i,i}(t,x)-\varrho(t,x)\,|V(t,x)|^2\right]
\end{aligned}$$

and

$$
\begin{aligned}
q_i(t,x) &= \\
&\frac{m}{2}\left[r_i - 2\sum_{j=1}^{3} V_j\, L_{i,j} + l_i\,|V|^2 - V_i \sum_{j=1}^{3} L_{j,j} + 2\,V_i \sum_{j=1}^{3} V_j\, l_j - V_i\,|V|^2\,\varrho\right] \\
&= \frac{m}{2}\left[r_i - 2\sum_{j=1}^{3} V_j\, L_{i,j} - V_i \sum_{j=1}^{3} L_{j,j} + 2\,\varrho\, V_i\,|V|^2\right] \\
&= \frac{m}{2}\, r_i - \sum_{j=1}^{3} V_j\, P_{i,j} - \frac{3\,k}{2}\, V_i\, \varrho\, T - \frac{m}{2}\,\varrho\, V_i\,|V|^2\,,
\end{aligned}
$$

for $i, j = 1, 2, 3$. Thus, the system of equations (1.67) implies

$$
\frac{\partial}{\partial t}\,\varrho(t,x) + \sum_{i=1}^{3} \frac{\partial}{\partial x_i}\Big[V_i(t,x)\,\varrho(t,x)\Big] = 0\,, \tag{1.68}
$$

$$
\begin{aligned}
&\frac{\partial}{\partial t}\Big[\varrho(t,x)\,V_j(t,x)\Big] + \\
&\sum_{i=1}^{3} \frac{\partial}{\partial x_i}\Big[V_i(t,x)\,\varrho(t,x)\,V_j(t,x)\Big] = -\frac{1}{m}\sum_{i=1}^{3} \frac{\partial}{\partial x_i}\,P_{i,j}(t,x)\,, \qquad j = 1,2,3\,,
\end{aligned} \tag{1.69}
$$

and

$$
\begin{aligned}
&\frac{\partial}{\partial t}\left[\frac{3\,k}{2\,m}\,\varrho(t,x)\,T(t,x) + \frac{1}{2}\,\varrho(t,x)\,|V(t,x)|^2\right] + \\
&\qquad \sum_{i=1}^{3} \frac{\partial}{\partial x_i}\left[V_i(t,x)\left(\frac{3\,k}{2\,m}\,\varrho(t,x)\,T(t,x) + \frac{1}{2}\,\varrho(t,x)\,|V(t,x)|^2\right)\right] = \\
&\qquad\qquad -\frac{1}{m}\sum_{i=1}^{3} \frac{\partial}{\partial x_i}\left[q_i(t,x) + \sum_{j=1}^{3} P_{i,j}(t,x)\,V_j(t,x)\right].
\end{aligned} \tag{1.70}
$$

Equation (1.68) transforms into

$$
\frac{\partial}{\partial t}\,\varrho(t,x) + \big(V(t,x), \nabla_x\big)\,\varrho(t,x) + \varrho(t,x)\,\mathrm{div}\,V(t,x) = 0\,. \tag{1.71}
$$

Using (1.68), the left-hand side of equation (1.69) transforms into

$$
\begin{aligned}
&\frac{\partial}{\partial t}\Big[\varrho(t,x)\Big]V_j(t,x) + \varrho(t,x)\,\frac{\partial}{\partial t}\Big[V_j(t,x)\Big] + \\
&\quad \sum_{i=1}^{3} \frac{\partial}{\partial x_i}\Big[V_i(t,x)\,\varrho(t,x)\Big]V_j(t,x) + \sum_{i=1}^{3} V_i(t,x)\,\varrho(t,x)\,\frac{\partial}{\partial x_i}\Big[V_j(t,x)\Big] \\
&= \varrho(t,x)\left[\frac{\partial}{\partial t}\,V_j(t,x) + \big(V(t,x), \nabla_x\big)\,V_j(t,x)\right]
\end{aligned}
$$

so that equation (1.69) takes the form

$$\frac{\partial}{\partial t}\, V_j(t,x) + \big(V(t,x), \nabla_x\big)\, V_j(t,x) = -\frac{1}{m\, \varrho(t,x)} \sum_{i=1}^{3} \frac{\partial}{\partial x_i}\, P_{i,j}(t,x)\,, \qquad j = 1,2,3\,. \tag{1.72}$$

The two parts of the left-hand side of equation (1.70) transform into

$$\begin{aligned} &\frac{\partial}{\partial t}\Big[\varrho(t,x)\Big] T(t,x) + \varrho(t,x)\, \frac{\partial}{\partial t}\Big[T(t,x)\Big] + \\ &\quad \sum_{i=1}^{3} \frac{\partial}{\partial x_i}\Big[V_i(t,x)\varrho(t,x)\Big] T(t,x) + \sum_{i=1}^{3} V_i(t,x)\, \varrho(t,x)\, \frac{\partial}{\partial x_i}\Big[T(t,x)\Big] \\ &= \varrho(t,x) \left[\frac{\partial}{\partial t}\, T(t,x) + \big(V(t,x), \nabla_x\big)\, T(t,x)\right] \end{aligned}$$

and

$$\begin{aligned} &\frac{1}{2}\Bigg(\sum_{j=1}^{3} \frac{\partial}{\partial t}\Big[\varrho(t,x)\, V_j(t,x)\Big] V_j(t,x) + \sum_{j=1}^{3} \varrho(t,x)\, V_j(t,x) \frac{\partial}{\partial t}\Big[V_j(t,x)\Big] + \\ &\qquad \sum_{i=1}^{3}\sum_{j=1}^{3} \frac{\partial}{\partial x_i}\Big[V_i(t,x)\, \varrho(t,x)\, V_j(t,x)\Big] V_j(t,x) + \\ &\qquad\quad \sum_{i=1}^{3}\sum_{j=1}^{3} V_i(t,x)\, \varrho(t,x)\, V_j(t,x)\, \frac{\partial}{\partial x_i}\Big[V_j(t,x)\Big]\Bigg) \\ &= \frac{1}{2}\sum_{j=1}^{3} V_j(t,x) \left[-\frac{1}{m}\sum_{i=1}^{3} \frac{\partial}{\partial x_i}\, P_{i,j}(t,x)\right] + \\ &\qquad \frac{1}{2}\sum_{j=1}^{3} \varrho(t,x)\, V_j(t,x) \left[-\frac{1}{m\, \varrho(t,x)} \sum_{i=1}^{3} \frac{\partial}{\partial x_i}\, P_{i,j}(t,x)\right] \\ &= -\frac{1}{m}\sum_{j=1}^{3} V_j(t,x) \sum_{i=1}^{3} \frac{\partial}{\partial x_i}\, P_{i,j}(t,x) \end{aligned}$$

so that equation (1.70) takes the form

$$\begin{aligned} &\frac{\partial}{\partial t}\, T(t,x) + \big(V(t,x), \nabla_x\big)\, T(t,x) = \\ &\quad -\frac{2}{3k\, \varrho(t,x)} \left(\operatorname{div} q(t,x) + \sum_{i,j=1}^{3} P_{i,j}(t,x) \frac{\partial}{\partial x_i}\, V_j(t,x)\right). \end{aligned} \tag{1.73}$$

The system (1.71), (1.72), (1.73) contains five equations for 13 unknown functions ϱ, V, P and q. Note that the symmetric matrix P is defined by its upper triangle.

If the distribution function is a Maxwellian, i.e.

$$f(t,x,v) = \varrho(t,x)\left[\frac{m}{2\pi\, k\, T(t,x)}\right]^{\frac{3}{2}} \exp\left(-\frac{m\,|v-V(t,x)|^2}{2\,k\,T(t,x)}\right),$$

then one obtains

$$P_{i,j}(t,x) = p(t,x)\,\delta_{i,j}\,, \qquad q_i(t,x) = 0\,, \qquad i,j = 1,2,3\,. \tag{1.74}$$

Assuming that the gas under consideration is close to equilibrium, i.e. its distribution function is close to a Maxwellian, property (1.74) can be used as a closure relation. Then the number of unknown functions reduces to five. These functions are the density ϱ, the stream velocity V and the temperature T (or, equivalently, the pressure p). Equations (1.71), (1.72) and (1.73) reduce to the **Euler equations**

$$\frac{\partial}{\partial t}\,\varrho(t,x) + \big(V(t,x),\nabla_x\big)\,\varrho(t,x) + \varrho(t,x)\,\mathrm{div}\,V(t,x) = 0\,,$$

$$\frac{\partial}{\partial t}\,V_j(t,x) + \big(V(t,x),\nabla_x\big)\,V_j(t,x) + \frac{k}{m\,\varrho(t,x)}\,\frac{\partial}{\partial x_j}\Big[\varrho(t,x)\,T(t,x)\Big] = 0\,, \qquad j = 1,2,3\,,$$

and

$$\frac{\partial}{\partial t}\,T(t,x) + \big(V(t,x),\nabla_x\big)\,T(t,x) + \frac{2}{3}\,T(t,x)\,\mathrm{div}\,V(t,x) = 0\,.$$

They describe a so-called Euler (or ideal) fluid.

Besides (1.74), other closure relations (also called constitutive equations) are used. If one assumes

$$P_{i,j}(t,x) = p(t,x)\,\delta_{i,j} - \mu\left[\frac{\partial}{\partial x_i}\,V_j(t,x) + \frac{\partial}{\partial x_j}\,V_i(t,x)\right] - \lambda\,\delta_{i,j}\,\mathrm{div}\,V(t,x)\,,$$

$$q_i(t,x) = -\kappa\,\frac{\partial}{\partial x_i}\,T(t,x)\,, \qquad i,j = 1,2,3\,,$$

then equations (1.71)-(1.73) reduce to the **Navier-Stokes equations**. They describe a so-called Navier-Stokes-Fourier (or viscous and thermally conducting) fluid. Here μ, λ are the viscosity coefficients and κ is the heat conduction coefficient. All these coefficients can be functions of the density ϱ and the temperature T.

1.8 Criterion of local equilibrium

If the distribution function f is close to a Maxwell distribution, then one can expect that the description of the flow by the Boltzmann equation is close

to its description by the system of Euler equations. The numerical solution of the Boltzmann equation is, in general, much more complicated than the numerical solution of the Euler equations, because the distribution function depends on seven variables. In contrast, the system of Euler equations contains five unknown functions depending on four variables. Therefore it makes sense to divide the domain D into two subdomains with the kinetic description of the flow by the Boltzmann equation in the first subdomain and with the hydrodynamic description by the Euler equations in the second subdomain.

In this section we derive a functional that indicates the deviation of the distribution function f from a Maxwell distribution with the same density, stream velocity and temperature. In the derivation we skip the arguments t, x which are assumed to be fixed. Note that (cf. (1.2))

$$f_{\mathrm{eq}}(v) = \varrho \left(\frac{m}{kT}\right)^{\frac{3}{2}} M_{0,1}\left(\frac{v-V}{\sqrt{kT/m}}\right).$$

In analogy we first introduce the normalized function

$$\tilde{f}(v) = \frac{1}{\varrho}\left(\frac{kT}{m}\right)^{\frac{3}{2}} f\left(V + v\sqrt{kT/m}\right) \tag{1.75}$$

and study its deviation from $M_{0,1}$. The general case is then found by an appropriate rescaling.

We consider a function

$$\psi(v) = a + (b, v) + (Cv, v) + (d, v)\,|v|^2 + e\,|v|^4\,, \tag{1.76}$$

where the parameters $a, e \in \mathbb{R}$, $b, d \in \mathbb{R}^3$, $C \in \mathbb{R}^{3\times 3}$ are chosen in such a way that

$$\int_{\mathbb{R}^3} \varphi(v)\, M_{0,1}(v)\Big[1 + \psi(v)\Big]\, dv = \int_{\mathbb{R}^3} \varphi(v)\, \tilde{f}(v)\, dv\,, \tag{1.77}$$

for the test functions

$$\varphi(v) = 1\,,\ v_i\,,\ v_i v_j\,,\ v_i\,|v|^2\,,\ |v|^4\,, \qquad i, j = 1, 2, 3\,.$$

Note that there are 14 equations and 14 unknown variables. The weighted $\mathbb{L}_2$-norm of the function (1.76)

$$\left(\int_{\mathbb{R}^3} \psi(v)^2\, M_{0,1}(v)\, dv\right)^{\frac{1}{2}} \tag{1.78}$$

will be used as a measure of deviation from local equilibrium.

Conditions (1.77) are transformed into

$$\int_{\mathbb{R}^3} \psi(v)\, M_{0,1}(v)\, dv = 0\,, \tag{1.79a}$$

$$\int_{\mathbb{R}^3} v_i\, \psi(v)\, M_{0,1}(v)\, dv = 0\,, \tag{1.79b}$$

$$\int_{\mathbb{R}^3} v_i\, v_j\, \psi(v)\, M_{0,1}(v)\, dv = \tilde{\tau}_{i,j}\,, \tag{1.79c}$$

$$\int_{\mathbb{R}^3} v_i\, |v|^2\, \psi(v)\, M_{0,1}(v)\, dv = 2\,\tilde{q}_i\,, \tag{1.79d}$$

$$\int_{\mathbb{R}^3} |v|^4\, \psi(v)\, M_{0,1}(v)\, dv = \tilde{\gamma}\,, \tag{1.79e}$$

where the notations

$$\tilde{\tau}_{i,j} = \int_{\mathbb{R}^3} v_i\, v_j\, \tilde{f}(v)\, dv - \delta_{i,j}\,, \tag{1.80}$$

$$\tilde{q}_i = \frac{1}{2} \int_{\mathbb{R}^3} v_i\, |v|^2\, \tilde{f}(v)\, dv \tag{1.81}$$

and (cf. (A.5))

$$\tilde{\gamma} = \int_{\mathbb{R}^3} |v|^4\, \tilde{f}(v)\, dv - 15 \tag{1.82}$$

are used. Note that

$$\int_{\mathbb{R}^3} \tilde{f}(v)\, dv = 1\,, \quad \int_{\mathbb{R}^3} v\, \tilde{f}(v)\, dv = 0\,, \quad \int_{\mathbb{R}^3} |v|^2\, \tilde{f}(v)\, dv = 3\,. \tag{1.83}$$

Using Lemma A.1, all integrals in (1.79a)-(1.79e) can be computed so that one obtains a system of equations for the parameters a, b, C, d and e

$$a + \operatorname{tr} C + 15\, e = 0\,, \tag{1.84a}$$

$$b_i + 5\, d_i = 0\,, \tag{1.84b}$$

$$a\, \delta_{i,j} + 2\, C_{i,j} + \operatorname{tr} C\, \delta_{i,j} + 35\, e\, \delta_{i,j} = \tilde{\tau}_{i,j}\,, \tag{1.84c}$$

$$5\, b_i + 35\, d_i = 2\, \tilde{q}_i\,, \tag{1.84d}$$

$$15\, a + 35 \operatorname{tr} C + 945\, e = \tilde{\gamma}\,, \tag{1.84e}$$

where $i, j = 1, 2, 3$. Note that

$$\sum_{k,l=1}^{3} C_{k,l} \int_{\mathbb{R}^3} v_i\, v_j\, v_k\, v_l\, M_{0,1}(v)\, dv = 2\, C_{i,j} \qquad \text{if} \quad i \neq j$$

and

$$\sum_{k,l=1}^{3} C_{k,l} \int_{\mathbb{R}^3} v_i^2 \, v_k \, v_l \, M_{0,1}(v) \, dv =$$

$$\sum_{k=1}^{3} C_{k,k} \int_{\mathbb{R}^3} v_i^2 \, v_k^2 \, M_{0,1}(v) \, dv = \sum_{k=1}^{3} C_{k,k} + 2 \, C_{i,i} \qquad \text{if} \quad i = j \, .$$

From (1.84b) and (1.84d) we immediately obtain

$$b_i = -\tilde{q}_i \, , \qquad d_i = \frac{1}{5} \, \tilde{q}_i \, , \qquad i = 1, 2, 3 \, . \tag{1.85}$$

Taking trace of the matrices in equation (1.84c) and using $\operatorname{tr} \tilde{\tau} = 0$ (cf. (1.83)), we obtain a linear system for the scalar parameters $a, \operatorname{tr} C$ and e,

$$\begin{pmatrix} 1 & 1 & 15 \\ 3 & 5 & 105 \\ 15 & 35 & 945 \end{pmatrix} \begin{pmatrix} a \\ \operatorname{tr} C \\ e \end{pmatrix} = \begin{pmatrix} 0 \\ 0 \\ \tilde{\gamma} \end{pmatrix} .$$

Thus these parameters are

$$a = \frac{1}{8} \, \tilde{\gamma} \, , \quad \operatorname{tr} C = -\frac{1}{4} \, \tilde{\gamma} \, , \quad e = \frac{1}{120} \, \tilde{\gamma} \, . \tag{1.86}$$

Using the equation (1.84c) we get

$$C_{i,j} = \frac{1}{2} \, \tilde{\tau}_{i,j} - \frac{\tilde{\gamma}}{12} \, \delta_{i,j} \, , \qquad i, j = 1, 2, 3 \, . \tag{1.87}$$

The function (1.76) is now entirely defined by (1.85)-(1.87).

According to (1.79a)-(1.79e) one obtains (cf. (1.78))

$$\begin{aligned} \int_{\mathbb{R}^3} \psi(v)^2 \, M_{0,1}(v) \, dv &= \sum_{i,j=1}^{3} C_{i,j} \, \tilde{\tau}_{i,j} + 2 \sum_{i=1}^{3} d_i \, \tilde{q}_i + e \, \tilde{\gamma} \\ &= \frac{1}{2} \sum_{i,j=1}^{3} \tilde{\tau}_{i,j}^2 - \frac{\tilde{\gamma}}{12} \sum_{i=1}^{3} \tilde{\tau}_{i,i} + \frac{2}{5} \sum_{i=1}^{3} \tilde{q}_i^2 + \frac{1}{120} \, \tilde{\gamma}^2 \\ &= \frac{1}{2} \, ||\tilde{\tau}||_F^2 + \frac{2}{5} \, |\tilde{q}|^2 + \frac{1}{120} \, \tilde{\gamma}^2 \, , \end{aligned} \tag{1.88}$$

where

$$||A||_F = \sqrt{\sum_{i,j=1}^{3} a_{i,j}^2} \tag{1.89}$$

denotes the Frobenius norm of a matrix A.

Finally we express the auxiliary quantities (1.80)-(1.82) through the standard macroscopic quantities (defined by the function f). Using (1.75) one obtains

$$\tilde{\tau}_{i,j} = \frac{1}{\varrho}\left(\frac{k\,T}{m}\right)^{\frac{3}{2}} \int_{\mathbb{R}^3} v_i\, v_j\, f\left(V + v\,\sqrt{k\,T/m}\right) dv - \delta_{i,j}$$
$$= \frac{1}{\varrho}\,\frac{m}{k\,T} \int_{\mathbb{R}^3} (v_i - V_i)\,(v_j - V_j)\, f(v)\, dv - \delta_{i,j} = \frac{1}{\varrho\, k\, T}\Big[P_{i,j} - p\,\delta_{i,j}\Big],$$

$$\tilde{q}_i = \frac{1}{\varrho}\left(\frac{k\,T}{m}\right)^{\frac{3}{2}} \frac{1}{2} \int_{\mathbb{R}^3} v_i\, |v|^2\, f\left(V + v\,\sqrt{k\,T/m}\right) dv$$
$$= \frac{1}{\varrho}\left(\frac{m}{k\,T}\right)^{\frac{3}{2}} \frac{1}{2} \int_{\mathbb{R}^3} (v_i - V_i)\, |v - V|^2\, f(v)\, dv = \frac{1}{\varrho\, k\, T}\left(\frac{m}{k\,T}\right)^{\frac{1}{2}} q_i$$

and

$$\tilde{\gamma} = \frac{1}{\varrho}\left(\frac{k\,T}{m}\right)^{\frac{3}{2}} \int_{\mathbb{R}^3} |v|^4\, f\left(V + v\,\sqrt{k\,T/m}\right) dv - 15$$
$$= \frac{1}{\varrho}\left(\frac{m}{k\,T}\right)^{2} \int_{\mathbb{R}^3} |v - V|^4\, f(v)\, dv - 15 = \frac{1}{\varrho}\left(\frac{m}{k\,T}\right)^{2} \gamma\,,$$

where

$$\gamma = \gamma(t,x) = \int_{\mathbb{R}^3} |v - V(t,x)|^4\, f(t,x,v)\, dv - 15\,\varrho(t,x)\left(\frac{k\,T(t,x)}{m}\right)^2. \quad (1.90)$$

Thus, according to (1.88), the quantity (1.78) takes the form (cf. (1.89))

$$Crit(t,x) = \frac{1}{\varrho\, k\, T}\left(\frac{1}{2}\,||P - p\,I||_F^2 + \frac{2\,m}{5\,k\,T}\,|q|^2 + \frac{m^4}{120\,k^2\,T^2}\,\gamma^2\right)^{1/2}. \quad (1.91)$$

The dimensionless function (1.91) will be used as a criterion of local equilibrium.

1.9 Scaling transformations

For different purposes it is reasonable to use some scaling for the Boltzmann equation in order to work with dimensionless variables and functions. Let

$$\varrho_0 > 0\,, \qquad V_0 > 0\,, \qquad X_0 > 0\,, \qquad t_0 = \frac{X_0}{V_0}$$

be the typical density, speed, length and time of the problem. According to (1.50), the typical speed is proportional to the square root of the typical temperature T_0, e.g., $V_0 = \sqrt{k\,T_0/m}$. Consider the dimensionless variables

$$\tilde{t} = \frac{t}{t_0}\,, \qquad \tilde{x} = \frac{x}{X_0}\,, \qquad \tilde{v} = \frac{v}{V_0}$$

and introduce the dimensionless function

$$\tilde f(\tilde t,\tilde x,\tilde v)=\tilde c\,f(t,x,v)\,,\qquad \tilde c=V_0^3\,\varrho_0^{-1}\,,$$

where ϱ_0 is the typical density (number per volume). One obtains

$$\begin{aligned}\frac{\partial}{\partial t}\,f(t,x,v)&=\frac{1}{\tilde c\,t_0}\,\frac{\partial}{\partial\tilde t}\,\tilde f(\tilde t,\tilde x,\tilde v)\,,\\ (v,\nabla_x)\,f(t,x,v)&=\frac{V_0}{\tilde c\,X_0}\,(\tilde v,\nabla_{\tilde x})\,\tilde f(\tilde t,\tilde x,\tilde v)=\frac{1}{\tilde c\,t_0}\,(\tilde v,\nabla_{\tilde x})\,\tilde f(\tilde t,\tilde x,\tilde v)\end{aligned}$$

and

$$\begin{aligned}&\int_{\mathbb{R}^3}\int_{\mathcal{S}^2}B(v,w,e)\times\\ &\quad\Big[f(t,x,v'(v,w,e))\,f(t,x,w'(v,w,e))-f(t,x,v)\,f(t,x,w)\Big]de\,dw\\ &=\frac{V_0^3}{\tilde c^2}\int_{\mathbb{R}^3}\int_{\mathcal{S}^2}B(v,w,e)\Big[\tilde f(\tilde t,\tilde x,V_0^{-1}\,v'(v,w,e))\,\tilde f(\tilde t,\tilde x,V_0^{-1}\,w'(v,w,e))-\\ &\qquad\tilde f(\tilde t,\tilde x,V_0^{-1}\,v)\,\tilde f(\tilde t,\tilde x,V_0^{-1}\,w)\Big]de\,d\tilde w\\ &=\frac{V_0^3}{\tilde c^2}\int_{\mathbb{R}^3}\int_{\mathcal{S}^2}B(v,w,e)\times\\ &\qquad\Big[\tilde f(\tilde t,\tilde x,v'(\tilde v,\tilde w,e))\,\tilde f(\tilde t,\tilde x,w'(\tilde v,\tilde w,e))-\tilde f(\tilde t,\tilde x,\tilde v)\,\tilde f(\tilde t,\tilde x,\tilde w)\Big]de\,d\tilde w\,.\end{aligned}$$

Thus, the new function satisfies

$$\begin{aligned}&\frac{\partial}{\partial\tilde t}\,\tilde f(\tilde t,\tilde x,\tilde v)+(\tilde v,\nabla_{\tilde x})\,\tilde f(\tilde t,\tilde x,\tilde v)=t_0\,\varrho_0\int_{\mathbb{R}^3}\int_{\mathcal{S}^2}B(V_0\,\tilde v,V_0\,\tilde w,e)\times\\ &\quad\Big[\tilde f(\tilde t,\tilde x,v'(\tilde v,\tilde w,e))\,\tilde f(\tilde t,\tilde x,w'(\tilde v,\tilde w,e))-\tilde f(\tilde t,\tilde x,\tilde v)\,\tilde f(\tilde t,\tilde x,\tilde w)\Big]de\,d\tilde w\,.\end{aligned}\tag{1.92}$$

Using the form (1.10) one obtains

$$B(V_0\,\tilde v,V_0\,\tilde w,e)=V_0\,|\tilde v-\tilde w|\,\frac{b(V_0\,|\tilde v-\tilde w|,\theta)}{\sin\theta}\,,\qquad\theta=\arccos\frac{(\tilde v-\tilde w,e)}{|\tilde v-\tilde w|}\,.$$

Taking into account the definition of the equilibrium mean free path (cf. (1.51))

$$L_0=\frac{1}{\sqrt{2}\,\pi\,d^2\,\varrho_0}$$

and of the **Knudsen number**

$$\mathrm{Kn}=\frac{L_0}{X_0}\,,\tag{1.93}$$

equation (1.92) is transformed into

$$\frac{\partial}{\partial \tilde{t}}\,\tilde{f}(\tilde{t},\tilde{x},\tilde{v}) + (\tilde{v},\nabla_{\tilde{x}})\,\tilde{f}(\tilde{t},\tilde{x},\tilde{v}) = \frac{1}{\mathrm{Kn}}\int_{\mathbb{R}^3}\int_{\mathcal{S}^2}\tilde{B}(\tilde{v},\tilde{w},e)\times \tag{1.94}$$
$$\Big[\tilde{f}(\tilde{t},\tilde{x},v'(\tilde{v},\tilde{w},e))\,\tilde{f}(\tilde{t},\tilde{x},w'(\tilde{v},\tilde{w},e)) - \tilde{f}(\tilde{t},\tilde{x},\tilde{v})\,\tilde{f}(\tilde{t},\tilde{x},\tilde{w})\Big]\,de\,d\tilde{w}\,.$$

where the collision kernel has the form

$$\tilde{B}(\tilde{v},\tilde{w},e) = \frac{|\tilde{v}-\tilde{w}|}{\sqrt{2}\,\pi\,d^2}\,\frac{\tilde{b}(|\tilde{v}-\tilde{w}|,\theta)}{\sin\theta}\,,\qquad \theta = \arccos\frac{(\tilde{v}-\tilde{w},e)}{|\tilde{v}-\tilde{w}|}\,,$$

with

$$\tilde{b}(|\tilde{v}-\tilde{w}|,\theta) = b(V_0\,|\tilde{v}-\tilde{w}|,\theta)\,.$$

Note that $\tilde{B}$ is dimensionless.

In the hard sphere case the **scaled Boltzmann equation** (1.94) takes the form (cf. (1.28))

$$\frac{\partial}{\partial t}\,f(t,x,v) + (v,\nabla_x)\,f(t,x,v) = \tag{1.95}$$
$$\frac{1}{4\sqrt{2}\pi\,\mathrm{Kn}}\int_{\mathbb{R}^3}\int_{\mathcal{S}^2}|v-w|\Big[f(t,x,v')\,f(t,x,w') - f(t,x,v)\,f(t,x,w)\Big]\,de\,dw\,,$$

where v', w' are defined in (1.6), or (cf. (1.18))

$$\frac{\partial}{\partial t}\,f(t,x,v) + (v,\nabla_x)\,f(t,x,v) = \frac{1}{2\sqrt{2}\pi\,\mathrm{Kn}}\times$$
$$\int_{\mathbb{R}^3}\int_{\mathcal{S}^2}|(e,v-w)|\Big[f(t,x,v^*)\,f(t,x,w^*) - f(t,x,v)\,f(t,x,w)\Big]\,de\,dw\,,$$

where v^* and w^* are defined in (1.12).

1.10 Comments and bibliographic remarks

Section 1.1

The Boltzmann equation (1.3) first appeared in [36]. The history of kinetic theory and, in particular, of Boltzmann's contributions is described in [49].

Section 1.2

Fig. 1.1 has been adapted from [82]. Both collision transformations (1.6) and (1.12) are used in the literature. Though equivalent, one of them may be preferable in a certain context. As we will see later, (1.6) is slightly more convenient for numerical purposes, since the corresponding distribution of the direction vector e is uniform (cf. (1.29)), while depending on the relative velocity (cf. (1.30)) in the case of (1.12).

Section 1.3

A discussion of soft and hard interactions can be found, for example, in [60] and [48, Sect. 2.4, 2.5]. The notion of "Maxwell molecules" refers to a paper by Maxwell in 1866, according to [48, p.71]. The variable diameter hard sphere model was introduced in [23] in order to correct the non-realistic temperature dependence of the viscosity coefficient in the hard sphere model, while keeping its main advantages such as the finite total cross-section and the isotropic scattering. There are further models for collision kernels and differential cross-sections in the literature, e.g., in [25], [78], [113], [114].

Section 1.4

First studies of boundary conditions for the Boltzmann equation go back to Maxwell 1879 (cf. [48, p.118, Ref. 11]). Concerning a more detailed discussion of boundary conditions we refer to [51, Ch. 8], [48, Ch. III], [25, Sect. 4.5]. A rather intuitive interpretation of boundary conditions will be given in Chapter 2 on the basis of stochastic models.

Section 1.5

The measurement data were taken from [131] and [40]. Concerning the mean free path, the following simple argument is given in [48, p.19]: On average there is only one other molecule in the cylinder of base πd^2 and height L so that $\varrho \pi d^2 L \sim 1$ and $L \sim 1/(\varrho \pi d^2)$. Formula (1.51) has been taken from [25, p.91]. Note that $L >> d$ is an assumption for the validity of the equation. Concerning the speed of sound, we refer to [48, p.233] and [25, pp.25, 64, 82, 165].

Section 1.6

The first discussion on collision invariants is due to Boltzmann himself. Later the problem was addressed by many authors. The corresponding references and a proof of Lemma 1.12 are given in [51, p.36]. In the non-homogeneous case the situation with the H-functional is more complicated. The corresponding discussion can be found in [51, p.51]. The curve in Fig. 1.2 was obtained in [100] using a conservative deterministic scheme for the Boltzmann equation and an adaptive trapezoid quadrature for the integral (1.64).

Section 1.7

Concerning closure relations we refer to [48, p.85]. Note the remark from [25, p.186]: "from the kinetic theory point of view, both the Euler and Navier-Stokes equations may be regarded as 'five moment' solutions of the Boltzmann equation, the former being valid for the Kn $\to$ 0 limit and the latter for Kn $<<$ 1."

Section 1.8

The problem of detecting local equilibrium using some macroscopic quantities was discussed by several authors. In [123] the quantity (criterion)

$$Crit(t,x) = \frac{c}{T(t,x)} \, ||P(t,x) - p(t,x)\, I||_F$$

was derived on the basis of physical intuition. In [135], [38] the heat flux based criterion

$$Crit(t,x) = \frac{c}{T(t,x)^{3/2}} \, |q(t,x)|$$

was used. Here $c > 0$ denotes some constant. Note that the functional (1.91) uses only moments of the function f so that it can be computed using stochastic numerics. The question how to decide where the hydrodynamic description is sufficient and how to couple the numerical procedures for the Boltzmann and Euler equations was investigated by a number of authors [37], [74], [101], [103], [117], [102], [199], [200], [201], [168].

Section 1.9

The dimensionless Knudsen number (cf. [107]) defined in (1.93) describes the degree of rarefaction of a gas. For small Knudsen numbers the collisions between particles become dominating.

2

Related Markov processes

2.1 Boltzmann type piecewise-deterministic Markov processes

A piecewise-deterministic Markov process is a jump process that changes its state in a deterministic way between jumps. Here we introduce a class of piecewise-deterministic Markov processes related to Boltzmann type equations. The processes describe the behavior of a system of particles. Each particle is characterized by its position, velocity and weight. The number of particles in the system is variable.

2.1.1 Free flow and state space

Consider the system of ordinary differential equations

$$\frac{d}{dt}\, x(t) = v(t)\,, \qquad \frac{d}{dt}\, v(t) = \mathcal{E}(x(t))\,, \qquad t \geq 0\,, \tag{2.1}$$

with initial condition

$$x(0) = x\,, \qquad v(0) = v\,, \qquad x, v \in \mathbb{R}^3\,. \tag{2.2}$$

Assume the force term $\mathcal{E}$ is globally Lipschitz continuous so that no explosion occurs. The unique solution $X(t,x,v), V(t,x,v)$ of (2.1), (2.2) is called **free flow** and determines the behavior of the particles between jumps. In the special case $\mathcal{E} = 0$ one obtains

$$X(t,x,v) = x + t\,v\,, \qquad V(t,x,v) = v\,, \qquad t \geq 0\,.$$

Note that t, x and v are dimensionless variables.

We first define the state space of a single particle. Denote by

$$\partial_{in}\left(D \times \mathbb{R}^3\right) = \tag{2.3}$$
$$\left\{(x,v) \in \partial D \times \mathbb{R}^3 \,:\, X(s,x,v) \in D\,, \quad \forall s \in (0,t)\,, \quad \text{for some } t > 0\right\}$$

the part of the boundary from which the free flow goes inside the domain D, and by

$$\partial_{out}\left(D\times\mathbb{R}^3\right)= \tag{2.4}$$
$$\Big\{(x,v)\in\partial D\times\mathbb{R}^3\,:\,X(-s,x,v)\in D\,,\quad \forall s\in(0,t)\,,\quad \text{for some } t>0\Big\}$$

the part of the boundary at which the free flow goes outside the domain. The state space of a single particle is

$$E_1=\tilde{E}_1\times(0,\infty)\,, \tag{2.5}$$

where

$$\tilde{E}_1=\left(D\times\mathbb{R}^3\right)\cup\Big(\partial_{in}\left(D\times\mathbb{R}^3\right)\setminus\partial_{out}\left(D\times\mathbb{R}^3\right)\Big). \tag{2.6}$$

It is the open set $D\times\mathbb{R}^3\times(0,\infty)$ extended by some part of its boundary, which is characterized by the free flow.

The state space of the process is

$$E=\bigcup_{\nu=1}^{\infty}(E_1)^{\nu}\cup\{(0)\}\,.$$

Elements of E are denoted by

$$z=(\nu,\zeta)\,:\quad \nu=1,2,\dots\,,\quad \zeta=(x_1,v_1,g_1;\dots;x_\nu,v_\nu,g_\nu)\,, \tag{2.7}$$

and (0) is the zero-state of the system. Define a metric ϱ on E in such a way that

$$\lim_{n\to\infty}\varrho((\nu_n,\zeta_n),(\nu,\zeta))=0\iff$$
$$\exists\, l\,:\,\nu_n=\nu\,,\ \forall\, n\geq l\quad\text{and}\quad\lim_{k\to\infty}\zeta_{l+k}=\zeta\text{ in }\mathbb{R}^{7\nu}\,.$$

2.1.2 Construction of sample paths

For $z=(\nu,\zeta)\in E$ (cf. (2.7)) define the **exit time**

$$t_*(z)=\min_{1\leq i\leq\nu}\bar{t}_*(x_i,v_i)\,, \tag{2.8}$$

where (cf. (2.6))

$$\bar{t}_*(x,v)=\begin{cases}\inf\{t>0\,:\,X(t,x,v)\in\partial D\}\,,\\ \infty\,,\quad\text{if no such time exists}\,,\end{cases}\qquad\text{for}\quad(x,v)\in\tilde{E}_1\,.$$

Introduce the set of exit states

$$\Gamma=\Big\{(\nu,\zeta)\,:\,\zeta=\mathcal{X}_\nu(t_*(\nu,\zeta'),\zeta')\,,\ \text{for some }(\nu,\zeta')\in E\Big\}, \tag{2.9}$$

where

$$\mathcal{X}_\nu(t,\zeta) = \Big(X(t,x_1,v_1), V(t,x_1,v_1), g_1; \ldots; X(t,x_\nu,v_\nu), V(t,x_\nu,v_\nu), g_\nu\Big). \tag{2.10}$$

Consider a kernel Q mapping E into $\mathcal{M}(E)$, a rate function

$$\lambda(z) = Q(z,E)\,, \tag{2.11}$$

and a kernel $Q_{\rm ref}$ mapping Γ into the set of probability measures on $(E,\mathcal{B}(E))$.

Starting at z, the particles move according to the free flow,

$$Z(t) = \mathcal{X}_\nu(t,\zeta)\,, \qquad t < \tau_1\,. \tag{2.12}$$

The random **jump time** τ_1 satisfies (cf. (2.8))

$$\mathrm{Prob}(\tau_1 > t) = \chi_{[0,t_*(z))}(t)\, \exp\left(-\int_0^t \lambda(\nu, \mathcal{X}_\nu(s,\zeta))\, ds\right), \quad t \geq 0\,. \tag{2.13}$$

Note that $\tau_1 \leq t_*(z)$ and

$$\mathrm{Prob}(\tau_1 = t_*(z)) = \exp\left(-\int_0^{t_*(z)} \lambda(\nu, \mathcal{X}_\nu(s,\zeta))\, ds\right).$$

At time τ_1 the process jumps into a state z_1. This state is distributed according to the **transition measure**

$$\begin{cases} \lambda(\bar z)^{-1} Q(\bar z, dz_1)\,, & \text{if} \quad \tau_1 < t_*(z)\,, \\ Q_{\rm ref}(\bar z, dz_1) \quad , & \text{if} \quad \tau_1 = t_*(z)\,, \end{cases} \tag{2.14}$$

where $\bar z = \mathcal{X}_\nu(\tau_1,\zeta)$. Then the construction is repeated with z_1 replacing z, and τ_2 replacing τ_1.

It is assumed that, for every $z \in E$, the mean number of jumps on finite time intervals is finite, i.e.

$$\mathbb{E} \sum_{k=1}^{\infty} \chi_{[0,S]}(\tau_k) < \infty\,, \qquad \forall\, S \geq 0\,. \tag{2.15}$$

2.1.3 Jump behavior

The system performs jumps of two different types, corresponding to the cases $\bar z \in E$ and $\bar z \in \Gamma$ in (2.14).

Jumps of type A occur while the system is in the state space and would stay there for a non-zero time interval. These (un-enforced) jumps are generated by the rate function (2.11). Examples are

- collisions of particles (type A1),

- scattering of particles (type A2),
- death (annihilation, absorption) of particles (type A3),
- birth (creation) of new particles (type A4).

Jumps of type B occur when the system is about to leave the state space. These (enforced) jumps are caused by the free flow hitting the boundary. Examples are

- reflection of particles at the boundary,
- absorption (outflow) of particles at the boundary.

Jumps of type A

We consider a kernel of the form

$$Q(z;d\tilde{z}) = Q_{\mathrm{coll}}(z;d\tilde{z}) + Q_{\mathrm{scat}}(z;d\tilde{z}) + Q_{-}(z;d\tilde{z}) + Q_{+}(z;d\tilde{z})\,, \tag{2.16}$$

where $z \in E$ (cf. (2.7)). We describe the jumps by some deterministic transformation depending on random parameters.

A1: Collisions of particles

The basic jump transformation is

$$[J_{\mathrm{coll}}(z;i,j,\theta)]_k = \begin{cases} (x_k, v_k, g_k) & \text{, if} \quad k \le \nu\,,\ k \ne i,j\,, \\ (x_{\mathrm{coll}}, v_{\mathrm{coll}}, \gamma_{\mathrm{coll}}(z;i,j,\theta)) & \text{, if} \quad k = i\,, \\ (y_{\mathrm{coll}}, w_{\mathrm{coll}}, \gamma_{\mathrm{coll}}(z;i,j,\theta)) & \text{, if} \quad k = j\,, \\ (x_i, v_i, g_i - \gamma_{\mathrm{coll}}(z;i,j,\theta)) & \text{, if} \quad k = \nu+1\,, \\ (x_j, v_j, g_j - \gamma_{\mathrm{coll}}(z;i,j,\theta)), & \text{if} \quad k = \nu+2\,, \end{cases} \tag{2.17}$$

where θ belongs to some parameter set Θ_{coll}, and the functions $x_{\mathrm{coll}}, v_{\mathrm{coll}}$, $y_{\mathrm{coll}}, w_{\mathrm{coll}}$ depend on the arguments $(x_i, v_i, x_j, v_j, \theta)$. The weight transfer function should satisfy

$$0 \le \gamma_{\mathrm{coll}}(z;i,j,\theta) \le \min(g_i, g_j)\,, \tag{2.18}$$

in order to keep the weights non-negative. The kernel

$$Q_{\mathrm{coll}}(z;d\tilde{z}) = \frac{1}{2} \sum_{1 \le i \ne j \le \nu} \int_{\Theta_{\mathrm{coll}}} \delta_{J_{\mathrm{coll}}(z;i,j,\theta)}(d\tilde{z})\, p_{\mathrm{coll}}(z;i,j,d\theta)\,, \tag{2.19}$$

which is concentrated on $(E_1)^{\nu} \cup (E_1)^{\nu+1} \cup (E_1)^{\nu+2}$ (cf. (2.5)), is a mixture of Dirac measures. Particles with weight zero are removed from the system.

A2: Scattering of particles

The basic jump transformation is

$$[J_{\mathrm{scat}}(z;i,\theta)]_j = \begin{cases} (x_j, v_j, g_j) & , \quad \text{if} \quad j \neq i\,, \\ (x_{\mathrm{scat}}, v_{\mathrm{scat}}, \gamma_{\mathrm{scat}}(z;i,\theta))\,, & \text{if} \quad j = i\,, \end{cases} \tag{2.20}$$

where θ belongs to some parameter set Θ_{scat}, and the functions $x_{\mathrm{scat}}, v_{\mathrm{scat}}$ depend on the arguments (x_i, v_i, θ). The weight transfer function γ_{scat} is strictly positive. The kernel

$$Q_{\mathrm{scat}}(z; d\tilde{z}) = \sum_{i=1}^{\nu} \int_{\Theta_{\mathrm{scat}}} \delta_{J_{\mathrm{scat}}(z;i,\theta)}(d\tilde{z})\, p_{\mathrm{scat}}(z; i, d\theta) \tag{2.21}$$

is concentrated on $(E_1)^{\nu}$.

A3: Annihilation of particles

The basic jump transformation is

$$[J_-(z;i)]_j = \begin{cases} (x_j, v_j, g_j) & , \quad \text{if} \quad j \neq i\,, \\ (x_i, v_i, g_i - \gamma_-(z;i))\,, & \text{if} \quad j = i\,. \end{cases}$$

The weight transfer function should satisfy

$$0 \leq \gamma_-(z;i) \leq g_i\,,$$

in order to keep the weights non-negative. The kernel

$$Q_-(z; d\tilde{z}) = \sum_{i=1}^{\nu} \delta_{J_-(z;i)}(d\tilde{z})\, p_-(z;i) \tag{2.22}$$

is concentrated on $(E_1)^{\nu-1} \cup (E_1)^{\nu}$. Particles with weight zero are removed from the system.

A4: Creation of new particles

The basic jump transformation is

$$[J_+(z;x,v)]_j = \begin{cases} (x_j, v_j, g_j) & , \quad \text{if} \quad j \leq \nu\,, \\ (x, v, \gamma_+(z;x,v))\,, & \text{if} \quad j = \nu + 1\,, \end{cases} \tag{2.23}$$

where $(x, v) \in \tilde{E}_1$ (cf. (2.6)). The weight transfer function γ_+ is strictly positive. The kernel

$$Q_+(z; d\tilde{z}) = \int_{\tilde{E}_1} \delta_{J_+(z;x,v)}(d\tilde{z})\, p_+(z; dx, dv) \tag{2.24}$$

is concentrated on $(E_1)^{\nu+1}$.

Jumps of type B

Here we consider the reflection of particles at the boundary (including absorption, or outflow). Let $z \in \Gamma$ (cf. (2.9)) and define

$$I(z) = \{i = 1, \dots, \nu \,:\, x_i \in \partial D\}\,.$$

Note that (cf. (2.4))

$$I(z) \neq \emptyset\,, \qquad (x_i, v_i) \in \partial_{out}\left(D \times \mathbb{R}^3\right),\ \forall\, i \in I(z)\,, \qquad x_i \in D\,,\ \forall\, i \notin I(z)\,.$$

Particles (x_i, v_i, g_i) with $i \notin I(z)$ remain unchanged. Particles (x_i, v_i, g_i) with $i \in I(z)$ are treated independently, according to some reflection kernel that satisfies (cf. (2.6))

$$p_{\mathrm{ref}}(x, v, g; \tilde{E}_1) \leq 1\,, \qquad \forall\,(x, v) \in \partial_{out}\left(D \times \mathbb{R}^3\right), \quad g > 0\,. \tag{2.25}$$

Namely, these particles disappear with the absorption probability

$$1 - p_{\mathrm{ref}}(x_i, v_i, g_i; \tilde{E}_1)\,. \tag{2.26}$$

With probability $p_{\mathrm{ref}}(x_i, v_i, g_i; \tilde{E}_1)$, they are reflected (jump into (y, w)) according to the distribution

$$\frac{1}{p_{\mathrm{ref}}(x_i, v_i, g_i; \tilde{E}_1)}\, p_{\mathrm{ref}}(x_i, v_i, g_i; dy, dw)\,, \tag{2.27}$$

and obtain weight $\gamma_{\mathrm{ref}}(x_i, v_i, g_i; y, w)$.

The formal description is as follows. The basic jump transformation is

$$[J_{\mathrm{ref}}(z; \alpha)]_j = \tag{2.28}$$
$$\begin{cases} (x_j, v_j, g_j) & , \quad \text{if} \quad j \notin I(z)\,, \\ (x_j, v_j, 0) & , \quad \text{if} \quad j \in I(z)\,,\ \alpha_j = 0\,, \\ (y_j, w_j, \gamma_{\mathrm{ref}}(x_j, v_j, g_j; y_j, w_j)) & , \quad \text{if} \quad j \in I(z)\,,\ \alpha_j = (y_j, w_j)\,, \end{cases}$$

where $\alpha \in \left(\{0\} \cup \tilde{E}_1\right)^{I(z)}$. The weight transfer function γ_{ref} is non-negative. The transition measure

$$Q_{\mathrm{ref}}(z; d\tilde{z}) = \int_{\{\alpha\}} \delta_{J_{\mathrm{ref}}(z;\alpha)}(d\tilde{z}) \prod_{j \in I(z)} \Big[\delta_0(d\alpha_j)\Big[1 - p_{\mathrm{ref}}(x_j, v_j, g_j; \tilde{E}_1)\Big] + \int_{\tilde{E}_1} \delta_{(y_j, w_j)}(d\alpha_j)\, p_{\mathrm{ref}}(x_j, v_j, g_j; dy_j, dw_j)\Big] \tag{2.29}$$

is concentrated on $(E_1)^{\nu} \cup \ldots \cup (E_1)^{\nu - \nu'}$, where ν' is the number of elements in the set $I(z)$. If only one particle hits the boundary at the same time, i.e. $I(z) = \{i\}$, then the transition measure (2.29) takes the form

$$Q_{\mathrm{ref}}(z; d\tilde{z}) = \delta_{J_{\mathrm{ref}}(z;0)}(d\tilde{z})\Big[1 - p_{\mathrm{ref}}(x_i, v_i, g_i; \tilde{E}_1)\Big] + \int_{\tilde{E}_1} \delta_{J_{\mathrm{ref}}(z;y,w)}(d\tilde{z})\, p_{\mathrm{ref}}(x_i, v_i, g_i; dy, dw)\,.$$

Particles with weight zero are removed from the system.

2.1.4 Extended generator

The extended generator of the process takes the form

$$\begin{aligned}\mathcal{A}\,\Phi(z) = &\sum_{i=1}^{\nu} \big(v_i, \nabla_{x_i}\big)\,\Phi(z) + \sum_{i=1}^{\nu} \big(\mathcal{E}(x_i), \nabla_{v_i}\big)\,\Phi(z) + \\ &\frac{1}{2} \sum_{1\le i\ne j\le \nu} \int_{\Theta_{\mathrm{coll}}} \Big[\Phi(J_{\mathrm{coll}}(z;i,j,\theta)) - \Phi(z)\Big] p_{\mathrm{coll}}(z;i,j,d\theta) \\ &+ \sum_{i=1}^{\nu} \int_{\Theta_{\mathrm{scat}}} \Big[\Phi(J_{\mathrm{scat}}(z;i,\theta)) - \Phi(z)\Big] p_{\mathrm{scat}}(z;i,d\theta) \\ &+ \sum_{i=1}^{\nu} \Big[\Phi(J_{-}(z;i)) - \Phi(z)\Big] p_{-}(z;i) \\ &+ \int_{\tilde{E}_1} \Big[\Phi(J_{+}(z;x,v)) - \Phi(z)\Big] p_{+}(z;dx,dv)\,. \end{aligned} \tag{2.30}$$

The domain of the generator contains functions Φ on E satisfying several conditions. We specify these conditions (in terms of φ) for functions of the form

$$\Phi(z) = \sum_{j=1}^{\nu} g_j\,\varphi(x_j, v_j)\,, \qquad \Phi_0 = 0\,, \tag{2.31}$$

which will be of special interest in the next section. Note that (cf. (2.10))

$$\Phi(\nu, \mathcal{X}_\nu(t,\zeta)) = \sum_{j=1}^{\nu} g_j\,\varphi(X(t,x_j,v_j), V(t,x_j,v_j))\,. \tag{2.32}$$

Condition 1 The functions are differentiable along the flow,

$$\exists\, \frac{d}{dt}\,\Phi(\nu, \mathcal{X}_\nu(t,\zeta))\Big|_{t=0}\,, \qquad \forall\,(\nu,\zeta) \in E\,.$$

According to (2.32), this condition is fulfilled for functions of the form (2.31) provided that

$$\exists\, \frac{d}{dt}\,\varphi(X(t,x,v), V(t,x,v))\Big|_{t=0}\,, \qquad \forall\,(x,v) \in \tilde{E}_1\,. \tag{2.33}$$

Condition 2 The functions can be continuously extended to the outgoing boundary,

$$\exists \lim_{t\searrow 0}\, \Phi(\nu, \mathcal{X}_\nu(-t,\zeta)) =: \Phi(\nu,\zeta)\,, \qquad \forall\,(\nu,\zeta) \in \Gamma\,.$$

According to (2.32), this condition is fulfilled for functions of the form (2.31) provided that

$$\exists \lim_{t\searrow 0} \varphi(X(-t,x,v),V(-t,x,v)) =: \varphi(x,v)\,, \qquad \forall\, x\in\partial D\,,\ v\in\mathbb{R}^3_{\rm out}(x)\,. \tag{2.34}$$

Boundary condition The functions satisfy

$$\Phi(z) = \int_E \Phi(\tilde z)\, Q_{\rm ref}(z,d\tilde z)\,, \qquad \forall\, z\in\Gamma\,.$$

With (2.29), this condition takes the form

$$\Phi(z) = \int_{\{\alpha\}} \Phi(J_{\rm ref}(z;\alpha)) \prod_{j\in I(z)} \Big[\delta_0(d\alpha_j)\Big[1-p_{\rm ref}(x_j,v_j,g_j;\tilde E_1)\Big] + \int_{\tilde E_1} \delta_{(y_j,w_j)}(d\alpha_j)\, p_{\rm ref}(x_j,v_j,g_j;dy_j,dw_j)\Big]\,. \tag{2.35}$$

Taking into account (2.28) and considering functions of the form (2.31), one obtains that condition (2.35) is fulfilled if

$$\begin{aligned}
&\sum_{j=1}^{\nu} g_j\,\varphi(x_j,v_j) = \sum_{j=1}^{\nu}\Phi_j(z) = \sum_{j\notin I(z)} g_j\,\varphi(x_j,v_j) + \\
&\quad \sum_{j\in I(z)} \int_{\{0\}\cup\tilde E_1} \Phi_j(J_{\rm ref}(z;\alpha))\Big[\delta_0(d\alpha_j)\Big[1-p_{\rm ref}(x_j,v_j,g_j;\tilde E_1)\Big] + \\
&\qquad \int_{\tilde E_1} \delta_{(y,w)}(d\alpha_j)\, p_{\rm ref}(x_j,v_j,g_j;dy,dw)\Big] \\
&= \sum_{j\notin I(z)} g_j\,\varphi(x_j,v_j) + \\
&\quad \sum_{j\in I(z)} \int_{\tilde E_1} \varphi(y,w)\,\gamma_{\rm ref}(x_j,v_j,g_j;y,w)\, p_{\rm ref}(x_j,v_j,g_j;dy,dw)\,.
\end{aligned} \tag{2.36}$$

Finally, condition (2.36) reduces to (cf. (2.6))

$$\varphi(x,v) = \int_{\tilde E_1} \varphi(y,w)\,\frac{\gamma_{\rm ref}(x,v,g;y,w)}{g}\, p_{\rm ref}(x,v,g;dy,dw)\,, \qquad \forall\,(x,v)\in\partial_{out}\left(D\times\mathbb{R}^3\right),\quad g>0\,. \tag{2.37}$$

Condition 3 The functions satisfy

$$\mathbb{E}\sum_k \chi_{[0,S]}(\tau_k)\,|\Phi(Z(\tau_k)) - \Phi(Z(\tau_k-))| < \infty\,, \qquad \forall\, S\ge 0\,, \tag{2.38}$$

i.e., for the process $\Phi(Z(t))$, the mean sum of absolute jump widths on finite time intervals is finite.

For the functions satisfying the above conditions, one obtains that

$$\Phi(Z(t)) - \Phi(Z(0)) - \int_0^t \mathcal{A}\,\Phi(Z(s))\,ds\,, \qquad t \geq 0\,, \tag{2.39}$$

is a martingale, uniformly integrable on any finite time interval.

Example 2.1. Consider the special case of a deterministic process, when $\lambda = 0$ (cf. (2.11)) and $D = \mathbb{R}^3$. The process takes the form

$$Z(t) = \mathcal{X}_\nu(t,\zeta)\,, \qquad t \geq 0\,, \qquad\qquad Z(0) = (\nu,\zeta)\,,$$

and satisfies

$$\frac{d}{dt}\,\Phi(Z(t)) = \sum_{i=1}^{\nu} (v_i, \nabla_{x_i})\,\Phi(Z(t)) + \sum_{i=1}^{\nu} (\mathcal{E}(x_i), \nabla_{v_i})\,\Phi(Z(t))\,,$$

for any continuously differentiable Φ.

2.2 Heuristic derivation of the limiting equation

2.2.1 Equation for measures

Let the process depend on some parameter n. We consider functions Φ of the form (2.31) belonging to the domain of the generator. According to (2.39), one obtains the representation

$$\int_{\tilde{E}_1} \varphi(x,v)\,\mu^{(n)}(t,dx,dv) = \tag{2.40}$$
$$\int_{\tilde{E}_1} \varphi(x,v)\,\mu^{(n)}(0,dx,dv) + \int_0^t \mathcal{A}^{(n)}\Phi(Z^{(n)}(s))\,ds + M^{(n)}(\varphi,t)\,,$$

where

$$\mu^{(n)}(t,dx,dv) = \sum_{j=1}^{\nu(t)} g_j(t)\,\delta_{x_j(t)}(dx)\,\delta_{v_j(t)}(dv)\,, \qquad t \geq 0\,, \tag{2.41}$$

is the **empirical measure** of the process and $M^{(n)}$ denotes a martingale term. The generator (2.30) takes the form

$$(\mathcal{A}^{(n)}\Phi)(z) = \tag{2.42}$$
$$\sum_{j=1}^{\nu} g_j\,(v_j, \nabla_{x_j})\,\varphi(x_j,v_j) + \sum_{i=1}^{\nu} g_j\,(\mathcal{E}(x_i), \nabla_{v_i})\,\varphi(x_j,v_j) +$$

$$
\begin{aligned}
&\frac{1}{2}\sum_{1\le i\ne j\le \nu}\int_{\Theta_{\rm coll}}\gamma^{(n)}_{\rm coll}(z;i,j,\theta)\,\times\\
&\Big[\varphi(x_{\rm coll},v_{\rm coll})+\varphi(y_{\rm coll},w_{\rm coll})-\varphi(x_i,v_i)-\varphi(x_j,v_j)\Big]p^{(n)}_{\rm coll}(z;i,j,d\theta)\\
&+\sum_{i=1}^{\nu}\int_{\Theta_{\rm scat}}\Big[\gamma^{(n)}_{\rm scat}(z;i,\theta)\,\varphi(x_{\rm scat},v_{\rm scat})-g_i\,\varphi(x_i,v_i)\Big]p^{(n)}_{\rm scat}(z;i,d\theta)\\
&+\sum_{i=1}^{\nu}\Big[-\gamma^{(n)}_{-}(z;i)\,\varphi(x_i,v_i)\,p^{(n)}_{-}(z;i)\Big]\\
&+\int_{\tilde E_1}\gamma^{(n)}_{+}(z;x,v)\,\varphi(x,v)\,p^{(n)}_{+}(z;dx,dv)\,.
\end{aligned}
$$

Assume

$$
\gamma^{(n)}_{\rm coll}(z;i,j,\theta)\,p^{(n)}_{\rm coll}(z;i,j,d\theta)=q^{(n)}_{\rm coll}(x_i,v_i,x_j,v_j,d\theta)\,g_i\,g_j\,, \tag{2.43}
$$

$$
\gamma^{(n)}_{\rm scat}(z;i,\theta)\,p^{(n)}_{\rm scat}(z;i,d\theta)=q_{\rm scat}(x_i,v_i,d\theta)\,g_i\,, \tag{2.44}
$$

$$
p^{(n)}_{\rm scat}(z;i,\Theta_{\rm scat})=q_{\rm scat}(x_i,v_i,\Theta_{\rm scat})\,, \tag{2.45}
$$

$$
\gamma^{(n)}_{-}(z;i)\,p^{(n)}_{-}(z;i)=g_i\,q_{-}(x_i,v_i) \tag{2.46}
$$

and

$$
\gamma^{(n)}_{+}(z;x,v)\,p^{(n)}_{+}(z;dx,dv)=q_{+}(dx,dv)\,. \tag{2.47}
$$

Then (2.42) implies

$$
\begin{aligned}
(\mathcal{A}^{(n)}\,\Phi)(Z^{(n)}(s))&=\int_{\tilde E_1}\big(v,\nabla_x\big)\,\varphi(x,v)\,\mu^{(n)}(s,dx,dv)+\\
&\int_{\tilde E_1}\big(\mathcal{E}(x),\nabla_v\big)\,\varphi(x,v)\,\mu^{(n)}(s,dx,dv)\\
&+\frac{1}{2}\int_{\tilde E_1}\int_{\tilde E_1}\int_{\Theta_{\rm coll}}\Big[\varphi(x_{\rm coll}(x,v,y,w,\theta),v_{\rm coll}(x,v,y,w,\theta))+\\
&\varphi(y_{\rm coll}(x,v,y,w,\theta),w_{\rm coll}(x,v,y,w,\theta))-\varphi(x,v)-\varphi(y,w)\Big]\times\\
&q^{(n)}_{\rm coll}(x,v,y,w,d\theta)\,\mu^{(n)}(s,dx,dv)\,\mu^{(n)}(s,dy,dw)+R^{(n)}(\varphi,s)\\
&+\int_{\tilde E_1}\int_{\Theta_{\rm scat}}\Big[\varphi(x_{\rm scat}(x,v,\theta),v_{\rm scat}(x,v,\theta))-\varphi(x,v)\Big]\times\\
&q_{\rm scat}(x,v,d\theta)\,\mu^{(n)}(s,dx,dv)\\
&-\int_{\tilde E_1}\varphi(x,v)\,q_{-}(x,v)\,\mu^{(n)}(s,dx,dv)+\int_{\tilde E_1}\varphi(x,v)\,q_{+}(dx,dv)\,.
\end{aligned} \tag{2.48}
$$

Here $R^{(n)}(\varphi, s)$ denotes the remainder corresponding to summation of equal indices in the double sum of the collision term.

Assume that

$$\lim_{n\to\infty} q_{\rm coll}^{(n)}(x, v, y, w, d\theta) = q_{\rm coll}(x, v, y, w, d\theta) \tag{2.49}$$

and let the martingale term $M^{(n)}$ and the remainder $R^{(n)}$ vanish as $n \to \infty$. If the empirical measures (2.41) converge to some deterministic limit, i.e.

$$\lim_{n\to\infty} \mu^{(n)}(t) = F(t)\,, \qquad \forall\, t \geq 0\,,$$

then one obtains from (2.40) and (2.48) the limiting equation for measures (cf. (2.6)),

$$\begin{aligned}
&\frac{d}{dt}\int_{\tilde{E}_1} \varphi(x,v)\, F(t,dx,dv) = \qquad (2.50)\\
&\quad \int_{\tilde{E}_1} (v, \nabla_x)\, \varphi(x,v)\, F(t,dx,dv) + \int_{\tilde{E}_1} (\mathcal{E}(x), \nabla_v)\, \varphi(x,v)\, F(t,dx,dv)\\
&+ \frac{1}{2}\int_{\tilde{E}_1}\int_{\tilde{E}_1}\int_{\Theta_{\rm coll}} \Big[\varphi(x_{\rm coll}(x,v,y,w,\theta), v_{\rm coll}(x,v,y,w,\theta)) +\\
&\qquad \varphi(y_{\rm coll}(x,v,y,w,\theta), w_{\rm coll}(x,v,y,w,\theta)) - \varphi(x,v) - \varphi(y,w)\Big] \times\\
&\qquad q_{\rm coll}(x,v,y,w,d\theta)\, F(t,dx,dv)\, F(t,dy,dw)\\
&+ \int_{\tilde{E}_1}\int_{\Theta_{\rm scat}} \Big[\varphi(x_{\rm scat}(x,v,\theta), v_{\rm scat}(x,v,\theta)) - \varphi(x,v)\Big] \times\\
&\qquad q_{\rm scat}(x,v,d\theta)\, F(t,dx,dv)\\
&- \int_{\tilde{E}_1} \varphi(x,v)\, q_-(x,v)\, F(t,dx,dv) + \int_{\tilde{E}_1} \varphi(x,v)\, q_+(dx,dv)\,.
\end{aligned}$$

The test functions φ satisfy the regularity conditions (2.33), (2.34). Assume

$$\gamma_{\rm ref}^{(n)}(x,v,g;y,w)\, p_{\rm ref}^{(n)}(x,v,g;dy,dw) = g\, q_{\rm ref}(x,v;dy,dw)\,. \tag{2.51}$$

Then the boundary condition (2.37) takes the form

$$\varphi(x,v) = \int_{\tilde{E}_1} \varphi(y,w)\, q_{\rm ref}(x,v;dy,dw)\,, \quad \forall\,(x,v) \in \partial_{out}\left(D \times \mathbb{R}^3\right). \tag{2.52}$$

2.2.2 Equation for densities

Assuming

$$F(t,dx,dv) = f(t,x,v)\,dx\,dv\,,$$

we are going to derive an equation for sufficiently regular densities f. To this end we introduce additional restrictions on the various parameters.

We consider the standard example of a collision jump (2.17), where

$$\begin{aligned} x_{\rm coll}(x,v,y,w,e) &= x\,, \qquad & v_{\rm coll}(x,v,y,w,e) &= v'(v,w,e)\,,\\ y_{\rm coll}(x,v,y,w,e) &= y\,, \qquad & w_{\rm coll}(x,v,y,w,e) &= w'(v,w,e)\,,\\ e &\in \mathcal{S}^2 = \Theta_{\rm coll} \end{aligned} \tag{2.53}$$

and v', w' denote the collision transformation (1.6). We assume

$$q_{\rm coll}(x,v,y,w,de) = h(x,y)\,B(v,w,e)\,de\,, \tag{2.54}$$

where h is a symmetric function and B is a collision kernel of the form (1.10).

We consider the standard example of a scattering jump (2.20), where

$$\begin{aligned} x_{\rm scat}(x,v,w,e) &= x\,, \qquad & v_{\rm scat}(x,v,w,e) &= v'(v,w,e)\,,\\ (w,e) &\in \mathbb{R}^3\times\mathcal{S}^2 = \Theta_{\rm scat} \end{aligned} \tag{2.55}$$

and v' denotes the collision transformation (1.6). We assume

$$q_{\rm scat}(x,v,dw,de) = M_{\rm scat}(x,w)\,B_{\rm scat}(v,w,e)\,dw\,de\,, \tag{2.56}$$

where $B_{\rm scat}$ is another collision kernel of the form (1.10) and $M_{\rm scat}$ is some non-negative function representing a "background medium".

Let the domain D have a smooth boundary. We assume (slightly abusing notations)

$$q_+(dx,dv) = q_+(x,v)\,dx\,dv \quad \text{on} \quad D\times\mathbb{R}^3\,, \tag{2.57}$$

$$q_+(dx,dv) = q_{\rm in}(x,v)\,\sigma(dx)\,dv \quad \text{on} \quad \partial D\times\mathbb{R}^3 \tag{2.58}$$

and

$$q_{\rm ref}(x,v;dy,dw) = q_{\rm ref}(x,v;y,w)\,\sigma(dy)\,dw\,. \tag{2.59}$$

In general, particles are allowed to jump from the boundary inside the domain. According to (2.59), they stay at the boundary.

Note that (cf. (2.3))

$$\Big\{(x,v)\in\partial D\times\mathbb{R}^3\ :\ v\in\mathbb{R}^3_{in}(x)\Big\}\subset\partial_{in}\left(D\times\mathbb{R}^3\right)$$

and (cf. (2.4))

$$\Big\{(x,v)\in\partial D\times\mathbb{R}^3\ :\ v\in\mathbb{R}^3_{out}(x)\Big\}\subset\partial_{out}\left(D\times\mathbb{R}^3\right).$$

Condition (2.52) on the test functions takes the form (cf. (2.6))

$$\begin{aligned} \varphi(x,v) = \int_{\partial D}\int_{\mathbb{R}^3_{in}(y)} &\varphi(y,w)\,q_{\rm ref}(x,v;y,w)\,dw\,\sigma(dy)\,,\\ &\forall x\in\partial D\,,\quad v\in\mathbb{R}^3_{\rm out}(x)\,. \end{aligned} \tag{2.60}$$

Note that

$$\int_D (v,\nabla_x)(\varphi)(x,v)\, f(t,x,v)\, dx = \\ -\int_D \varphi(x,v)\, (v,\nabla_x)(f)(t,x,v)\, dx - \int_{\partial D} \varphi(x,v)\, f(t,x,v)\, \big(v,n(x)\big)\, \sigma(dx)$$

and

$$\int_{\mathbb{R}^3} (\mathcal{E}(x),\nabla_v)(\varphi)(x,v)\, f(t,x,v)\, dv = \\ -\int_{\mathbb{R}^3} \varphi(x,v)\, (\mathcal{E}(x),\nabla_v)(f)(t,x,v)\, dv\,.$$

Then, using Lemma 1.10, equation (2.50) transforms into

$$\begin{aligned} &\frac{d}{dt}\int_D\int_{\mathbb{R}^3} \varphi(x,v)\, f(t,x,v)\, dv\, dx + \int_D\int_{\mathbb{R}^3} \varphi(x,v)\, \big(v,\nabla_x\big)\, f(t,x,v)\, dv\, dx \\ &+ \int_{\partial D}\int_{\mathbb{R}^3} \varphi(x,v)\, f(t,x,v)\, \big(v,n(x)\big)\, dv\, \sigma(dx) \\ &+ \int_D\int_{\mathbb{R}^3} \varphi(x,v)\, \big(\mathcal{E}(x),\nabla_v\big)\, f(t,x,v)\, dv\, dx = \qquad (2.61) \\ &\int_D\int_{\mathbb{R}^3}\int_D\int_{\mathbb{R}^3}\int_{\mathcal{S}^2} \varphi(x,v)\, h(x,y)\, B(v,w,e)\, \times \\ &\Big[f(t,x,v'(v,w,e))\, f(t,y,w'(v,w,e)) - f(t,x,v)\, f(t,y,w)\Big]\, de\, dw\, dy\, dv\, dx \\ &+ \int_D\int_{\mathbb{R}^3}\int_{\mathbb{R}^3}\int_{\mathcal{S}^2} \varphi(x,v)\, B_{\mathrm{scat}}(v,w,e)\Big[f(t,x,v'(v,w,e))\, \times \\ &\quad M_{\mathrm{scat}}(x,w'(v,w,e)) - f(t,x,v)\, M_{\mathrm{scat}}(x,w)\Big]\, de\, dw\, dv\, dx \\ &+ \int_{\partial D}\int_{\mathbb{R}^3_{in}(x)} \varphi(x,v)\, q_{in}(x,v)\, dv\, \sigma(dx) \\ &+ \int_D\int_{\mathbb{R}^3} \varphi(x,v)\, q_+(x,v)\, dv\, dx - \int_D\int_{\mathbb{R}^3} \varphi(x,v)\, q_-(x,v)\, f(t,x,v)\, dv\, dx\,. \end{aligned}$$

Choosing (cf. (2.60))

$$\varphi(x,v) = 0\,, \qquad x \in \partial D\,,$$

and removing test functions, one obtains from (2.61) an equation for the densities

$$\begin{aligned} &\frac{\partial}{\partial t}\, f(t,x,v) + \big(v,\nabla_x\big)\, f(t,x,v) + \big(\mathcal{E}(x),\nabla_v\big)\, f(t,x,v) = \qquad (2.62) \\ &q_+(x,v) - q_-(x,v)\, f(t,x,v) + \int_D\int_{\mathbb{R}^3}\int_{\mathcal{S}^2} h(x,y)\, B(v,w,e)\, \times \end{aligned}$$

$$\Big[f(t,x,v'(v,w,e))\,f(t,y,w'(v,w,e)) - f(t,x,v)\,f(t,y,w)\Big]\,de\,dw\,dy$$
$$+\int_{\mathbb{R}^3}\int_{\mathcal{S}^2} B_{\rm scat}(v,w,e)\times$$
$$\Big[f(t,x,v'(v,w,e))\,M_{\rm scat}(x,w'(v,w,e)) - f(t,x,v)\,M_{\rm scat}(x,w)\Big]\,de\,dw\,.$$

2.2.3 Boundary conditions

Note that (2.61) and (2.62) imply

$$\int_{\partial D}\int_{\mathbb{R}^3}\varphi(x,v)\,f(t,x,v)\,\big(v,n(x)\big)\,dv\,\sigma(dx) = \int_{\partial D}\int_{\mathbb{R}^3_{in}(x)}\varphi(x,v)\,q_{in}(x,v)\,dv\,\sigma(dx)\,. \tag{2.63}$$

Using (2.60), one obtains the equality

$$\begin{aligned}
&\int_{\partial D}\int_{\mathbb{R}^3}\varphi(x,v)\,f(t,x,v)\,\big(v,n(x)\big)\,dv\,\sigma(dx) = \\
&\quad\int_{\partial D}\int_{\mathbb{R}^3_{in}(x)}\varphi(x,v)\,f(t,x,v)\,\big(v,n(x)\big)\,dv\,\sigma(dx) + \\
&\quad\int_{\partial D}\int_{\mathbb{R}^3_{out}(x)}\int_{\partial D}\int_{\mathbb{R}^3_{in}(y)}\varphi(y,w)\times \\
&\qquad\qquad q_{\rm ref}(x,v;y,w)\,dw\,\sigma(dy)\,f(t,x,v)\,\big(v,n(x)\big)\,dv\,\sigma(dx) \\
&= \int_{\partial D}\int_{\mathbb{R}^3_{in}(x)}\varphi(x,v)\Big[f(t,x,v)\,\big(v,n(x)\big) + \\
&\quad\int_{\partial D}\int_{\mathbb{R}^3_{out}(y)} q_{\rm ref}(y,w;x,v)\,f(t,y,w)\,\big(w,n(y)\big)\,dw\,\sigma(dy)\Big]\,dv\,\sigma(dx)\,,
\end{aligned}$$

for any fixed $x\in\partial D$. Consequently, it follows from equation (2.63) that

$$\begin{aligned}
&\int_{\partial D}\int_{\mathbb{R}^3_{in}(x)}\varphi(x,v)\Big[f(t,x,v)\,\big(v,n(x)\big)+ \\
&\quad\int_{\partial D}\int_{\mathbb{R}^3_{out}(y)} q_{\rm ref}(y,w;x,v)\,f(t,y,w)\,\big(w,n(y)\big)\,dw\,\sigma(dy)\Big]\,dv\,\sigma(dx) \\
&= \int_{\partial D}\int_{\mathbb{R}^3_{in}(x)}\varphi(x,v)\,q_{in}(x,v)\,dv\,\sigma(dx)\,.
\end{aligned}$$

Removing the test functions we conclude that the function f satisfies the boundary condition

$$f(t,x,v)\,\big(v,n(x)\big) = q_{in}(x,v) + \int_{\partial D}\int_{\mathbb{R}^3_{out}(y)} q_{\rm ref}(y,w;x,v)\,f(t,y,w)\,\big|\big(w,n(y)\big)\big|\,dw\,\sigma(dy)\,, \tag{2.64}$$

for any $x\in\partial D$ and $v\in\mathbb{R}^3_{in}(x)$.

2.3 Special cases and bibliographic remarks

2.3.1 Boltzmann equation and boundary conditions

We have derived equation (2.62) with the boundary condition (2.64). Here we consider some special cases.

The equation

$$\frac{\partial}{\partial t} f(t,x,v) + \big(v, \nabla_x\big) f(t,x,v) + \big(\mathcal{E}(x), \nabla_v\big) f(t,x,v) = \tag{2.65}$$
$$\int_D \int_{\mathbb{R}^3} \int_{\mathcal{S}^2} h(x,y)\, B(v,w,e) \times$$
$$\Big[f(t,x,v^*(v,w,e))\, f(t,y,w^*(v,w,e)) - f(t,x,v)\, f(t,y,w) \Big] de\, dw\, dy$$

is called **mollified** Boltzmann equation (cf. [48, Sect. VIII.3]). It was introduced in [140] and reduces formally to the Boltzmann equation if the "mollifier" h is a delta-function (see also [166]).

The equation

$$\frac{\partial}{\partial t} f(t,x,v) + \big(v, \nabla_x\big) f(t,x,v) + \big(\mathcal{E}(x), \nabla_v\big) f(t,x,v) =$$
$$\int_{\mathbb{R}^3} \int_{\mathcal{S}^2} B_{\text{scat}}(v,w,e) \times$$
$$\Big[f(t,x,v^*(v,w,e))\, M_{\text{scat}}(x,w^*(v,w,e)) - f(t,x,v)\, M_{\text{scat}}(x,w) \Big] de\, dw$$

is called **linear** Boltzmann equation (cf. [48, Sect. IV.3]). It has been widely used in the field of neutron transport in connection with the development of nuclear technology.

If (with a slight abuse of notation)

$$q_{\text{ref}}(x,v;y,w) = \delta(x-y)\, q_{\text{ref}}(x,v;w)\,, \tag{2.66}$$

then particles hitting the boundary do not change their position. The boundary condition (2.64) takes the form

$$f(t,x,v)\,\big(v, n(x)\big) = \tag{2.67}$$
$$q_{in}(x,v) + \int_{\mathbb{R}^3_{out}(x)} q_{\text{ref}}(x,w;v)\, f(t,x,w)\, \big|\big(w, n(x)\big)\big|\, dw\,,$$

where $t \geq 0$, $x \in \partial D$ and $v \in \mathbb{R}^3_{in}(x)$.

If there is complete absorption at the boundary, i.e. $q_{\text{ref}} \equiv 0$, then one obtains from (2.67) the **inflow boundary condition** (cf. (1.36))

$$f(t,x,v)\,\big(v, n(x)\big) = q_{in}(x,v)\,. \tag{2.68}$$

Such boundary conditions were used in [157, p.338].

If there is no inflow, i.e. $q_{in} \equiv 0$, then one obtains from (2.67) the boundary condition

$$f(t,x,v)\,(v,n(x)) = \int_{\mathbb{R}^3_{out}(x)} q_{\mathrm{ref}}(x,w;v)\, f(t,x,w)\,|(w,n(x))|\,dw\,, \tag{2.69}$$

which includes absorption (cf. [48, Section III.1]).

If the reflection kernel has the form

$$q_{\mathrm{ref}}(x,w;v) = (1-\alpha)\,\delta(v-w+2\,n(x)\,(n(x),w)) + \alpha\, M_b(x,v)\,(v,n(x))\,, \tag{2.70}$$

for some $\alpha \in [0,1]$, where M_b is an appropriately normalized boundary Maxwellian (cf. (1.39)), then condition (2.69) takes the form of the so-called **Maxwell boundary condition** (cf. [48, Sect. III.5])

$$\begin{aligned} f(t,x,v) &= (1-\alpha)\, f(t,x,v-2\,n(x)\,(n(x),v)) \\ &\quad + \alpha\, M_b(x,v) \int_{\mathbb{R}^3_{out}(x)} f(t,x,w)\,|(w,n(x))|\,dw\,. \end{aligned} \tag{2.71}$$

Note that $v = w - 2\,n(x)\,(n(x),w)$ is equivalent to $w = v - 2\,n(x)\,(n(x),v)$, and $|(v-2\,n(x)\,(n(x),v),n(x))| = |(v,n(x))|$. Condition (2.71) covers the special cases of specular reflection (cf. (1.37)) and of diffuse reflection (cf. (1.38)), which are obtained for $\alpha = 0$ and $\alpha = 1$, respectively.

2.3.2 Boltzmann type processes

The theory of piecewise-deterministic processes has been presented in the monograph [54] (cf. also [53] and the discussion therein). Note the remark from [54, p.60]: "Assumption (2.15) is usually quite easily checked in applications, but it is hard to formulate general conditions under which it holds, because of the complicated interaction between flow, λ, Q, and the geometry of the boundary." An analogous statement applies to assumption (2.38).

Coupling of process parameters and parameters of the equation

Using the restrictions made in the formal derivation of the limiting equation for densities (2.62), (2.64), we recall the relationship between various process parameters and the corresponding parameters of the equation.

Restrictions (2.43), (2.49), (2.53) and (2.54) were made concerning the process parameters related to **collision jumps**. Correspondingly, we assume that the weight transfer function and the intensity function are coupled to the parameters h and B via the relation

$$\gamma^{(n)}_{\mathrm{coll}}(z;i,j,e)\, p^{(n)}_{\mathrm{coll}}(z;i,j,de) = g_i\, g_j\, h^{(n)}(x_i,x_j)\, B(v_i,v_j,e)\,de\,, \tag{2.72}$$

where

$$\lim_{n\to\infty} h^{(n)}(x,y) = h(x,y)\,.$$

Restrictions (2.44), (2.45), (2.55) and (2.56) were made concerning the process parameters related to **scattering jumps**. Correspondingly, the weight transfer function and the intensity function are coupled to the parameters $M_{\rm scat}$ and $B_{\rm scat}$ via the relations

$$\gamma^{(n)}_{\rm scat}(z;i,w,e)\,p^{(n)}_{\rm scat}(z;i,dw,de) = g_i\,M_{\rm scat}(x_i,w)\,B_{\rm scat}(v_i,w,e)\,dw\,de \qquad (2.73)$$

and

$$\int_{\mathcal{S}^2}\int_{\mathbb{R}^3} p^{(n)}_{\rm scat}(z;i,dw,de) = \int_{\mathcal{S}^2}\int_{\mathbb{R}^3} M_{\rm scat}(x_i,w)\,B_{\rm scat}(v_i,w,e)\,dw\,de\,. \qquad (2.74)$$

The weight transfer function and the intensity function related to **annihilation jumps** are coupled to the parameter q_- via the relation (2.46),

$$\gamma^{(n)}_-(z;i)\,p^{(n)}_-(z;i) = g_i\,q_-(x_i,v_i)\,. \qquad (2.75)$$

Restrictions (2.47), (2.57) and (2.58) were made concerning the process parameters related to **creation jumps**. We introduce analogous notations distinguishing between creation inside the domain and on its boundary. Correspondingly, the weight transfer functions and the intensity functions are coupled to the parameters q_+ and $q_{\rm in}$ via the relations

$$\gamma^{(n)}_+(z;x,v)\,p^{(n)}_+(z;dx,dv) = q_+(x,v)\,dx\,dv \quad \text{on} \quad D\times\mathbb{R}^3 \qquad (2.76)$$

and

$$\gamma^{(n)}_{\rm in}(z;x,v)\,p^{(n)}_{\rm in}(z;dx,dv) = q_{\rm in}(x,v)\,\sigma(dx)\,dv \quad \text{on} \quad \partial D\times\mathbb{R}^3\,. \qquad (2.77)$$

Note that $p^{(n)}_{\rm in}$ is concentrated on the set

$$\Big\{(x,v)\ :\ x\in\partial D\,,\ v\in\mathbb{R}^3_{in}(x)\Big\}. \qquad (2.78)$$

Restrictions (2.51) and (2.59) were made concerning the process parameters related to **reflection jumps**. Correspondingly, the weight transfer function and the reflection kernel are coupled to the parameter $q_{\rm ref}$ via the relation

$$\gamma^{(n)}_{\rm ref}(x,v,g;y,w)\,p^{(n)}_{\rm ref}(x,v,g;dy,dw) = g\,q_{\rm ref}(x,v;y,w)\,\sigma(dy)\,dw\,. \qquad (2.79)$$

Note that $p^{(n)}_{\rm ref}$ is concentrated on the set (2.78) and satisfies (cf. (2.25))

$$\int_{\partial D}\int_{\mathbb{R}^3} p^{(n)}_{\rm ref}(x,v,g;dy,dw) \le 1\,, \quad \forall\, x\in\partial D\,,\ v\in\mathbb{R}^3_{out}(x)\,,\ g>0\,. \qquad (2.80)$$

Generating trajectories of the process

Now we specify the procedure of generating trajectories of the process from Section 2.1.2. According to (2.72), (2.73), (2.75)-(2.77), one obtains (cf. (2.19), (2.21), (2.22), (2.24), (2.57), (2.58))

$$Q^{(n)}_{\mathrm{coll}}(z;d\tilde z) = \frac{1}{2}\sum_{1\le i\ne j\le \nu}\int_{\mathcal{S}^2}\delta_{J_{\mathrm{coll}}(z;i,j,e)}(d\tilde z)\frac{g_i\,g_j}{\gamma^{(n)}_{\mathrm{coll}}(z;i,j,e)}\,h^{(n)}(x_i,x_j)\,B(v_i,v_j,e)\,de\,, \tag{2.81}$$

$$Q^{(n)}_{\mathrm{scat}}(z;d\tilde z) = \sum_{i=1}^{\nu}\int_{\mathcal{S}^2}\int_{\mathbb{R}^3}\delta_{J_{\mathrm{scat}}(z;i,w,e)}(d\tilde z)\times \frac{g_i}{\gamma^{(n)}_{\mathrm{scat}}(z;i,w,e)}\,M_{\mathrm{scat}}(x_i,w)\,B_{\mathrm{scat}}(v_i,w,e)\,dw\,de\,, \tag{2.82}$$

$$Q^{(n)}_{-}(z;d\tilde z) = \sum_{i=1}^{\nu}\delta_{J_-(z;i)}(d\tilde z)\,\frac{g_i}{\gamma^{(n)}_{-}(z;i)}\,q_-(x_i,v_i)\,, \tag{2.83}$$

$$Q^{(n)}_{+}(z;d\tilde z) = \int_D\int_{\mathbb{R}^3}\delta_{J_+(z;x,v)}(d\tilde z)\,\frac{q_+(x,v)}{\gamma^{(n)}_{+}(z;x,v)}\,dv\,dx \tag{2.84}$$

and

$$Q^{(n)}_{\mathrm{in}}(z;d\tilde z) = \int_{\partial D}\int_{\mathbb{R}^3_{in}(x)}\delta_{J_{\mathrm{in}}(z;x,v)}(d\tilde z)\,\frac{q_{\mathrm{in}}(x,v)}{\gamma^{(n)}_{\mathrm{in}}(z;x,v)}\,dv\,\sigma(dx)\,. \tag{2.85}$$

The process moves according to the free flow (2.12), (2.10) until some random jump time τ_1 is reached. The probability distribution (2.13) of this time is determined by the free flow and the rate function (2.11), which takes the form (cf. (2.16))

$$\lambda^{(n)}(z) = Q^{(n)}_{\mathrm{coll}}(z;E) + Q^{(n)}_{\mathrm{scat}}(z;E) + Q^{(n)}_{-}(z;E) + Q^{(n)}_{+}(z;E) + Q^{(n)}_{\mathrm{in}}(z;E)\,.$$

At τ_1, the process jumps into a state z_1, which is distributed according to (2.14).

If no particle hits the boundary at τ_1, then z_1 is randomly chosen according to the distribution (cf. (2.16))

$$\frac{1}{Q^{(n)}_{\mathrm{coll}}(\bar z;E)}\,Q^{(n)}_{\mathrm{coll}}(\bar z;dz_1)\,,\qquad \text{with probability}\quad \frac{Q^{(n)}_{\mathrm{coll}}(\bar z;E)}{\lambda^{(n)}(\bar z)}\,, \tag{2.86}$$

$$\frac{1}{Q^{(n)}_{\rm scat}(\bar z;E)}\,Q^{(n)}_{\rm scat}(\bar z;dz_1)\,,\qquad \text{with probability}\quad \frac{Q^{(n)}_{\rm scat}(\bar z;E)}{\lambda^{(n)}(\bar z)}\,, \tag{2.87}$$

$$\frac{1}{Q^{(n)}_{-}(\bar z;E)}\,Q^{(n)}_{-}(\bar z;dz_1)\,,\qquad \text{with probability}\quad \frac{Q^{(n)}_{-}(\bar z;E)}{\lambda^{(n)}(\bar z)}\,, \tag{2.88}$$

$$\frac{1}{Q^{(n)}_{+}(\bar z;E)}\,Q^{(n)}_{+}(\bar z;dz_1)\,,\qquad \text{with probability}\quad \frac{Q^{(n)}_{+}(\bar z;E)}{\lambda^{(n)}(\bar z)}\,, \tag{2.89}$$

and

$$\frac{1}{Q^{(n)}_{\rm in}(\bar z;E)}\,Q^{(n)}_{\rm in}(\bar z;dz_1)\,,\qquad \text{with probability}\quad \frac{Q^{(n)}_{\rm in}(\bar z;E)}{\lambda^{(n)}(\bar z)}\,, \tag{2.90}$$

where $\bar z$ is the state of the process just before the jump.

If some particles hit the boundary at τ_1, then z_1 is distributed according to (2.29). Thus, a particle (x,v,g) is either absorbed or reflected into

$$\Big(y,w,\gamma^{(n)}_{\rm ref}(x,v,g;y,w)\Big)\,.$$

According to (2.79), the absorption probability (2.26) takes the form

$$1-\int_{\partial D}\int_{\mathbb{R}^3_{in}(y)}\frac{g}{\gamma^{(n)}_{\rm ref}(x,v,g;y,w)}\,q_{\rm ref}(x,v;y,w)\,dw\,\sigma(dy) \tag{2.91}$$

and the distribution (2.27) of (y,w) is

$$\frac{\gamma^{(n)}_{\rm ref}(x,v,g;y,w)^{-1}\,q_{\rm ref}(x,v;y,w)\,dw\,\sigma(dy)}{\int_{\partial D}\int_{\mathbb{R}^3_{in}(\tilde y)}\gamma^{(n)}_{\rm ref}(x,v,g;\tilde y,\tilde w)^{-1}\,q_{\rm ref}(x,v;\tilde y,\tilde w)\,d\tilde w\,\sigma(d\tilde y)}\,. \tag{2.92}$$

Constant weights

In this case each particle has the same weight $\bar g^{(n)}$ and all weight transfer functions equal $\bar g^{(n)}$. We refer to Remark 3.5 concerning the choice of this "standard weight". The formulas below suggest the appropriate normalization of the process parameters with respect to n (in terms of $\bar g^{(n)}$). Moreover, they provide a probabilistic interpretation of the various parameters of the equation.

The parameters $h^{(n)}$ and B determine via (2.81), (2.86) the rate function of collision jumps

$$Q^{(n)}_{\rm coll}(\bar z;E)=\frac{\bar g^{(n)}}{2}\sum_{1\le i\ne j\le\nu}h^{(n)}(\bar x_i,\bar x_j)\int_{\mathcal{S}^2}B(\bar v_i,\bar v_j,e)\,de \tag{2.93}$$

and the distribution of the jump parameters. The indices i, j of the collision partners are chosen according to the probabilities

$$\frac{\bar{g}^{(n)}\, h^{(n)}(\bar{x}_i, \bar{x}_j) \int_{\mathcal{S}^2} B(\bar{v}_i, \bar{v}_j, e)\, de}{2\, Q^{(n)}_{\mathrm{coll}}(\bar{z}; E)} \tag{2.94}$$

and, given i, j , the direction vector e is chosen according to the density

$$\frac{B(\bar{v}_i, \bar{v}_j, e)}{\int_{\mathcal{S}^2} B(\bar{v}_i, \bar{v}_j, \tilde{e})\, d\tilde{e}}\,. \tag{2.95}$$

The parameters M_{scat} and B_{scat} determine via (2.82), (2.87) the rate function of scattering jumps

$$Q^{(n)}_{\mathrm{scat}}(\bar{z}; E) = \sum_{i=1}^{\nu} \int_{\mathcal{S}^2} \int_{\mathbb{R}^3} M_{\mathrm{scat}}(\bar{x}_i, w)\, B_{\mathrm{scat}}(\bar{v}_i, w, e)\, dw\, de \tag{2.96}$$

and the distribution of the jump parameters. The index i of the scattered particle is chosen according to the probabilities

$$\frac{\int_{\mathbb{R}^3} \int_{\mathcal{S}^2} M_{\mathrm{scat}}(\bar{x}_i, w)\, B_{\mathrm{scat}}(\bar{v}_i, w, e)\, de\, dw}{Q^{(n)}_{\mathrm{scat}}(\bar{z}; E)}\,. \tag{2.97}$$

Given i , the background velocity w is chosen according to the density

$$\frac{M_{\mathrm{scat}}(\bar{x}_i, w) \int_{\mathcal{S}^2} B_{\mathrm{scat}}(\bar{v}_i, w, e)\, de}{\int_{\mathbb{R}^3} \int_{\mathcal{S}^2} M_{\mathrm{scat}}(\bar{x}_i, \tilde{w})\, B_{\mathrm{scat}}(\bar{v}_i, \tilde{w}, \tilde{e})\, d\tilde{e}\, d\tilde{w}} \tag{2.98}$$

and, given i, w , the direction vector e is chosen according to the density

$$\frac{B_{\mathrm{scat}}(\bar{v}_i, w, e)}{\int_{\mathcal{S}^2} B_{\mathrm{scat}}(\bar{v}_i, w, \tilde{e})\, d\tilde{e}}\,. \tag{2.99}$$

The parameter q_- determines via (2.83), (2.88) the rate function of annihilation jumps

$$Q^{(n)}_{-}(\bar{z}; E) = \sum_{i=1}^{\nu} q_-(\bar{x}_i, \bar{v}_i) \tag{2.100}$$

and the distribution of the jump parameter. The index i of the annihilated particle is chosen according to the probabilities

$$\frac{q_-(\bar{x}_i, \bar{v}_i)}{Q^{(n)}_{-}(\bar{z}; E)}\,. \tag{2.101}$$

The parameters q_+ and q_{in} determine via (2.84), (2.85), (2.89), (2.90) the rate functions of creation jumps

$$Q_+^{(n)}(\bar{z};E) = \frac{1}{\bar{g}^{(n)}} \int_D \int_{\mathbb{R}^3} q_+(x,v)\, dv\, dx\,, \tag{2.102}$$
$$Q_{\rm in}^{(n)}(\bar{z};E) = \frac{1}{\bar{g}^{(n)}} \int_{\partial D} \int_{\mathbb{R}^3_{in}(x)} q_{\rm in}(x,v)\, dv\, \sigma(dx)$$

and the distribution of the jump parameters. A new particle is created either inside the domain D, according to the density

$$\frac{q_+(x,v)}{\bar{g}^{(n)}\, Q_+^{(n)}(\bar{z};E)}\,, \tag{2.103}$$

or at the boundary of the domain, according to the density

$$\frac{q_{\rm in}(x,v)}{\bar{g}^{(n)}\, Q_{\rm in}^{(n)}(\bar{z};E)}\,.$$

The parameter $q_{\rm ref}$ determines the probability distribution of reflection jumps. Namely, a particle (x,v) hitting the boundary disappears with the absorption probability (cf. (2.91))

$$1 - \int_{\partial D} \int_{\mathbb{R}^3_{in}(y)} q_{\rm ref}(x,v;y,w)\, dw\, \sigma(dy)\,.$$

Otherwise, it is reflected (jumps into (y,w)) according to the distribution (cf. (2.92))

$$\frac{q_{\rm ref}(x,v;y,w)\, dw\, \sigma(dy)}{\int_{\partial D} \int_{\mathbb{R}^3_{in}(\tilde{y})} q_{\rm ref}(x,v;\tilde{y},\tilde{w})\, d\tilde{w}\, \sigma(d\tilde{y})}\,.$$

Note that (2.80), (2.79) imply the restriction

$$\int_{\partial D} \int_{\mathbb{R}^3_{in}(y)} q_{\rm ref}(x,v;y,w)\, dw\, \sigma(dy) \le 1\,, \qquad \forall\, x \in \partial D\,,\ v \in \mathbb{R}^3_{out}(x)\,.$$

Variable weights

Finally we discuss the general case of variable weights. Note that the behavior of the process is not uniquely determined by the parameters of the equation. For a given set of parameters, there is a whole class of processes corresponding to this equation in the limit $n \to \infty$. In this sense, the parameters of the process are **degrees of freedom**. They can be used for the purpose of modifying the procedure of "direct simulation" (constant weights), leading to more efficient numerical algorithms. Here we consider some of these degrees of freedom as examples. The others will be studied in connection with the numerical procedures in Chapter 3.

In the case of scattering jumps, conditions (2.73), (2.74) imply (cf. (2.82))

$$Q^{(n)}_{\mathrm{scat}}(z;E) = \sum_{i=1}^{\nu} \int_{\mathbb{R}^3} \int_{\mathcal{S}^2} M_{\mathrm{scat}}(x_i,w)\, B_{\mathrm{scat}}(v_i,w,e)\, de\, dw\,.$$

Thus, the rate function is completely determined by the parameters of the equation (cf. (2.96)). Beside this, the distribution of the jump parameters i, w, e can be changed compared to the choice (2.97)-(2.99). The change in distribution is compensated by an appropriate change in the weight transfer function according to (2.73).

In the case of annihilation jumps, both the rate function and the distribution of the jump parameters can be changed compared to direct simulation (2.100), (2.101). For example, the choice

$$\gamma^{(n)}_{-}(z;i) = \frac{g_i}{1+\kappa_-}\,, \qquad \kappa_- \geq 0\,,$$

leads to an increased (compared to (2.100)) rate function

$$Q^{(n)}_{-}(z;E) = (1+\kappa_-) \sum_{i=1}^{\nu} q_-(x_i,v_i)\,,$$

while the distribution of the jump parameters remains the same (compared to (2.101)). Here annihilation events occur more often, but particles do not disappear completely.

In the case of creation jumps inside the domain, both the rate function and the distribution of the jump parameters can be changed compared to direct simulation (2.102), (2.103). According to (2.84), the choice

$$\gamma^{(n)}_{+}(z;x,v) = \frac{\bar{g}^{(n)}}{\kappa_+(x,v)} \tag{2.104}$$

leads to a rate function

$$Q^{(n)}_{+}(z;E) = \frac{1}{\bar{g}^{(n)}} \int_D \int_{\mathbb{R}^3} \kappa_+(x,v)\, q_+(x,v)\, dv\, dx\,,$$

while the distribution of the new particle is

$$\frac{\kappa_+(x,v)\, q_+(x,v)}{\bar{g}^{(n)}\, Q^{(n)}_{+}(z;E)}\,. \tag{2.105}$$

The function κ_+ is assumed to satisfy

$$\inf_{x,v} \kappa_+(x,v) > 0\,.$$

It can be used to favor certain states of the created particles, according to (2.105). This change in distribution is compensated by a correspondingly lower weight of the created particles, according to (2.104).

2.3.3 History

Here we consider a stochastic particle system

$$\Big(x_1(t), v_1(t), \dots, x_n(t), v_n(t)\Big), \qquad t \geq 0\,, \tag{2.106}$$

determined by the infinitesimal generator (cf. (2.30))

$$\mathcal{A}\,\Phi(z) = \sum_{i=1}^{n} \Big[(v_i, \nabla_{x_i}) + (\mathcal{E}, \nabla_{v_i})\Big]\Phi(z) + \tag{2.107}$$
$$\frac{1}{2\,n} \sum_{1 \leq i \neq j \leq n} \int_{\mathcal{S}^2} \Big[\Phi(J(z,i,j,e)) - \Phi(z)\Big]\, q^{(n)}(x_i, v_i, x_j, v_j, e)\, de\,,$$

where (cf. (1.12))

$$[J(z,i,j,e)]_k = \begin{cases} (x_k, v_k) & \text{, if} \quad k \neq i,j\,, \\ (x_i, v^*(v_i, v_j, e)) & \text{, if} \quad k = i\,, \\ (x_j, w^*(v_i, v_j, e)) & \text{, if} \quad k = j\,, \end{cases} \tag{2.108}$$

and

$$z = (x_1, v_1, \dots, x_n, v_n)\,, \qquad x_i, v_i \in \mathbb{R}^3\,, \quad i = 1, \dots, n\,. \tag{2.109}$$

Note that a version of **Kolmogorov's forward equation** for a Markov process with density p and generator $\mathcal{A}$ reads

$$\frac{\partial}{\partial t}\, p(t,z) = \mathcal{A}^*\, p(t,z)\,, \tag{2.110}$$

where $\mathcal{A}^*$ is the adjoint operator. Let $p^{(n)}(t,z)$ denote the n–particle density of the process (2.106). Using properties of the collision transformation and some symmetry assumption on $q^{(n)}$, one obtains from (2.110) the equation

$$\frac{\partial}{\partial t}\, p^{(n)}(t,z) + \sum_{i=1}^{n} \Big[(v_i, \nabla_{x_i}) + (\mathcal{E}, \nabla_{v_i})\Big] p^{(n)}(t,z) = \tag{2.111}$$
$$\frac{1}{2\,n} \sum_{1 \leq i \neq j \leq n} \int_{\mathcal{S}^2} \Big[p^{(n)}(t, J(z,i,j,e)) - p^{(n)}(t,z)\Big] q^{(n)}(x_i, v_i, x_j, v_j, e)\, de\,.$$

Differential equations for the density functions of Markov processes were introduced by A. N. Kolmogorov (1903-1987) in his paper [108] in 1931. After a detailed consideration of the pure diffusion and jump cases, an equation for the one-dimensional mixed case is given in the last section, and a remark concerning the multi-dimensional mixed case is contained in the conclusion. A more detailed investigation of the mixed case is given by W. Feller (1906-1970) in [63].

The process (2.106) with the generator (2.107), (2.108) is related to the Boltzmann equation

$$\frac{\partial}{\partial t} f(t,x,v) + (v, \nabla_x) f(t,x,v) + (\mathcal{E}, \nabla_v) f(t,x,v) = \tag{2.112}$$
$$\int_{\mathbb{R}^3} \int_{\mathcal{S}^2} B(v,w,e) \times$$
$$\Big[f(t,x,v^*(v,w,e))\, f(t,x,w^*(v,w,e)) - f(t,x,v)\, f(t,x,w) \Big] de\, dw\,.$$

The study of this relationship was started by M. A. Leontovich (1903-1981) in his paper [121] in 1935. Using the method of generating functions, Leontovich first studied the cases of "monomolecular processes" (independent particles) and of "bimolecular processes" with discrete states (e.g. a finite number of velocities). Under some assumptions on the initial state, it was shown that the expectations of the relative numbers of particles in the bimolecular scheme asymptotically (as $n \to \infty$) solve the corresponding deterministic equation. The process related to the Boltzmann equation (2.112) was described via equation (2.111) (even including a boundary condition of specular reflection). Concerning the asymptotic behavior of the process, Leontovich pointed out the following. Let $p_k^{(n)}$ denote the marginal distributions corresponding to the density $p^{(n)}$. If

$$\lim_{n\to\infty} p_2^{(n)}(t,x_1,v_1,x_2,v_2) = \lim_{n\to\infty} p_1^{(n)}(t,x_1,v_1) \lim_{n\to\infty} p_1^{(n)}(t,x_2,v_2) \tag{2.113}$$

and

$$\lim_{n\to\infty} q^{(n)}(x,v,y,w,e) = \delta(x-y)\, B(v,w,e)\,, \tag{2.114}$$

then the function

$$f(t,x,v) = \lim_{n\to\infty} p_1^{(n)}(t,x,v)$$

solves the Boltzmann equation. Leontovich noted that he was not able to prove a limit theorem in analogy with the discrete case, though he strongly believes that such a theorem holds.

Independently, the problem was tackled by M. Kac (1914-1984) in his paper [91] in 1956. Considering the spatially homogeneous Boltzmann equation

$$\frac{\partial}{\partial t} f(t,v) = \tag{2.115}$$
$$\int_{\mathbb{R}^3} \int_{\mathcal{S}^2} B(v,w,e) \Big[f(t,v^*(v,w,e))\, f(t,w^*(v,w,e)) - f(t,v)\, f(t,w) \Big] de\, dw$$

Kac introduced a process governed by the Kolmogorov equation

$$\frac{\partial}{\partial t}\, p^{(n)}(t,z) = \tag{2.116}$$
$$\frac{1}{2\,n} \sum_{1\le i\ne j\le n} \int_{\mathcal{S}^2} \Big[p^{(n)}(t, J(z,i,j,e)) - p^{(n)}(t,z)\Big] B(v_i, v_j, e)\, de\,,$$

where $z = (v_1, \dots, v_n)$ and J is appropriately adapted, compared to (2.108). He studied its asymptotic behavior and proved (in a simplified situation) that $\lim_{n\to\infty} p_1^{(n)}$ satisfies the Boltzmann equation. We cite from p.175 (using our notations): "To get (2.115) one must only assume that

$$p_2^{(n)}(t, v, w) \sim p_1^{(n)}(t, v)\, p_1^{(n)}(t, w)$$

for all v, w in the allowable range. One is immediately faced with the difficulty that since $p^{(n)}(t,z)$ is uniquely determined by $p^{(n)}(0,z)$ no additional assumptions on $p^{(n)}(t,z)$ can be made unless they can be deduced from some postulated properties of $p^{(n)}(0,z)$.

A moment's reflection will convince us that in order to derive (2.115) the following theorem must first be proved.

Basic Theorem Let $p^{(n)}(t,z)$ be a sequence of probability density functions ... having the "Boltzmann property"

$$\lim_{n\to\infty} p_k^{(n)}(0, v_1, \dots, v_k) = \prod_{i=1}^{k} \lim_{n\to\infty} p_1^{(n)}(0, v_i)\,. \tag{2.117}$$

Then $p^{(n)}(t,z)$ [that is, solutions of (2.116)] also have the "Boltzmann property":

$$\lim_{n\to\infty} p_k^{(n)}(t, v_1, \dots, v_k) = \prod_{i=1}^{k} \lim_{n\to\infty} p_1^{(n)}(t, v_i)\,. \tag{2.118}$$

In other words, the Boltzmann property propagates in time!"

Kac calls equation (2.116) the **master equation** referring to the paper [154] published by G. E. Uhlenbeck (1900-1988) and co-workers in 1940. There, a stochastic particle system was used to model the shower formation by fast electrons. We cite from p.353 (adapting to our notation): "When the probabilities of the elementary processes are known, one can write down a continuity equation for $p^{(n)}$, from which all other equations can be derived and which we call therefore the "master" equation."

Besides [91] (proceedings of a conference in 1954/1955), Kac published the two books [92] (ten lectures given in 1956) and [93] (extension of 12 lectures given in 1957) containing more material related to the stochastic approach to the Boltzmann equation. In [92] the factorization property (2.118) is also called the "chaos property" (indicating asymptotic independence), and the statement of the basic theorem is called **propagation of chaos**. The following remark is made in [93, p.131]: "The primary disadvantage of the

master equation approach ... lies in the difficulty (if not impossibility!) of extending it to the nonspatially uniform case."

Kac returns to this point in later publications. We cite from [96, p.385] (proceedings of a conference in 1972 celebrating the 100-th anniversary of the Boltzmann equation): "The master equation approach suffers from a major deficiency. It is limited to the spatially homogeneous case. It seems impossible to bring in streaming terms while at the same time treating collisions as random events. The explanation of this I believe lies in the fact that in a gas streaming and collisions come from the same source i.e. the Hamiltonian of the system. It thus appears that the full Boltzmann equation (i.e., with streaming terms) can be interpreted as a probabilistic equation only by going back to the Γ-space and postulating an initial probability density ... There are other drawbacks e.g., that in spite of many efforts propagation of chaos has not yet been proved for a single realistic case." In the paper [124, p.462] (submitted in 1975) one reads: "The idea, apparently first used by Nordsieck, Lamb, and Uhlenbeck [154], is to treat the evolution of the system as a random process. ... [later, same page] ... This approach is intrinsically limited to the spatially homogeneous case, for the treatment of the elementary events (the molecular collisions) as random transitions depends on the suppression - or averaging - of the position coordinates."

In 1983 the soviet journal "Uspekhi Fizicheskikh Nauk" published a series of papers honoring Leontovich (who would have had his 80th birthday). The importance and influence of the paper [121] were discussed by Yu. L. Klimontovich (1924-2002) in [105]. In particular, the footnote on page 691 throws some light on how Kac learned about the early Leontovich-paper. We cite (from Russian): "During a school on statistical physics in Jadwisin (Poland) M. Kac told me the following. After his book appeared in Russian, one of the Leningrad physicists sent him a copy of [121]. M. Kac asked me: "How he (Leontovich) could know and understand all this in 1935?" ... I mentioned the friendship and collaboration of M. A. Leontovich and A. N. Kolmogorov. M. Kac immediately replied: "So Kolmogorov taught him all this"."

In fact, Leontovich refers in [121] to Kolmogorov's paper [108] concerning the rigorous derivation of the basic differential equation for Markov processes with finitely many states. On the other hand, Kolmogorov refers to a paper by Leontovich [122], and even to a joint paper with Leontovich [109], when motivating the importance of the new probabilistic concepts, introduced in his book [110], for concrete physical problems. Moreover, Kolmogorov refereed the paper [121] for the "Zentralblatt für Mathematik und ihre Grenzgebiete" (see Zbl. 0012.26802).

The conference mentioned by Klimontovich obviously took place in 1977 (cf. [52], [97], [104]). The Russian translation [94] of [93] appeared in 1965, while the translation [95] (referred to in [105]) of [92] appeared only in 1967. Unfortunately, there seems to be no other written evidence about the "Kac-Leontovich relationship". The paper [98], which appeared in 1979, contains on page 47 the same statement as in [124] (cited above) concerning the spatially

homogeneous case. In 1986 a special issue of the "Annals of Probability" was dedicated to the memory of Kac. His contributions to mathematical physics were reviewed in [198]. Here, the stochastic models for the Boltzmann equation are mentioned, but no remark concerning Leontovich is made.

Before continuing the historical excursion, we recall the pathwise behavior of the process (2.106) with the generator (2.107), (2.108). Assume $D = \mathbb{R}^3$ so that no boundary conditions are involved. Starting at $z = (x_1, v_1, \dots, x_n, v_n)$ the process moves according to the free flow, i.e. (cf. (2.12), (2.10), (2.1))

$$Z(t) = \Big(X(t, x_1, v_1), V(t, x_1, v_1), \dots, X(t, x_n, v_n), V(t, x_n, v_n)\Big)$$

until a random jump time τ_1 is reached. The probability distribution of this time is determined by (cf. (2.13))

$$\mathrm{Prob}(\tau_1 > t) = \exp\left(-\int_0^t \lambda^{(n)}(Z(s))\, ds\right), \qquad t \geq 0\,,$$

where (cf. (2.81), (2.93))

$$\lambda^{(n)}(z) = \frac{1}{2\,n} \sum_{1 \leq i \neq j \leq n} \int_{\mathcal{S}^2} q^{(n)}(x_i, v_i, x_j, v_j, e)\, de\,.$$

At the random time τ_1 the process jumps into a state z_1, which is obtained from the state $\bar{z}$ of the process just before the jump by a two-particle interaction. Namely, two indices i, j and a direction vector e are chosen according to the probability density

$$\frac{q^{(n)}(\bar{x}_i, \bar{v}_i, \bar{x}_j, \bar{v}_j, e)}{2\,n\,\lambda^{(n)}(\bar{z})}\,,$$

and the velocities $\bar{v}_i, \bar{v}_j$ are replaced using the collision transformation (1.12). In view of (2.114), a reasonable specification is (cf. (2.94), (2.95))

$$q^{(n)}(x, v, y, w, e) = h^{(n)}(x, y)\, B(v, w, e)\,,$$

where $h^{(n)}$ approximates the delta-function. Choosing

$$h^{(n)}(x, y) = \begin{cases} c_n^{-1}\,, & \text{if} \quad |x - y| \leq \varepsilon^{(n)}\,, \\ 0 \quad , & \text{otherwise}\,, \end{cases}$$

where c_n is the volume of the ball of radius $\varepsilon^{(n)}$, one observes that only those particles can collide which are closer to each other than the interaction distance $\varepsilon^{(n)}$.

In [106, Ch. 9] Klimontovich rewrites the Leontovich equation (2.111) with

$$q^{(n)}(x, v, y, w, e) = \delta(x - y)\, B(v, w, e)\,, \tag{2.119}$$

saying (on page 144): "Delta-function $\delta(x_i - x_j)$ indicates that the colliding particles belong to one and the same point." In [105] the equation is written in the same form, but the following remark is made (on page 693): "...the 'width' of the function $\delta(x_i - x_j)$ is characterized by the quantity l_Φ." This quantity is introduced on p. 692 as a "physically infinitesimally small" length interval. Note that equation (2.111) with $q^{(n)}$ given in (2.119) has been formally derived by C. Cercignani in the paper [46] in 1975 (see also his report on the book [106] in MR 96g:82049 and Zbl. 0889.60100).

However, describing the Leontovich equation from [121] as equation (2.111) with $q^{(n)}$ given in (2.119) is definitely misleading. The basic goal of that paper was to introduce an appropriate stochastic process so that "equation (2.112) occurs as the limiting equation for the mathematical expectations as $n \to \infty$" (p. 213). But the process with the choice (2.119) does not make much sense, since, except for some singular configurations, the particles do not interact at all. In [46, p. 220] the author remarks (concerning equation (2.111) with $q^{(n)}$ given in (2.119)): "The singular nature of the equation ... raises serious questions about its meaning and validity." Unfortunately, the paper [121] contains many misprints that have to be corrected from the context. In the following we cite using our notations. On page 224 Leontovich considers random transitions

$$(\bar{x}_1, \bar{v}_1, \dots, \bar{x}_n, \bar{v}_n) \to (x_1, v_1, \dots, x_n, v_n)$$

where (formula (39))

$$x_k = \bar{x}_k\,, \qquad k = 1, 2, \dots, n\,,$$

and all but two of the velocities before and after the collision are equal, while $\bar{v}_k$ and $\bar{v}_i$ are transformed according to the rule (1.12). Concerning the transition probabilities $q^{(n)}(\bar{x}_k, \bar{v}_k, \bar{x}_i, \bar{v}_i, e)$ (introduced in formula (41)) he notes that they "depend on the positions of the particles $\bar{x}_k$ and $\bar{x}_i$ and are different from zero only if their distance does not exceed a certain quantity." Assuming (formula (45))

$$q^{(n)}(x, v, y, w, e) = q^{(n)}(x, v^*(v, w, e), y, w^*(v, w, e), e)$$

and (formula (64))

$$q^{(n)}(x, v, y, w, e) = q^{(n)}(y, w, x, v, e)$$

Leontovich obtains (equation (63))

$$\begin{aligned} &\frac{\partial}{\partial t}\, p_1^{(n)}(t, x, v) + (v, \nabla_x)\, p_1^{(n)}(t, x, v) + (\mathcal{E}, \nabla_v)\, p_1^{(n)}(t, x, v) = \\ &\int_{\mathbb{R}^3} \int_{\mathbb{R}^3} \int_{\mathcal{S}^2} q^{(n)}(x, v, y, w, e) \times \\ &\Big[p_2^{(n)}(t, x, v^*(v, w, e), y, w^*(v, w, e)) - p_2^{(n)}(t, x, v, y, w) \Big]\, de\, dw\, dy\,. \end{aligned} \tag{2.120}$$

The following arguments are given at the last half page of the paper. Relation (2.120) takes the form of the "basic equation of gas theory" (2.112) if one replaces $p_2^{(n)}$ by the product of $p_1^{(n)}$. Such replacement can be justified if one proves a "limit theorem" (for $n \to \infty$) in analogy with the case of a discrete state space. Then (2.120) takes the form

$$\frac{\partial}{\partial t} f(t,x,v) + (v, \nabla_x) f(t,x,v) + (\mathcal{E}, \nabla_v) f(t,x,v) = \int_{\mathbb{R}^3} \int_{\mathbb{R}^3} \int_{\mathcal{S}^2} q(x,v,y,w,e) \times \Big[f(t,x,v^*(v,w,e)) f(t,y,w^*(v,w,e)) - f(t,x,v) f(t,y,w) \Big] de\, dw\, dy\,.$$

Complete agreement with (2.113) in the "hard sphere case" is obtained if we put

$$q(x,v,y,w,e) = |(v-w,e)|\, \delta(x-y)\,. \tag{2.121}$$

From this context we concluded that relation (2.121) is meant to hold only after taking the limit $n \to \infty$. But since in the paper dependence on n is not explicitly expressed, and the same notations are used for the objects before and after taking the limit, a misinterpretation is possible.

Spatially homogeneous case

Research in the field of stochastic particle systems related to the Boltzmann equation was restricted to the spatially homogeneous case during a long period after Kac's paper [91]. In H. P. McKean's paper [134] published in 1975 one reads (on p.436) "I do not know how to handle the streaming". Concerning the history of the approach the author notes "The model stems from Lamb-Nordsieck-Uhlenbeck [154], though first employed in the present connection by Siegert [184] and by Kac [91]." Propagation of chaos was first studied for a simplified two-dimensional model called "Kac's caricature of a Maxwellian gas" (cf. [132], [133]). The result was generalized to the three-dimensional model (assuming cut-off and some smoothness of the solution to the Boltzmann equation) by F. A. Grünbaum in his doctoral dissertation (supervised by McKean) in 1971 (cf. [73]). Further references are [161], [162], [163], [164], [195], [196], [197], [143], [192], [193], [194], [187], [81], [64], [18].

It turns out (cf. [197], [193]) that the chaos property (2.117) (i.e., the asymptotic factorization) is equivalent to the convergence in distribution of the empirical measures

$$\mu^{(n)}(t) = \frac{1}{n} \sum_{i=1}^{n} \delta_{v_i(t)} \tag{2.122}$$

to a deterministic limit. The objects (2.122) are considered as random variables with values in the space of measures on the state space of a single

particle. Thus, the basic theorem can be reformulated as the propagation of convergence of empirical measures (cf. [203]). In this setup, it is natural to study the convergence not only for fixed t, but also in the space of measure–valued functions of t (functional law of large numbers).

Spatially inhomogeneous case

The spatially inhomogeneous case was treated by C. Cercignani in the paper [47] (submitted 11/1982) in 1983. He considered a system of "soft spheres", where "molecules collide at distances randomly given by a probability distribution" (p. 491), and proved propagation of chaos (modulo a uniqueness theorem). The limiting equation is the mollified Boltzmann equation (2.65).

A more general approach was developed by A.V. Skorokhod in the book [185] published in 1983. In Chapter 2 he considered a Markov process $Z(t) = (Z_i(t))_{i=1}^n$ (describing it via stochastic differential equations with respect to Poisson measures) with the generator

$$\mathcal{A}\Phi(z) = \sum_{i=1}^{n} \big(b(z_i), \nabla_{z_i}\big)\, \Phi(z) + \frac{1}{2\,n} \sum_{1\le i\ne j\le n} \int_{\Theta} \Big[\Phi(J(z,i,j,\vartheta)) - \Phi(z)\Big]\, \pi(d\vartheta)\,,$$

where Φ is an appropriate test function, $z = (z_1, \dots, z_n) \in \mathcal{Z}^n$, and

$$[J(z,i,j,e)]_k = \begin{cases} z_k & , \text{ if } \quad k \ne i,j\,, \\ z_i + \beta(z_i, z_j, \vartheta)\,, & \text{if } \quad k = i\,, \\ z_j + \beta(z_j, z_i, \vartheta)\,, & \text{if } \quad k = j\,. \end{cases}$$

The symbol $\mathcal{Z}$ denotes the state space of a single particle, π is a measure on a parameter set Θ, and f is a function on $\mathcal{Z}\times\mathcal{Z}\times\Theta$. This model is more general than the Leontovich model (2.107), (2.108), as far as the gradient terms and the jump transformation J are concerned. However, the distribution π of the jump parameter ϑ does not depend on the state z. It was proved that the corresponding empirical measures (cf. (2.122)) converge (for any t) to a deterministic limit $\lambda(t)$ which satisfies the equation

$$\frac{d}{dt}\int_{\mathcal{Z}} \varphi(z)\,\lambda(t,dz) = \int_{\mathcal{Z}} \big(b(z), \nabla_z\big)\,\varphi(z)\,\lambda(t,dz) + \int_{\mathcal{Z}}\int_{\mathcal{Z}} \left\{ \int_{\Theta} \Big[\varphi(z_1 + \beta(z_1,z_2,\vartheta)) - \varphi(z_1)\Big]\,\pi(d\vartheta)\right\} \lambda(t,dz_1)\,\lambda(t,dz_2)\,,$$

for appropriate test functions φ.

Further references concerning the spatially inhomogeneous case are [66], [6], [149], [126], [116], [17], [205], [207], [72]. Developing the stochastic approach to the Boltzmann equation, systems with a general binary interaction

between particles and a general (Markovian) single particle evolution (including spatial motion) were considered. Results concerning the approximation of the solution to the corresponding nonlinear kinetic equation by the particle system (including the order of convergence) were obtained in [149], [72] covering the case of bounded intensities and a constant (in time) number of particles. Boundedness of the intensities restricts the results to the mollified Boltzmann equation (2.65). Partial results concerning the non-mollified case are [44] (one-dimensional model), [170], [171], [173] (discrete velocities), [136] (small initial data). Recent results related to the Enskog equation were obtained in [172] .

Convergence in the stationary case

Finally we mention a result from [45] concerning convergence in the stationary case. In many applications studying the equilibrium behavior of gas flows is of primary interest. To this end, time averaging over trajectories of the corresponding particle system is used,

$$\frac{1}{k}\sum_{j=1}^{k}\left[\frac{1}{n}\sum_{i=1}^{n}\varphi(x_i(t_j),v_i(t_j))\right], \qquad t_j=\bar{t}+j\,\Delta t\,,$$

where φ is a test function and $\bar{t}$ is some starting time for averaging. To justify this procedure (for $k\to\infty$), one has to study the connection between the stationary density of the process and the stationary Boltzmann equation. From the results mentioned above one can obtain information about the limit $\lim_{t\to\infty}\lim_{n\to\infty} p_1^{(n)}(t,x,v)$ while here one is interested in the limit $\lim_{n\to\infty}\lim_{t\to\infty} p_1^{(n)}(t,x,v)$. The identity of both quantities is not at all obvious.

Consider the (mollified) stationary Boltzmann equation

$$(v,\nabla_x)\,\bar{f}(x,v)=\varepsilon\int_D\int_{\mathbb{R}^3}\int_{\mathcal{S}^2} h(x,y)\,B(v,w,e)\times \tag{2.123}$$

$$\Big[\bar{f}(x,v^*(v,w,e))\,\bar{f}(y,w^*(v,w,e))-\bar{f}(x,v)\,\bar{f}(y,w)\Big]de\,dw\,dy\,,$$

with the boundary condition of "diffuse reflection", and introduce the notation

$$\bar{f}_k(x_1,v_1,\ldots,x_k,v_k)=\prod_{i=1}^{k}\bar{f}(x_i,v_i)\,.$$

Consider the stationary density of the n-particle process $\bar{p}^{(n)}$ and the corresponding marginals

$$\bar{p}_k^{(n)}(x_1,v_1,\ldots,x_k,v_k)\,.$$

Then the following result holds.

THEOREM [45, Th. 2.5] There exists $\varepsilon_0 > 0$ such that

$$||\bar{p}_k^{(n)} - \bar{f}_k||_{L^1} \leq \frac{c^k}{n}, \qquad \forall\, n > k,$$

for any $0 < \varepsilon \leq \varepsilon_0$ and $k = 1, 2, \ldots$, where c does not depend on ε, k, n.

Note that, beside the asymptotic factorization itself, one even obtains an order of convergence. The main restriction, the smallness of the right-hand side of the Boltzmann equation (2.123), is due to the fact that the proof uses perturbation from the collision-less situation. Further assumptions concern the domain D (smooth, convex, bounded), the collision kernel B (bounded) and some cut-off of small velocities.

We refer to [9], [10] concerning other results on the approximation of the solution to the stationary Boltzmann equation by time averages of stochastic particle systems.

3

Stochastic weighted particle method

Here we reduce the generality of Chapter 2. We skip the external force as well as scattering and annihilation of particles. We consider creation of particles only at the boundary of the domain (inflow). We assume that particles hitting the boundary do not change their positions. This avoids overloading the presentation, and allows us to concentrate on the main ideas. Moreover, we make the assumptions of Section 2.2.2, which were used in the formal derivation of the limiting equation for densities.

According to (2.53) the jump transformation (2.17) related to collisions takes the form

$$[J_{\mathrm{coll}}(z;i,j,e)]_k = \begin{cases} (x_k, v_k, g_k) & , \quad \text{if} \quad k \le \nu\,,\ k \ne i,j\,, \\ (x_i, v'(v_i,v_j,e), \gamma_{\mathrm{coll}}(z;i,j,e)) & , \quad \text{if} \quad k = i\,, \\ (x_j, w'(v_i,v_j,e), \gamma_{\mathrm{coll}}(z;i,j,e)) & , \quad \text{if} \quad k = j\,, \\ (x_i, v_i, g_i - \gamma_{\mathrm{coll}}(z;i,j,e)) & , \quad \text{if} \quad k = \nu+1\,, \\ (x_j, v_j, g_j - \gamma_{\mathrm{coll}}(z;i,j,e)) & , \quad \text{if} \quad k = \nu+2\,, \end{cases} \tag{3.1}$$

where (cf. (2.7))

$$z = \Big(\nu, (x_1,v_1,g_1), \ldots, (x_\nu, v_\nu, g_\nu)\Big) \tag{3.2}$$

and v', w' denote the collision transformation (1.6). We consider the collision weight transfer function

$$\gamma_{\mathrm{coll}}(z;i,j,e) = [1+\kappa(z;i,j,e)]^{-1}\, \min(g_i, g_j)\,, \tag{3.3}$$

where the weight transfer parameter κ is non-negative so that condition (2.18) is satisfied. According to (2.54) we choose

$$p_{\mathrm{coll}}(z;i,j,de) = [1+\kappa(z;i,j,e)]\, h(x_i,x_j)\, B(v_i,v_j,e)\, \max(g_i,g_j)\, de \tag{3.4}$$

so that (2.43) and (2.49) are satisfied. Note that both functions (3.3) and (3.4) do not depend on the convergence parameter n.

The jump transformation (2.23) related to creation events is denoted by (cf. (2.58))

$$\Big[J_{\rm in}^{(n)}(z;x,v)\Big]_k = \begin{cases} (x_k, v_k, g_k) & , \quad \text{if} \quad k \le \nu\,, \\ (x, v, \gamma_{\rm in}^{(n)}(x,v))\,, & \text{if} \quad k = \nu+1\,. \end{cases}$$

The inflow weight transfer function $\gamma_{\rm in}^{(n)}$ and the inflow intensity function $p_{\rm in}^{(n)}$ are assumed not to depend on the state z. They are concentrated on the set (cf. (2.78))

$$\Big\{(x,v)\ :\ x \in \partial D\,,\ v \in \mathbb{R}^3_{in}(x)\Big\} \tag{3.5}$$

and coupled via condition (cf. (2.47), (2.77))

$$\gamma_{\rm in}^{(n)}(x,v)\, p_{\rm in}^{(n)}(x,v) = q_{\rm in}(x,v)\,. \tag{3.6}$$

The weight transfer function and the reflection kernel, related to jumps at the boundary, are coupled via condition (cf. (2.79), (2.66))

$$\gamma_{\rm ref}(x,v,g;y,w)\, p_{\rm ref}(x,v,g;dy,dw) = g\,\delta_x(dy)\, q_{\rm ref}(x,v;w)\,dw\,. \tag{3.7}$$

Both parameters do not depend on n. The reflection kernel $p_{\rm ref}$ is concentrated on the set (3.5) and satisfies (cf. (2.80))

$$\int_{\partial D}\int_{\mathbb{R}^3} p_{\rm ref}(x,v,g;dy,dw) \le 1\,, \qquad \forall\, x \in \partial D\,, \quad v \in \mathbb{R}^3_{out}(x)\,, \quad g > 0\,. \tag{3.8}$$

The extended generator (2.30) of the corresponding particle system takes the form

$$\begin{aligned} \mathcal{A}^{(n)}\Phi(z) = \sum_{i=1}^{\nu} (v_i, \nabla_{x_i})\,\Phi(z) + \frac{1}{2}\sum_{1\le i\ne j\le \nu}\int_{\mathcal{S}^2}\Big[\Phi(J_{\rm coll}(z;i,j,e)) - \Phi(z)\Big]\times \\ [1+\kappa(z;i,j,e)]\,h(x_i,x_j)\,B(v_i,v_j,e)\,\max(g_i,g_j)\,de + \\ \int_{\partial D}\int_{\mathbb{R}^3_{in}(x)}\Big[\Phi(J_{\rm in}^{(n)}(z;x,v)) - \Phi(z)\Big]p_{\rm in}^{(n)}(x,v)\,dv\,\sigma(dx)\,. \end{aligned} \tag{3.9}$$

The limiting equation (2.62) is

$$\begin{aligned} \frac{\partial}{\partial t}\,f(t,x,v) + (v,\nabla_x) f(t,x,v) = \int_D\int_{\mathbb{R}^3}\int_{\mathcal{S}^2} h(x,y)\,B(v,w,e)\times \\ \Big[f(t,x,v'(v,w,e))\,f(t,y,w'(v,w,e)) - f(t,x,v)\,f(t,y,w)\Big]de\,dw\,dy\,, \end{aligned} \tag{3.10}$$

with the boundary condition (cf. (2.67))

$$f(t,x,v)\,\big(v,n(x)\big) = q_{in}(x,v) + \int_{\mathbb{R}^3_{out}(x)} q_{\mathrm{ref}}(x,w;v)\, f(t,x,w)\,\big|\big(w,n(x)\big)\big|\,dw\,, \qquad \forall\, x\in\partial D\,,\ v\in\mathbb{R}^3_{in}(x)\,, \tag{3.11}$$

and the initial condition

$$f(0,x,v) = f_0(x,v)\,, \tag{3.12}$$

for some non-negative integrable function f_0.

The dependence of the process on the convergence parameter n is restricted to the initial state (resolution of f_0) and to the inflow intensity (resolution of q_{in}). It will be specified in Sections 3.1.1 and 3.2.2, respectively. For example, n can be the number of particles in the system at time zero, or the average number of particles entering the system during a unit time interval. Correspondingly, this parameter influences the weights of the particles. In the case of "direct simulation", all particles have some standard weight $\bar{g}^{(n)}$. In the general case, all particle weights are bounded by some maximal weight $g^{(n)}_{\max}$.

3.1 The DSMC framework

3.1.1 Generating the initial state

The first step is the approximation of the initial measure

$$F_0(dx,dv) = f_0(x,v)\,dx\,dv\,,$$

corresponding to the initial condition (3.12) of the Boltzmann equation, by a system of particles

$$Z^{(n)}(0) = \Big(x_i(0), v_i(0), g_i(0)\Big)_{i=1}^{\nu(0)}\,. \tag{3.13}$$

Approximation means that the empirical measure of the system

$$\mu^{(n)}(0,dx,dv) = \sum_{i=1}^{\nu(0)} g_i(0)\,\delta_{(x_i(0),v_i(0))}(dx,dv) \tag{3.14}$$

converges to F_0 in an appropriate sense. The notion of convergence will be specified in Section 3.4.2. The initial state (3.13) can be determined by any probabilistic rule, but also deterministic approximations are possible, provided convergence holds.

For example, one can generate n independent particles according to the probability density

$$\frac{f_0(x,v)}{\int_D \int_{\mathbb{R}^3} f_0(y,w)\,dw\,dy}\,,$$

with weights

$$\bar{g}^{(n)} = \frac{1}{n} \int_D \int_{\mathbb{R}^3} f_0(y,w)\, dw\, dy\,. \tag{3.15}$$

Then (cf. (3.14))

$$\lim_{n\to\infty} \int_D \int_{\mathbb{R}^3} \varphi(x,v)\, \mu^{(n)}(0,dx,dv) = \int_D \int_{\mathbb{R}^3} \varphi(x,v)\, F_0(dx,dv)\,, \tag{3.16}$$

for any integrable test function φ, by the law of large numbers. If f_0 is identically zero (vacuum), then the empty system (consisting of no particles) satisfies (3.16).

More generally, n independent particles $(x_i(0), v_i(0))$ are generated according to some probability density p_0, with weights

$$g_i(0) = \frac{1}{n}\, \frac{f_0(x_i(0), v_i(0))}{p_0(x_i(0), v_i(0))}\,, \qquad i = 1, \ldots, n\,.$$

Here one assumes that all weights are bounded by $g^{(n)}_{\max}$. Convergence in the sense of (3.16) follows from the law of large numbers.

3.1.2 Decoupling of free flow and collisions

For reasons of numerical efficiency, the time evolution of the system is approximated via a splitting technique using some time discretization

$$t_k = k\, \Delta t\,, \qquad k = 0, 1, \ldots\,, \tag{3.17}$$

where $\Delta t > 0$ is called **time step**. This leads to a decoupling of free flow and collisions.

One part of the evolution is determined by the generator (3.9) without the collision term, i.e.

$$\begin{aligned} \mathcal{A}^{(n)}_{\text{free}} \Phi(z) = \sum_{i=1}^{\nu} (v_i, \nabla_{x_i})\, \Phi(z) + \\ \int_{\partial D} \int_{\mathbb{R}^3_{in}(x)} \Big[\Phi(J^{(n)}_{\text{in}}(z;x,v)) - \Phi(z)\Big] p^{(n)}_{\text{in}}(x,v)\, dv\, \sigma(dx)\,. \end{aligned} \tag{3.18}$$

In this part there is no interaction among the particles. If a particle hits the boundary, then its state changes according to the boundary condition. New particles are created according to the inflow term.

The other part of the evolution is determined by the generator (3.9) keeping only the collision term, i.e.

$$\begin{aligned} \mathcal{A}_{\text{coll}} \Phi(z) = \frac{1}{2} \sum_{1\le i\ne j\le \nu} \int_{\mathcal{S}^2} \Big[\Phi(J_{\text{coll}}(z;i,j,e)) - \Phi(z)\Big] h(x_i, x_j) \times \\ [1 + \kappa(z;i,j,e)]\, B(v_i, v_j, e)\, \max(g_i, g_j)\, de\,. \end{aligned} \tag{3.19}$$

Here the positions of the particles remain unchanged.

A detailed description of both parts follows in Sections 3.2 and 3.3, respectively. The free flow and collision simulation steps are combined in an appropriate way (e.g., the final state of the system after the free flow step serves as the initial state for the collision simulation step, etc.).

3.1.3 Limiting equations

The splitting technique leads to a corresponding approximation of the limiting equation (3.10). Consider the auxiliary functions (cf. (3.17))

$$f^{(1,k)}(t,x,v)\,,\quad f^{(2,k)}(t,x,v)\,,\qquad t\in[t_k,t_{k+1}]\,,\quad (x,v)\in D\times\mathbb{R}^3\,,$$

where $k=0,1,\dots$. These functions are determined by two systems of equations coupled via their initial conditions. The first system, which corresponds to the free flow simulation steps, has the form

$$\frac{\partial}{\partial t}\,f^{(1,k)}(t,x,v)+(v,\nabla_x)f^{(1,k)}(t,x,v)=0\,,$$

with boundary condition (3.11) and initial condition

$$f^{(1,k)}(t_k,x,v)=f^{(2,k-1)}(t_k,v)\,,\quad k=1,2,\dots\,,\qquad f^{(1,0)}(0,x,v)=f_0(x,v)\,.$$

The second system, which corresponds to the collision simulation steps, has the form

$$\begin{aligned}\frac{\partial}{\partial t}\,f^{(2,k)}(t,x,v)&=\int_D\int_{\mathbb{R}^3}\int_{\mathcal{S}^2}h(x,y)\,B(v,w,e)\times\\&\Big[f^{(2,k)}(t,x,v')\,f^{(2,k)}(t,y,w')-f^{(2,k)}(t,x,v)\,f^{(2,k)}(t,y,w)\Big]de\,dw\,dy\,,\end{aligned}\tag{3.20}$$

with initial condition

$$f^{(2,k)}(t_k,x,v)=f^{(1,k)}(t_{k+1},x,v)\,,\qquad k=0,1,\dots\,.$$

The limiting density $\hat f$ satisfies

$$\hat f(t_k,x,v)=f^{(2,k-1)}(t_k,x,v)\,,\qquad k=1,2,\dots\,,\qquad \hat f(0,x,v)=f_0(x,v)\,.$$

3.1.4 Calculation of functionals

Consider functionals of the form

$$\Psi(t)=\int_D\int_{\mathbb{R}^3}\varphi(x,v)\,f(t,x,v)\,dv\,dx\,.\tag{3.21}$$

They have the physical dimension of the quantity φ. The functionals (3.21) are approximated by the random variable

$$\xi^{(n)}(t) = \sum_{i=1}^{\nu(t)} g_i(t)\,\varphi(x_i(t), v_i(t))\,. \tag{3.22}$$

In order to estimate and to reduce the random fluctuations of (3.22), a number N of independent ensembles of particles is generated. The corresponding values of the random variable are denoted by $\xi_1^{(n)}(t), \ldots, \xi_N^{(n)}(t)$. The **empirical mean value** of the random variable (3.22), i.e.

$$\eta_1^{(n,N)}(t) = \frac{1}{N}\sum_{j=1}^{N} \xi_j^{(n)}(t)\,, \tag{3.23}$$

is then used as an approximation to the functional (3.21). The error of this approximation is $|\eta_1^{(n,N)}(t) - \Psi(t)|$ consisting of the following two components.

The **systematic error** is the difference between the mathematical expectation of the random variable (3.22) and the exact value of the functional, i.e.

$$e_{sys}^{(n)}(t) = \mathbb{E}\,\xi^{(n)}(t) - \Psi(t)\,. \tag{3.24}$$

The **statistical error** is the difference between the empirical mean value and the expected value of the random variable, i.e.

$$e_{stat}^{(n,N)}(t) = \eta_1^{(n,N)}(t) - \mathbb{E}\,\xi^{(n)}(t)\,.$$

A **confidence interval** for the expectation of the random variable $\xi^{(n)}(t)$ is obtained as

$$I_p = \left[\eta_1^{(n,N)}(t) - \lambda_p\sqrt{\frac{\operatorname{Var}\xi^{(n)}(t)}{N}}\,,\ \eta_1^{(n,N)}(t) + \lambda_p\sqrt{\frac{\operatorname{Var}\xi^{(n)}(t)}{N}}\right], \tag{3.25}$$

where

$$\operatorname{Var}\xi^{(n)}(t) := \mathbb{E}\left[\xi^{(n)}(t) - \mathbb{E}\,\xi^{(n)}(t)\right]^2 = \mathbb{E}\left[\xi^{(n)}(t)\right]^2 - \left[\mathbb{E}\,\xi^{(n)}(t)\right]^2 \tag{3.26}$$

is the variance of the random variable (3.22) and $p \in (0,1)$ is the confidence level. This means that

$$\operatorname{Prob}\left\{\mathbb{E}\,\xi^{(n)}(t) \notin I_p\right\} = \operatorname{Prob}\left\{|e_{stat}^{(n,N)}(t)| \geq \lambda_p\sqrt{\frac{\operatorname{Var}\xi^{(n)}(t)}{N}}\right\} \sim p\,.$$

For example, $p = 0.999$ corresponds to $\lambda_p \sim 3.2$. Thus, the value

$$c^{(n,N)}(t) = \lambda_p\sqrt{\frac{\operatorname{Var}\xi^{(n)}(t)}{N}}$$

is a probabilistic upper bound for the statistical error.

The variance (3.26) is approximated by the corresponding empirical value, i.e.

$$\operatorname{Var} \xi^{(n)}(t) \sim \eta_2^{(n,N)}(t) - \left[\eta_1^{(n,N)}(t)\right]^2,$$

where

$$\eta_2^{(n,N)}(t) = \frac{1}{N} \sum_{j=1}^{N} \left[\xi_j^{(n)}(t)\right]^2$$

is the empirical second moment of the random variable (3.22).

3.2 Free flow part

We describe the time evolution for $t \geq 0$, in order to avoid indexing with respect to the time discretization (3.17). The system evolves according to the infinitesimal generator (3.18), i.e. there is free flow of particles

$$\frac{d}{dt} x_i(t) = v_i(t), \qquad t \geq 0, \tag{3.27}$$

until they hit the boundary. In that case, particles are treated according to the boundary condition, i.e. they are reflected (and move further according to (3.27)) or absorbed. The simulation stops when the time Δt is over.

The inflow mechanism is not influenced by the behavior of the system so that it can be modeled independently.

3.2.1 Modeling of boundary conditions

The behavior of particles hitting the boundary is determined by the parameters p_{ref} and γ_{ref}, which are coupled to the corresponding parameter of the equation via (3.7). The reflection kernel p_{ref}, which determines both the absorption probability and the reflection law, is concentrated on the set (3.5) (of positions at the boundary and in-going velocities) and satisfies (3.8). A particle (x, v, g) is absorbed with probability (2.91), that is

$$1 - \int_{\partial D} \int_{\mathbb{R}^3} p_{\text{ref}}(x, v, g; dy, dw). \tag{3.28}$$

With remaining probability the particle is reflected, i.e., it jumps into the state

$$\Big(y, w, \gamma_{\text{ref}}(x, v, g; y, w)\Big),$$

where y, w are distributed according to (2.92), that is

$$\frac{p_{\mathrm{ref}}(x,v,g;dy,dw)}{\int_{\partial D}\int_{\mathbb{R}^3} p_{\mathrm{ref}}(x,v,g;d\tilde{y},d\tilde{w})}\,. \tag{3.29}$$

Note that, due to (3.7), particles do not change their positions.

Example 3.1. The case of "direct simulation" corresponds to the choice

$$p_{\mathrm{ref}}(x,v,g;dy,dw) = \delta_x(dy)\, q_{\mathrm{ref}}(x,v;w)\, dw \tag{3.30}$$

and

$$\gamma_{\mathrm{ref}}(x,v,g;y,w) = g\,. \tag{3.31}$$

The absorption probability (3.28) and the reflection law (3.29) take the form

$$1 - \int_{\mathbb{R}^3_{\mathrm{in}}(x)} q_{\mathrm{ref}}(x,v;w)\, dw \tag{3.32}$$

and

$$\delta_x(dy)\, \frac{q_{\mathrm{ref}}(x,v;w)\, dw}{\int_{\mathbb{R}^3_{\mathrm{in}}(x)} q_{\mathrm{ref}}(x,v;\tilde{w})\, d\tilde{w}}\,, \tag{3.33}$$

respectively. Note that (3.8) implies

$$\int_{\mathbb{R}^3_{\mathrm{in}}(x)} q_{\mathrm{ref}}(x,v;w)\, dw \le 1$$

as a necessary condition. The Maxwell boundary condition (2.71) corresponds to the reflection kernel (2.70). In this case the absorption probability (3.32) is zero. With probability α, the new velocity of the particle is generated according to

$$M_b(x,w)\,\big(w, n(x)\big)\,, \qquad w \in \mathbb{R}^3_{\mathrm{in}}(x)\,,$$

where M_b is an appropriately normalized boundary Maxwellian (cf. (1.39)). With probability $1-\alpha$, the new velocity is calculated as

$$w = v - 2\, n(x)\,\big(n(x), v\big)\,, \tag{3.34}$$

according to specular reflection. Note that (3.34) implies $w \in \mathbb{R}^3_{\mathrm{in}}(x)$. ■

Any change of the reflection kernel p_{ref} or the weight transfer function γ_{ref} (compared to (3.30), (3.31)) is compensated by a corresponding change of the other parameter, according to (3.7).

Example 3.2. Here we illustrate how the absorption probability can be modified, compared to the direct simulation case (3.32). Choosing

$$\gamma_{\mathrm{ref}}(x,v,g;y,w) = g\,\kappa_{\mathrm{ref}}\,, \qquad \kappa_{\mathrm{ref}} > 0\,, \tag{3.35}$$

one obtains from (3.7)

$$p_{\mathrm{ref}}(x,v,g;dy,dw) = \frac{1}{\kappa_{\mathrm{ref}}}\,\delta_x(dy)\,q_{\mathrm{ref}}(x,v;w)\,dw\,.$$

The corresponding reflection law (3.29) is the same as in the case of direct simulation, namely (3.33), but the absorption probability (3.28) takes the form

$$1 - \frac{1}{\kappa_{\mathrm{ref}}}\int_{\mathbb{R}^3_{in}(x)} q_{\mathrm{ref}}(x,v;w)\,dw\,,$$

instead of (3.32). According to (3.8), one obtains the restriction

$$\kappa_{\mathrm{ref}} \geq \int_{\mathbb{R}^3_{in}(x)} q_{\mathrm{ref}}(x,v;w)\,dw\,. \tag{3.36}$$

In the case

$$\int_{\mathbb{R}^3_{in}(x)} q_{\mathrm{ref}}(x,v;w)\,dw < 1$$

there is absorption in the direct simulation scheme. This "natural" absorption can be avoided by choosing

$$\kappa_{\mathrm{ref}} = \int_{\mathbb{R}^3_{in}(x)} q_{\mathrm{ref}}(x,v;w)\,dw\,.$$

Then the particle is always reflected at the boundary, but it looses some weight proportional to the reflection probability that corresponds to direct simulation. On the other hand, absorption can be artificially intensified or even introduced. Assume, for example, that there is no natural absorption, i.e.

$$\int_{\mathbb{R}^3_{in}(x)} q_{\mathrm{ref}}(x,v;w)\,dw = 1\,.$$

Choosing $\kappa_{\mathrm{ref}} > 1$, the particle is either absorbed (with probability $1 - \kappa_{\mathrm{ref}}^{-1}$) or reflected, gaining some weight according to (3.35). Note that even the case

$$\int_{\mathbb{R}^3_{in}(x)} q_{\mathrm{ref}}(x,v;w)\,dw > 1$$

is covered. This case can not be interpreted in terms of "direct simulation", since some increase of weight at the boundary is necessary, according to (3.36), (3.35).

Example 3.3. Here we illustrate how the reflection law can be modified, compared to the direct simulation case (3.30). Consider the case of diffuse reflection (cf. (2.70) with $\alpha = 1$), i.e.

$$q_{\mathrm{ref}}(x, v; w) = M_b(x, w)\,(w, n(x))\,.$$

Choosing

$$p_{\mathrm{ref}}(x, v, g; dy, dw) = \delta_x(dy)\,\tilde{M}_b(x, w)\,(w, n(x))\,dw$$

one obtains from (3.7)

$$\gamma_{\mathrm{ref}}(x, v, g; y, w) = g\,\frac{M_b(x, w)}{\tilde{M}_b(x, w)}\,. \tag{3.37}$$

Here $\tilde{M}_b$ is a Maxwellian with a modified temperature, or even with some mean velocity showing inside the domain, such that (cf. (1.35) and Lemma A.2)

$$\int_{\mathbb{R}^3_{in}(x)} \tilde{M}_b(x, w)\,(w, n(x))\,dw = 1\,.$$

Note that (3.8) is satisfied and the absorption probability (3.28) is zero. The new velocity of the particle is generated according to

$$\tilde{M}_b(x, w)\,(w, n(x))\,, \qquad w \in \mathbb{R}^3_{\mathrm{in}}(x)\,.$$

The new weight is given by (3.37).

3.2.2 Modeling of inflow

The inflow of particles at the boundary is determined by the parameters $p^{(n)}_{\mathrm{in}}$ and $\gamma^{(n)}_{\mathrm{in}}$, which are coupled to the corresponding parameter of the equation via (3.6). The intensity function $p^{(n)}_{\mathrm{in}}$ determines both the frequency of creation jumps and the distribution of the created particles. Its support is the set (3.5) of positions at the boundary and in-going velocities. The inflow intensity is denoted by

$$\lambda^{(n)}_{\mathrm{in}} = \int_{\partial D} \int_{\mathbb{R}^3_{in}(x)} p^{(n)}_{\mathrm{in}}(x, v)\,dv\,\sigma(dx)\,. \tag{3.38}$$

Each jump consists in creating a particle

$$\left(x, v, \gamma^{(n)}_{\mathrm{in}}(x, v)\right),$$

where the position $x \in \partial D$ and the velocity $v \in \mathbb{R}^3_{in}(x)$ are distributed according to the inflow law

$$\frac{1}{\lambda_{\rm in}^{(n)}}\, p_{\rm in}^{(n)}(x,v)\,. \tag{3.39}$$

The expected number of particles entering the domain during the time step Δt is

$$\lambda_{\rm in}^{(n)}\,\Delta t\,. \tag{3.40}$$

The expected value of the weight of a new particle is

$$\frac{1}{\lambda_{\rm in}^{(n)}} \int_{\partial D} \int_{\mathbb{R}^3_{in}(x)} \gamma_{\rm in}^{(n)}(x,v)\, p_{\rm in}^{(n)}(x,v)\, dv\, \sigma(dx) = \frac{F_{in}}{\lambda_{\rm in}^{(n)}}\,,$$

according to (3.6), where

$$F_{in} = \int_{\partial D} \int_{\mathbb{R}^3_{in}(x)} q_{\rm in}(x,v)\, dv\, \sigma(dx)\,. \tag{3.41}$$

The expected overall weight created during Δt is (cf. (3.40))

$$\lambda_{\rm in}^{(n)}\,\Delta t\,\frac{F_{in}}{\lambda_{\rm in}^{(n)}} = F_{in}\,\Delta t \tag{3.42}$$

and does not depend on $\gamma_{\rm in}^{(n)}$, $p_{\rm in}^{(n)}$.

Example 3.4. The case of "direct simulation" corresponds to the choice

$$\gamma_{\rm in}^{(n)}(x,v) = \bar{g}^{(n)} \tag{3.43}$$

and

$$p_{\rm in}^{(n)}(x,v) = \frac{1}{\bar{g}^{(n)}}\, q_{\rm in}(x,v)\,, \tag{3.44}$$

where $\bar{g}^{(n)} > 0$ is some "standard weight" (cf. Remark 3.5). The inflow intensity (3.38) takes the form (cf. (3.41))

$$\lambda_{\rm in}^{(n)} = \frac{F_{in}}{\bar{g}^{(n)}} \tag{3.45}$$

and the inflow law (3.39) is

$$\frac{1}{F_{\rm in}}\, q_{\rm in}(x,v)\,. \tag{3.46}$$

All incoming particles get the weight $\bar{g}^{(n)}$.

A case of special interest is

$$q_{in}(x,v) = \chi_{\Gamma_{in}}(x)\,\chi_{\{(w,e)>0\}}(v)\, M_{in}(v)\,(v,e)\,, \tag{3.47}$$

where

$$M_{in}(v) = \frac{\varrho_{in}}{(2\pi T_{in})^{3/2}} \exp\left(-\frac{|v - V_{in}|^2}{2T_{in}}\right) \tag{3.48}$$

is an inflow Maxwellian and

$$e = n(x)\,, \qquad \forall\, x \in \Gamma_{in} \subset \partial D\,. \tag{3.49}$$

Here the inflow is restricted to some plane part of the boundary. The inflow intensity is (3.45) with (cf. Lemma A.2)

$$F_{in} = \tag{3.50}$$
$$\varrho_{in}\,\sigma(\Gamma_{in})\left\{\sqrt{\frac{T_{in}}{2\pi}}\,\exp\left(-\frac{(V_{in},e)^2}{2T_{in}}\right) + \frac{(V_{in},e)}{2}\left[1 + \operatorname{erf}\left(\frac{(V_{in},e)}{\sqrt{2T_{in}}}\right)\right]\right\}.$$

According to the inflow law (3.46), the position of the incoming particle is distributed uniformly on Γ_{in} and its velocity is generated according to

$$\frac{\sigma(\Gamma_{in})}{F_{in}}\,\chi_{\{(w,e)>0\}}(v)\,M_{in}(v)\,(v,e)\,. \tag{3.51}$$

Remark 3.5. If $f_0 \neq 0$ then the standard weight $\bar{g}^{(n)}$ is determined during the generation of the initial state (e.g., via (3.15)). If $f_0 = 0$ then the dependence of the process on the convergence parameter n is determined during the inflow modeling. For example, one can choose $\lambda_{\rm in}^{(n)} = n$ so that, according to (3.40), n is the expected number of particles entering the system during a unit time interval. The standard particle weight is then

$$\bar{g}^{(n)} = \frac{1}{n}\int_{\partial D}\int_{\mathbb{R}^3_{in}(x)} q_{\rm in}(x,v)\,dv\,\sigma(dx)\,,$$

according to (3.45), (3.41).

Remark 3.6. Typically, $\bar{g}^{(n)} \sim 1/n$ so that $\lambda_{\rm in}^{(n)} \sim n$ is large. In this case, deterministic time steps $1/\lambda_{\rm in}^{(n)}$ can be used. This means that a deterministic number of particles is created. Alternatively, at the end some random step can be added, to make the expectation correct. However, the stochastic mechanism described above is more stable in extreme situations (low particle numbers, large time steps, etc.).

Remark 3.7. The boundary condition

$$f(t,x,v) = f_{in}(x,v) \tag{3.52}$$

corresponds to the choice (cf. (2.68))

$$q_{in}(x,v) = f_{in}(x,v)\,(v, n(x))\,.$$

Note that (3.52) applies to $v \in \mathbb{R}^3_{in}(x)$, and there is no condition for $v \in \mathbb{R}^3_{out}(x)$. Complete absorption is determined by the condition $q_{\rm ref} \equiv 0$, not by $f(x,v) = 0$ for $v \in \mathbb{R}^3_{out}(x)$. ■

Any change of the inflow intensity function $p_{\rm in}^{(n)}$ or the inflow weight transfer function $\gamma_{\rm in}^{(n)}$ (compared to (3.43), (3.44)) is compensated by a corresponding change of the other parameter, according to (3.6).

Example 3.8. We consider the choice

$$p_{in}^{(n)}(x,v) = \frac{1}{\kappa_{\rm in}} \frac{F_{in}}{\bar g^{(n)}} \Big[(1-c_{in})\, \tilde F_{in}^{-1}\, \tilde q_{in}(x,v) + c_{in}\, F_{in}^{-1}\, q_{in}(x,v) \Big] \tag{3.53}$$

and

$$\gamma_{in}^{(n)}(x,v) = \kappa_{\rm in}\, \bar g^{(n)}\, \frac{F_{in}^{-1}\, q_{in}(x,v)}{(1-c_{in})\, \tilde F_{in}^{-1}\, \tilde q_{in}(x,v) + c_{in}\, F_{in}^{-1}\, q_{in}(x,v)}\,, \tag{3.54}$$

for some $\kappa_{\rm in} > 0$ and $c_{in} \in [0,1]$. The function $\tilde q_{in}$ is given on the set (3.5) and $\tilde F_{in}$ is defined in analogy with (3.41). While q_{in} determines the main stream of the inflow, the parameter $\tilde q_{in}$ describes some auxiliary stream. Note that (3.6) is satisfied. The inflow intensity (3.38) is

$$\lambda_{\rm in}^{(n)} = \frac{1}{\kappa_{\rm in}} \frac{F_{in}}{\bar g^{(n)}} \tag{3.55}$$

and the inflow law (3.39) takes the form

$$(1-c_{in})\, \tilde F_{in}^{-1}\, \tilde q_{in}(x,v) + c_{in}\, F_{in}^{-1}\, q_{in}(x,v)\,. \tag{3.56}$$

Thus, position x and velocity v of the new particle are generated according to the main stream, with probability c_{in}, and according to the auxiliary stream, with probability $1-c_{in}$. The weight of a new particle is determined by (3.54) and has the upper bound

$$\kappa_{\rm in}\, \bar g^{(n)}\, \min\left(\frac{1}{c_{in}}\,,\ \frac{\tilde F_{in}}{(1-c_{in})\, F_{in}}\, \sup_{x,v}\, \frac{q_{in}(x,v)}{\tilde q_{in}(x,v)} \right).$$

Note that Example 3.4 is obtained for $\kappa_{\rm in} = c_{in} = 1$. The choice $\kappa_{\rm in} \neq 1$ modifies the inflow intensity, while the choice $c_{in} < 1$ corresponds to a change of the inflow law.

In the special case (3.47)-(3.49) we consider the intensity function of the auxiliary stream in the form

$$\tilde q_{in}(x,v) = \chi_{\Gamma_{in}}(x)\, \chi_{\{(w,e)>0\}}(v)\, \tilde M_{in}(v)\, (v,e)\,, \tag{3.57}$$

where

$$\tilde M_{in}(v) = \frac{\varrho_{in}}{(2\pi\,\tau\,T_{in})^{3/2}} \exp\left(-\frac{|v-V_{in}|^2}{2\,\tau\,T_{in}} \right) \qquad \text{for some} \quad \tau > 0\,.$$

Note that $\tilde F_{in}$ is given by (3.50) with T_{in} replaced by $\tau\, T_{in}$. The inflow intensity is (3.55). According to the inflow law (3.56), the position of the incoming

particle is distributed uniformly on Γ_{in}. Its velocity is generated according to (3.51) with probability c_{in}, and according to

$$\frac{\sigma(\Gamma_{in})}{\tilde{F}_{in}}\,\chi_{\{(w,e)>0\}}(v)\,\tilde{M}_{in}(v)\,(v,e)\,,$$

with probability $1-c_{in}$. The weight of a new particle (3.54) takes the form

$$\gamma_{in}^{(n)}(x,v)=\kappa_{\mathrm{in}}\,\bar{g}^{(n)}\,\frac{1}{(1-c_{in})\,(F_{in}/\tilde{F}_{in})\,(\tilde{M}_{in}(v)/M_{in}(v))+c_{in}}\,.$$

Remark 3.9. In the case (3.53), (3.54) with $c_{in}=0$, all particles are created according to the auxiliary stream, with weights

$$\kappa_{\mathrm{in}}\,\bar{g}^{(n)}\,\frac{\tilde{F}_{in}\,q_{in}(x,v)}{F_{in}\,\tilde{q}_{in}(x,v)}\,.$$

If $\tilde{q}_{in}$ differs significantly from q_{in}, then only very few particles representing the main stream are created. However, those particles have very large weights. The expected overall weight of particles created during a time interval of length Δt is given in (3.42). However, its actual value fluctuates very strongly around this correct value, and is mostly too small. The effect of strongly fluctuating weights is not desirable since the value $g_{\max}^{(n)}$ controls the convergence (cf. Theorem 3.22).

3.3 Collision part

We describe the time evolution for $t\geq 0$, in order to avoid indexing with respect to the time discretization (3.17). The system evolves according to the infinitesimal generator (3.19), i.e. particles collide changing their velocities. An artificially decreased weight transfer during collisions (cf. (3.3)) is compensated by an appropriately increased intensity of collisions (cf. (3.4)). The simulation stops when the time Δt is over.

3.3.1 Cell structure

For reasons of numerical efficiency, some partition

$$D=\bigcup_{l=1}^{l_c} D_l \tag{3.58}$$

of the spatial domain into a finite number of disjoint cells is introduced, and a mollifying function of the form

$$h(x,y)=\frac{1}{|D_l|}\sum_{l=1}^{l_c}\chi_{D_l}(x)\,\chi_{D_l}(y) \tag{3.59}$$

is used. Here $|D_l|$ denotes the volume of the cell D_l. The cell structure leads to a decoupling of collision cell processes, if one assumes that the weight transfer parameter is of the form

$$\kappa(z;i,j,e) = \sum_{l=1}^{l_c} \chi_{D_l}(x_i)\,\chi_{D_l}(x_j)\,\kappa_l(z^{(l)};i,j,e)\,, \tag{3.60}$$

where (cf. (3.2))

$$z^{(l)} = \{(x_i,v_i,g_i)\,:\,x_i \in D_l\}\,. \tag{3.61}$$

Indeed, the generator (3.19) takes the form

$$\mathcal{A}_{\rm coll}(\Phi)(z) = \sum_{l=1}^{l_c} \mathcal{A}_{{\rm coll},l}(\Phi)(z)\,,$$

where (cf. (3.1), (3.3))

$$\mathcal{A}_{{\rm coll},l}(\Phi)(z) = \frac{1}{2\,|D_l|} \sum_{1\le i\ne j\le \nu} \chi_{D_l}(x_i)\,\chi_{D_l}(x_j)\,\max(g_i,g_j)\times \tag{3.62}$$

$$\int_{\mathcal{S}^2} \Big[\Phi(J_{{\rm coll},l}(z;i,j,e)) - \Phi(z)\Big][1+\kappa_l(z^{(l)};i,j,e)]\,B(v_i,v_j,e)\,de\,,$$

with

$$[J_{{\rm coll},l}(z;i,j,e)]_k = \tag{3.63}$$

$$\begin{cases} (x_k,v_k,g_k) & , \quad \text{if} \quad k\le\nu\,,\ k\ne i,j\,,\\ (x_i,v'(v_i,v_j,e),\gamma_{{\rm coll},l}(z^{(l)};i,j,e)) & , \quad \text{if} \quad k=i\,,\\ (x_j,w'(v_i,v_j,e),\gamma_{{\rm coll},l}(z^{(l)};i,j,e)) & , \quad \text{if} \quad k=j\,,\\ (x_i,v_i,g_i-\gamma_{{\rm coll},l}(z^{(l)};i,j,e)) & , \quad \text{if} \quad k=\nu+1\,,\\ (x_j,v_j,g_j-\gamma_{{\rm coll},l}(z^{(l)};i,j,e)) & , \quad \text{if} \quad k=\nu+2\,, \end{cases}$$

and

$$\gamma_{{\rm coll},l}(z^{(l)};i,j,e) = [1+\kappa_l(z^{(l)};i,j,e)]^{-1}\,\min(g_i,g_j)\,. \tag{3.64}$$

Thus, there is no interaction between different cells, and collisions of the particles are simulated independently in each cell, according to the generators (3.62).

The limiting equation (3.20) of the collision step is replaced by a system of limiting equations corresponding to different cells, i.e.

$$f^{(2,k)}(t,x,v) = \sum_{l=1}^{l_c} \chi_{D_l}(x)\,f_l^{(2,k)}(t,x,v)\,, \tag{3.65}$$

where

$$\frac{\partial}{\partial t}\,f_l^{(2,k)}(t,x,v) = \frac{1}{|D_l|}\int_{D_l}\int_{\mathbb{R}^3}\int_{\mathcal{S}^2} B(v,w,e)\times \tag{3.66}$$

$$\Big[f_l^{(2,k)}(t,x,v')\,f_l^{(2,k)}(t,y,w') - f_l^{(2,k)}(t,x,v)\,f_l^{(2,k)}(t,y,w)\Big]\,de\,dw\,dy\,.$$

3.3.2 Fictitious collisions

Here we introduce a modification of the Markov jump process with the generator (cf. (3.62))

$$\mathcal{A}_{\mathrm{coll},l}(\Phi)(z) = \int_{\mathcal{Z}} \Big[\Phi(\tilde{z}) - \Phi(z)\Big] Q_{\mathrm{coll},l}(z; d\tilde{z})\,, \tag{3.67}$$

where

$$Q_{\mathrm{coll},l}(z; d\tilde{z}) = \frac{1}{2} \sum_{1\le i\ne j\le \nu} \int_{\mathcal{S}^2} \delta_{J_{\mathrm{coll},l}(z;i,j,e)}(d\tilde{z})\; p_{\mathrm{coll},l}(z; i, j, e)\, de$$

and

$$\begin{aligned} &p_{\mathrm{coll},l}(z; i, j, e) = \\ &\frac{1}{|D_l|}\, \chi_{D_l}(x_i)\, \chi_{D_l}(x_j)\; \max(g_i, g_j)\, [1 + \kappa_l(z^{(l)}; i, j, e)]\, B(v_i, v_j, e)\,. \end{aligned} \tag{3.68}$$

Let $\hat{p}_{\mathrm{coll},l}$ be a function such that

$$\int_{\mathcal{S}^2} p_{\mathrm{coll},l}(z; i, j, e)\, de \le \hat{p}_{\mathrm{coll},l}(z; i, j) \tag{3.69}$$

and define

$$\begin{aligned} \hat{Q}_{\mathrm{coll},l}(z; d\tilde{z}) = {} & \frac{1}{2} \sum_{1\le i\ne j\le \nu} \int_{\mathcal{S}^2} \delta_{J_{\mathrm{coll},l}(z;i,j,e)}(d\tilde{z})\, p_{\mathrm{coll},l}(z; i, j, e)\, de + \\ & \frac{1}{2} \sum_{1\le i\ne j\le \nu} \delta_z(d\tilde{z}) \left[\hat{p}_{\mathrm{coll},l}(z; i, j) - \int_{\mathcal{S}^2} p_{\mathrm{coll},l}(z; i, j, e)\, de\right]. \end{aligned}$$

Remark 3.10. The generator (3.67) does not change if one replaces $Q_{\mathrm{coll},l}$ by $\hat{Q}_{\mathrm{coll},l}$. Thus, the distribution of the Markov process and therefore its convergence properties do not depend on the function $\hat{p}_{\mathrm{coll},l}$. However, the choice of this function is of importance for numerical purposes, since it provides different ways of generating trajectories of the process. ■

The pathwise behavior of a Markov jump process with the rate function

$$\hat{\lambda}_{\mathrm{coll},l}(z) = \frac{1}{2} \sum_{1\le i\ne j\le \nu} \hat{p}_{\mathrm{coll},l}(z; i, j) \tag{3.70}$$

and the transition measure

$$\hat{\lambda}_{\mathrm{coll},l}(z)^{-1}\, \hat{Q}_{\mathrm{coll},l}(z; d\tilde{z}) \tag{3.71}$$

is described as follows. Coming to a state z, the process stays there for a random **waiting time** $\tau(z)$, which has an exponential distribution with the parameter (3.70), i.e.

$$\mathrm{Prob}(\tau(z) > t) = \exp(-\hat{\lambda}_{\mathrm{coll},l}(z)\, t)\,.$$

After the time $\tau(z)$, the process jumps into a state $\tilde{z}$, which is distributed according to the transition measure (3.71). This measure takes the form

$$\begin{aligned}\hat{\lambda}_{\mathrm{coll},l}(z)^{-1}\hat{Q}_{\mathrm{coll},l}(z;d\tilde{z}) = \sum_{1\le i\ne j\le \nu} \frac{\hat{p}_{\mathrm{coll},l}(z;i,j)}{2\,\hat{\lambda}_{\mathrm{coll},l}(z)} \times \\ \left\{ \frac{\int_{\mathcal{S}^2} p_{\mathrm{coll},l}(z;i,j,e)\,de}{\hat{p}_{\mathrm{coll},l}(z;i,j)} \int_{\mathcal{S}^2} \delta_{J_{\mathrm{coll},l}(z;i,j,e)}(d\tilde{z})\, \frac{p_{\mathrm{coll},l}(z;i,j,e)\,de}{\int_{\mathcal{S}^2} p_{\mathrm{coll},l}(z;i,j,e)\,de} \right. \\ \left. + \delta_z(d\tilde{z}) \left[1 - \frac{\int_{\mathcal{S}^2} p_{\mathrm{coll},l}(z;i,j,e)\,de}{\hat{p}_{\mathrm{coll},l}(z;i,j)}\right] \right\}\end{aligned}$$

representing a superposition of simpler distributions. Consequently, the distribution of the indices i, j is determined by the probabilities

$$\frac{\hat{p}_{\mathrm{coll},l}(z;i,j)}{2\,\hat{\lambda}_{\mathrm{coll},l}(z)} = \frac{\hat{p}_{\mathrm{coll},l}(z;i,j)}{\sum_{1\le i\ne j\le \nu} \hat{p}_{\mathrm{coll},l}(z;i,j)}\,, \qquad 1 \le i \ne j \le \nu\,. \tag{3.72}$$

Given i and j, the new state is $\tilde{z} = z$ with probability

$$1 - \frac{\int_{\mathcal{S}^2} p_{\mathrm{coll},l}(z;i,j,e)\,de}{\hat{p}_{\mathrm{coll},l}(z;i,j)}\,. \tag{3.73}$$

Expression (3.73) is therefore called probability of a fictitious collision. Otherwise, i.e. with the remaining probability, the new state is

$$\tilde{z} = J_{\mathrm{coll},l}(z;i,j,e)\,,$$

where the distribution of the direction vector $e \in \mathcal{S}^2$ is

$$\frac{p_{\mathrm{coll},l}(z;i,j,e)}{\int_{\mathcal{S}^2} p_{\mathrm{coll},l}(z;i,j,e)\,de} = \frac{[1+\kappa_l(z^{(l)};i,j,e)]\,B(v_i,v_j,e)}{\int_{\mathcal{S}^2}[1+\kappa_l(z^{(l)};i,j,e)]\,B(v_i,v_j,e)\,de}\,. \tag{3.74}$$

Remark 3.11. Note that the expectation of the random waiting time $\tau(z)$ is $\hat{\lambda}_{\mathrm{coll},l}(z)^{-1}$. If this value is sufficiently small (cf. (3.68)-(3.70) and Remark 3.6), then the random time step can be replaced by the deterministic approximation

$$\hat{\tau}(z) = \hat{\lambda}_{\mathrm{coll},l}(z)^{-1}\,.$$

3.3.3 Majorant condition

Here we specify the majorant condition (3.69). We assume that the collision kernel satisfies

$$\int_{\mathcal{S}^2} B(v,w,e)\,de \le c_B\,|v-w|^{\varepsilon}\,, \qquad \forall\, v,w \in \mathbb{R}^3\,,$$

for some $\varepsilon \in [0,2)$ and some constant c_B. Note that

$$\max(g_i, g_j) \le g_i + g_j - g_{\min,l}\,, \qquad \forall i,j\,:\, x_i, x_j \in D_l\,,$$

where

$$g_{\min,l} = g_{\min,l}(z) \le \min_{i\,:\,x_i \in D_l} g_i \tag{3.75}$$

is a lower bound for the particle weights in the cell. Furthermore, let

$$C_{\kappa,l} \ge \kappa_l(z^{(l)}; i, j, e) \ge 0$$

be an upper bound for the weight transfer parameter. Then condition (3.69) is fulfilled provided that (cf. (3.68))

$$\hat{p}_{\mathrm{coll},l}(z; i, j) \ge \frac{1}{|D_l|}\,\chi_{D_l}(x_i)\,\chi_{D_l}(x_j)\,[g_i + g_j - g_{\min,l}]\,[1 + C_{\kappa,l}]\,c_B\,|v_i - v_j|^{\varepsilon}\,. \tag{3.76}$$

In the following subsections, we will construct several **majorants** $\hat{p}_{\mathrm{coll},l}$ satisfying (3.76), and discuss the resulting procedures for generating trajectories of the process.

Considering a state z of the form (3.2), we introduce the notations

$$\varrho(z) = \sum_{i=1}^{\nu} g_i\,, \tag{3.77}$$

$$V(z) = \frac{1}{\varrho(z)} \sum_{i=1}^{\nu} g_i\, v_i\,, \tag{3.78}$$

$$\varepsilon(z) = \sum_{i=1}^{\nu} g_i\,|v_i|^2 \tag{3.79}$$

and

$$T(z) = \frac{1}{3\,\varrho(z)} \sum_{i=1}^{\nu} g_i\,|v_i - V(z)|^2 = \frac{1}{3}\left[\frac{1}{\varrho(z)}\,\varepsilon(z) - |V(z)|^2\right]. \tag{3.80}$$

Note that the quantities (3.77)–(3.80) are preserved during the collision simulation step. For the cell system (3.61) we introduce the number of particles in the cell D_l

$$\nu_l = \sum_{i=1}^{\nu} \chi_{D_l}(x_i)\,, \tag{3.81}$$

the local density

$$\varrho_l = \varrho(z^{(l)}) = \sum_{i\,:\,x_i \in D_l} g_i \,, \tag{3.82}$$

the local mean velocity

$$V_l = V(z^{(l)}) = \frac{1}{\varrho_l} \sum_{i\,:\,x_i \in D_l} g_i \, v_i \tag{3.83}$$

and the local temperature

$$T_l = T(z^{(l)}) = \frac{1}{3\,\varrho_l} \sum_{i\,:\,x_i \in D_l} g_i \, |v_i - V_l|^2 = \frac{1}{3} \left[\frac{1}{\varrho_l} \sum_{i\,:\,x_i \in D_l} g_i \, |v_i|^2 - |V_l|^2 \right]. \tag{3.84}$$

Note that

$$\begin{aligned} \sum_{j\,:\,x_j \in D_l} g_j \, |v_i - v_j|^2 &= \sum_{j\,:\,x_j \in D_l} g_j \Big[|v_i - V_l|^2 - 2\,(v_i - V_l, v_j - V_l) + |v_j - V_l|^2 \Big] \\ &= |v_i - V_l|^2 \, \varrho_l + 3\, T_l \, \varrho_l \end{aligned} \tag{3.85}$$

and

$$\sum_{i,j\,:\,x_i, x_j \in D_l} g_i \, g_j \, |v_i - v_j|^2 = 6\, T_l \, \varrho_l^2 \,. \tag{3.86}$$

Remark 3.12. In the case of variable weights it is reasonable to choose (cf. (3.75))

$$g_{\min,l} = 0 \,, \tag{3.87}$$

since the algorithm becomes simpler and $g_{\min,l}$ is usually very small anyway. However, we keep $g_{\min,l}$ in the formulas in order to cover the case of "direct simulation" (constant weights).

3.3.4 Global upper bound for the relative velocity norm

Here we consider an upper bound for the relative particle velocities in the cell,

$$U_l = U_l(z) \geq \max_{i \neq j\,:\,x_i, x_j \in D_l} |v_i - v_j| \,. \tag{3.88}$$

Note that

$$U_l = 2 \max_{i\,:\,x_i \in D_l} |v_i - V_l|$$

is a possible choice. According to (3.88), the function

$$\hat{p}_{\mathrm{coll},l}(z;i,j) = \frac{1}{|D_l|}\,\chi_{D_l}(x_i)\,\chi_{D_l}(x_j)\,[g_i + g_j - g_{\min,l}]\,[1 + C_{\kappa,l}]\,c_B\,U_l^\varepsilon$$

satisfies (3.76). The corresponding waiting time parameter (3.70) takes the form

$$\begin{aligned}\hat{\lambda}_{\mathrm{coll},l}(z) &= \frac{1}{2\,|D_l|}\,[1 + C_{\kappa,l}]\,c_B\,U_l^\varepsilon \sum_{i\neq j\,:\,x_i,x_j\in D_l} [g_i + g_j - g_{\min,l}] \\ &= \frac{1}{2\,|D_l|}\,[1 + C_{\kappa,l}]\,c_B\,U_l^\varepsilon\,(\nu_l - 1)\,[2\,\varrho_l - \nu_l\,g_{\min,l}]\,. \end{aligned} \tag{3.89}$$

The indices of the collision partners are distributed according to the probabilities (3.72),

$$\frac{g_i + g_j - g_{\min,l}}{(\nu_l - 1)\,[2\,\varrho_l - \nu_l\,g_{\min,l}]}\,, \tag{3.90}$$

among particles belonging to the cell D_l. The probability of a fictitious collision (3.73) is (cf. (3.68))

$$1 - \frac{\max(g_i, g_j)}{g_i + g_j - g_{\min,l}}\,\frac{\int_{\mathcal{S}^2}[1 + \kappa_l(z^{(l)};i,j,e)]\,B(v_i,v_j,e)\,de}{[1 + C_{\kappa,l}]\,c_B\,U_l^\varepsilon}\,. \tag{3.91}$$

Finally, the distribution of the direction vector is (3.74).

Example 3.13. In the case of constant weights,

$$\begin{aligned} g_i &= \bar{g}^{(n)}\,, \quad i = 1,\dots,n\,, \qquad \kappa_l = C_{\kappa,l} = 0\,, \\ g_{\min,l} &= \bar{g}^{(n)}\,, \qquad \varrho_l = \bar{g}^{(n)}\,\nu_l\,, \end{aligned} \tag{3.92}$$

one obtains the waiting time parameter

$$\hat{\lambda}_{\mathrm{coll},l}(z) = \frac{\nu_l\,(\nu_l - 1)}{2\,|D_l|}\,\bar{g}^{(n)}\,c_B\,U_l^\varepsilon\,, \tag{3.93}$$

uniform distribution of indices, the probability of a fictitious collision

$$1 - \frac{\int_{\mathcal{S}^2} B(v_i,v_j,e)\,de}{c_B\,U_l^\varepsilon}$$

and the distribution of the direction vector

$$\frac{B(v_i,v_j,e)}{\int_{\mathcal{S}^2} B(v_i,v_j,e)\,de}\,. \tag{3.94}$$

Example 3.14. In the case of variable weights we assume (3.87) and

$$\kappa_l = C_{\kappa,l}\,. \tag{3.95}$$

Then the waiting time parameter (3.89) takes the form

$$\hat{\lambda}_{\mathrm{coll},l}(z) = \frac{1}{|D_l|}\,[1 + C_{\kappa,l}]\,c_B\,U_l^{\varepsilon}\,(\nu_l - 1)\,\varrho_l\,.$$

According to the index distribution (3.90), first the index i is chosen with probability

$$\frac{(\nu_l - 2)\,g_i + \varrho_l}{2\,(\nu_l - 1)\,\varrho_l}\,, \tag{3.96}$$

and then, given i, the index j is chosen with probability

$$\frac{g_i + g_j}{(\nu_l - 2)\,g_i + \varrho_l}\,. \tag{3.97}$$

The probability of a fictitious collision (3.91) takes the form

$$1 - \frac{\max(g_i, g_j)}{g_i + g_j}\,\frac{\int_{S^2} B(v_i, v_j, e)\,de}{c_B\,U_l^{\varepsilon}}\,,$$

and the distribution of the direction vector is (3.94). Both distributions (3.96) and (3.97) are of the form

$$\frac{c_1 + p_i}{c_2}\,, \qquad i = 1, \ldots, k\,. \tag{3.98}$$

They may be modeled by the acceptance-rejection technique (cf. Section B.1.1). For example, choose i uniformly and check the condition

$$\eta \le \frac{c_1 + p_i}{c_1 + p_{\max}}\,,$$

where η is uniformly on $[0, 1]$ and

$$p_{\max} \ge \max_{i=1,\ldots,k} p_i\,.$$

3.3.5 Shells in the velocity space

Here we use some non-global upper bound for the relative particle velocities in the cell. Consider some values

$$0 < b_1 < \ldots < b_K\,, \qquad K \ge 1\,, \tag{3.99}$$

where (cf. (3.83), (3.84))

$$\frac{|v_i - V_l|}{\sqrt{T_l}} \le b_K\,, \qquad \forall i\,:\, x_i \in D_l\,. \tag{3.100}$$

Define

$$\hat{b}(v) = \min\left\{ b_k\,,\ k = 1, \dots, K\,:\, \frac{|v - V_l|}{\sqrt{T_l}} \le b_k \right\} \tag{3.101}$$

and note that

$$\frac{|v_i - V_l|}{\sqrt{T_l}} \le \hat{b}(v_i)\,, \qquad \forall i\,:\, x_i \in D_l\,. \tag{3.102}$$

The function $\hat{b}$ taking values $b_1, \dots, b_K$ provides a certain non-global majorant for the normalized velocities. Using the estimate

$$|a+b|^\varepsilon \le \max(1, 2^{\varepsilon-1})\,(a^\varepsilon + b^\varepsilon)\,, \qquad a, b, \varepsilon > 0\,,$$

one obtains

$$\begin{aligned} |v_i - v_j|^\varepsilon &\le \max(1, 2^{\varepsilon-1})\, T_l^{\frac{\varepsilon}{2}} \left[\left(\frac{|v_i - V_l|}{\sqrt{T_l}} \right)^\varepsilon + \left(\frac{|v_j - V_l|}{\sqrt{T_l}} \right)^\varepsilon \right] \\ &\le \max(1, 2^{\varepsilon-1})\, T_l^{\frac{\varepsilon}{2}} \left[\hat{b}(v_i)^\varepsilon + \hat{b}(v_j)^\varepsilon \right]. \end{aligned} \tag{3.103}$$

According to (3.103), the function

$$\begin{aligned} \hat{p}_{\mathrm{coll},l}(z; i, j) = \frac{1}{|D_l|}\, \chi_{D_l}(x_i)\, \chi_{D_l}(x_j) \times \\ [g_i + g_j - g_{\min,l}]\, [1 + C_{\kappa,l}]\, c_B\, \max(1, 2^{\varepsilon-1})\, T_l^{\frac{\varepsilon}{2}} \left[\hat{b}(v_i)^\varepsilon + \hat{b}(v_j)^\varepsilon \right] \end{aligned} \tag{3.104}$$

satisfies (3.76).

We introduce the notation

$$I_k = \{ i\,:\, \hat{b}(v_i) = b_k \}\,, \qquad k = 1, \dots, K\,, \tag{3.105}$$

for the groups of indices of particles with normalized velocities having a given individual majorant, or belonging to a given shell in the velocity space. Let $|I_k|$ denote the number of those particles and

$$\gamma_k = \sum_{i \in I_k} g_i\,, \qquad k = 1, \dots, K\,, \tag{3.106}$$

denote their weight. Note that (cf. (3.82), (3.81))

$$\sum_{k=1}^{K} \gamma_k = \varrho_l\,, \qquad \sum_{k=1}^{K} |I_k| = \nu_l\,.$$

With the majorant (3.104), the waiting time parameter (3.70) takes the form

$$\begin{aligned}\hat\lambda_{\mathrm{coll},l}(z) &= \frac{1}{2\,|D_l|}\,[1+C_{\kappa,l}]\,c_B\,\max(1,2^{\varepsilon-1})\,T_l^{\frac{\varepsilon}{2}}\times\\ &\qquad\sum_{i\neq j\,:\,x_i,x_j\in D_l}[g_i+g_j-g_{\min,l}]\left[\hat b(v_i)^\varepsilon+\hat b(v_j)^\varepsilon\right]\\ &= \frac{1}{|D_l|}\,[1+C_{\kappa,l}]\,c_B\,\max(1,2^{\varepsilon-1})\,T_l^{\frac{\varepsilon}{2}}\times\\ &\quad\left[(\nu_l-2)\sum_{i\,:\,x_i\in D_l}g_i\,\hat b(v_i)^\varepsilon+\Big[\varrho_l-(\nu_l-1)\,g_{\min,l}\Big]\sum_{i\,:\,x_i\in D_l}\hat b(v_i)^\varepsilon\right]\\ &= \frac{1}{|D_l|}\,[1+C_{\kappa,l}]\,c_B\,\max(1,2^{\varepsilon-1})\,T_l^{\frac{\varepsilon}{2}}\times\\ &\quad\left[(\nu_l-2)\sum_{k=1}^K\gamma_k\,b_k^\varepsilon+\Big[\varrho_l-(\nu_l-1)\,g_{\min,l}\Big]\sum_{k=1}^K|I_k|\,b_k^\varepsilon\right].\end{aligned}\tag{3.107}$$

According to (3.72) the distribution of the indices i,j is

$$\frac{[g_i+g_j-g_{\min,l}]\left[\hat b(v_i)^\varepsilon+\hat b(v_j)^\varepsilon\right]}{2\left[(\nu_l-2)\sum_{k=1}^K\gamma_k\,b_k^\varepsilon+[\varrho_l-(\nu_l-1)\,g_{\min,l}]\sum_{k=1}^K|I_k|\,b_k^\varepsilon\right]}\tag{3.108}$$

among particles belonging to the cell D_l. The probability of a fictitious collision (3.73) is (cf. (3.68))

$$1-\frac{\int_{\mathcal{S}^2}[1+\kappa_l(z^{(l)};i,j,e)]\,B(v_i,v_j,e)\,de}{[1+C_{\kappa,l}]\,c_B\,\max(1,2^{\varepsilon-1})\,T_l^{\frac{\varepsilon}{2}}\,[\hat b(v_i)^\varepsilon+\hat b(v_j)^\varepsilon]}\,\frac{\max(g_i,g_j)}{[g_i+g_j-g_{\min,l}]}\,.\tag{3.109}$$

Finally, the distribution of the direction vector is (3.74).

Note that (3.108) is a mixture of two distributions, which are symmetric to each other. Therefore, the indices i,j are chosen according to

$$\frac{[g_i+g_j-g_{\min,l}]\,\hat b(v_i)^\varepsilon}{(\nu_l-2)\sum_{k=1}^K\gamma_k\,b_k^\varepsilon+[\varrho_l-(\nu_l-1)\,g_{\min,l}]\sum_{k=1}^K|I_k|\,b_k^\varepsilon}\,,$$

and their order is changed with probability $\frac{1}{2}$. This last step can be omitted since the result of the jump does not depend on the order of the indices (provided κ_l is symmetric, cf. (3.63), (3.64)). Thus, the index i is distributed according to

$$\frac{g_i\,\hat b(v_i)^\varepsilon\,(\nu_l-2)+[\varrho_l-(\nu_l-1)\,g_{\min,l}]\,\hat b(v_i)^\varepsilon}{(\nu_l-2)\sum_{k=1}^K\gamma_k\,b_k^\varepsilon+[\varrho_l-(\nu_l-1)\,g_{\min,l}]\sum_{k=1}^K|I_k|\,b_k^\varepsilon}\,.$$

First the shell index $k=1,\dots,K$ is chosen according to the probabilities

$$\frac{\gamma_k\, b_k^\varepsilon\,(\nu_l-2)+[\varrho_l-(\nu_l-1)\,g_{\min,l}]\,|I_k|\,b_k^\varepsilon}{(\nu_l-2)\sum_{k=1}^K \gamma_k\, b_k^\varepsilon+[\varrho_l-(\nu_l-1)\,g_{\min,l}]\sum_{k=1}^K |I_k|\,b_k^\varepsilon}\,, \tag{3.110}$$

and then the particle in the shell is chosen according to the probabilities

$$\frac{g_i\,(\nu_l-2)+\varrho_l-(\nu_l-1)\,g_{\min,l}}{\gamma_k\,(\nu_l-2)+[\varrho_l-(\nu_l-1)\,g_{\min,l}]\,|I_k|}\,. \tag{3.111}$$

Given i, the index $j\neq i$ is distributed according to the probabilities

$$\frac{g_i+g_j-g_{\min,l}}{g_i\,(\nu_l-2)+\varrho_l-(\nu_l-1)\,g_{\min,l}}\,. \tag{3.112}$$

Example 3.15. In the case of constant weights (3.92) one obtains (cf. (3.106))

$$\gamma_k=\bar g^{(n)}\,|I_k|\,.$$

The waiting time parameter (3.107) takes the form

$$\begin{aligned}\hat\lambda_{\mathrm{coll},l}(z)&=\frac{1}{|D_l|}\,c_B\,\max(1,2^{\varepsilon-1})\,T_l^{\frac{\varepsilon}{2}}\,\times\\&\qquad\left[(\nu_l-2)\sum_{k=1}^K\bar g^{(n)}\,|I_k|\,b_k^\varepsilon+[\nu_l\,\bar g^{(n)}-(\nu_l-1)\,\bar g^{(n)}]\sum_{k=1}^K|I_k|\,b_k^\varepsilon\right]\\&=\frac{1}{|D_l|}\,c_B\,\max(1,2^{\varepsilon-1})\,T_l^{\frac{\varepsilon}{2}}\,(\nu_l-1)\,\bar g^{(n)}\sum_{k=1}^K|I_k|\,b_k^\varepsilon\,.\end{aligned} \tag{3.113}$$

The shell index $k=1,\dots,K$ is generated according to the probabilities (3.110),

$$\frac{|I_k|\,b_k^\varepsilon}{\sum_{k=1}^K|I_k|\,b_k^\varepsilon}\,, \tag{3.114}$$

and the particle index i in that shell is chosen uniformly, according to (3.111). Given i, the parameter $j\neq i$ is generated uniformly, according to (3.112). The probability of a fictitious collision (3.109) is

$$1-\frac{\int_{S^2}B(v_i,v_j,e)\,de}{c_B\,\max(1,2^{\varepsilon-1})\,T_l^{\frac{\varepsilon}{2}}\,[\hat b(v_i)^\varepsilon+\hat b(v_j)^\varepsilon]}\,.$$

The distribution of the direction vector is (3.94).

Remark 3.16. The value of b_K is increased (if necessary) during the simulation. The values of $|I_k|$ have to be updated after each collision. If some $|I_k|$ equals zero, then the corresponding group is simply not chosen (cf. (3.114)).

Example 3.17. In the case of variable weights we assume (3.87) and (3.95). Then the waiting time parameter (3.107) takes the form

$$\hat{\lambda}_{\mathrm{coll},l}(z) = \frac{1}{|D_l|}\,[1+C_{\kappa,l}]\,c_B\,\max(1,2^{\varepsilon-1})\,T_l^{\frac{\varepsilon}{2}}\left[(\nu_l-2)\sum_{k=1}^{K}\gamma_k\,b_k^{\varepsilon}+\varrho_l\sum_{k=1}^{K}|I_k|\,b_k^{\varepsilon}\right].$$

The shell index $k = 1,\dots,K$ is generated according to the probabilities (3.110),

$$\frac{\gamma_k\,b_k^{\varepsilon}\,(\nu_l-2)+\varrho_l\,|I_k|\,b_k^{\varepsilon}}{(\nu_l-2)\sum_{k=1}^{K}\gamma_k\,b_k^{\varepsilon}+\varrho_l\sum_{k=1}^{K}|I_k|\,b_k^{\varepsilon}}\,,$$

and the particle index in that shell is chosen according to the probabilities (3.111),

$$\frac{g_i\,(\nu_l-2)+\varrho_l}{\gamma_k\,(\nu_l-2)+\varrho_l\,|I_k|}\,. \tag{3.115}$$

Given i, the index $j\neq i$ is distributed according to the probabilities (3.112),

$$\frac{g_i+g_j}{g_i\,(\nu_l-2)+\varrho_l}\,. \tag{3.116}$$

The probability of a fictitious collision (3.109) takes the form

$$1-\frac{\int_{S^2}B(v_i,v_j,e)\,de}{c_B\,\max(1,2^{\varepsilon-1})\,T_l^{\frac{\varepsilon}{2}}\,[\hat{b}(v_i)^{\varepsilon}+\hat{b}(v_j)^{\varepsilon}]}\,\frac{\max(g_i,g_j)}{[g_i+g_j]}\,, \tag{3.117}$$

and the distribution of the direction vector is (3.94).

Remark 3.18. Note that the effort for generating the shell index is proportional to the number of shells. The distributions (3.115) and (3.116) are of the form (3.98) and can be modeled by an appropriate acceptance-rejection technique (cf. Section B.1.1). For example, maximum weights in the shells can be used.

3.3.6 Temperature time counter

Here we consider another upper bound for the relative particle velocity in the cell, using the local temperature (3.84). Note that

$$|v-w|^{\varepsilon}=T_l^{\frac{\varepsilon}{2}}\left(\frac{|v-w|}{\sqrt{T_l}}\right)^{\varepsilon}\le T_l^{\frac{\varepsilon}{2}}\left[\alpha\,\frac{|v-w|^2}{T_l}+\beta\right], \tag{3.118}$$

where $\alpha,\beta>0$ are such that

$$x^{\varepsilon}\le\alpha\,x^2+\beta\,,\qquad \forall x\ge 0\,. \tag{3.119}$$

According to (3.118), the function

$$\hat{p}_{\mathrm{coll},l}(z;i,j) = \frac{1}{|D_l|}\,\chi_{D_l}(x_i)\,\chi_{D_l}(x_j)\,[g_i+g_j-g_{\min,l}]\,[1+C_{\kappa,l}]\,c_B\,T_l^{\frac{\varepsilon}{2}}\left[\alpha\,\frac{|v_i-v_j|^2}{T_l}+\beta\right]. \tag{3.120}$$

satisfies (3.76).

With the majorant (3.120), the waiting time parameter (3.70) takes the form (cf. (3.85))

$$\begin{aligned}\hat{\lambda}_{\mathrm{coll},l}(z) &= \frac{1}{2\,|D_l|}\,[1+C_{\kappa,l}]\,c_B\,T_l^{\frac{\varepsilon}{2}}\left[\frac{2\,\alpha}{T_l}\sum_{i,j\,:\,x_i,x_j\in D_l} g_i\,|v_i-v_j|^2+\right.\\ &\left.\quad 2\,\beta\,\varrho_l\,(\nu_l-1)-g_{\min,l}\left(\frac{\alpha}{T_l}\sum_{i,j\,:\,x_i,x_j\in D_l}|v_i-v_j|^2+\beta\,\nu_l\,(\nu_l-1)\right)\right]\\ &= \frac{1}{2\,|D_l|}\,[1+C_{\kappa,l}]\,c_B\,T_l^{\frac{\varepsilon}{2}}\left[\alpha\left(\frac{2\,\varrho_l}{T_l}\sum_{i\,:\,x_i\in D_l}|v_i-V_l|^2+6\,\varrho_l\,\nu_l-\right.\right.\\ &\left.\left.\quad\frac{g_{\min,l}}{T_l}\sum_{i,j\,:\,x_i,x_j\in D_l}|v_i-v_j|^2\right)+\beta\Big(2\,\varrho_l\,(\nu_l-1)-g_{\min,l}\,\nu_l\,(\nu_l-1)\Big)\right]\\ &= \frac{1}{2\,|D_l|}\,[1+C_{\kappa,l}]\,c_B\,T_l^{\frac{\varepsilon}{2}}\Big(c_1\,\alpha+c_2\,\beta\Big).\end{aligned} \tag{3.121}$$

In order to increase the expected time step, we minimize the expression (3.121) with respect to α,β satisfying (3.119).

Lemma 3.19. *For any $c_1,\,c_2>0$, the expression $c_1\,\alpha+c_2\,\beta$ takes its minimum from among the α,β satisfying (3.119) for*

$$\alpha=\alpha_*=\left(\frac{c_1}{c_2}\right)^{\frac{\varepsilon}{2}-1}\,\frac{\varepsilon}{2} \tag{3.122}$$

and

$$\beta=\beta_*=\left(\frac{c_1}{c_2}\right)^{\frac{\varepsilon}{2}}\left(1-\frac{\varepsilon}{2}\right). \tag{3.123}$$

The minimum value is

$$c_1\,\alpha_*+c_2\,\beta_*=c_1^{\frac{\varepsilon}{2}}\,c_2^{1-\frac{\varepsilon}{2}}. \tag{3.124}$$

Proof. The function

$$\varphi(x)=\alpha\,x^2-x^\varepsilon+\beta\,,\qquad x\ge 0\,,\quad \alpha,\beta>0\,,\quad \varepsilon\in(0,2)\,,$$

takes its minimum at some point x_0 satisfying $\varphi'(x_0) = 0$ so that

$$x_0 = \Big(\frac{\varepsilon}{2\,\alpha}\Big)^{\frac{1}{2-\varepsilon}} \qquad \text{or} \qquad \alpha = \frac{\varepsilon\, x_0^{\varepsilon-2}}{2}\,. \tag{3.125}$$

The minimum is non-negative if

$$\beta \geq x_0^{\varepsilon} - \alpha\, x_0^2 = x_0^{\varepsilon}\left(1 - \frac{\varepsilon}{2}\right). \tag{3.126}$$

In order to minimize the expression $c_1\,\alpha + c_2\,\beta$, we consider the function

$$\psi(x_0) = c_1\,\frac{\varepsilon\, x_0^{\varepsilon-2}}{2} + c_2\, x_0^{\varepsilon}\left(1 - \frac{\varepsilon}{2}\right).$$

Condition

$$\psi'(x_*) = \frac{c_1}{2}\,(\varepsilon-2)\,\varepsilon\, x_*^{\varepsilon-3} + c_2\,\varepsilon\, x_*^{\varepsilon-1}\left(1 - \frac{\varepsilon}{2}\right) = 0$$

implies $x_* = \sqrt{c_1/c_2}$. Thus, formulas (3.122)-(3.124) follow from (3.125) and (3.126). ■

With the optimal choice (3.122), (3.123) of the parameters α, β, the waiting time parameter (3.121) takes the form (cf. (3.124))

$$\hat{\lambda}_{\mathrm{coll},l}(z) = \frac{1}{2\,|D_l|}\,[1 + C_{\kappa,l}]\,c_B\,T_l^{\frac{\varepsilon}{2}}\,c_1^{\frac{\varepsilon}{2}}\,c_2^{1-\frac{\varepsilon}{2}}\,, \tag{3.127}$$

where

$$c_1 = c_1(z) = \frac{2\,\varrho_l}{T_l}\sum_{i\,:\,x_i\in D_l}|v_i - V_l|^2 + 6\,\varrho_l\,\nu_l - \frac{g_{\min,l}}{T_l}\sum_{i,j\,:\,x_i,x_j\in D_l}|v_i - v_j|^2 \tag{3.128}$$

and

$$c_2 = c_2(z) = 2\,\varrho_l\,(\nu_l - 1) - g_{\min,l}\,\nu_l\,(\nu_l - 1)\,. \tag{3.129}$$

According to (3.72), the distribution of the indices i, j is (cf. (3.120), (3.127), (3.122), (3.123))

$$\frac{(g_i + g_j - g_{\min,l})\left[\alpha_*\,\frac{|v_i - v_j|^2}{T_l} + \beta_*\right]}{c_1^{\frac{\varepsilon}{2}}\,c_2^{1-\frac{\varepsilon}{2}}} = \tag{3.130}$$

$$(g_i + g_j - g_{\min,l})\left[\frac{\varepsilon}{2\,c_1}\,\frac{|v_i - v_j|^2}{T_l} + \frac{1}{c_2}\left(1 - \frac{\varepsilon}{2}\right)\right].$$

The probability of a fictitious collision (3.73) is (cf. (3.68), (3.120))

$$1-\frac{\max(g_i,g_j)}{[g_i+g_j-g_{\min,l}]}\,\frac{\int_{\mathcal{S}^2}[1+\kappa_l(z^{(l)};i,j,e)]\,B(v_i,v_j,e)\,de}{[1+C_{\kappa,l}]\,c_B\,T_l^{\frac{\varepsilon}{2}}\left[\alpha_*\,\frac{|v_i-v_j|^2}{T_l}+\beta_*\right]}=1-\tag{3.131}$$

$$\frac{\max(g_i,g_j)}{[g_i+g_j-g_{\min,l}]}\,\frac{\int_{\mathcal{S}^2}[1+\kappa_l(z^{(l)};i,j,e)]\,B(v_i,v_j,e)\,de}{[1+C_{\kappa,l}]\,c_B\,T_l^{\frac{\varepsilon}{2}}\left[\left(\frac{c_1}{c_2}\right)^{\frac{\varepsilon}{2}-1}\frac{\varepsilon}{2}\,\frac{|v_i-v_j|^2}{T_l}+\left(\frac{c_1}{c_2}\right)^{\frac{\varepsilon}{2}}\left(1-\frac{\varepsilon}{2}\right)\right]}.$$

The distribution of the direction vector is (3.74).

Constant weights

Now we specify the general procedure in the case of constant weights (3.92). One obtains (cf. (3.128), (3.129), (3.122), (3.123), (3.86), (3.84))

$$c_1=\frac{2\,\bar g^{(n)}\,\nu_l}{T_l}\,3\,\nu_l\,T_l+6\,\bar g^{(n)}\,\nu_l^2-\frac{\bar g^{(n)}}{T_l}\,6\,T_l\,\nu_l^2=6\,\bar g^{(n)}\,\nu_l^2\tag{3.132}$$

and

$$c_2=2\,\bar g^{(n)}\,\nu_l\,(\nu_l-1)-\bar g^{(n)}\,\nu_l\,(\nu_l-1)=\bar g^{(n)}\,\nu_l\,(\nu_l-1)\,.\tag{3.133}$$

The waiting time parameter (3.127) takes the form

$$\begin{aligned}\hat\lambda_{\mathrm{coll},l}(z)&=\frac{1}{2\,|D_l|}\,c_B\,T_l^{\frac{\varepsilon}{2}}\,\bar g^{(n)}\,\nu_l\,(\nu_l-1)\left(\frac{6\,\nu_l}{\nu_l-1}\right)^{\frac{\varepsilon}{2}}\\&=\frac{\bar g^{(n)}}{2\,|D_l|}\,c_B\,\nu_l\,(\nu_l-1)\left(6\,T_l\,\frac{\nu_l}{\nu_l-1}\right)^{\frac{\varepsilon}{2}}.\end{aligned}\tag{3.134}$$

The distribution (3.130) of the indices i,j is

$$\frac{\varepsilon}{12\,\nu_l^2}\,\frac{|v_i-v_j|^2}{T_l}+\frac{1}{\nu_l\,(\nu_l-1)}\,\left(1-\frac{\varepsilon}{2}\right).\tag{3.135}$$

The probability of a fictitious collision (3.131) is

$$1-\frac{\int_{\mathcal{S}^2}B(v_i,v_j,e)\,de}{c_B\,T_l^{\frac{\varepsilon}{2}}\left[\frac{\varepsilon}{2}\left(\frac{6\,\nu_l}{\nu_l-1}\right)^{\frac{\varepsilon}{2}-1}\,\frac{|v_i-v_j|^2}{T_l}+\left(1-\frac{\varepsilon}{2}\right)\left(\frac{6\,\nu_l}{\nu_l-1}\right)^{\frac{\varepsilon}{2}}\right]}.$$

The distribution of the direction vector is (3.94).

Remark 3.20. If the rough estimate

$$\left(\frac{|v-w|}{\sqrt{T_l}}\right)^{\varepsilon}\le\frac{|v-w|^2}{T_l}+1$$

was used in (3.118), instead of optimizing α,β, then one would obtain (3.127) with c_1+c_2 instead of $c_1^{\frac{\varepsilon}{2}}\,c_2^{1-\frac{\varepsilon}{2}}$. Using (3.132), (3.133) one gets

$$\hat{\lambda}_{\mathrm{coll},l}(z) = \frac{\bar{g}^{(n)}}{2\,|D_l|}\, c_B\, \nu_l\, T_l^{\frac{\varepsilon}{2}}\, (7\,\nu_l - 1)$$

instead of (3.134), i.e. a factor $(7\,\nu_l - 1)$ instead of $(\nu_l - 1)\left(\frac{6\,\nu_l}{\nu_l - 1}\right)^{\frac{\varepsilon}{2}}$, or, asymptotically, 7 instead of $6^{\frac{\varepsilon}{2}}$. Thus, the time steps would be considerably bigger. ■

Note that (3.86) implies (cf. (3.88))

$$6\,T_l\,(\bar{g}^{(n)}\,\nu_l)^2 = (\bar{g}^{(n)})^2 \sum_{i\neq j\,:\,x_i,x_j\in D_l} |v_i - v_j|^2 \leq (\bar{g}^{(n)})^2\,\nu_l\,(\nu_l - 1)\,U_l^2$$

so that

$$6\,T_l\,\frac{\nu_l}{\nu_l - 1} \leq U_l^2\,. \tag{3.136}$$

Thus, the waiting time parameter (3.134) is always bigger than the waiting time parameter (3.93) obtained for the global upper bound. The corresponding time steps may differ by several orders of magnitude, as the following example shows.

Example 3.21. Consider the spatially homogeneous case and the measure

$$c\,\delta_{-w\,\frac{1-c}{c}}(dv) + (1-c)\,\delta_w(dv)\,, \qquad w\in\mathbb{R}^3\,, \quad c\in(0,1)\,.$$

An approximating particle system is

$$v_i = -w\,\frac{1-c}{c}\,, \quad i = 1,\ldots,[c\,n]\,, \qquad v_i = w\,, \quad i = [c\,n]+1,\ldots,n\,,$$

where [.] denotes the integer part. We have (cf. (3.83), (3.84))

$$V^{(n)} = -w\,\frac{1-c}{c}\,\frac{[c\,n]}{n} + w\left(1 - \frac{[c\,n]}{n}\right) \quad \to \quad 0\,,$$

$$3\,T^{(n)} = |w|^2\,\frac{(1-c)^2}{c^2}\,\frac{[c\,n]}{n} + |w|^2\left(1 - \frac{[c\,n]}{n}\right) - [V^{(n)}]^2 \quad \to \quad |w|^2\,\frac{1-c}{c}$$

and

$$U^{(n)} = \max_{i,j}|v_i - v_j| = |w|\,\frac{1}{c}$$

so that

$$\lim_{n\to\infty}\frac{U^{(n)}}{\sqrt{6\,T^{(n)}}} = \frac{1}{\sqrt{2\,c\,(1-c)}}\,. \tag{3.137}$$

In the case $c = 0.5$ the limit in (3.137) is $\sqrt{2}$ being relatively close to the lower bound given by (3.136). If $c\sim 0$ or $c\sim 1$, then the right-hand side of (3.137) is arbitrarily large. ■

However, the distribution of the indices (3.135) is much more complicated than the uniform distribution related to the time counter (3.93) obtained for the global upper bound. We represent the probabilities (3.135) in the form $p_{i,j} = p_i\, p_{j|i}\,,$ where the probability of i is (cf. (3.85))

$$p_i = \sum_j p_{i,j} = \frac{\varepsilon}{12\,\nu_l}\,\frac{|v_i - V_l|^2}{T_l} + \frac{1}{\nu_l}\left(1 - \frac{\varepsilon}{4}\right) \tag{3.138}$$

and the conditional probability of j given i takes the form

$$p_{j|i} = \frac{p_{i,j}}{p_i} = \frac{\frac{\varepsilon}{12\,\nu_l}\,\frac{|v_i - v_j|^2}{T_l} + \frac{1}{\nu_l - 1}\left(1 - \frac{\varepsilon}{2}\right)}{\frac{\varepsilon}{12}\,\frac{|v_i - V_l|^2}{T_l} + 1 - \frac{\varepsilon}{4}}\,. \tag{3.139}$$

Both distributions (3.138) and (3.139) are generated using the acceptance-rejection technique (cf. Section B.1.1). We apply the idea of ordering the particles with respect to the absolute values of their normalized velocities (cf. (3.99)-(3.102)).

The distribution of the first index i is generated using (cf. (B.1))

$$X = \{i = 1, 2, \ldots, n \,:\, x_i \in D_l\}$$

and

$$f_i = \frac{\varepsilon}{12}\,\frac{|v_i - V_l|^2}{T_l} + 1 - \frac{\varepsilon}{4}\,, \qquad F_i = \frac{\varepsilon}{12}\,\hat{b}(v_i)^2 + 1 - \frac{\varepsilon}{4}\,.$$

Since (cf. (3.105))

$$\sum_j F_j =$$

$$\sum_{k=1}^{K} \sum_{j\,:\,\hat{b}(v_j) = b_k} F_j = \sum_{k=1}^{K} |I_k|\left(\frac{\varepsilon}{12}\,b_k^2 + 1 - \frac{\varepsilon}{4}\right) = \frac{\varepsilon}{12}\,\sum_{k=1}^{K} |I_k|\,b_k^2 + \nu_l\left(1 - \frac{\varepsilon}{4}\right),$$

the distribution (B.2) takes the form

$$\frac{F_i}{\sum_j F_j} = \frac{\frac{\varepsilon}{12}\,\sum_{k=1}^{K} |I_k|\,b_k^2}{\frac{\varepsilon}{12}\,\sum_{k=1}^{K} |I_k|\,b_k^2 + \nu_l\,(1 - \frac{\varepsilon}{4})}\,\frac{\hat{b}(v_i)^2}{\sum_{k=1}^{K} |I_k|\,b_k^2} + \frac{\nu_l\,(1 - \frac{\varepsilon}{4})}{\frac{\varepsilon}{12}\,\sum_{k=1}^{K} |I_k|\,b_k^2 + \nu_l\,(1 - \frac{\varepsilon}{4})}\,\frac{1}{\nu_l}\,.$$

According to this representation the index i is distributed uniformly with probability

$$\frac{\nu_l\,(1 - \frac{\varepsilon}{4})}{\frac{\varepsilon}{12}\,\sum_{k=1}^{K} |I_k|\,b_k^2 + \nu_l\,(1 - \frac{\varepsilon}{4})}\,.$$

With probability

$$1 - \frac{\nu_l \left(1 - \frac{\varepsilon}{4}\right)}{\frac{\varepsilon}{12} \sum_{k=1}^{K} |I_k|\, b_k^2 + \nu_l \left(1 - \frac{\varepsilon}{4}\right)} ,$$

the index i is distributed according to the distribution

$$\frac{\hat{b}(v_i)^2}{\sum_{k=1}^{K} |I_k|\, b_k^2} .$$

Thus, first the number of a group of indices is chosen according to the probabilities

$$\frac{|I_k|\, b_k^2}{\sum_{\mu=1}^{K} |I_\mu|\, b_\mu^2} , \qquad k = 1, \ldots, K ,$$

and then the index i is chosen uniformly in the group I_k. Finally, the index i is accepted with probability

$$\frac{\frac{\varepsilon}{12} \frac{|v_i - V_l|^2}{T_l} + 1 - \frac{\varepsilon}{4}}{\frac{\varepsilon}{12} \hat{b}(v_i)^2 + 1 - \frac{\varepsilon}{4}} .$$

The distribution of the second index j is generated using (cf. (B.1))

$$X_i = \{j = 1, 2, \ldots, n \,:\, j \neq i \,,\; x_j \in D_l\} ,$$

$$f_{j|i} = \frac{\varepsilon}{12} \frac{|v_i - v_j|^2}{T} + \frac{\nu_l}{\nu_l - 1} \left(1 - \frac{\varepsilon}{2}\right)$$

and (cf. (3.103) with $\varepsilon = 2$)

$$F_{j|i} = \frac{\varepsilon}{6} \left[\hat{b}(v_i)^2 + \hat{b}(v_j)^2\right] + \frac{\nu_l}{\nu_l - 1} \left(1 - \frac{\varepsilon}{2}\right) .$$

Since

$$\sum_{j:\, j \neq i} F_{j|i} = (\nu_l - 2) \frac{\varepsilon}{6} \hat{b}(v_i)^2 + \nu_l \left(1 - \frac{\varepsilon}{2}\right) + \frac{\varepsilon}{6} \sum_{k=1}^{K} |I_k|\, b_k^2 ,$$

the distribution (B.2) takes the form

$$\frac{F_{j|i}}{\sum_{\mu:\, \mu \neq i} F_{\mu|i}} = \frac{(\nu_l - 1) \left[\frac{\varepsilon}{6} \hat{b}(v_i)^2 + \frac{\nu_l}{\nu_l - 1} \left(1 - \frac{\varepsilon}{2}\right)\right]}{(\nu_l - 2) \frac{\varepsilon}{6} \hat{b}(v_i)^2 + \nu_l \left(1 - \frac{\varepsilon}{2}\right) + \frac{\varepsilon}{6} \sum_{k=1}^{K} |I_k|\, b_k^2} \frac{1}{(\nu_l - 1)} +$$
$$\frac{\frac{\varepsilon}{6} \left[\sum_{k=1}^{K} |I_k|\, b_k^2 - \hat{b}(v_i)^2\right]}{(\nu_l - 2) \frac{\varepsilon}{6} \hat{b}(v_i)^2 + \nu_l \left(1 - \frac{\varepsilon}{2}\right) + \frac{\varepsilon}{6} \sum_{k=1}^{K} |I_k|\, b_k^2} \frac{\hat{b}(v_j)^2}{\left[\sum_{k=1}^{K} |I_k|\, b_k^2 - \hat{b}(v_i)^2\right]} .$$

According to this representation the index $j \neq i$ is distributed uniformly, with probability

$$\frac{(\nu_l - 1)\left[\frac{\varepsilon}{6}\,\hat{b}(v_i)^2 + \frac{\nu_l}{\nu_l - 1}\left(1 - \frac{\varepsilon}{2}\right)\right]}{(\nu_l - 2)\,\frac{\varepsilon}{6}\,\hat{b}(v_i)^2 + \nu_l\left(1 - \frac{\varepsilon}{2}\right) + \frac{\varepsilon}{6}\,\sum_{k=1}^{K} |I_k|\, b_k^2}\,.$$

With probability

$$1 - \frac{(\nu_l - 1)\left[\frac{\varepsilon}{6}\,\hat{b}(v_i)^2 + \frac{\nu_l}{\nu_l - 1}\left(1 - \frac{\varepsilon}{2}\right)\right]}{(\nu_l - 2)\,\frac{\varepsilon}{6}\,\hat{b}(v_i)^2 + \nu_l\left(1 - \frac{\varepsilon}{2}\right) + \frac{\varepsilon}{6}\,\sum_{k=1}^{K} |I_k|\, b_k^2}\,,$$

the index $j \neq i$ is distributed according to

$$\frac{\hat{b}(v_j)^2}{\sum_{k=1}^{K} |I_k|\, b_k^2 - \hat{b}(v_i)^2}\,.$$

Thus, first the number of the group is chosen according to the probabilities

$$\frac{|I_k|\, b_k^2 - \chi_{I_k}(i)\,\hat{b}(v_i)^2}{\sum_{\mu=1}^{K} |I_\mu|\, b_\mu^2 - \hat{b}(v_i)^2}\,, \qquad k = 1, \ldots, K\,,$$

and then the index j is generated uniformly in the corresponding group. Finally, the index j is accepted with probability

$$\frac{\frac{\varepsilon}{12}\,\frac{|v_i - v_j|^2}{T_l} + \frac{\nu_l}{\nu_l - 1}\left(1 - \frac{\varepsilon}{2}\right)}{\frac{\varepsilon}{6}\left[\hat{b}(v_i)^2 + \hat{b}(v_j)^2\right] + \frac{\nu_l}{\nu_l - 1}\left(1 - \frac{\varepsilon}{2}\right)}\,.$$

Variable weights

Finally, we consider a simplification of the general procedure in the case of variable weights. Assuming (3.87) and (3.95), one obtains (cf. (3.128), (3.129))

$$c_1 = \frac{2\,\varrho_l}{T_l} \sum_{i\,:\,x_i \in D_l} |v_i - V_l|^2 + 6\,\varrho_l\,\nu_l \qquad \text{and} \qquad c_2 = 2\,\varrho_l\,(\nu_l - 1)\,.$$

The waiting time parameter (3.127) takes the form

$$\hat{\lambda}_{\mathrm{coll},l}(z) = \frac{1}{|D_l|}\,[1 + C_{\kappa,l}]\,c_B\,T_l^{\frac{\varepsilon}{2}}\,\varrho_l\,(\nu_l - 1)\left(\frac{1}{T_l\,(\nu_l - 1)} \sum_{i\,:\,x_i \in D_l} |v_i - V_l|^2 + \frac{3\,\nu_l}{\nu_l - 1}\right)^{\frac{\varepsilon}{2}}\,.$$

The distribution (3.130) of the indices i, j is

$$(g_i + g_j)\left[\frac{\varepsilon}{2\,c_1}\,\frac{|v_i - v_j|^2}{T_l} + \frac{1}{c_2}\left(1 - \frac{\varepsilon}{2}\right)\right].$$

The probability of a fictitious collision (3.131) is

$$1 - \frac{\max(g_i, g_j)}{[g_i + g_j]}\,\frac{\int_{\mathcal{S}^2} B(v_i, v_j, e)\,de}{c_B\,T_l^{\frac{\varepsilon}{2}}\left[\left(\frac{c_1}{c_2}\right)^{\frac{\varepsilon}{2}-1}\,\frac{\varepsilon}{2}\,\frac{|v_i - v_j|^2}{T_l} + \left(\frac{c_1}{c_2}\right)^{\frac{\varepsilon}{2}}\left(1 - \frac{\varepsilon}{2}\right)\right]}.$$

The distribution of the direction vector is (3.94).

3.4 Controlling the number of particles

Modeling collisions by weighted particles leads to an increase in the number of particles. Thus in most situations (except when absorption is strong enough) it is necessary to control the number of simulation particles, i.e. to reduce the system when it becomes too large. In this section we modify the collision part described in Section 3.3 so that the number of particles in the system remains bounded. For the modified procedure, we prove a convergence theorem.

3.4.1 Collision processes with reduction

We introduce a sequence of Markov processes

$$Z^{(n)}(t) = \left((x_i^{(n)}(t), v_i^{(n)}(t), g_i^{(n)}(t))\,,\quad i = 1, \dots, \nu^{(n)}(t)\right),\quad t \geq 0\,,\quad n = 1, 2, \dots\,. \tag{3.140}$$

The state spaces are

$$\mathcal{Z}^{(n)} = \left\{z \in \mathcal{Z}' :\quad \sum_{i=1}^{\nu} g_i \leq C_\mu\,,\quad \max_{i=1,\dots,\nu} g_i \leq g_{\max}^{(n)}\,,\quad \nu \leq \nu_{\max}^{(n)} + 2\right\}, \tag{3.141}$$

where

$$\mathcal{Z}' = \left\{\left(x_1, v_1, g_1; \dots; x_\nu, v_\nu, g_\nu\right) :\quad \nu = 1, 2, \dots\,,\right.$$
$$\left. x_i \in D\,,\quad v_i \in \mathbb{R}^3\,,\quad g_i > 0\,,\quad i = 1, \dots, \nu\right\}.$$

The parameter $C_\mu > 0$ determines a bound for the mass of the system, the parameters $g_{\max}^{(n)} > 0$ are bounds for the individual particle weights, and the parameters $\nu_{\max}^{(n)} > 0$ are some particle number bounds indicating reduction

jumps. The time evolution of the processes (3.140) is determined by the generators

$$\mathcal{A}^{(n)}\Phi(z) = \int_{\mathcal{Z}^{(n)}} [\Phi(\tilde{z}) - \Phi(z)]\, Q^{(n)}(z, d\tilde{z})\,, \qquad z \in \mathcal{Z}^{(n)}\,, \tag{3.142}$$

where

$$Q^{(n)}(z, d\tilde{z}) = \begin{cases} Q_{\text{coll}}(z; d\tilde{z})\,, & \text{if} \quad \nu \le \nu_{\max}^{(n)}\,, \\ \\ Q_{\text{red}}^{(n)}(z; d\tilde{z})\,, & \text{if} \quad \nu > \nu_{\max}^{(n)}\,, \end{cases} \tag{3.143}$$

and Φ are appropriate test functions on $\mathcal{Z}^{(n)}$.

The transition measure, corresponding to collision jumps, is (cf. (3.19))

$$Q_{\text{coll}}(z; d\tilde{z}) = \frac{1}{2} \sum_{1 \le i \ne j \le \nu} \int_{\mathcal{S}^2} \delta_{J_{\text{coll}}(z;i,j,e)}(d\tilde{z})\, p_{\text{coll}}(z; i, j, e)\, de\,, \tag{3.144}$$

where $z \in \mathcal{Z}^{(n)}$ and the jump transformation has the form (cf. (3.1))

$$[J_{\text{coll}}(z; i, j, e)]_k = \begin{cases} (x_k, v_k, g_k) & , \quad \text{if} \quad k \le \nu\,,\ k \ne i, j\,, \\ (x_i, v'(v_i, v_j, e), \gamma_{\text{coll}}(z; i, j, e)) & , \quad \text{if} \quad k = i\,, \\ (x_j, w'(v_i, v_j, e), \gamma_{\text{coll}}(z; i, j, e)) & , \quad \text{if} \quad k = j\,, \\ (x_i, v_i, g_i - \gamma_{\text{coll}}(z; i, j, e)) & , \quad \text{if} \quad k = \nu + 1\,, \\ (x_j, v_j, g_j - \gamma_{\text{coll}}(z; i, j, e)) & , \quad \text{if} \quad k = \nu + 2\,. \end{cases} \tag{3.145}$$

The weight transfer function is defined as (cf. (3.64))

$$\gamma_{\text{coll}}(z; i, j, e) = \frac{1}{1 + \kappa(z; i, j, e)}\, \min(g_i, g_j)\,, \tag{3.146}$$

where the weight transfer parameter satisfies

$$0 \le \kappa(z; i, j, e) \le C_\kappa\,, \qquad \text{for some} \quad C_\kappa > 0\,. \tag{3.147}$$

Particles with zero weights are removed from the system. The intensity function has the form

$$p_{\text{coll}}(z; i, j, e) = [1 + \kappa(z; i, j, e)]\, \max(g_i, g_j)\, h(x_i, x_j)\, B(v_i, v_j, e)\,. \tag{3.148}$$

The mollifying function and the collision kernel are assumed to satisfy

$$\sup_{(x,v),(y,w) \in D \times \mathbb{R}^3} h(x, y) \int_{\mathcal{S}^2} B(v, w, e)\, de \le C_b\,, \quad \text{for some } C_b > 0\,. \tag{3.149}$$

Note that

$$J_{\text{coll}}(z; i, j, e) \in \mathcal{Z}^{(n)}\,, \qquad \forall\, z \in \mathcal{Z}^{(n)} : \nu \le \nu_{\max}^{(n)}\,,\ 1 \le i \ne j \le \nu\,,\ e \in \mathcal{S}^2\,,$$

since collision jumps are mass-preserving, do not increase the maximum particle weight, and increase the number of particles by at most two.

The transition measure, corresponding to **reduction jumps**, is represented in the form

$$Q^{(n)}_{\mathrm{red}}(z;d\tilde{z}) = \lambda^{(n)}_{\mathrm{red}}\, P^{(n)}_{\mathrm{red}}(z;d\tilde{z})\,, \tag{3.150}$$

where $\lambda^{(n)}_{\mathrm{red}} > 0$ is some waiting time parameter (cf. Remark 3.23) and the **reduction measure** $P^{(n)}_{\mathrm{red}}$ satisfies

$$P^{(n)}_{\mathrm{red}}(z;\mathcal{Z}^{(n)}) = 1\,, \qquad \forall\, z \in \mathcal{Z}^{(n)} \;:\; \nu > \nu^{(n)}_{\max}\,. \tag{3.151}$$

Examples of this measure will be given in Section 3.4.4.

Using assumptions (3.147) and (3.149), one obtains (cf. (3.144), (3.141))

$$\begin{aligned} &\lambda_{\mathrm{coll}}(z) = Q_{\mathrm{coll}}(z,\mathcal{Z}^{(n)}) = \qquad\qquad (3.152)\\ &\quad \frac{1}{2}\sum_{1\le i\ne j\le \nu}\int_{\mathcal{S}^2}[1+\kappa(z;i,j,e)]\,\max(g_i,g_j)\,h(x_i,x_j)\,B(v_i,v_j,e)\,de\\ &\le (1+C_\kappa)\,C_b\,\nu\sum_{i=1}^{\nu} g_i \le (1+C_\kappa)\,C_b\,C_\mu\,\nu\,, \qquad \forall\, z\in\mathcal{Z}^{(n)}\,, \end{aligned}$$

and (cf. (3.150))

$$\begin{aligned} Q^{(n)}(z,\mathcal{Z}^{(n)}) &= \chi_{\{\nu\le\nu^{(n)}_{\max}\}}(z)\,\lambda_{\mathrm{coll}}(z) + \chi_{\{\nu>\nu^{(n)}_{\max}\}}(z)\,\lambda^{(n)}_{\mathrm{red}}\\ &\le (1+C_\kappa)\,C_b\,C_\mu\,\nu^{(n)}_{\max} + \lambda^{(n)}_{\mathrm{red}}\,, \qquad \forall\, z\in\mathcal{Z}^{(n)}\,. \end{aligned}$$

Thus, the generators (3.142) are bounded and their domains consist of all measurable bounded functions Φ on $\mathcal{Z}^{(n)}$.

3.4.2 Convergence theorem

Here we study the asymptotic behavior (as $n \to \infty$) of the processes (3.140). Consider the **bounded Lipschitz metric**

$$\begin{aligned} &\varrho_L(m_1,m_2) = \qquad\qquad (3.153)\\ &\sup_{||\varphi||_L\le 1}\left|\int_{D\times\mathbb{R}^3}\varphi(x,v)\,m_1(dx,dv) - \int_{D\times\mathbb{R}^3}\varphi(x,v)\,m_2(dx,dv)\right| \end{aligned}$$

on the space $\mathcal{M}(D\times\mathbb{R}^3)$, where

$$||\varphi||_L = \max\left\{||\varphi||_\infty\,,\ \sup_{(x,v)\ne(y,w)\in D\times\mathbb{R}^3}\frac{|\varphi(x,v)-\varphi(y,w)|}{|x-y|+|v-w|}\right\}. \tag{3.154}$$

We introduce the sets

$$\mathcal{D}_r := \{\varphi_r \,:\, ||\varphi||_L \le 1\}\,, \qquad r > 0\,, \tag{3.155}$$

where

$$\varphi_r(x,v) = \begin{cases} \varphi(x,v) & , \quad \text{if} \quad |v| \le r\,, \\ (r+1-|v|)\,\varphi(x,v)\,, & \text{if} \quad |v| \in [r, r+1]\,, \\ 0 & , \quad \text{if} \quad |v| \ge r+1\,, \end{cases} \tag{3.156}$$

and $(x,v) \in D \times \mathbb{R}^3$. In this section we assume the position domain D to be compact.

We first collect several assumptions concerning the process parameters in order to shorten the formulation of the theorem. We assume that the particle weight bounds satisfies

$$\lim_{n\to\infty} g_{\max}^{(n)} = 0\,, \tag{3.157}$$

that the particle number bounds indicating reduction satisfies

$$\lim_{n\to\infty} \nu_{\max}^{(n)} = \infty \tag{3.158}$$

and that the parameters of the waiting time before reduction satisfies

$$\lim_{n\to\infty} \lambda_{\mathrm{red}}^{(n)} = \infty\,. \tag{3.159}$$

We make three assumptions concerning the reduction measure. The first assumption assures that the reduction effect is sufficiently strong. It has the form

$$P_{\mathrm{red}}^{(n)}(z; \mathcal{Z}^{(n)}(\delta)) = 1\,, \qquad \forall\, z \in \mathcal{Z}^{(n)} \,:\, \nu > \nu_{\max}^{(n)}\,, \tag{3.160}$$

for some $\delta \in (0,1)$, where

$$\mathcal{Z}^{(n)}(\delta) = \Big\{ z \in \mathcal{Z}^{(n)} \,:\, \nu \le (1-\delta)\,\nu_{\max}^{(n)} \Big\}. \tag{3.161}$$

The second assumption assures that reduction is sufficiently precise. It has the form

$$\lim_{r\to\infty} \limsup_{n\to\infty} \mathbb{E} \sup_{\varphi\in\mathcal{D}_r} \sup_{s\in[0,S]} \tag{3.162}$$
$$\chi_{\{\nu>\nu_{\max}^{(n)}\}}(Z^{(n)}(s)) \int_{\mathcal{Z}^{(n)}} \Big[\Phi(\tilde{z}) - \Phi(Z^{(n)}(s))\Big]^2 P_{\mathrm{red}}^{(n)}(Z^{(n)}(s); d\tilde{z}) = 0\,,$$

for any $S > 0$, where

$$\Phi(z) = \sum_{i=1}^{\nu} g_i\, \varphi(x_i, v_i)\,, \qquad z \in \mathcal{Z}^{(n)}\,. \tag{3.163}$$

The third assumption restricts the increase of energy during reduction (cf. (3.79)). It has the form

$$\int_{\mathcal{Z}^{(n)}} \varepsilon(\tilde{z})\, P_{\mathrm{red}}^{(n)}(z; d\tilde{z}) \le c\,\varepsilon(z)\,, \qquad \forall\, z \in \mathcal{Z}^{(n)} \,:\, \nu > \nu_{\max}^{(n)}\,, \tag{3.164}$$

for some $c > 0$.

Finally, the mollifying function and the collision kernel are assumed to satisfy

$$\begin{aligned} &\int_{\mathcal{S}^2} |h(x,y)\, B(v,w,e) - h(x_1,y_1)\, B(v_1,w_1,e)|\, de \le \\ &\quad C_L \Big[|x - x_1| + |y - y_1| + |v - v_1| + |w - w_1| \Big], \quad \text{for some} \quad C_L > 0\,, \end{aligned} \tag{3.165}$$

and the collision transformation is assumed to satisfy

$$\begin{aligned} &|v'(v,w,e) - v'(v_1,w_1,e)| + |w'(v,w,e) - w'(v_1,w_1,e)| \\ &\qquad \le C' \Big[|v - v_1| + |w - w_1| \Big], \qquad \text{for some} \quad C' \ge 1\,, \end{aligned} \tag{3.166}$$

and

$$|v'(v,w,e)|^2 + |w'(v,w,e)|^2 \le |v|^2 + |w|^2\,. \tag{3.167}$$

Theorem 3.22. *Let F be a function of time $t \ge 0$ with values in $\mathcal{M}(D \times \mathbb{R}^3)$ satisfying the equation*

$$\begin{aligned} &\int_{D\times\mathbb{R}^3} \varphi(x,v)\, F(t, dx, dv) = \int_{D\times\mathbb{R}^3} \varphi(x,v)\, F_0(dx, dv) + \\ &\frac{1}{2} \int_0^t \int_{D\times\mathbb{R}^3} \int_{D\times\mathbb{R}^3} \int_{\mathcal{S}^2} \Big[\varphi(x, v'(v,w,e)) + \varphi(y, w'(v,w,e)) \\ &- \varphi(x,v) - \varphi(y,w) \Big] h(x,y)\, B(v,w,e)\, de\, F(s, dx, dv)\, F(s, dy, dw)\, ds\,, \end{aligned} \tag{3.168}$$

for all test functions φ on $D \times \mathbb{R}^3$ such that $||\varphi||_L < \infty$. Assume the solution is such that

$$\sup_{t\in[0,S]} F(t, D \times \mathbb{R}^3) \le c(S)\, F_0(D \times \mathbb{R}^3) \tag{3.169}$$

and

$$\sup_{t\in[0,S]} \int_{D\times\mathbb{R}^3} |v|^2\, F(t, dx, dv) \le c(S) \int_{D\times\mathbb{R}^3} |v|^2\, F_0(dx, dv)\,, \tag{3.170}$$

for arbitrary $S \ge 0$ and some constants $c(S) > 0$. Let the assumptions (3.147), (3.149), (3.157)-(3.160), (3.162) and (3.164)-(3.167) be fulfilled and let

$$\mu^{(n)}(t,dx,dv) = \sum_{i=1}^{\nu^{(n)}(t)} g_i^{(n)}(t)\,\delta_{x_i^{(n)}(t)}(dx)\,\delta_{v_i^{(n)}(t)}(dv)\,, \qquad t \geq 0\,, \tag{3.171}$$

denote the sequence of empirical measures of the processes (3.140). If

$$\lim_{n\to\infty} \mathbb{E}\,\varrho_L(\mu^{(n)}(0), F_0) = 0 \tag{3.172}$$

and

$$\limsup_{n\to\infty} \mathbb{E} \int_{D\times\mathbb{R}^3} |v|^2\,\mu^{(n)}(0,dx,dv) < \infty\,, \tag{3.173}$$

then

$$\lim_{n\to\infty} \mathbb{E} \sup_{t\in[0,S]} \varrho_L(\mu^{(n)}(t), F(t)) = 0\,, \qquad \forall\, S > 0\,. \tag{3.174}$$

Remark 3.23. The only restriction on the parameter $\lambda_{\mathrm{red}}^{(n)}$ is (3.159). It would be rather natural to consider the choice $\lambda_{\mathrm{red}}^{(n)} = \infty$, which corresponds to an immediate reduction of the system, when the particle number bound is exceeded. This is actually done in the implementation of the algorithm. However, avoiding the introduction of the artificial parameter $\lambda_{\mathrm{red}}^{(n)}$ would lead to a complicated structure of some of the collision jumps making the proof of the convergence theorem technically more difficult.

Remark 3.24. Assumptions (3.166) and (3.167) are fulfilled for the collision transformations (1.6) and (1.12), as well as for modifications related to inelastic collisions.

Remark 3.25. Assumptions (3.172) and (3.173) imply

$$\int_{D\times\mathbb{R}^3} |v|^2\,F_0(dx,dv) < \infty\,. \tag{3.175}$$

Indeed, according to (3.172) one obtains (cf. Lemmas A.4 and A.6)

$$\begin{aligned}\int_{D\times\mathbb{R}^3} \min\left(r,|v|^2\right) F_0(dx,dv) &= \lim_{n\to\infty} \mathbb{E} \int_{D\times\mathbb{R}^3} \min\left(r,|v|^2\right) \mu^{(n)}(0,dx,dv) \\ &\leq \limsup_{n\to\infty} \mathbb{E} \int_{D\times\mathbb{R}^3} |v|^2\,\mu^{(n)}(0,dx,dv)\,,\end{aligned}$$

for any $r > 0$. Consequently,

$$\int_{D\times\mathbb{R}^3} |v|^2\,F_0(dx,dv) \leq \limsup_{n\to\infty} \mathbb{E} \int_{D\times\mathbb{R}^3} |v|^2\,\mu^{(n)}(0,dx,dv)$$

and (3.175) follows from (3.173).

Remark 3.26. The limiting equation (3.168) is a weak form of equation (3.20) related to the collision simulation step. This can be established using arguments from the proof of Lemma 1.11. However, since there is a regularity assumption on the mollifier h (cf. (3.165)), the convergence result cannot be directly applied to equation (3.20) with h defined in (3.59). For this choice of the mollifier, the equation is replaced by a system of cell equations (cf. (3.65), (3.66)). The convergence result can be applied to each cell equation. The result for equation (3.20) with h defined in (3.59) follows from Corollary A.5 and Theorem A.8, since $F(t, \partial D_l \times \mathbb{R}^3) = 0$ (cf. Remark A.9). Note that equation (3.66) reduces to the spatially homogeneous Boltzmann equation if the initial condition is spatially homogeneous.

Remark 3.27. Assumptions (3.160), (3.162) and (3.164) concerning the reduction measure are kept very general in order to provide freedom for the construction of new procedures. Concrete examples and more explicit sufficient convergence conditions will be given in Section 3.4.4.

3.4.3 Proof of the convergence theorem

The starting point for the study of the convergence behavior is the representation

$$\Phi(Z^{(n)}(t)) = \Phi(Z^{(n)}(0)) + \int_0^t \mathcal{A}^{(n)}(\Phi)(Z^{(n)}(s))\, ds + M^{(n)}(\varphi, t)\,, \tag{3.176}$$

where Φ is of the form (3.163), φ is bounded and measurable on $D \times \mathbb{R}^3$ and $M^{(n)}$ is a martingale satisfying

$$\mathbb{E}\, M^{(n)}(\varphi, t)^2 = \mathbb{E} \int_0^t [\mathcal{A}^{(n)}\Phi^2 - 2\,\Phi\,\mathcal{A}^{(n)}\Phi](Z^{(n)}(s))\, ds\,. \tag{3.177}$$

Note that, since (cf. (3.77))

$$|\Phi(z)| \le ||\varphi||_\infty\, \varrho(z) \tag{3.178}$$

and $\varrho(z) \le C_\mu$, the function Φ is bounded on $\mathcal{Z}^{(n)}$ provided that φ is bounded on $D \times \mathbb{R}^3$. The function Φ is measurable for measurable φ.

For $k = 1, 2$, it follows from (3.144)-(3.146) and (3.148) that

$$\begin{aligned}
&\int_{\mathcal{Z}} [\Phi(\tilde{z}) - \Phi(z)]^k\, Q_{\mathrm{coll}}(z, d\tilde{z}) = \qquad (3.179)\\
&\quad \frac{1}{2} \sum_{1 \le i \ne j \le \nu} \int_{\mathcal{S}^2} [\Phi(J_{\mathrm{coll}}(z; i, j, e)) - \Phi(z)]^k\, p_{\mathrm{coll}}(z; i, j, e)\, de\\
&= \frac{1}{2} \sum_{1 \le i \ne j \le \nu} \int_{\mathcal{S}^2} \Big[\varphi(x_i, v'(v_i, v_j, e)) + \varphi(x_j, w'(v_i, v_j, e)) -
\end{aligned}$$

$$\varphi(x_i,v_i)-\varphi(x_j,v_j)\Big]^k\,\gamma_{\rm coll}(z;i,j,e)^k\,p_{\rm coll}(z;i,j,e)\,de$$
$$=\frac{1}{2}\sum_{1\le i\ne j\le\nu} g_i\,g_j\int_{\mathcal{S}^2}\Big[\varphi(x_i,v'(v_i,v_j,e))+\varphi(x_j,w'(v_i,v_j,e))-\varphi(x_i,v_i)-$$
$$\varphi(x_j,v_j)\Big]^k\,\gamma_{\rm coll}(z;i,j,e)^{k-1}\,h(x_i,x_j)\,B(v_i,v_j,e)\,de\,.$$

Using (3.179) (with $k=1$), we conclude that (cf. (3.142), (3.143))

$$\mathcal{A}^{(n)}(\Phi)(z)=\frac{1}{2}\sum_{i,j=1}^{\nu} g_i\,g_j\int_{\mathcal{S}^2}\Big[\varphi(x_i,v'(v_i,v_j,e))+\varphi(x_j,w'(v_i,v_j,e))-$$
$$\varphi(x_i,v_i)-\varphi(x_j,v_j)\Big]h(x_i,x_j)\,B(v_i,v_j,e)\,de+R_1^{(n)}(\varphi,z)-R_2^{(n)}(\varphi,z)\,,$$

where

$$R_1^{(n)}(\varphi,z)=\chi_{\{\nu>\nu_{\max}^{(n)}\}}(z)\int_{\mathcal{Z}}[\Phi(\tilde z)-\Phi(z)]\,Q_{\rm red}^{(n)}(z;d\tilde z)\tag{3.180}$$

and

$$R_2^{(n)}(\varphi,z)=\frac{1}{2}\sum_{i=1}^{\nu} g_i^2\int_{\mathcal{S}^2}\Big[\varphi(x_i,v'(v_i,v_i,e))+\tag{3.181}$$
$$\varphi(x_i,w'(v_i,v_i,e))-\varphi(x_i,v_i)-\varphi(x_i,v_i)\Big]h(x_i,x_i)\,B(v_i,v_i,e)\,de$$
$$+\,\chi_{\{\nu>\nu_{\max}^{(n)}\}}(z)\,\frac{1}{2}\sum_{1\le i\ne j\le\nu} g_i\,g_j\int_{\mathcal{S}^2}\Big[\varphi(x_i,v'(v_i,v_j,e))+$$
$$\varphi(x_j,w'(v_i,v_j,e))-\varphi(x_i,v_i)-\varphi(x_j,v_j)\Big]h(x_i,x_j)\,B(v_i,v_j,e)\,de\,.$$

Taking into account the definition (3.171) one obtains

$$\mathcal{A}^{(n)}(\Phi)(Z^{(n)}(s))\;=\;R_1^{(n)}(\varphi,Z^{(n)}(s))-R_2^{(n)}(\varphi,Z^{(n)}(s))+$$
$$\frac{1}{2}\int_{D\times\mathbb{R}^3}\int_{D\times\mathbb{R}^3}\int_{\mathcal{S}^2}\Big[\varphi(x,v'(v,w,e))+\varphi(y,w'(v,w,e))-\varphi(x,v)-$$
$$\varphi(y,w)\Big]h(x,y)\,B(v,w,e)\,de\,\mu^{(n)}(s,dx,dv)\,\mu^{(n)}(s,dy,dw)$$

and

$$\Phi(Z^{(n)}(t))=\int_{D\times\mathbb{R}^3}\varphi(x,v)\,\mu^{(n)}(t,dx,dv)\,.$$

Consequently, (3.176) takes the form

$$\int_{D\times\mathbb{R}^3}\varphi(x,v)\,\mu^{(n)}(t,dx,dv)=\tag{3.182}$$

$$\int_{D\times\mathbb{R}^3} \varphi(x,v)\,\mu^{(n)}(0,dx,dv) + \int_0^t \mathcal{B}(\varphi,\mu^{(n)}(s))\,ds + \int_0^t R_1^{(n)}(\varphi,Z^{(n)}(s))\,ds - \int_0^t R_2^{(n)}(\varphi,Z^{(n)}(s))\,ds + M^{(n)}(\varphi,t)\,,$$

with the notation

$$\mathcal{B}(\varphi,m) = \frac{1}{2}\int_{D\times\mathbb{R}^3}\int_{D\times\mathbb{R}^3}\int_{\mathcal{S}^2}\Big[\varphi(x,v'(v,w,e)) + \varphi(y,w'(v,w,e)) - \varphi(x,v) - \varphi(y,w)\Big]h(x,y)\,B(v,w,e)\,de\,m(dx,dv)\,m(dy,dw)\,, \tag{3.183}$$

for $m \in \mathcal{M}(D\times\mathbb{R}^3)$. Note that the expected limiting equation (3.168) takes the form

$$\int_{D\times\mathbb{R}^3} \varphi(x,v)\,F(t,dx,dv) = \int_{D\times\mathbb{R}^3} \varphi(x,v)\,F_0(dx,dv) + \int_0^t \mathcal{B}(\varphi,F(s))\,ds\,. \tag{3.184}$$

We prepare the proof of Theorem 3.22 by several lemmas. We use the notations $\mathcal{Z}^{(n)}(0)$ (cf. (3.161)) for the set of all starting points of collision jumps and

$$\mathcal{Z}^{(n)} \setminus \mathcal{Z}^{(n)}(0) = \Big\{z \in \mathcal{Z}^{(n)} \,:\, \nu > \nu_{\max}^{(n)}\Big\}$$

for the set of all starting points of reduction jumps. Consider the family of processes

$$Z_{t,z}^{(n)}(s)\,, \quad s \geq t \geq 0\,, \quad z \in \mathcal{Z}^{(n)}\,, \qquad Z_{t,z}^{(n)}(t) = z\,,$$

and let

$$\tau_{t,z}^{(n)} = \inf\Big\{s > t \,:\, Z_{t,z}^{(n)}(s) \in \mathcal{Z}^{(n)} \setminus \mathcal{Z}^{(n)}(0)\Big\} \tag{3.185}$$

be the first moment of reaching $\mathcal{Z}^{(n)} \setminus \mathcal{Z}^{(n)}(0)$. The joint distribution function of $\Big(\tau_{t,z}^{(n)}, Z_{t,z}^{(n)}(\tau_{t,z}^{(n)})\Big)$ is denoted by $P_{t,z}^{(n)}$. Note that

$$P_{t,z}^{(n)}(ds,d\tilde{z}) = \delta_{t,z}(ds,d\tilde{z})\,, \qquad z \in \mathcal{Z}^{(n)} \setminus \mathcal{Z}^{(n)}(0)\,. \tag{3.186}$$

Let $H_{t,z}^{(n)}$ denote the joint distribution of time and state after the first jump of the process starting in z at time t. Note that (cf. (3.143), (3.150))

$$H_{t,z}^{(n)}(ds,d\tilde{z}) = \lambda_{\rm red}^{(n)}\,\exp(-\lambda_{\rm red}^{(n)}\,(s-t))\,ds\,P_{\rm red}^{(n)}(z;d\tilde{z})\,, \tag{3.187}$$

for all $z \in \mathcal{Z}^{(n)} \setminus \mathcal{Z}^{(n)}(0)$. Introduce the kernel

$$K^{(n)}(t,z;dt_1,dz_1) = \int_t^\infty \int_{\mathcal{Z}^{(n)}\setminus\mathcal{Z}^{(n)}(0)} P^{(n)}_{t,z}(ds,d\tilde{z})\, H^{(n)}_{s,\tilde{z}}(dt_1,dz_1)\,, \qquad (3.188)$$

which represents the joint distribution of time and state after the first reduction jump of the process starting in z at time t. The iterated kernels are denoted by

$$K^{(n)}_{l+1}(t,z;dt_2,dz_2) = \int_t^\infty \int_{\mathcal{Z}} K^{(n)}(t,z;dt_1,dz_1)\, K^{(n)}_l(t_1,z_1;dt_2,dz_2)\,, \quad (3.189)$$

where $l = 1,2,\ldots$ and $K^{(n)}_1 = K^{(n)}$. Note that $K^{(n)}_l(t,z;[t,t+S],\mathcal{Z}^{(n)})$ is the probability that the process starting at time t in state z performs at least l reduction jumps on the time interval $[t,t+S]$.

In the proofs of the lemmas we skip the superscripts indicating the dependence on n.

Lemma 3.28. *Assume (3.147), (3.149) and (3.158). Then (cf. (3.161))*

$$\lim_{n\to\infty} \sup_{t\geq 0\,,\, z\in\mathcal{Z}^{(n)}(\varepsilon)} K^{(n)}(t,z;[t,t+\Delta t],\mathcal{Z}^{(n)}) = 0\,, \qquad (3.190)$$

for any $\varepsilon \in (0,1)$ *and*

$$\Delta t < \frac{\varepsilon}{2\,(1+C_\kappa)\,C_b\,C_\mu}\,. \qquad (3.191)$$

Proof. It follows from (3.188) that, for $u \geq t$,

$$K(t,z;[t,u],\mathcal{Z}) = \int_t^\infty \int_{\mathcal{Z}\setminus\mathcal{Z}(0)} P_{t,z}(ds,d\tilde{z})\, H_{s,\tilde{z}}([t,u],\mathcal{Z}) = \qquad (3.192)$$

$$\int_t^u \int_{\mathcal{Z}\setminus\mathcal{Z}(0)} P_{t,z}(ds,d\tilde{z})\, H_{s,\tilde{z}}([s,u],\mathcal{Z}) \leq P_{t,z}([t,u],\mathcal{Z}) = 1 - \mathrm{Prob}(\tau_{t,z}\geq u)\,.$$

Introduce

$$k_{\min}(\varepsilon) = \left[\frac{\varepsilon\,\nu_{\max}}{2}\right], \qquad (3.193)$$

where $[x]$ denotes the integer part of a real number x. Since each collision increases the number of particles by at most 2 and, according to (3.161),

$$\nu + 2\,k_{\min}(\varepsilon) \leq (1-\varepsilon)\,\nu_{\max} + \varepsilon\,\nu_{\max} = \nu_{\max}\,, \qquad \forall\, z\in\mathcal{Z}(\varepsilon)\,,$$

there will be at least $k_{\min}(\varepsilon)$ jumps before the particle number bound $\nu_{\max}$ is crossed for the first time, when the system starts in $\mathcal{Z}(\varepsilon)$. Therefore, we obtain $\tau_{t,z} \geq \sigma_{t,z}(k_{\min}(\varepsilon))$ and

$$\mathrm{Prob}(\tau_{t,z}\geq u) \geq \mathrm{Prob}(\sigma_{t,z}(k_{\min}(\varepsilon))\geq u)\,, \qquad \forall\, z\in\mathcal{Z}(\varepsilon)\,, \qquad (3.194)$$

where $\sigma_{t,z}(k)$, $k = 1, 2, \dots$, denotes the moment of the k-th jump of the process starting in z at time t. The waiting times before the first $k_{\min}(\varepsilon)$ jumps of the process starting in $\mathcal{Z}(\varepsilon)$ have the parameter $\lambda_{\rm coll}(z)$. According to (3.147), (3.149) and (3.152), we conclude that

$$\mathrm{Prob}(\sigma_{t,z}(k_{\min}(\varepsilon)) \geq u) \geq \mathrm{Prob}(\sigma'(k_{\min}(\varepsilon)) \geq u - t)\,, \qquad (3.195)$$

for all $z \in \mathcal{Z}(\varepsilon)$, where $\sigma'(k)$ denotes the k-th jump time of a process with waiting time parameter

$$(1 + C_\kappa)\, C_b\, C_\mu\, \nu_{\max}\,. \qquad (3.196)$$

Note that

$$\mathrm{Prob}(\sigma'(k_{\min}(\varepsilon)) \geq u - t) = \mathrm{Prob}\left(\sum_{i=1}^{k_{\min}(\varepsilon)} \xi_i \geq u - t\right), \qquad (3.197)$$

where (ξ_i) are independent random variables exponentially distributed with parameter (3.196). Using (3.192), (3.194), (3.195) and (3.197), one concludes that

$$\sup_{t\geq 0\,,\, z\in\mathcal{Z}(\varepsilon)} K(t, z; [t, t+\Delta t], \mathcal{Z}) \leq 1 - \mathrm{Prob}\left(\sum_{i=1}^{k_{\min}(\varepsilon)} \xi_i \geq \Delta t\right). \qquad (3.198)$$

According to (3.158) one obtains (cf. (3.196), (3.193))

$$\mathbb{E} \sum_{i=1}^{k_{\min}(\varepsilon)} \xi_i = \frac{k_{\min}(\varepsilon)}{(1 + C_\kappa)\, C_b\, C_\mu\, \nu_{\max}} \to \frac{\varepsilon}{2\,(1 + C_\kappa)\, C_b\, C_\mu}\,, \qquad \text{as} \quad n \to \infty\,,$$

and

$$\mathrm{Var} \sum_{i=1}^{k_{\min}(\varepsilon)} \xi_i = \frac{k_{\min}(\varepsilon)}{[(1 + C_\kappa)\, C_b\, C_\mu\, \nu_{\max}]^2} \to 0\,, \qquad \text{as} \quad n \to \infty\,,$$

so that

$$\sum_{i=1}^{k_{\min}(\varepsilon)} \xi_i \to \frac{\varepsilon}{2\,(1 + C_\kappa)\, C_b\, C_\mu} \qquad \text{in probability}\,, \qquad \text{as} \quad n \to \infty\,,$$

according to Lemma A.6. Thus, (3.190) follows from (3.198) and (3.191). ∎

Lemma 3.29. *Let (3.160) and the assumptions of Lemma 3.28 hold. Then (cf. (3.189))*

$$\lim_{n\to\infty} \sup_{t\geq 0\,,\, z\in\mathcal{Z}^{(n)}} K_l^{(n)}(t, z; [t, t+S], \mathcal{Z}^{(n)}) = 0\,, \qquad (3.199)$$

for any $S > 0$ *and*

$$l > \frac{2\,S\,(1 + C_\kappa)\, C_b\, C_\mu}{\delta}\,. \qquad (3.200)$$

Proof. We first show that

$$\sup_{t\geq 0\,,\, z\in\mathcal{Z}(\delta)} K_l(t,z;[t,t+l\,\Delta t],\mathcal{Z}) \leq l \sup_{t\geq 0\,,\, z\in\mathcal{Z}(\delta)} K(t,z;[t,t+\Delta t],\mathcal{Z})\,, \tag{3.201}$$

for any $\Delta t > 0$ and $l = 1, 2, \ldots$. For $l = 1$, the assertion is obviously fulfilled. For $l \geq 1$, we obtain from (3.160) that

$$\begin{aligned}
&K_{l+1}(t,z;[t,t+(l+1)\Delta t],\mathcal{Z}) = \\
&\quad \int_t^\infty \int_{\mathcal{Z}} K(t,z;dt_1,dz_1)\, K_l(t_1,z_1;[t,t+(l+1)\Delta t],\mathcal{Z}) \\
&= \int_t^{t+\Delta t} \int_{\mathcal{Z}} K(t,z;dt_1,dz_1)\, K_l(t_1,z_1;[t,t+(l+1)\Delta t],\mathcal{Z}) + \\
&\quad \int_{t+\Delta t}^{t+(l+1)\Delta t} \int_{\mathcal{Z}} K(t,z;dt_1,dz_1)\, K_l(t_1,z_1;[t,t+(l+1)\Delta t],\mathcal{Z}) \\
&\leq K(t,z;[t,t+\Delta t],\mathcal{Z}) + \\
&\quad \int_{t+\Delta t}^{t+(l+1)\Delta t} \int_{\mathcal{Z}(\delta)} K(t,z;dt_1,dz_1)\, K_l(t_1,z_1;[t_1,t_1+l\Delta t],\mathcal{Z}) \\
&\leq K(t,z;[t,t+\Delta t],\mathcal{Z}) + \sup_{t\geq 0\,,\, z\in\mathcal{Z}(\delta)} K_l(t,z;[t,t+l\Delta t],\mathcal{Z})\,.
\end{aligned}$$

Thus, (3.201) follows by induction. Using again (3.160), we obtain

$$\begin{aligned}
K_{l+1}(t,z;[t,t+S],\mathcal{Z}) &= \int_t^\infty \int_{\mathcal{Z}(\delta)} K(t,z;dt_1,dz_1)\, K_l(t_1,z_1;[t,t+S],\mathcal{Z}) \\
&\leq \sup_{t\geq 0\,,\, z\in\mathcal{Z}(\delta)} K_l(t,z;[t,t+S],\mathcal{Z})\,, \qquad \forall\, l \geq 1\,.
\end{aligned} \tag{3.202}$$

If l satisfies (3.200) then there exists Δt such that $S \leq l\,\Delta t$ and (3.191) holds with $\varepsilon = \delta$. Thus, (3.199) follows from (3.202), (3.201) and Lemma 3.28. ∎

Lemma 3.30. *Let the assumptions of Lemma 3.29 hold. Then*

$$\limsup_{n\to\infty} \mathbb{E}\left[\lambda_{\mathrm{red}}^{(n)} \int_0^S \chi_{\{\nu>\nu_{\max}^{(n)}\}}(Z^{(n)}(s))\, ds\right]^2 < \infty\,, \qquad \forall\, S > 0\,.$$

Proof. Introduce the function

$$A(t,z) = \mathbb{E}_{t,z}\left[\lambda_{\mathrm{red}} \int_t^S \chi_{\{\nu>\nu_{\max}\}}(Z(u))\, du\right]^2, \qquad t \in [0,S]\,, \quad z \in \mathcal{Z}\,,$$

where $\mathbb{E}_{t,z}$ denotes conditional expectation. For $z \in \mathcal{Z}(0)$, one obtains (cf. (3.185))

$$
\begin{aligned}
A(t,z) &= \int_t^\infty \int_{\mathcal{Z}\setminus\mathcal{Z}(0)} P_{t,z}(ds,d\tilde{z}) \times \\
&\quad \mathbb{E}_{t,z}\left(\left[\lambda_{\mathrm{red}} \int_t^S \chi_{\{\nu>\nu_{\max}\}}(Z(u))\,du \right]^2 \,\middle|\, \tau_{t,z}=s\,,\, Z(\tau_{t,z})=\tilde{z} \right) \\
&= \int_t^S \int_{\mathcal{Z}\setminus\mathcal{Z}(0)} P_{t,z}(ds,d\tilde{z}) \times \\
&\quad \mathbb{E}_{t,z}\left(\left[\lambda_{\mathrm{red}} \int_t^S \chi_{\{\nu>\nu_{\max}\}}(Z(u))\,du \right]^2 \,\middle|\, \tau_{t,z}=s\,,\, Z(\tau_{t,z})=\tilde{z} \right) \\
&= \int_t^S \int_{\mathcal{Z}\setminus\mathcal{Z}(0)} P_{t,z}(ds,d\tilde{z}) \times \\
&\quad \mathbb{E}_{t,z}\left(\left[\lambda_{\mathrm{red}} \int_s^S \chi_{\{\nu>\nu_{\max}\}}(Z(u))\,du \right]^2 \,\middle|\, \tau_{t,z}=s\,,\, Z(\tau_{t,z})=\tilde{z} \right) \\
&= \int_t^S \int_{\mathcal{Z}\setminus\mathcal{Z}(0)} \mathbb{E}_{s,\tilde{z}}\left[\lambda_{\mathrm{red}} \int_s^S \chi_{\{\nu>\nu_{\max}\}}(Z(u))\,du \right]^2 P_{t,z}(ds,d\tilde{z}) \\
&= \int_t^S \int_{\mathcal{Z}\setminus\mathcal{Z}(0)} A(s,\tilde{z})\, P_{t,z}(ds,d\tilde{z})\,. \qquad (3.203)
\end{aligned}
$$

Let $\sigma_{t,z}$ be the moment of the first jump of the process starting in z at time t. For $\tilde{z} \in \mathcal{Z}\setminus\mathcal{Z}(0)$ and $s \in [0,S]$, one obtains

$$
\begin{aligned}
A(s,\tilde{z}) &= \int_s^\infty \int_{\mathcal{Z}} H_{s,\tilde{z}}(dt,dz) \times \\
&\quad \mathbb{E}_{s,\tilde{z}}\left(\left[\lambda_{\mathrm{red}} \int_s^S \chi_{\{\nu>\nu_{\max}\}}(Z(u))\,du \right]^2 \,\middle|\, \sigma_{s,\tilde{z}}=t\,,\, Z(\sigma_{s,\tilde{z}})=z \right) \\
&= \int_S^\infty \int_{\mathcal{Z}} H_{s,\tilde{z}}(dt,dz) \times \\
&\quad \mathbb{E}_{s,\tilde{z}}\left(\left[\lambda_{\mathrm{red}} \int_s^S \chi_{\{\nu>\nu_{\max}\}}(Z(u))\,du \right]^2 \,\middle|\, \sigma_{s,\tilde{z}}=t\,,\, Z(\sigma_{s,\tilde{z}})=z \right) \\
&\quad + \int_s^S \int_{\mathcal{Z}} H_{s,\tilde{z}}(dt,dz) \times \\
&\quad \mathbb{E}_{s,\tilde{z}}\left(\left[\lambda_{\mathrm{red}} \int_s^S \chi_{\{\nu>\nu_{\max}\}}(Z(u))\,du \right]^2 \,\middle|\, \sigma_{s,\tilde{z}}=t\,,\, Z(\sigma_{s,\tilde{z}})=z \right) \\
&\le \left[\lambda_{\mathrm{red}}\,(S-s) \right]^2 H_{s,\tilde{z}}([S,\infty),\mathcal{Z}) + 2\int_s^S \int_{\mathcal{Z}} H_{s,\tilde{z}}(dt,dz) \times
\end{aligned}
$$

$$\mathbb{E}_{s,\tilde{z}}\left(\left[\lambda_{\rm red}\int_t^S \chi_{\{\nu>\nu_{\max}\}}(Z(u))\,du\right]^2\,\middle|\,\sigma_{s,\tilde{z}}=t\,,\,Z(\sigma_{s,\tilde{z}})=z\right)$$
$$+2\int_s^S\int_{\mathcal{Z}} H_{s,\tilde{z}}(dt,dz)\times$$
$$\mathbb{E}_{s,\tilde{z}}\left(\left[\lambda_{\rm red}\int_s^t \chi_{\{\nu>\nu_{\max}\}}(Z(u))\,du\right]^2\,\middle|\,\sigma_{s,\tilde{z}}=t\,,\,Z(\sigma_{s,\tilde{z}})=z\right)$$
$$\le \lambda_{\rm red}^2\int_S^\infty (t-s)^2\,H_{s,\tilde{z}}(dt,\mathcal{Z}) \tag{3.204}$$
$$+2\int_s^S\int_{\mathcal{Z}} A(t,z)\,H_{s,\tilde{z}}(dt,dz)+2\,\lambda_{\rm red}^2\int_s^S (t-s)^2\,H_{s,\tilde{z}}(dt,\mathcal{Z})\,.$$

Thus, (3.203) and (3.204) imply, for $z\in\mathcal{Z}(0)$,

$$A(t,z)\le\int_t^S\int_{\mathcal{Z}\setminus\mathcal{Z}(0)} P_{t,z}(ds,d\tilde{z})\int_s^S\int_{\mathcal{Z}} H_{s,\tilde{z}}(dt_1,dz_1)\,A(t_1,z_1)+a(t,z)\,, \tag{3.205}$$

where

$$a(t,z)=2\,\lambda_{\rm red}^2\int_t^S\int_{\mathcal{Z}\setminus\mathcal{Z}(0)}\int_s^\infty (u-s)^2\,H_{s,\tilde{z}}(du,\mathcal{Z})\,P_{t,z}(ds,d\tilde{z})\,.$$

For any $s\ge 0$ and $\tilde{z}\in\mathcal{Z}\setminus\mathcal{Z}(0)$, one obtains (cf. (3.187))

$$\int_s^\infty (u-s)^2\,H_{s,\tilde{z}}(du,\mathcal{Z})=\frac{2}{\lambda_{\rm red}^2}$$

and

$$a(t,z)\le 4\,. \tag{3.206}$$

Note that inequality (3.205) holds also for $z\in\mathcal{Z}\setminus\mathcal{Z}(0)$, according to (3.186) and (3.204). Inequalities (3.205) and (3.206) imply (cf. (3.188))

$$A(t,z)\le 2\int_t^S\int_{\mathcal{Z}} K(t,z;dt_1,dz_1)\,A(t_1,z_1)+4\,, \tag{3.207}$$

where $t\in[0,S]$ and $z\in\mathcal{Z}$. Iterating (3.207) one obtains

$$A(t,z)\le 2^l\int_t^S\int_{\mathcal{Z}} K_l(t,z;dt_1,dz_1)\,A(t_1,z_1)+2^{l+2}\,. \tag{3.208}$$

Note that

$$A(t,z)\le\lambda_{\rm red}^2\,S^2\,,\qquad\forall\,t\in[0,S]\,,\quad z\in\mathcal{Z}\,.$$

Iterating (3.208) one obtains

$$A(t,z) \le 2^{l+2} \sum_{k=0}^{N-1} \Big(2^l \, ||K_l||\Big)^k + \Big(2^l \, ||K_l||\Big)^N \lambda_{\rm red}^2 \, S^2 \,, \qquad (3.209)$$

for any $N = 1, 2, \dots$, where

$$||K_l|| = \sup_{t \ge 0 \,,\, z \in \mathcal{Z}} K_l(t, z; [t, t+S], \mathcal{Z}) \,.$$

According to Lemma 3.29, there exists l such that $2^l \, ||K_l|| \le C$, for some $C < 1$ and sufficiently large n . Consequently, (3.209) implies

$$A(t,z) \le \frac{2^{l+2}}{1-C}$$

and the assertion follows. ∎

Lemma 3.31. *Let (3.164), (3.167), (3.173) and the assumptions of Lemma 3.29 hold. Then*

$$\lim_{r \to \infty} \limsup_{n \to \infty} \mathbb{E} \sup_{t \in [0,S]} \mu^{(n)}(t, \{(x,v) : \, |v| \ge r\}) = 0 \,, \qquad \forall \, S > 0 \,.$$

Proof. Introduce the function

$$A(t,z) = \mathbb{E}_{t,z} \sup_{u \in [t,S]} \mu(u, \{|v| \ge r\}) \,, \qquad t \in [0,S] \,, \quad z \in \mathcal{Z} \,. \qquad (3.210)$$

Let $\tau'_{t,z}$ denote the moment of the first reduction jump, when starting in z at time t . One obtains

$$\begin{aligned}
A(t,z) &= \int_t^\infty \int_{\mathcal{Z}} K(t,z; dt_1, dz_1) \times \\
&\qquad \mathbb{E}_{t,z} \Big\{ \sup_{u \in [t,S]} \mu(u, \{|v| \ge r\}) \, \Big| \, \tau'_{t,z} = t_1, Z(\tau'_{t,z}) = z_1 \Big\} \\
&\le \int_S^\infty \int_{\mathcal{Z}} K(t,z; dt_1, dz_1) \times \\
&\qquad \mathbb{E}_{t,z} \Big\{ \sup_{u \in [t,S]} \mu(u, \{|v| \ge r\}) \, \Big| \, \tau'_{t,z} = t_1, Z(\tau'_{t,z}) = z_1 \Big\} \\
&\quad + \int_t^S \int_{\mathcal{Z}} K(t,z; dt_1, dz_1) \times \\
&\qquad \mathbb{E}_{t,z} \Big\{ \sup_{u \in [t,t_1]} \mu(u, \{|v| \ge r\}) \, \Big| \, \tau'_{t,z} = t_1, Z(\tau'_{t,z}) = z_1 \Big\} \\
&\quad + \int_t^S \int_{\mathcal{Z}} K(t,z; dt_1, dz_1) \times \\
&\qquad \mathbb{E}_{t,z} \Big\{ \sup_{u \in [t_1,S]} \mu(u, \{|v| \ge r\}) \, \Big| \, \tau'_{t,z} = t_1, Z(\tau'_{t,z}) = z_1 \Big\} \\
&= a(t,z) + \int_t^S \int_{\mathcal{Z}} K(t,z; dt_1, dz_1) \, A(t_1, z_1) \,, \qquad (3.211)
\end{aligned}$$

where

$$a(t,z) = \mathbb{E}_{t,z} \sup_{u\in[t,\min(S,\tau'_{t,z})]} \mu(u,\{|v|\geq r\})\,.$$

Using the fact that the function $\int_{D\times\mathbb{R}^3} |v|^2\,\mu(u,dx,dv)$ takes at most two different values for $u\in[t,\min(S,\tau'_{t,z})]$, one obtains

$$\begin{aligned} a(t,z) &\leq \frac{1}{r^2}\,\mathbb{E}_{t,z} \sup_{u\in[t,\min(S,\tau'_{t,z})]} \int_{D\times\mathbb{R}^3} |v|^2\,\mu(u,dx,dv) \\ &\leq \frac{1}{r^2}\left[\mathbb{E}_{t,z}\int_{D\times\mathbb{R}^3} |v|^2\,\mu(t,dx,dv) + \mathbb{E}_{t,z}\int_{D\times\mathbb{R}^3} |v|^2\,\mu(\tau'_{t,z},dx,dv)\right] \\ &= \frac{1}{r^2}\left[\varepsilon(z) + \int_t^\infty\int_{\mathcal{Z}} \varepsilon(z_1)\,K(t,z;dt_1,dz_1)\right], \end{aligned} \tag{3.212}$$

where ε is defined in (3.79). It follows from (3.164) that (cf. (3.187))

$$\int_s^\infty\int_{\mathcal{Z}} \varepsilon(z_1)\,H_{s,\tilde{z}}(dt_1,dz_1) = \int_{\mathcal{Z}} \varepsilon(z_1)\,P_{\mathrm{red}}(\tilde{z};dz_1) \leq c\,\varepsilon(\tilde{z})$$

and from (3.167) that

$$\int_t^\infty\int_{\mathcal{Z}\setminus\mathcal{Z}(0)} \varepsilon(\tilde{z})\,P_{t,z}(ds,d\tilde{z}) \leq \varepsilon(z)\,.$$

Thus, one concludes that (cf. (3.188))

$$\begin{aligned} &\int_t^\infty\int_{\mathcal{Z}} \varepsilon(z_1)\,K(t,z;dt_1,dz_1) = \\ &\quad \int_t^\infty\int_{\mathcal{Z}} \varepsilon(z_1) \int_t^\infty\int_{\mathcal{Z}\setminus\mathcal{Z}(0)} P_{t,z}(ds,d\tilde{z})\,H_{s,\tilde{z}}(dt_1,dz_1) \\ &= \int_t^\infty\int_{\mathcal{Z}\setminus\mathcal{Z}(0)} \int_s^\infty\int_{\mathcal{Z}} \varepsilon(z_1)\,H_{s,\tilde{z}}(dt_1,dz_1)\,P_{t,z}(ds,d\tilde{z}) \\ &\leq c\int_t^\infty\int_{\mathcal{Z}\setminus\mathcal{Z}(0)} \varepsilon(\tilde{z})\,P_{t,z}(ds,d\tilde{z}) \leq c\,\varepsilon(z)\,. \end{aligned} \tag{3.213}$$

Using (3.211), (3.212) and (3.213), one obtains

$$A(t,z) \leq \int_t^S\int_{\mathcal{Z}} K(t,z;dt_1,dz_1)\,A(t_1,z_1) + \frac{1+c}{r^2}\,\varepsilon(z)\,. \tag{3.214}$$

Note that $A(t,z)\leq C_\mu$, according to (3.141) and (3.210). Iterating (3.214) and using (3.213), one obtains (cf. (3.189))

$$A(t,z) \leq C_\mu\,K_l(t,z;[t,S],\mathcal{Z}) + \frac{(1+c)\sum_{k=0}^{l-1} c^k}{r^2}\,\varepsilon(z)\,, \tag{3.215}$$

for any $l \geq 1$. Choosing l sufficiently large, it follows from (3.215) and Lemma 3.29 that

$$\limsup_{n\to\infty} \mathbb{E} \sup_{t\in[0,S]} \mu(t,\{|v| \geq r\}) \leq \frac{(1+c)\sum_{k=0}^{l-1} c^k}{r^2} \limsup_{n\to\infty} \mathbb{E}\,\varepsilon(Z(0))\,.$$

Thus, the assertion is a consequence of (3.173). ∎

Lemma 3.32. *Let (3.157), (3.162) and the assumptions of Lemma 3.30 hold. Then (cf. (3.176), (3.155))*

$$\lim_{r\to\infty} \limsup_{n\to\infty} \mathbb{E} \sup_{t\in[0,S]} \sup_{\varphi\in\mathcal{D}_r} |M^{(n)}(\varphi,t)| = 0\,, \qquad \forall\, S > 0\,.$$

Proof. The set $\mathcal{D}_r$ is compact in the space of continuous functions on the set $\{(x,v) \in D\times\mathbb{R}^3 : \ |v| \leq r+1\}$ (cf. (3.156)). Consequently, for any $\varepsilon > 0$, there exists a finite subset $\{\psi_i;\ i = 1,\dots,I(\varepsilon)\}$ of $\mathcal{D}_r$ such that

$$\min_i ||\psi - \psi_i||_\infty \leq \varepsilon\,, \qquad \forall\, \psi \in \mathcal{D}_r\,.$$

This implies the estimate

$$|M(\psi,t)| \leq \sup_{||\varphi||_\infty\leq\varepsilon} |M(\varphi,t)| + \sum_{i=1}^{I(\varepsilon)} |M(\psi_i,t)|\,, \qquad \forall\, \psi \in \mathcal{D}_r\,. \tag{3.216}$$

According to (3.142), (3.143), (3.179) with $k = 1$, (3.141) and (3.149), it follows that

$$|\mathcal{A}(\Phi)(z)| \leq 2\,||\varphi||_\infty\, C_b\, C_\mu^2 + \chi_{\{\nu>\nu_{\max}\}}(z) \left| \int_{\mathcal{Z}} [\Phi(\tilde z) - \Phi(z)]\, Q_{\rm red}(z; d\tilde z) \right|.$$

Thus, using (3.151) and (3.141), we obtain (cf. (3.176), (3.163))

$$\begin{aligned} |M(\varphi,t)| &\leq 2\,||\varphi||_\infty\, C_\mu\,[1 + C_b\, t\, C_\mu] + \\ &\int_0^t \chi_{\{\nu>\nu_{\max}\}}(Z(s)) \left| \int_{\mathcal{Z}} [\Phi(\tilde z) - \Phi(Z(s))]\, Q_{\rm red}(Z(s), d\tilde z) \right| ds \\ &\leq 2\,||\varphi||_\infty\, C_\mu\,[1 + C_b\, t\, C_\mu] + 2\,||\varphi||_\infty\, C_\mu\, \lambda_{\rm red} \int_0^t \chi_{\{\nu>\nu_{\max}\}}(Z(s))\, ds\,. \end{aligned} \tag{3.217}$$

Now (3.217) and (3.216) imply

$$\begin{aligned} \sup_{t\in[0,S]} \sup_{\varphi\in\mathcal{D}_r} |M(\varphi,t)| &\leq \sum_{i=1}^{I(\varepsilon)} \sup_{t\in[0,S]} |M(\psi_i,t)| + \\ &2\,\varepsilon\, C_\mu \left[1 + C_b\, S\, C_\mu + \lambda_{\rm red} \int_0^S \chi_{\{\nu>\nu_{\max}\}}(Z(s))\, ds \right]. \end{aligned} \tag{3.218}$$

The martingale inequality gives

$$\mathbb{E}\sup_{t\in[0,S]}|M(\varphi,t)|\le 2\left(\mathbb{E}\,M(\varphi,S)^2\right)^{\frac12}\,. \tag{3.219}$$

Using the elementary identity $a^2-b^2=2(a-b)b+(a-b)^2$, one obtains

$$\mathcal{A}\Phi^2(z)=2\,\Phi(z)\,\mathcal{A}\Phi(z)+\int_{\mathcal{Z}}[\Phi(\tilde z)-\Phi(z)]^2\,Q(z,d\tilde z)\,,$$

so that, according to (3.143) and (3.179) with $k=2$,

$$\begin{aligned}\mathcal{A}\Phi^2(z)-2\,\Phi(z)\,\mathcal{A}\Phi(z)=\chi_{\{\nu\le\nu_{\max}\}}(z)\,\frac12\sum_{1\le i\ne j\le\nu}g_i\,g_j\times\\ \int_{\mathcal{S}^2}\Big[\varphi(x_i,v'(v_i,v_j,e))+\varphi(x_j,w'(v_i,v_j,e))-\varphi(x_i,v_i)-\varphi(x_j,v_j)\Big]^2\times\\ \gamma_{\rm coll}(z;i,j,e)\,h(x_i,x_j)\,B(v_i,v_j,e)\,de\\ +\,\chi_{\{\nu>\nu_{\max}\}}(z)\int_{\mathcal{Z}}[\Phi(\tilde z)-\Phi(z)]^2\;Q_{\rm red}(z;d\tilde z)\,.\end{aligned}$$

Using (3.146) and (3.149), we conclude that (cf. (3.141))

$$\begin{aligned}&\mathcal{A}\Phi^2(z)-2\,\Phi(z)\,\mathcal{A}\Phi(z)\le\\ &\quad 8\,||\varphi||_\infty^2\,C_b\,C_\mu^2\,g_{\max}+\chi_{\{\nu>\nu_{\max}\}}(z)\int_{\mathcal{Z}}[\Phi(\tilde z)-\Phi(z)]^2\;Q_{\rm red}(z;d\tilde z)\,.\end{aligned}$$

Now (3.177) implies

$$\begin{aligned}&\mathbb{E}\,M(\varphi,S)^2\;\le\;8\,||\varphi||_\infty^2\,C_b\,C_\mu^2\,S\,g_{\max}+\\ &\mathbb{E}\int_0^S\left[\chi_{\{\nu>\nu_{\max}\}}(Z(s))\,\lambda_{\rm red}\int_{\mathcal{Z}}[\Phi(\tilde z)-\Phi(Z(s))]^2\;P_{\rm red}(Z(s);d\tilde z)\right]ds\,.\end{aligned} \tag{3.220}$$

Using (3.218), (3.219), (3.220) and $\sqrt{a^2+b^2}\le|a|+|b|$, we obtain

$$\begin{aligned}&\mathbb{E}\sup_{t\in[0,S]}\sup_{\varphi\in\mathcal{D}_r}|M(\varphi,t)|\le 2\,I(\varepsilon)\,C_\mu\,\sqrt{8\,C_b\,S\,g_{\max}}+2\sum_{i=1}^{I(\varepsilon)}\\ &\left(\mathbb{E}\int_0^S\left[\chi_{\{\nu>\nu_{\max}\}}(Z(s))\,\lambda_{\rm red}\int_{\mathcal{Z}}[\Phi_i(\tilde z)-\Phi_i(Z(s))]^2\;P_{\rm red}(Z(s);d\tilde z)\right]ds\right)^{\frac12}\\ &+2\,\varepsilon\,C_\mu\left[1+C_b\,S\,C_\mu+\lambda_{\rm red}\,\mathbb{E}\int_0^S\chi_{\{\nu>\nu_{\max}\}}(Z(s))\,ds\right]\\ &\le\quad 2\,I(\varepsilon)\,C_\mu\,\sqrt{8\,C_b\,S\,g_{\max}}+\\ &2\,\varepsilon\,C_\mu\left[1+C_b\,S\,C_\mu+\lambda_{\rm red}\,\mathbb{E}\int_0^S\chi_{\{\nu>\nu_{\max}\}}(Z(s))\,ds\right]+\end{aligned}$$

$$2\,I(\varepsilon)\left(\mathbb{E}\left[\lambda_{\rm red}\int_0^S \chi_{\{\nu>\nu_{\max}\}}(Z(s))\,ds\right]^2\right)^{\frac14}\times$$

$$\left(\mathbb{E}\left[\sup_{\varphi\in\mathcal{D}_r}\sup_{s\in[0,S]}\chi_{\{\nu>\nu_{\max}\}}(Z(s))\int_{\mathcal{Z}}[\Phi(\tilde z)-\Phi(Z(s))]^2\,P_{\rm red}(Z(s);d\tilde z)\right]^2\right)^{\frac14},$$

where Φ_i denotes the function (3.163) with $\varphi=\psi_i$. Using (3.157), Lemma 3.30 and (3.162), we conclude that

$$\limsup_{n\to\infty}\mathbb{E}\sup_{t\in[0,S]}\sup_{\varphi\in\mathcal{D}_r}|M(\varphi,t)|\le$$
$$2\,\varepsilon\,C_\mu\left[1+C_b\,S\,C_\mu+\limsup_{n\to\infty}\lambda_{\rm red}\,\mathbb{E}\int_0^S\chi_{\{\nu>\nu_{\max}\}}(Z(s))\,ds\right].$$

Since $\varepsilon>0$ is arbitrary, the assertion follows from Lemma 3.30. ∎

Lemma 3.33. *Let (3.162) and the assumptions of Lemma 3.30 hold. Then (cf. (3.180), (3.155))*

$$\lim_{r\to\infty}\limsup_{n\to\infty}\mathbb{E}\int_0^S\sup_{\varphi\in\mathcal{D}_r}|R_1^{(n)}(\varphi,Z^{(n)}(s))|\,ds=0\,,\qquad\forall\,S>0\,.$$

Proof. One obtains (cf. (3.150))

$$\mathbb{E}\int_0^S\sup_{\varphi\in\mathcal{D}_r}|R_1(\varphi,Z(s))|\,ds\le$$
$$\mathbb{E}\int_0^S\left[\chi_{\{\nu>\nu_{\max}\}}(Z(s))\,\lambda_{\rm red}\sup_{\varphi\in\mathcal{D}_r}\int_{\mathcal{Z}}|\Phi(\tilde z)-\Phi(Z(s))|\,P_{\rm red}(Z(s);d\tilde z)\right]ds$$
$$\le\left(\mathbb{E}\left[\lambda_{\rm red}\int_0^S\chi_{\{\nu>\nu_{\max}\}}(Z(s))\,ds\right]^2\right)^{\frac12}\times$$
$$\left(\mathbb{E}\sup_{\varphi\in\mathcal{D}_r}\sup_{s\in[0,S]}\chi_{\{\nu>\nu_{\max}\}}(Z(s))\int_{\mathcal{Z}}[\Phi(\tilde z)-\Phi(Z(s))]^2\,P_{\rm red}(Z(s);d\tilde z)\right)^{\frac12},$$

and the assertion follows from Lemma 3.30 and (3.162). ∎

Lemma 3.34. *Let (3.157), (3.159) and the assumptions of Lemma 3.30 hold. Then (cf. (3.181), (3.155))*

$$\lim_{n\to\infty}\mathbb{E}\int_0^S\sup_{\varphi\in\mathcal{D}_r}|R_2^{(n)}(\varphi,Z^{(n)}(s))|\,ds=0\,,\qquad\forall\,S>0\,,\quad r>0\,.$$

Proof. It follows from (3.149) that

$$|R_2(\varphi,z)| \le 2\,||\varphi||_\infty\, C_b \left[\sum_{i=1}^{\nu} g_i^2 + \chi_{\{\nu>\nu_{\max}\}}(z) \sum_{1\le i\ne j\le \nu} g_i\, g_j\right].$$

Thus, taking into account (3.141), we obtain

$$\int_0^S \sup_{\varphi\in\mathcal{D}_r} |R_2(\varphi, Z(s))|\, ds \le 2\, C_b \left[C_\mu\, g_{\max}^{(n)} + C_\mu^2 \int_0^S \chi_{\{\nu>\nu_{\max}\}}(Z(s))\, ds\right],$$

and the assertion follows from (3.157), (3.159) and Lemma 3.30. ∎

Lemma 3.35. *Assume (3.149), (3.165) and (3.166). Then (cf. (3.183), (3.153), (3.154))*

$$\begin{aligned}&|\mathcal{B}(\varphi,m) - \mathcal{B}(\varphi,m_1)| \le \\ &\quad 2\,C'\,(C_b + C_L)\,||\varphi||_L\, \varrho_L(m,m_1)\Big[m(D\times\mathbb{R}^3) + m_1(D\times\mathbb{R}^3)\Big],\end{aligned}$$

for any $m, m_1 \in \mathcal{M}(D\times\mathbb{R}^3)$.

Proof. Introduce

$$\begin{aligned}b(\varphi)(x,v,y,w) = \frac{1}{2}\int_{\mathcal{S}^2} \Big[&\varphi(x, v'(v,w,e)) + \\ &\varphi(y, w'(v,w,e)) - \varphi(x,v) - \varphi(y,w)\Big] h(x,y)\, B(v,w,e)\, de\end{aligned}$$

and

$$\begin{aligned}b_1(\varphi,m)(x,v) &= \int_{D\times\mathbb{R}^3} b(\varphi)(x,v,y,w)\, m(dy,dw)\,, \\ b_2(\varphi,m)(y,w) &= \int_{D\times\mathbb{R}^3} b(\varphi)(x,v,y,w)\, m(dx,dv)\,.\end{aligned}$$

According to (3.149), (3.165) and (3.166) one obtains

$$\begin{aligned}&|b(\varphi)(x,v,y,w) - b(\varphi)(x_1,v_1,y_1,w_1)| \le \\ &\quad 2\,C'\,(C_b + C_L)\,||\varphi||_L \Big[|x-x_1| + |v-v_1| + |y-y_1| + |w-w_1|\Big]\end{aligned}$$

and, for $i = 1, 2$,

$$\begin{aligned}&|b_i(\varphi,m)(x,v) - b_i(\varphi,m)(x_1,v_1)| \le \\ &\quad 2\,C'\,(C_b + C_L)\,||\varphi||_L\, m(D\times\mathbb{R}^3)\Big[|x-x_1| + |v-v_1|\Big].\end{aligned} \tag{3.221}$$

It follows from (3.221) and

$$|b_i(\varphi,m)(x,v)| \le 2\,||\varphi||_\infty\, C_b\, m(D\times\mathbb{R}^3)\,, \qquad i=1,2\,,$$

that

$$||b_i(\varphi,m)||_L \le 2\,C'\,(C_b+C_L)\,||\varphi||_L\, m(D\times\mathbb{R}^3)\,, \qquad i=1,2\,. \tag{3.222}$$

Finally, since

$$\int_{D\times\mathbb{R}^3}\int_{D\times\mathbb{R}^3} b(\varphi)(x,v,y,w)\,m(dx,dv)\,m_1(dy,dw) = \int_{D\times\mathbb{R}^3} b_2(\varphi,m)(y,w)\,m_1(dy,dw) = \int_{D\times\mathbb{R}^3} b_1(\varphi,m_1)(x,v)\,m(dx,dv)$$

and

$$\mathcal{B}(\varphi,m) = \int_{D\times\mathbb{R}^3} b_2(\varphi,m)(y,w)\,m(dy,dw) = \int_{D\times\mathbb{R}^3} b_1(\varphi,m)(x,v)\,m(dx,dv)\,,$$

one obtains

$$\begin{aligned}
&|\mathcal{B}(\varphi,m)-\mathcal{B}(\varphi,m_1)| \le \\
&\quad\left|\int_{D\times\mathbb{R}^3} b_2(\varphi,m)(y,w)\,m(dy,dw) - \int_{D\times\mathbb{R}^3} b_2(\varphi,m)(y,w)\,m_1(dy,dw)\right| + \\
&\quad\left|\int_{D\times\mathbb{R}^3} b_1(\varphi,m_1)(x,v)\,m(dx,dv) - \int_{D\times\mathbb{R}^3} b_1(\varphi,m_1)(x,v)\,m_1(dx,dv)\right| \\
&\le \Big[||b_2(\varphi,m)||_L + ||b_1(\varphi,m_1)||_L\Big]\,\varrho_L(m,m_1)\,,
\end{aligned}$$

and the assertion follows from (3.222). ∎

Proof of Theorem 3.22. Note that functions of the form (3.156) satisfy

$$||\varphi_r||_L \le 2\,||\varphi||_L\,. \tag{3.223}$$

According to (3.182), (3.184) we obtain

$$\begin{aligned}
&|\langle\varphi,\mu^{(n)}(t)\rangle - \langle\varphi,F(t)\rangle| \le \\
&\quad |\langle\varphi_r,\mu^{(n)}(t)\rangle - \langle\varphi_r,F(t)\rangle| + |\langle\varphi-\varphi_r,\mu^{(n)}(t)\rangle| + |\langle\varphi-\varphi_r,F(t)\rangle| \\
&\le |\langle\varphi_r,\mu^{(n)}(0)\rangle - \langle\varphi_r,F_0\rangle| + \int_0^t |\mathcal{B}(\varphi_r,\mu^{(n)}(s)) - \mathcal{B}(\varphi_r,F(s))|\,ds + \\
&\quad |M^{(n)}(\varphi_r,t)| + \int_0^t |R_1^{(n)}(\varphi_r,Z^{(n)}(s))|\,ds + \int_0^t |R_2^{(n)}(\varphi_r,Z^{(n)}(s))|\,ds + \\
&\quad ||\varphi||_\infty\Big[\mu^{(n)}(t,\{(x,v):\,|v|\ge r\}) + F(t,\{(x,v):\,|v|\ge r\})\Big],
\end{aligned}\tag{3.224}$$

for any $r>0$. Using (3.223), (3.141), (3.169) and Lemma 3.35, we conclude from (3.224) that (cf. (3.153))

$$
\begin{aligned}
\varrho_L(\mu^{(n)}(t),F(t)) &\le 2\,\varrho_L(\mu^{(n)}(0),F_0) + \sup_{\varphi\in\mathcal{D}_r}|M^{(n)}(\varphi,t)| + \\
&\quad 4\,C'\,(C_b+C_L)\int_0^t \varrho_L(\mu^{(n)}(s),F(s))\Big[\mu^{(n)}(s,D\times\mathbb{R}^3)+F(s,D\times\mathbb{R}^3)\Big]ds \\
&\quad +\mu^{(n)}(t,\{(x,v):|v|\ge r\})+F(t,\{(x,v):|v|\ge r\}) + \\
&\quad \int_0^t \sup_{\varphi\in\mathcal{D}_r}|R_1^{(n)}(\varphi,Z^{(n)}(s))|\,ds + \int_0^t \sup_{\varphi\in\mathcal{D}_r}|R_2^{(n)}(\varphi,Z^{(n)}(s))|\,ds \\
&\le 4\,C'\,(C_b+C_L)\,[C_\mu + c(S)\,F_0(D\times\mathbb{R}^3)]\int_0^t \varrho_L(\mu^{(n)}(s),F(s))\,ds + \\
&\quad 2\,\varrho_L(\mu^{(n)}(0),F_0) + \sup_{s\in[0,S]}\sup_{\varphi\in\mathcal{D}_r}|M^{(n)}(\varphi,s)| + \\
&\quad \sup_{s\in[0,S]}\mu^{(n)}(s,\{(x,v):|v|\ge r\}) + \sup_{s\in[0,S]}F(s,\{(x,v):|v|\ge r\}) \\
&\quad + \int_0^S \sup_{\varphi\in\mathcal{D}_r}|R_1^{(n)}(\varphi,Z^{(n)}(s))|\,ds + \int_0^S \sup_{\varphi\in\mathcal{D}_r}|R_2^{(n)}(\varphi,Z^{(n)}(s))|\,ds\,,
\end{aligned}
$$

for any $t\in[0,S]$. Gronwall's inequality implies

$$
\begin{aligned}
&\sup_{t\in[0,S]}\varrho_L(\mu^{(n)}(t),F(t)) \le \qquad (3.225)\\
&\quad \exp\Big(4\,C'\,(C_b+C_L)\,[C_\mu + c(S)\,F_0(D\times\mathbb{R}^3)]\,S\Big)\times \\
&\quad \Bigg[2\,\varrho_L(\mu^{(n)}(0),F_0) + \sup_{s\in[0,S]}\sup_{\varphi\in\mathcal{D}_r}|M^{(n)}(\varphi,s)| + \\
&\quad \sup_{s\in[0,S]}\mu^{(n)}(s,\{(x,v):|v|\ge r\}) + \sup_{s\in[0,S]}F(s,\{(x,v):|v|\ge r\}) + \\
&\quad \int_0^S \sup_{\varphi\in\mathcal{D}_r}|R_1^{(n)}(\varphi,Z^{(n)}(s))|\,ds + \int_0^S \sup_{\varphi\in\mathcal{D}_r}|R_2^{(n)}(\varphi,Z^{(n)}(s))|\,ds\Bigg]\,.
\end{aligned}
$$

Since, according to (3.170),

$$
\begin{aligned}
\sup_{s\in[0,S]}F(s,\{(x,v):|v|\ge r\}) &\le \frac{1}{r^2}\sup_{s\in[0,S]}\int_{D\times\mathbb{R}^3}|v|^2\,F(s,dx,dv) \\
&\le \frac{c(S)}{r^2}\int_{D\times\mathbb{R}^3}|v|^2\,F_0(dx,dv)\,,
\end{aligned}
$$

assumptions (3.172) and (3.173) imply (cf. Remark 3.25)

$$
\lim_{r\to\infty}\sup_{s\in[0,S]}F(s,\{(x,v):|v|\ge r\}) = 0\,. \qquad (3.226)
$$

According to (3.226) and Lemmas 3.31-3.34, we finally obtain from (3.225)

$$\limsup_{n\to\infty} \mathbb{E} \sup_{t\in[0,S]} \varrho_L(\mu^{(n)}(t), F(t)) \le$$
$$2\exp\Big(4\,C'(C_b+C_L)\,[C_\mu + c(S)F_0(D\times\mathbb{R}^3)]\,S\Big) \limsup_{n\to\infty} \mathbb{E}\,\varrho_L(\mu^{(n)}(0), F_0)$$

so that (3.174) follows from (3.172). ∎

3.4.4 Construction of reduction measures

Here we construct several examples of reduction measures satisfying the assumptions (3.160), (3.162) and (3.164) of Theorem 3.22. Recall the notations (3.77)–(3.80).

General construction

The general reduction mechanism is described as follows. First a group formation procedure is applied to the state

$$z \in \mathcal{Z}^{(n)}_{\rm red} = \Big\{ z \in \mathcal{Z}^{(n)} \,:\, \nu > \nu^{(n)}_{\max} \Big\} \tag{3.227}$$

giving a family of groups

$$G^{(n)}_i(z) = \Big((x_{i,j}, v_{i,j}, g_{i,j}) \,, \quad j = 1, \dots, \nu_i \Big),$$
$$i = 1, \dots, \gamma^{(n)}(z) \,, \qquad \sum_{i=1}^{\gamma^{(n)}(z)} \nu_i = \nu \,. \tag{3.228}$$

Then each group $G^{(n)}_i(z)$ is replaced by a random system

$$\tilde z_i = \Big((\tilde x_{i,j}, \tilde v_{i,j}, \tilde g_{i,j}) \,, \quad j = 1, \dots, \tilde\nu_i \Big) \tag{3.229}$$

distributed according to some group reduction measure $P^{(n)}_{{\rm red},i}$ on $\mathcal{Z}^{(n)}$. The groups are treated independently so that the reduction measure takes the form

(3.230)

$$P^{(n)}_{\rm red}(z; d\tilde z) = \int_{\mathcal{Z}^{(n)}} \dots \int_{\mathcal{Z}^{(n)}} \delta_{J_{\rm red}(\tilde z_1, \dots, \tilde z_{\gamma^{(n)}(z)})}(d\tilde z) \prod_{i=1}^{\gamma^{(n)}(z)} P^{(n)}_{{\rm red},i}(G^{(n)}_i(z); d\tilde z_i) \,,$$

where $J_{\rm red}(\tilde z_1, \dots, \tilde z_\gamma)$ denotes the formation of a state $\tilde z$ from the subsystems $\tilde z_1, \dots, \tilde z_\gamma$. The group reduction measures are assumed to preserve mass, i.e.

$$\sum_{j=1}^{\tilde\nu_i} \tilde g_{i,j} = \sum_{j=1}^{\nu_i} g_{i,j} \qquad \text{a.s.} \quad \text{w.r.t.} \quad P^{(n)}_{{\rm red},i}(G^{(n)}_i(z); d\tilde z_i) \,. \tag{3.231}$$

Consequently, the measure (3.230) is concentrated on $\mathcal{Z}^{(n)}$.

Now we specify the assumptions of Theorem 3.22 for the reduction measure (3.230).

Remark 3.36. Assume that there exist $k_\gamma \geq 1$ and $\delta \in (0,1)$ such that (cf. (3.229))

$$\tilde{\nu}_i \leq k_\gamma \qquad \text{a.s.} \quad \text{w.r.t.} \quad P^{(n)}_{\text{red},i}(G^{(n)}_i(z); d\tilde{z}_i) \tag{3.232}$$

and

$$k_\gamma \, \gamma^{(n)}(z) \leq (1-\delta) \, \nu^{(n)}_{\max} , \tag{3.233}$$

for all $z \in \mathcal{Z}^{(n)}_{\text{red}}$ and $i = 1, \ldots, \gamma^{(n)}(z)$. Then one obtains

$$\sum_{i=1}^{\gamma^{(n)}(z)} \tilde{\nu}_i \leq (1-\delta) \, \nu^{(n)}_{\max} \qquad \text{a.s.} \quad \text{w.r.t.} \quad P^{(n)}_{\text{red}}(z; d\tilde{z})$$

so that assumption (3.160) is fulfilled. ■

Note that a function Φ of the form (3.163) satisfies (cf. (3.228)-(3.230))

$$\Phi(z) = \sum_{i=1}^{\gamma^{(n)}(z)} \sum_{j=1}^{\nu_i} g_{i,j} \, \varphi(x_{i,j}, v_{i,j}) = \sum_{i=1}^{\gamma^{(n)}(z)} \Phi(G^{(n)}_i(z)) \tag{3.234}$$

and

$$\Phi(J_{\text{red}}(\tilde{z}_1, \ldots, \tilde{z}_{\gamma(z)})) = \sum_{i=1}^{\gamma^{(n)}(z)} \Phi(\tilde{z}_i) \, . \tag{3.235}$$

Remark 3.37. Assume that there exists $c > 0$ such that

$$\int_{\mathcal{Z}^{(n)}} \varepsilon(\tilde{z}_i) \, P^{(n)}_{\text{red},i}(G^{(n)}_i(z); d\tilde{z}_i) \leq c \, \varepsilon(G^{(n)}_i(z)) \, , \tag{3.236}$$

for all $z \in \mathcal{Z}^{(n)}_{\text{red}}$ and $i = 1, \ldots, \gamma^{(n)}(z)$. Then, using (3.234) and (3.235), one obtains

$$\int_{\mathcal{Z}^{(n)}} \varepsilon(\tilde{z}) \, P^{(n)}_{\text{red}}(z; d\tilde{z}) =$$
$$\sum_{i=1}^{\gamma^{(n)}(z)} \int_{\mathcal{Z}^{(n)}} \varepsilon(\tilde{z}_i) \, P^{(n)}_{\text{red},i}(G^{(n)}_i(z); d\tilde{z}_i) \leq c \sum_{i=1}^{\gamma^{(n)}(z)} \varepsilon(G^{(n)}_i(z)) = c \, \varepsilon(z)$$

so that assumption (3.164) is fulfilled. ■

According to (3.234), (3.235), (3.178) and (3.231), the reduction measure (3.230) satisfies

$$\int_{\mathcal{Z}^{(n)}} [\Phi(\tilde{z}) - \Phi(z)]^2 \, P^{(n)}_{\mathrm{red}}(z; d\tilde{z}) =$$

$$\int_{\mathcal{Z}^{(n)}} \dots \int_{\mathcal{Z}^{(n)}} \left[\sum_{i=1}^{\gamma^{(n)}(z)} \Big[\Phi(\tilde{z}_i) - \Phi(G_i^{(n)}(z)) \Big] \right]^2 \prod_{i=1}^{\gamma^{(n)}(z)} P^{(n)}_{\mathrm{red},i}(G_i^{(n)}(z); d\tilde{z}_i)$$

$$\leq \sum_{i=1}^{\gamma^{(n)}(z)} \int_{\mathcal{Z}^{(n)}} \Big[\Phi(\tilde{z}_i) - \Phi(G_i^{(n)}(z)) \Big]^2 P^{(n)}_{\mathrm{red},i}(G_i^{(n)}(z); d\tilde{z}_i) +$$

$$\left(\sum_{i=1}^{\gamma^{(n)}(z)} \int_{\mathcal{Z}^{(n)}} \Big[\Phi(\tilde{z}_i) - \Phi(G_i^{(n)}(z)) \Big] P^{(n)}_{\mathrm{red},i}(G_i^{(n)}(z); d\tilde{z}_i) \right)^2$$

$$\leq 2\, ||\varphi||^2_\infty \sum_{i=1}^{\gamma^{(n)}(z)} \left[\int_{\mathcal{Z}^{(n)}} \varrho(\tilde{z}_i)^2 \, P^{(n)}_{\mathrm{red},i}(G_i^{(n)}(z); d\tilde{z}_i) + \varrho(G_i^{(n)}(z))^2 \right] + R^{(n)}(z)^2$$

$$\leq 4\, ||\varphi||^2_\infty \, C_\mu \max_{i=1,\dots,\gamma^{(n)}(z)} \varrho(G_i^{(n)}(z)) + R^{(n)}(z)^2 \,, \tag{3.237}$$

where

$$R^{(n)}(z) = \sum_{i=1}^{\gamma^{(n)}(z)} \left| \Phi(G_i^{(n)}(z)) - \int_{\mathcal{Z}^{(n)}} \Phi(\tilde{z}_i) P^{(n)}_{\mathrm{red},i}(G_i^{(n)}(z); d\tilde{z}_i) \right| . \tag{3.238}$$

Remark 3.38. Assume that

$$\varrho(G_i^{(n)}(z)) \leq C_G \, g^{(n)}_{\max} \qquad \text{for some} \quad C_G > 0 \tag{3.239}$$

and

$$\Phi(G_i^{(n)}(z)) = \int_{\mathcal{Z}^{(n)}} \Phi(\tilde{z}_i) P^{(n)}_{\mathrm{red},i}(G_i^{(n)}(z); d\tilde{z}_i) \,, \tag{3.240}$$

for all Φ of the form (3.163), $z \in \mathcal{Z}^{(n)}_{\mathrm{red}}$ and $i = 1, \dots, \gamma^{(n)}(z)$, Then (3.237), (3.238) and (3.157) imply

$$\lim_{n\to\infty} \sup_{||\varphi||_\infty \leq 1} \sup_{z \in \mathcal{Z}^{(n)}_{\mathrm{red}}} \int_{\mathcal{Z}^{(n)}} [\Phi(\tilde{z}) - \Phi(z)]^2 \, P^{(n)}_{\mathrm{red}}(z; d\tilde{z}) = 0 \,,$$

which is sufficient for assumption (3.162). ■

In order to weaken assumption (3.240), we consider functions Φ of the form (3.163) with $\varphi \in \mathcal{D}_r$ (cf. (3.155), (3.156)) and $r > 0$. Introduce the notations

$$I^{(n)}(z) = \Big\{ i = 1, 2, \dots, \gamma^{(n)}(z) \Big\} \tag{3.241}$$

and

$$I_r^{(n)}(z) = \Big\{ i \in I^{(n)}(z) : \, |v_{i,j}| < r+1 \quad \text{for some} \quad j = 1, \dots, \nu_i \Big\}. \tag{3.242}$$

Note that

$$|\Phi(z)| \le \varrho_r(z)\,, \tag{3.243}$$

where

$$\varrho_r(z) = \sum_{i=1}^{\nu} g_i \, \chi_{[0,r+1)}(|v|)\,, \qquad z \in \mathcal{Z}^{(n)}\,. \tag{3.244}$$

According to (3.243) and (3.242), the term (3.238) satisfies

$$R^{(n)}(z) = R_r^{(n)}(z) + \sum_{i \in I^{(n)}(z) \setminus I_r^{(n)}(z)} \left| \int_{\mathcal{Z}^{(n)}} \Phi(\tilde z_i)\, P_{\mathrm{red},i}^{(n)}(G_i^{(n)}(z); d\tilde z_i) \right|$$

$$\le R_r^{(n)}(z) + \sum_{i \in I^{(n)}(z) \setminus I_r^{(n)}(z)} \int_{\mathcal{Z}^{(n)}} \varrho_r(\tilde z_i)\, P_{\mathrm{red},i}^{(n)}(G_i^{(n)}(z); d\tilde z_i)\,, \tag{3.245}$$

where

$$R_r^{(n)}(z) = \sum_{i \in I_r^{(n)}(z)} \left| \Phi(G_i^{(n)}(z)) - \int_{\mathcal{Z}^{(n)}} \Phi(\tilde z_i)\, P_{\mathrm{red},i}^{(n)}(G_i^{(n)}(z); d\tilde z_i) \right|. \tag{3.246}$$

Remark 3.39. Assume (3.239),

$$\lim_{n\to\infty} \sup_{\varphi \in \mathcal{D}_r} \sup_{z \in \mathcal{Z}_{\mathrm{red}}^{(n)}} R_r^{(n)}(z) = 0 \tag{3.247}$$

and

$$\lim_{n\to\infty} \sup_{z \in \mathcal{Z}_{\mathrm{red}}^{(n)}} \sum_{i \in I^{(n)}(z) \setminus I_r^{(n)}(z)} \int_{\mathcal{Z}^{(n)}} \varrho_r(\tilde z_i)\, P_{\mathrm{red},i}^{(n)}(G_i^{(n)}(z); d\tilde z_i) = 0\,, \tag{3.248}$$

for any $r > 0$, where the notations (3.241), (3.242), (3.244) and (3.246) are used. Then (3.237), (3.238), (3.245) and (3.157) imply

$$\lim_{n\to\infty} \sup_{\varphi \in \mathcal{D}_r} \sup_{z \in \mathcal{Z}_{\mathrm{red}}^{(n)}} \int_{\mathcal{Z}^{(n)}} [\Phi(\tilde z) - \Phi(z)]^2\, P_{\mathrm{red}}^{(n)}(z; d\tilde z) = 0\,, \qquad \forall\, r > 0\,,$$

which is sufficient for assumption (3.162). ■

Finally, we remove assumption (3.248). According to (3.231), one obtains

$$\sum_{i \in I^{(n)}(z) \setminus I_r^{(n)}(z)} \int_{\mathcal{Z}^{(n)}} \varrho_r(\tilde z_i)\, P_{\mathrm{red},i}^{(n)}(G_i^{(n)}(z); d\tilde z_i) \le$$

$$\sum_{i \in I^{(n)}(z) \setminus I_r^{(n)}(z)} \int_{\mathcal{Z}^{(n)}} \varrho(\tilde z_i)\, P_{\mathrm{red},i}^{(n)}(G_i^{(n)}(z); d\tilde z_i) = \sum_{i \in I^{(n)}(z) \setminus I_r^{(n)}(z)} \varrho(G_i^{(n)}(z))$$

$$= \sum_{i \in I^{(n)}(z) \setminus I_r^{(n)}(z)} \sum_{j=1}^{\nu_i} g_{i,j}\, \chi_{[r+1,\infty)}(|v_{i,j}|) \le \sum_{i=1}^{\nu} g_i\, \chi_{[r+1,\infty)}(|v_i|)$$

so that (3.245) implies (cf. (3.171))

$$R^{(n)}(Z^{(n)}(s)) \le R_r^{(n)}(Z^{(n)}(s)) + \mu^{(n)}(s, \{(x,v) : |v| \ge r\}) . \quad (3.249)$$

Remark 3.40. Assume (3.239), (3.247) and let the assumptions of Lemma 3.31 hold. Then (3.237), (3.238), (3.249) and (3.157) imply

$$\begin{aligned} &\limsup_{n\to\infty} \mathbb{E} \sup_{\varphi\in\mathcal{D}_r} \sup_{s\in[0,S]} \\ &\quad \chi_{\{\nu>\nu_{\max}^{(n)}\}}(Z^{(n)}(s)) \int_{\mathcal{Z}^{(n)}} [\Phi(\tilde z) - \Phi(Z^{(n)}(s))]^2 P_{\mathrm{red}}^{(n)}(Z^{(n)}(s); d\tilde z) \\ &\le 2\, C_\mu \limsup_{n\to\infty} \mathbb{E} \sup_{s\in[0,S]} \mu^{(n)}(s, \{(x,v) : |v| \ge r\}) \end{aligned}$$

so that assumption (3.162) is a consequence of Lemma 3.31.

Group reduction measures

We prepare the construction of the reduction measure (3.230) by introducing several examples of group reduction measures satisfying assumption (3.231).

Example 3.41 (Unbiased reduction). Consider the measure

$$p_{\mathrm{red},1}(z; d\tilde z) = \frac{1}{\varrho(z)} \sum_{i=1}^{\nu} g_i\, \delta_{J_{\mathrm{red},1}(z;i)}(d\tilde z) , \quad (3.250)$$

where

$$J_{\mathrm{red},1}(z;i) = (x_i, v_i, \varrho(z)) , \quad i = 1, \dots, \nu .$$

Note that one particle is produced. Its weight is determined by conservation of mass. According to (3.250), its position and velocity are chosen randomly (with probabilities $g_i/\varrho(z)$) from all particles in the original system. Note that (cf. (3.163))

$$\begin{aligned} &\int_{\mathcal{Z}} \Phi(\tilde z)\, p_{\mathrm{red},1}(z; d\tilde z) = \quad (3.251) \\ &\frac{1}{\varrho(z)} \sum_{i=1}^{\nu} g_i\, \Phi(J_{\mathrm{red},1}(z;i)) = \frac{1}{\varrho(z)} \sum_{i=1}^{\nu} g_i\, \varrho(z)\, \varphi(x_i, v_i) = \Phi(z) , \end{aligned}$$

for arbitrary test functions φ.

Example 3.42 (Conservation of momentum). Consider the measure

$$p_{\mathrm{red},2}(z; d\tilde z) = \frac{1}{\varrho(z)} \sum_{i=1}^{\nu} g_i\, \delta_{J_{\mathrm{red},2}(z;i)}(d\tilde z) , \quad (3.252)$$

where

$$J_{\mathrm{red},2}(z;i) = \Big(x_i, V(z), \varrho(z)\Big)\,, \qquad i = 1,\dots,\nu\,.$$

Note that one particle is produced. Its weight and velocity are uniquely determined by conservation of mass and momentum. According to (3.252), its position is chosen randomly (with probabilities $g_i/\varrho(z)$) from all particles in the original system. The energy of the state after reduction satisfies

$$\varepsilon(J_{\mathrm{red},2}(z)) = \varrho(z)\,|V(z)|^2 \le \sum_{i=1}^{\nu} g_i\,|v_i|^2 = \varepsilon(z)\,. \tag{3.253}$$

Note that (cf. (3.163))

$$\begin{aligned}\int_{\mathcal{Z}} \Phi(\tilde z)\,p_{\mathrm{red},2}(z;d\tilde z) &= \frac{1}{\varrho(z)}\sum_{i=1}^{\nu} g_i\,\Phi(J_{\mathrm{red},2}(z;i))\\ &= \frac{1}{\varrho(z)}\sum_{i=1}^{\nu} g_i\,\varrho(z)\,\varphi(x_i,V(z)) = \sum_{i=1}^{\nu} g_i\,\varphi(x_i,V(z))\,,\end{aligned}$$

for arbitrary test functions φ. This implies

$$\begin{aligned}\left|\int_{\mathcal{Z}} \Phi(\tilde z)\,p_{\mathrm{red},2}(z;d\tilde z) - \Phi(z)\right| &= \left|\sum_{i=1}^{\nu} g_i\,\varphi(x_i,V(z)) - \sum_{i=1}^{\nu} g_i\,\varphi(x_i,v_i)\right|\\ &\le ||\varphi||_L \sum_{i=1}^{\nu} g_i\,|v_i - V(z)|\,.\end{aligned} \tag{3.254}$$

Example 3.43 (Conservation of momentum and energy). Consider the measure

$$p_{\mathrm{red},3}(z;d\tilde z) = \frac{1}{\varrho(z)^2}\sum_{i,j=1}^{\nu} g_i\,g_j \int_{\mathcal{S}^2} \delta_{J_{\mathrm{red},3}(z;i,j,e)}(d\tilde z)\,\sigma_{\mathrm{red}}(z;de)\,, \tag{3.255}$$

where

$$\begin{aligned}[J_{\mathrm{red},3}(z;i,j,e)]_1 &= \left(x_i, V(z) + \sqrt{3\,T(z)}\,e\,, \frac{\varrho(z)}{2}\right),\\ [J_{\mathrm{red},3}(z;i,j,e)]_2 &= \left(x_j, V(z) - \sqrt{3\,T(z)}\,e\,, \frac{\varrho(z)}{2}\right)\end{aligned} \tag{3.256}$$

and σ_{red} is some probability measure on $\mathcal{S}^2$. Note that two particles are produced. Each of them is given half of the weight of the original system. Their velocities are determined by conservation of momentum and energy up to a certain vector $e \in \mathcal{S}^2$. According to (3.255), their positions are chosen

randomly (with probabilities $g_i/\varrho(z)$) from all particles in the original system, and the distribution of e is $\sigma_{\rm red}$. Note that the energy of the state after reduction satisfies

$$\begin{aligned}\varepsilon(J_{\rm red,3}(z;i,j,e)) &= \frac{\varrho(z)}{2}\left[|V(z)+\sqrt{3\,T(z)}\,e|^2+|V(z)-\sqrt{3\,T(z)}\,e|^2\right]\\ &= \varrho(z)\Big[|V(z)|^2+3\,T(z)\Big] = \varepsilon(z)\,,\end{aligned}$$

for all $i,j=1,\ldots,\nu$ and $e\in\mathcal{S}^2$. Since (cf. (3.163))

$$\begin{aligned}&\Phi(J_{\rm red,3}(z;i,j,e)) =\\ &\frac{\varrho(z)}{2}\left[\varphi(x_i,V(z)+\sqrt{3\,T(z)}\,e)+\varphi(x_j,V(z)-\sqrt{3\,T(z)}\,e)\right],\end{aligned}$$

one obtains

$$\begin{aligned}&\int_{\mathcal{Z}}\Phi(\tilde z)\,p_{\rm red,3}(z;d\tilde z) = \frac{1}{\varrho(z)^2}\sum_{i,j=1}^{\nu} g_i\,g_j\int_{\mathcal{S}^2}\Phi(J_{\rm red,3}(z;i,j,e))\,\sigma_{\rm red}(z;de)\\ &=\frac{1}{2}\sum_{i=1}^{\nu} g_i\int_{\mathcal{S}^2}\varphi(x_i,V(z)+\sqrt{3\,T(z)}\,e)\,\sigma_{\rm red}(z;de)+\\ &\quad\frac{1}{2}\sum_{j=1}^{\nu} g_j\int_{\mathcal{S}^2}\varphi(x_j,V(z)-\sqrt{3\,T(z)}\,e)\,\sigma_{\rm red}(z;de)\,,\end{aligned}$$

for arbitrary test functions φ. This implies

$$\begin{aligned}&\left|\int_{\mathcal{Z}}\Phi(\tilde z)\,p_{\rm red,3}(z;d\tilde z)-\Phi(z)\right|\le\\ &\quad\frac{1}{2}\left|\sum_{i=1}^{\nu} g_i\int_{\mathcal{S}^2}\varphi(x_i,V(z)+\sqrt{3\,T(z)}\,e)\,\sigma_{\rm red}(z;de)-\sum_{i=1}^{\nu} g_i\,\varphi(x_i,v_i)\right|+\\ &\quad\frac{1}{2}\left|\sum_{i=1}^{\nu} g_i\int_{\mathcal{S}^2}\varphi(x_i,V(z)-\sqrt{3\,T(z)}\,e)\,\sigma_{\rm red}(z;de)-\sum_{i=1}^{\nu} g_i\,\varphi(x_i,v_i)\right|\\ &\le||\varphi||_L\left[\sum_{i=1}^{\nu} g_i\,|v_i-V(z)|+\varrho(z)\sqrt{3\,T(z)}\right].\end{aligned}\tag{3.257}$$

For example, $\sigma_{\rm red}$ can be the uniform distribution on $\mathcal{S}^2$. Another particular choice is

$$\sigma_{\rm red}(de)=\delta_{e(z)}(de)\,,$$

where

$$e_k(z)=\pm\frac{1}{\sqrt{3\,T(z)}}\sqrt{\frac{\varepsilon_k(z)}{\varrho(z)}-V_k(z)^2}\,,\quad \varepsilon_k(z)=\sum_{i=1}^{\nu} g_i\,v_{i,k}^2\,,\qquad k=1,2,3\,.$$

In this case one obtains

$$\varepsilon_k(J_{\mathrm{red},3}(z;i,j,e(z))) = \tag{3.258}$$
$$\frac{\varrho(z)}{2}\Big[[V_k(z)+\sqrt{3\,T(z)}\,e_k(z)]^2+[V_k(z)-\sqrt{3\,T(z)}\,e_k(z)]^2\Big]=\varepsilon_k(z)$$

so that even the energy components are preserved.

Example 3.44 (Conservation of momentum, energy and heat flux). Consider the measure

$$p_{\mathrm{red},4}(z;d\tilde z)=\frac{1}{\varrho(z)^2}\sum_{i,j=1}^{\nu} g_i\,g_j\,\delta_{J_{\mathrm{red},4}(z;i,j)}(d\tilde z)\,, \tag{3.259}$$

where

$$[J_{\mathrm{red},4}(z;i,j)]_1=\Big(x_i,\tilde v_1(z),\tilde g_1(z)\Big),\quad [J_{\mathrm{red},4}(z;i,j)]_2=\Big(x_j,\tilde v_2(z),\tilde g_2(z)\Big).$$

Note that two particles are produced. Their weights and velocities are uniquely determined by the conservation of mass, momentum, energy and also the heat flux vector of the system

$$q(z)=\frac{1}{2}\sum_{i=1}^{\nu} g_i\,(v_i-V(z))|v_i-V(z)|^2\,.$$

According to (3.259), their positions are chosen randomly (with probabilities $g_i/\varrho(z)$) from all particles in the original system. The case $q=0$ is covered by Example 3.43, since (cf. (3.256))

$$q(J_{\mathrm{red},3}(z;e))=\frac{3\,\varrho(z)\,T(z)}{4}\Big[\sqrt{3\,T(z)}\,e-\sqrt{3\,T(z)}\,e\Big]=0\,,$$

for any $e\in\mathcal{S}^2$. Thus, in the following derivation we assume $q\neq 0$. We consider velocities of the form

$$\tilde v_1=V(z)+\alpha\,e\,,\qquad \tilde v_2=V(z)-\beta\,e\,,\qquad e\in\mathcal{S}^2\,, \tag{3.260}$$

where α and β are positive numbers. The conservation properties imply

$$\varrho(z)=\varrho(\tilde z)=\tilde g_1+\tilde g_2\,, \tag{3.261}$$

$$\begin{aligned}\varrho(z)\,V(z)&=\varrho(\tilde z)\,V(\tilde z)=\tilde g_1\,[V(z)+\alpha\,e]+\tilde g_2\,[V(z)-\beta\,e]\\&=\varrho(z)\,V(z)+[\alpha\,\tilde g_1-\beta\,\tilde g_2]\,e\,,\end{aligned} \tag{3.262}$$

$$\begin{aligned}\varepsilon(z)&=\varepsilon(\tilde z)=\tilde g_1\,|V(z)+\alpha\,e|^2+\tilde g_2\,|V(z)-\beta\,e|^2\\&=\varrho(z)\,|V(z)|^2+2\,[\alpha\,\tilde g_1-\beta\,\tilde g_2]\,\big(V(z),e\big)+\tilde g_1\,\alpha^2+\tilde g_2\,\beta^2\\&=\varrho(z)\,|V(z)|^2+\tilde g_1\,\alpha^2+\tilde g_2\,\beta^2\end{aligned} \tag{3.263}$$

and

$$2\,q(z) = 2\,q(\tilde{z}) = [\tilde{g}_1\,\alpha^3 - \tilde{g}_2\,\beta^3]\,e\,. \tag{3.264}$$

From (3.262), (3.263) one obtains

$$\alpha\,\tilde{g}_1 = \beta\,\tilde{g}_2 \tag{3.265}$$

and (cf. (3.80))

$$\tilde{g}_1\,\alpha^2 + \tilde{g}_2\,\beta^2 = 3\,\varrho(z)\,T(z)\,. \tag{3.266}$$

Considering

$$\alpha = \theta\,\sqrt{3\,T(z)}\,, \qquad \theta > 0\,, \tag{3.267}$$

and using (3.265), one gets from (3.266) the relation

$$\begin{aligned}\tilde{g}_1\,\alpha^2 + \tilde{g}_2\,\beta^2 &= \tilde{g}_1\,\alpha^2 + \tilde{g}_2\,\frac{\tilde{g}_1^2}{\tilde{g}_2^2}\,\alpha^2 = 3\,\tilde{g}_1\,\theta^2\,T(z) + 3\,\frac{\tilde{g}_1^2}{\tilde{g}_2}\,\theta^2\,T(z)\\ &= 3\,\frac{\tilde{g}_1}{\tilde{g}_2}\,\theta^2\,T(z)\,(\tilde{g}_1 + \tilde{g}_2) = 3\,\varrho(z)\,T(z)\,\frac{\tilde{g}_1}{\tilde{g}_2}\,\theta^2 = 3\,\varrho(z)\,T(z)\,,\end{aligned}$$

which implies (cf. (3.261))

$$\tilde{g}_1 = \varrho(z)\frac{1}{1+\theta^2}\,, \qquad \tilde{g}_2 = \varrho(z)\frac{\theta^2}{1+\theta^2} \tag{3.268}$$

and (cf. (3.265))

$$\beta = \frac{\sqrt{3\,T(z)}}{\theta}\,. \tag{3.269}$$

From (3.264) one obtains

$$e = e(z) = \frac{q(z)}{|q(z)|} \tag{3.270}$$

and, using (3.267) and (3.268),

$$\begin{aligned}\tilde{g}_1\,\alpha^3 - \tilde{g}_2\,\beta^3 &= \varrho(z)\,\frac{1}{1+\theta^2}\,\theta^3\,[3\,T(z)]^{\frac{3}{2}} - \varrho(z)\,\frac{\theta^2}{1+\theta^2}\,\frac{[3\,T(z)]^{\frac{3}{2}}}{\theta^3} =\\ \varrho(z)\,\frac{[3\,T(z)]^{\frac{3}{2}}}{1+\theta^2}\,\left(\theta^3 - \frac{1}{\theta}\right) &= \varrho(z)\,\frac{[3\,T(z)]^{\frac{3}{2}}}{\theta}\,\left(\theta^2 - 1\right) = 2\,|q(z)|\,,\end{aligned}$$

which implies

$$\theta^2 - 2\frac{|q(z)|}{\varrho(z)\,[3\,T(z)]^{\frac{3}{2}}}\,\theta - 1 = 0\,. \tag{3.271}$$

Equation (3.271) is always solvable and only the solution

$$\theta = \theta(z) = \frac{|q(z)|}{\varrho(z)\,[3\,T(z)]^{\frac{3}{2}}} + \sqrt{1 + \frac{|q(z)|^2}{\varrho(z)^2\,[3\,T(z)]^3}}$$

is positive (cf. (3.267)). According to (3.267)-(3.270) and (3.260), the parameters of the two new particles are

$$\tilde{g}_1(z) = \frac{1}{1+\theta(z)^2}\,\varrho(z)\,, \qquad \tilde{g}_2(z) = \frac{\theta(z)^2}{1+\theta(z)^2}\,\varrho(z)\,, \tag{3.272}$$

$$\tilde{v}_1(z) = V(z) + \frac{\theta(z)\,\sqrt{3\,T(z)}}{|q(z)|}\,q(z)\,, \qquad \tilde{v}_2(z) = V(z) - \frac{\sqrt{3\,T(z)}}{\theta(z)\,|q(z)|}\,q(z)\,.$$

One obtains (cf. (3.163))

$$\begin{aligned}
\int_{\mathcal{Z}} \Phi(\tilde{z})\,p_{\mathrm{red},4}(z;d\tilde{z}) &= \frac{1}{\varrho(z)^2}\sum_{i,j=1}^{\nu} g_i\,g_j\,\Phi(J_{\mathrm{red},4}(z;i,j)) \\
&= \frac{1}{\varrho(z)^2}\sum_{i,j=1}^{\nu} g_i\,g_j\Big[\tilde{g}_1(z)\,\varphi(x_i,\tilde{v}_1(z)) + \tilde{g}_2(z)\,\varphi(x_j,\tilde{v}_2(z))\Big] \\
&= \frac{\tilde{g}_1(z)}{\varrho(z)}\sum_{i=1}^{\nu} g_i\,\varphi(x_i,\tilde{v}_1(z)) + \frac{\tilde{g}_2(z)}{\varrho(z)}\sum_{j=1}^{\nu} g_j\,\varphi(x_j,\tilde{v}_2(z))\,,
\end{aligned}$$

for arbitrary test function φ. This implies

$$\begin{aligned}
&\left|\int_{\mathcal{Z}} \Phi(\tilde{z})\,p_{\mathrm{red},4}(z;d\tilde{z}) - \Phi(z)\right| \le \frac{\tilde{g}_1(z)}{\varrho(z)}\sum_{i=1}^{\nu} g_i\Big|\varphi(x_i,\tilde{v}_1(z)) - \varphi(x_i,v_i)\Big| + \\
&\quad \frac{\tilde{g}_2(z)}{\varrho(z)}\sum_{j=1}^{\nu} g_j\Big|\varphi(x_j,\tilde{v}_2(z)) - \varphi(x_j,v_j)\Big| \\
&\le ||\varphi||_L\left[\sum_{i=1}^{\nu} g_i\,|v_i - V(z)| + \varrho(z)\,\sqrt{3\,T(z)}\left(\frac{\tilde{g}_1(z)\,\theta(z)}{\varrho(z)} + \frac{\tilde{g}_2(z)}{\varrho(z)\,\theta(z)}\right)\right] \\
&= ||\varphi||_L\left[\sum_{i=1}^{\nu} g_i\,|v_i - V(z)| + \varrho(z)\,\sqrt{3\,T(z)}\,\frac{2\,\theta(z)}{1+\theta(z)^2}\right] \\
&\le ||\varphi||_L\left[\sum_{i=1}^{\nu} g_i\,|v_i - V(z)| + \varrho(z)\,\sqrt{3\,T(z)}\right],
\end{aligned} \tag{3.273}$$

according to (3.272).

Examples of reduction measures

Finally, we introduce several combinations of group reduction measures from Examples 3.41-3.44 into a reduction measure (3.230) and check the assumptions of Theorem 3.22.

Example 3.45. We define

$$P^{(n)}_{\mathrm{red},i}(z;d\tilde{z}) = p_{\mathrm{red},1}(z;d\tilde{z})\,, \qquad i=1,\ldots,\gamma^{(n)}(z)\,,$$

according to Example 3.41. Note that (3.232) is fulfilled with $k_\gamma = 1$, and (3.236), (3.240) follow from (3.251). According to Remarks 3.36-3.38, the reduction measure (3.230) satisfies the assumptions of Theorem 3.22 for all group formation procedures such that (cf. (3.233), (3.239))

$$\gamma^{(n)}(z) \le (1-\delta)\,\nu^{(n)}_{\max} \qquad \text{for some } \delta\in(0,1) \tag{3.274}$$

and

$$\varrho(G^{(n)}_i(z)) \le g^{(n)}_{\max}\,, \tag{3.275}$$

for all $z\in\mathcal{Z}^{(n)}_{\mathrm{red}}$ (cf. (3.227)) and $i=1,\ldots,\gamma^{(n)}(z)$. Since particle weights are bounded by $g^{(n)}_{\max}$, it is always possible to form groups satisfying (3.275) and

$$\frac{1}{2}\,g^{(n)}_{\max} \le \varrho(G^{(n)}_i(z)) \qquad \text{for all but one } i\,. \tag{3.276}$$

Since the mass of the system is bounded by C_μ, (3.276) implies

$$\gamma^{(n)}(z) \le \frac{2\,C_\mu}{g^{(n)}_{\max}} + 1$$

so that assumption (3.274) can be satisfied if

$$\frac{2\,C_\mu + g^{(n)}_{\max}}{1-\delta} \le g^{(n)}_{\max}\,\nu^{(n)}_{\max} \qquad \text{for some } \delta\in(0,1)\,.$$

Note that there is a lot of freedom in the choice of the groups.

Example 3.46. We define

$$P^{(n)}_{\mathrm{red},i}(z;d\tilde{z}) = p_{\mathrm{red},k(i)}(z;d\tilde{z})\,, \qquad i=1,\ldots,\gamma^{(n)}(z)\,,$$

where $k(i)$ can take the values $2,3,4$, according to Examples 3.42-3.44. Note that (3.232) is fulfilled with $k_\gamma = 2$, and (3.236) is satisfied due to either energy conservation or (3.253). According to (3.254), (3.257), (3.273) and

$$\sum_{i=1}^{\nu} g_i\,|v_i - V(z)| \le \sqrt{\varrho(z)}\left(\sum_{i=1}^{\nu} g_i\,|v_i-V(z)|^2\right)^{\frac{1}{2}} = \varrho(z)\,\sqrt{3\,T(z)}\,,$$

one obtains

$$\sum_{i\in I^{(n)}_r(z)} \left|\int_{\mathcal{Z}^{(n)}} \Big[\Phi(\tilde{z}_i) - \Phi(G^{(n)}_i(z))\Big]\,P^{(n)}_{\mathrm{red},i}(G^{(n)}_i(z);d\tilde{z}_i)\right| \le$$

$$2\sqrt{3}\,||\varphi||_L \sum_{i\in I^{(n)}_r(z)} \varrho(G^{(n)}_i(z))\,\sqrt{T(G^{(n)}_i(z))}$$

so that (3.247) is fulfilled if (cf. (3.227))

$$\lim_{n\to\infty} \sup_{z\in\mathcal{Z}_{\rm red}^{(n)}} \sum_{i\in I_r^{(n)}(z)} \varrho(G_i^{(n)}(z)) \sqrt{T(G_i^{(n)}(z))} = 0\,, \qquad \forall\, r>0\,. \tag{3.277}$$

Since

$$3\,T(z) = \frac{1}{\varrho(z)} \sum_{i=1}^{\nu} g_i \left| v_i - \frac{1}{\varrho(z)} \sum_{j=1}^{\nu} g_j\, v_j \right|^2 = \frac{1}{\varrho(z)^3} \sum_{i=1}^{\nu} g_i \left| \sum_{j=1}^{\nu} g_j\, v_i - \sum_{j=1}^{\nu} g_j\, v_j \right|^2$$

and

$$\sqrt{3\,T(z)} \le \mathrm{diam}_v(z) := \max_{1\le i,j\le\nu} |v_i - v_j|\,,$$

a sufficient condition for (3.277) is

$$\lim_{n\to\infty} \sup_{z\in\mathcal{Z}_{\rm red}^{(n)}} \max_{i\in I_r^{(n)}(z)} \mathrm{diam}_v(G_i^{(n)}(z)) = 0\,, \qquad \forall\, r>0\,. \tag{3.278}$$

Consider a sequence of numbers $d_n > 0$ such that

$$\lim_{n\to\infty} d_n = \infty \tag{3.279}$$

and a sequence of set families

$$C_l^{(n)} \subset \mathbb{R}^3\,, \qquad l = 1,\dots,n\,,$$

such that

$$\Big\{ |v| \le d_n \Big\} \subset \bigcup_{l=1}^{n} C_l^{(n)} \tag{3.280}$$

and

$$\lim_{n\to\infty} \max_{1\le l\le n} \mathrm{diam}\, C_l^{(n)} = 0\,. \tag{3.281}$$

Assume that (cf. (3.228))

$$\begin{aligned} &\{v_{i,j}\,,\ j=1,\dots,\nu_i\} \subset C_l^{(n)}\,, \qquad \text{for some} \quad l=1,\dots,n\,, \\ &\text{or} \\ &\{v_{i,j}\,,\ j=1,\dots,\nu_i\} \cap C_l^{(n)} = \emptyset\,, \qquad \forall\, l=1,\dots,n\,, \end{aligned} \tag{3.282}$$

for all $z \in \mathcal{Z}_{\rm red}^{(n)}$ and $i = 1,\dots,\gamma^{(n)}(z)$. Then (3.278) follows from (3.279)-(3.281). According to Remarks 3.36, 3.37 and 3.40, the reduction measure

(3.230) satisfies the assumptions of Theorem 3.22 for all group formation procedures such that (cf. (3.233), (3.239))

$$2\,\gamma^{(n)}(z) \le (1-\delta)\,\nu_{\max}^{(n)} \qquad \text{for some } \delta \in (0,1)\,, \tag{3.283}$$

$$\varrho(G_i^{(n)}(z)) \le g_{\max}^{(n)} \tag{3.284}$$

and (3.282) holds, for all $z \in \mathcal{Z}_{\rm red}^{(n)}$ and $i = 1, \dots, \gamma^{(n)}(z)$. Since particle weights are bounded by $g_{\max}^{(n)}$, it is always possible to form groups satisfying (3.282) and (3.284). Since the mass of the system is bounded by C_μ, the number of groups satisfies (cf. (3.276))

$$\begin{aligned}\gamma^{(n)}(z) &\le \sum_{l=1}^{n} \left[\frac{2}{g_{\max}^{(n)}} \sum_{i:\, v_i \in C_l^{(n)}} g_i + 1 \right] + \frac{2}{g_{\max}^{(n)}} \sum_{i:\, v_i \notin C_l^{(n)}, \forall\, l} g_i + 1 \\ &\le \frac{2\,C_\mu}{g_{\max}^{(n)}} + n + 1\,.\end{aligned}$$

Thus, condition (3.283) can be satisfied, if

$$\frac{4\,C_\mu + 2\,(n+1)\,g_{\max}^{(n)}}{1-\delta} \le g_{\max}^{(n)}\,\nu_{\max}^{(n)} \qquad \text{for some } \delta \in (0,1)\,.$$

Note that there is a lot of freedom in the choice of the groups. One may choose $\gamma^{(n)}(z)$ arbitrary groups of weight less or equal than $g_{\max}^{(n)}$, each either contained in one of the sets $C_l^{(n)}$ or not intersecting with any of them, provided that $\gamma^{(n)}(z)$ satisfies (3.283). ■

Remark 3.47. In Example 3.46 there are no restrictions concerning the form of the groups outside $\cup_{l=1}^{n} C_l^{(n)}$. In order to apply Remark 3.39 instead of Remark 3.40, one would need to make some additional assumption, e.g., that the reduction outputs for those groups remain outside $\cup_{l=1}^{n} C_l^{(n)}$.

Group formation procedure

Under the above restrictions, the group formation procedure is rather arbitrary. In particular, the following method can be used iteratively. One determines the direction in which the group variation is greatest. Then the group is splitted with a plane perpendicular to that direction through the group mean. More specifically, one determines the group covariance matrix

$$R_{i,j}(z) = \frac{1}{\varrho(z)} \sum_{k=1}^{\nu} g_k\, v_{k,i}\, v_{k,j} - V_i(z)\, V_j(z)\,, \qquad i,j = 1,2,3\,.$$

The normal direction of the splitting plane is parallel to the eigenvector corresponding to the largest eigenvalue of $R(z)$.

3.5 Comments and bibliographic remarks

3.5.1 Some Monte Carlo history

The term "Monte Carlo method" occurs in the title of the paper [137] by N. Metropolis (1915-1999) and S. Ulam (1909-1984) in 1949, where earlier work by E. Fermi (1901-1954) and J. von Neumann (1903-1957) is mentioned. The method consists in generating samples of stochastic models in order to extract statistical information. An elementary random number generator is a roulette, though in practice deterministic algorithms (imitating random properties) are run on computers.

The method, which could be called "stochastic numerics", has a very wide range of applications. The objective may be the numerical approximation of deterministic quantities, like an integral or the solution to some integro-differential equation. However, in many situations one does not need any equation to study rather complicated phenomena. It is sufficient to have a model that includes probabilistic information about some basic events. Then one can use "direct simulation". This makes the method so attractive to people working in applications. Much of the literature is spread over very different fields, leading often to parallel developments.

The history of the Monte Carlo method is described in the literature. Early monographs are [43], [42], [77], [71], [189], [56], [188]. The extensive review paper [76] contains a list of 251 references. By now the mathematical search system *MathSciNet* names more than 120 matches, when asked: "Monte Carlo" in "title" AND "Entry type" = "Books (including proceedings)". The development of the Monte Carlo method as an important tool for applied problems is closely related to the development of computers (see the paper [3] written on the occasion of Metropolis' 70th birthday). The first significant field of application was radiation transport, where the linear Boltzmann equation is relevant.

In the field of nonlinear transport, the "test particle Monte Carlo method" was introduced in [79] and the "direct simulation Monte Carlo (or DSMC) method" goes back to [19] (homogeneous gas relaxation problem) and [20] (shock structure problem). We refer to [21], [25, Sects. 9.4, 11.1] and [26] concerning remarks on the historical development. The history of the subject is also reflected in the proceedings of the bi-annual conferences on "Rarefied Gas Dynamics" ranging from 1958 to the present (cf. [175], [174]).

3.5.2 Time counting procedures

First we recall the collision simulation without fictitious collisions. We consider the hard sphere collision kernel from Example 1.5 so that

$$\int_{\mathcal{S}^2} B(v,w,e)\,de = c_B\,|v-w|\,,$$

for some constant c_B. In the case of constant weights $\bar{g}^{(n)} = 1/n$, the parameter of the waiting time distribution (3.70) takes the form (cf. (3.68))

$$\begin{aligned}\lambda_{\mathrm{coll},l}(z) &= \frac{1}{2} \sum_{1 \le i \ne j \le \nu} \int_{\mathcal{S}^2} p_{\mathrm{coll},l}(z; i, j, e)\, de \\ &= \frac{c_B}{2\, n\, |D_l|} \sum_{i \ne j\,:\, x_i, x_j \in D_l} |v_i - v_j| \,. \end{aligned} \tag{3.285}$$

The distribution (3.72) of the indices i, j of the collision partners is

$$\frac{|v_i - v_j|}{\sum_{\alpha \ne \beta\,:\, x_\alpha, x_\beta \in D_l} |v_\alpha - v_\beta|} \,, \tag{3.286}$$

i.e. the pairs of particles are chosen with probability proportional to their relative velocity. The numerical implementation of this modeling procedure runs into difficulties, since, in general, there is quadratic effort (with respect to the number of particles in the cell) in the calculation of the waiting time parameter (3.285) or the probabilities (3.286).

The original idea to avoid this problem was introduced in Bird's "time counter method". Here the indices i, j are generated according to (3.286) by an acceptance-rejection technique, and the corresponding time step is computed as

$$\hat{\tau}(z, i, j) = \frac{2\, n\, |D_l|}{c_B\, \nu_l\, (\nu_l - 1)\, |v_i - v_j|} \,, \tag{3.287}$$

where ν_l denotes the number of particles in the cell D_l. Note that, according to (3.286),

$$\begin{aligned}\mathbb{E}\, \hat{\tau}(z, i, j) &= \sum_{i \ne j\,:\, x_i, x_j \in D_l} \hat{\tau}(z, i, j)\, \frac{|v_i - v_j|}{\sum_{\alpha \ne \beta\,:\, x_\alpha, x_\beta \in D_l} |v_\alpha - v_\beta|} \\ &= \frac{1}{\sum_{\alpha \ne \beta\,:\, x_\alpha, x_\beta \in D_l} |v_\alpha - v_\beta|} \sum_{i \ne j\,:\, x_i, x_j \in D_l} \frac{2\, n\, |D_l|}{c_B\, \nu_l\, (\nu_l - 1)} \\ &= \frac{2\, n\, |D_l|}{c_B \sum_{i \ne j\,:\, x_i, x_j \in D_l} |v_i - v_j|} = \lambda_{\mathrm{coll},l}(z)^{-1} \,. \end{aligned}$$

Thus, the time counter (3.287) has the correct expectation (3.285). However, the time counter method has some drawbacks. If, by chance, a pair (i, j) with a small relative velocity is chosen, then the time step (3.287) is large. This effect may create strong statistical fluctuations.

The idea of "fictitious collisions" is very general (cf. [61, Ch. 4, § 2]). In the context of the Boltzmann equation it has been introduced in various ways and under different names. A "null-collision technique" appeared in [112] (submitted 07/86), a "majorant frequency scheme" was derived in [89] (submitted

08/87), and the most commonly used "no time counter scheme" was introduced in [24] (submitted 1988). We refer to the review paper [88] and to [25, Section 11.1] for more comments on this issue.

The time counting procedure from Section 3.3.5 was introduced in [179]. DSMC with the waiting time parameter (3.113) is expected to be more efficient than DSMC with the waiting time parameter (3.93) if there are relatively few particles with large relative velocities (compared to V_l) while the majority of particles has moderate relative velocities. In these cases the individual majorant (3.103) will be significantly smaller than the global majorant (3.88). The corresponding time steps are much bigger so that fewer collisions are generated. However, a part of this advantage is lost due to the additional effort needed for the simulation. This effect has been illustrated in [179, Tables 1,2]. Numerical experiments for SWPM have not yet been performed.

The temperature time counter from Section 3.3.6 was introduced in [180]. The advantage of bigger time steps is partly lost due to the additional effort needed for simulation (cf. [180, Tables 1,2]). This procedure seems to be more appropriate for DSMC than for SWPM because of the constant time step.

3.5.3 Convergence and variance reduction

The study of the relationship between the stochastic simulation procedures and the Boltzmann equation was not much valued by the "father of DSMC" G. A. Bird a decade ago. We cite from [25, p.209]: "...it is much easier to introduce more complex and accurate models into the direct simulation environment than into the formal Boltzmann equation. ... To limit direct simulation objectives to a solution of the Boltzmann equation is unduly restrictive. ... Given the physical basis of the DSMC method, the existence, uniqueness and convergence issues that are important in the traditional mathematical analysis of equations, are largely irrelevant." Both cited arguments are convincing, but the conclusion is questionable. Surely the stochastic particle system carries much more information than the limiting equation. In particular, it allows one to study fluctuation phenomena. Moreover, introducing complex physical effects into the DSMC procedure is often straightforward.

However, one of the most important theoretical issues in Monte Carlo theory is the problem of **variance reduction**. Applied to direct simulation schemes, it means that the "natural" level of statistical fluctuations should be reduced in order to better estimate certain average quantities. In rarefied gas dynamics such quantities might be macroscopic characteristics of flows with high density gradients, or tails of the velocity distribution. We cite from [25, p.212]: "Systematic variance reduction has not been demonstrated for the DSMC method." This is in contrast to linear transport theory, where powerful variance reduction methods (like importance sampling) have been developed since the early days. We cite a classical statement from [202, p.68] (though it might be considered as being "politically incorrect" nowadays) "... the only good Monte Carlos are dead Monte Carlos – the Monte Carlos we

don't have to do. In other words, good Monte Carlo ducks chance processes as much as possible. In particular, if the last step of the process we are studying is a probability of reaction, it is wasteful ... to force a 'yes' or 'no' with a random number instead of accepting the numerical value of the probability of reaction and averaging this numerical value." Accordingly, the basic principle of variance reduction in linear transport is to let particles always go through the material (with appropriately reduced weights) instead of absorbing them all the time except a few events, when the particle comes through with its starting weight.

In nonlinear transport the situation is more complicated. Roughly speaking, variance reduction assumes having a parameter dependent class of models approximating the same object. The parameter is then chosen in order to reduce the variance, thus improving the stochastic convergence behavior. In the linear case, all random variables usually have the same expectation, corresponding to the quantities of interest. In the nonlinear case, it is also necessary to make parameter dependent models comparable. One way is to check that the random variables converge to the same limit, independently of the choice of the parameter. Thus, the convergence issue becomes important in this context, and limiting equations occur.

Following ideas used in the case of linear transport, a specific variance reduction strategy is to fill the position space (or larger parts of the velocity space) uniformly with particles, while the weights of these particles provide information about the actual density. In the general context the uniformity corresponds to the introduction of some deterministic components (regular grid, order, etc.). The stochastic weighted particle method (SWPM) is based on this strategy. The method consists of a class of algorithms containing certain degrees of freedom. For a special choice of these parameters the standard DSMC method is obtained. More general procedures of modeling particle collisions as well as inflow and boundary behavior are implemented. The degrees of freedom are used to control the behavior of the particle system, aiming at variance reduction. The basic idea of the method originates from [86], where random discrete velocity models were introduced (cf. also [84], [85], [87]). These models combine particle schemes (particles with changing velocities and fixed weights) and discrete velocity models (particles with fixed velocities and changing weights). SWPM was formulated in [177]. It is based on a partial random weight transfer during collisions, leading to an increase in the number of particles. Therefore appropriate reduction procedures are needed to control that quantity. Various deterministic procedures with different conservation properties were proposed in [176], and some error estimates were found. Low density regions have been successfully resolved with a moderate number of simulation particles in [181].

Further references related to weighted particles applied in the framework of different methods are [183], [39], [147], [138]. In [183] the author uses a reduction procedure requiring the conservation of all energy components (3.258).

Some convergence results for SWPM without reduction were obtained in [206], [178]. A convergence proof for SWPM with reduction has been proposed in [130]. The basic idea was the introduction of new stochastic reduction procedures that, on the one hand, do not possess all conservation properties of the deterministic procedures, but, on the other hand, have the correct expectation for a much larger class of functionals. This idea is quite natural in the context of stochastic particle methods. Theorem 3.22 presents an improved version of the result from [130] and includes the case of deterministic reduction. The proof follows the lines of [206], though other (more recent) approaches might be more elegant. The convergence result covers SWPM (including standard DSMC) with different collision transformations (cf. Remark 3.24). In particular, it can be applied to the Boltzmann equation with inelastic collisions.

Convergence for Bird's scheme (with the original time counter (3.287)) was proved in [204]. We note that the introduction of the "no time counter" schemes (1986-1988) makes the direct connection between practically relevant numerical procedures and Markov processes evident. Thus, results from the theory of stochastic processes are immediately applicable (cf. the discussion in Section 2.3.3). In particular, this has been done for the modeling procedures based on the Skorokhod approach through stochastic differential equations with respect to Poisson measures (cf. [5], [127], [125], [128]). Further aspects of convergence for Bird's scheme were studied in [167].

3.5.4 Nanbu's method

The interest in studying the connection between stochastic simulation procedures in rarefied gas dynamics and the Boltzmann equation was stimulated by K. Nanbu's paper [144] in 1980 (cf. the survey papers [145], [146], [83]). Starting from the Boltzmann equation, the author introduced certain approximations and derived a probabilistic particle scheme. In Nanbu's method the general DSMC framework of Section 3.1 is used, but the collision simulation is modified. We describe the collision simulation step on the time interval $[0, \Delta t]$ and give a convergence proof.

Let $(x_1(0), v_1(0), \ldots, x_n(0), v_n(0))$ be the state of the system at time zero. We consider the case of constant particle weights $1/n$. The collision kernel is assumed to satisfy

$$\sup_{v,w\in\mathbb{R}^3} \int_{\mathcal{S}^2} B(v,w,e)\, de < \infty \tag{3.288}$$

and the time step is such that

$$\Delta t\, \frac{1}{|D_l|} \sup_{v,w\in\mathbb{R}^3} \int_{\mathcal{S}^2} B(v,w,e)\, de \le 1\,. \tag{3.289}$$

The basic ingredient of Nanbu's approach is a decoupling of particle evolutions during the collision step. In addition, at most one collision per particle is allowed.

Each particle $(x_i(0), v_i(0))$, $i = 1, \ldots, n$, is treated independently in the following way. The particle does not collide on $[0, \Delta t]$, i.e.

$$v_i(\Delta t) = v_i(0)\,, \tag{3.290}$$

with probability

$$1 - \Delta t \, \frac{1}{|D_l|\, n} \sum_{j\,:\, x_j(0) \in D_l} \int_{\mathcal{S}^2} B(v_i(0), v_j(0), e)\, de\,, \tag{3.291}$$

where D_l is the spatial cell to which the particle belongs. Note that the expressions (3.291) are non-negative, according to (3.289). With the remaining probability, i.e.

$$\Delta t \, \frac{1}{|D_l|\, n} \sum_{j\,:\, x_j(0) \in D_l} \int_{\mathcal{S}^2} B(v_i(0), v_j(0), e)\, de\,, \tag{3.292}$$

the particle makes one collision. The index j of the collision partner is chosen according to the probabilities

$$\frac{\chi_{D_l}(x_j(0)) \int_{\mathcal{S}^2} B(v_i(0), v_j(0), e)\, de}{\sum_{k=1}^{n} \chi_{D_l}(x_k(0)) \int_{\mathcal{S}^2} B(v_i(0), v_k(0), e)\, de} \tag{3.293}$$

and the direction vector e is generated according to the probability density

$$\frac{B(v_i(0), v_j(0), e)}{\int_{\mathcal{S}^2} B(v_i(0), v_j(0), e')\, de'}\,. \tag{3.294}$$

The new velocity is defined as (cf. (1.12))

$$v_i(\Delta t) = v^*(v_i(0), v_j(0), e)\,. \tag{3.295}$$

The position does not change, i.e.

$$x_i(\Delta t) = x_i(0)\,. \tag{3.296}$$

Consider the empirical measures of the particle system

$$\mu^{(n)}(t, dx, dv) = \frac{1}{n} \sum_{i=1}^{n} \delta_{x_i(t)}(dx)\, \delta_{v_i(t)}(dv)\,, \qquad t = 0, \Delta t\,,$$

and their restrictions $\mu_l^{(n)}$ to the sets $D_l \times \mathbb{R}^3$. Let $f(0, x, v)$ be a non-negative function on $D \times \mathbb{R}^3$ such that

$$\int_D \int_{\mathbb{R}^3} f(0, x, v)\, dv\, dx = 1\,. \tag{3.297}$$

Define the function $f(\Delta t, x, v)$ on $D \times \mathbb{R}^3$ by its restrictions

$$f_l(\Delta t, x, v) = f(0, x, v) + \Delta t \, \frac{1}{|D_l|} \int_{D_l} \int_{\mathbb{R}^3} \int_{\mathcal{S}^2} B(v, w, e) \times \tag{3.298}$$
$$\Big[f(0, x, v^*(v, w, e)) \, f(0, y, w^*(v, w, e)) - f(0, x, v) \, f(0, y, w) \Big] de \, dw \, dy$$

on $D_l \times \mathbb{R}^3$. Note that the functions (3.298) are non-negative according to (3.289), (3.288), (3.297). Finally, we define the measures

$$F(t, dx, dv) = f(t, x, v) \, dx \, dv \,, \qquad t = 0, \Delta t \,, \tag{3.299}$$

and their restrictions F_l to the sets $D_l \times \mathbb{R}^3$.

Remark 3.48. The collision transformation (1.12) satisfies

$$|v^* - w^*| = |v - w| \,, \qquad (v^* - w^*, e) = (w - v, e) \,.$$

Moreover, the mapping

$$\mathcal{T}_e \, : \, (v, w) \, \to \, \Big(v^*(v, w, e), w^*(v, w, e) \Big)$$

has the properties

$$\mathcal{T}_e^2 = \mathcal{I} \,, \qquad \mathcal{T}_e^{-1} = \mathcal{T}_e \,, \qquad |\det \, \mathcal{T}_e| = 1 \,.$$

Theorem 3.49. *Let the collision kernel be bounded, continuous and such that*

$$B(v^*(v, w, e), w^*(v, w, e), e) = B(v, w, e) \,. \tag{3.300}$$

If

$$\lim_{n \to \infty} \mathbb{E} \, \varrho_L(\mu_l^{(n)}(0), F_l(0)) = 0 \tag{3.301}$$

then

$$\lim_{n \to \infty} \mathbb{E} \, \varrho_L(\mu_l^{(n)}(\Delta t), F_l(\Delta t)) = 0 \,,$$

where ϱ_L is defined in (3.153).

Proof. Let φ be any continuous bounded function on $D_l \times \mathbb{R}^3$. According to Remark 3.48 and (3.300), equation (3.298) implies

$$\langle \varphi, F_l(\Delta t) \rangle = \langle \varphi, F_l(0) \rangle + \Delta t \, \frac{1}{|D_l|} \int_{D_l} \int_{\mathbb{R}^3} \int_{D_l} \int_{\mathbb{R}^3} \int_{\mathcal{S}^2}$$
$$\Big[\varphi(x, v^*(v, w, e)) - \varphi(x, v) \Big] B(v, w, e) \, de \, F(0, dy, dw) \, F(0, dx, dv)$$
$$= \langle \varphi, F_l(0) \rangle + \Delta t \, \mathcal{B}_l(\varphi, F_l(0)) \,, \tag{3.302}$$

with the notation

$$\mathcal{B}_l(\varphi,\nu)=\frac{1}{|D_l|}\int_{D_l}\int_{\mathbb{R}^3}\int_{D_l}\int_{\mathbb{R}^3}\int_{\mathcal{S}^2}$$
$$\Big[\varphi(x,v^*(v,w,e))-\varphi(x,v)\Big]B(v,w,e)\,de\,\nu(dx,dv)\,\nu(dy,dw)\,.$$

It follows from (3.290)-(3.296) and conditional independence that

$$\begin{aligned}
\mathbb{E}\,\langle\varphi,\mu_l^{(n)}(\Delta t)\rangle &= \mathbb{E}\,\frac{1}{n}\sum_{i\,:\,x_i(0)\in D_l}\Bigg\{\\
&\varphi(x_i(0),v_i(0))\left[1-\Delta t\,\frac{1}{|D_l|\,n}\sum_{j\,:\,x_j(0)\in D_l}\int_{\mathcal{S}^2}B(v_i(0),v_j(0),e)\,de\right]+\\
&\Delta t\,\frac{1}{|D_l|\,n}\sum_{j\,:\,x_j(0)\in D_l}\int_{\mathcal{S}^2}\varphi(x_i(0),v^*(v_i(0),v_j(0),e))\,B(v_i(0),v_j(0),e)\,de\Bigg\}\\
&= \mathbb{E}\Bigg\{\langle\varphi,\mu_l^{(n)}(0)\rangle+\Delta t\,\frac{1}{|D_l|}\int_{D_l}\int_{\mathbb{R}^3}\int_{D_l}\int_{\mathbb{R}^3}\int_{\mathcal{S}^2}\\
&\Big[\varphi(x,v^*(v,w,e))-\varphi(x,v)\Big]B(v,w,e)\,de\,\mu_l^{(n)}(0,dy,dw)\,\mu_l^{(n)}(0,dx,dv)\Bigg\}\\
&= \mathbb{E}\left\{\langle\varphi,\mu_l^{(n)}(0)\rangle+\Delta t\,\mathcal{B}_l(\varphi,\mu_l^{(n)}(0))\right\} \qquad (3.303)
\end{aligned}$$

and

$$\begin{aligned}
\mathbb{E}\left(\langle\varphi,\mu_l^{(n)}(\Delta t)\rangle\right)^2 &= \mathbb{E}\,\frac{1}{n^2}\sum_{i\,:\,x_i(0)\in D_l}\varphi^2(x_i(\Delta t),v_i(\Delta t))+\\
&\mathbb{E}\left(\frac{1}{n}\sum_{i\,:\,x_i(0)\in D_l}\mathbb{E}\left\{\varphi(x_i(\Delta t),v_i(\Delta t))\Big|x_1(0),v_1(0),\dots,x_n(0),v_n(0)\right\}\right)^2-\\
&\mathbb{E}\,\frac{1}{n^2}\sum_{i\,:\,x_i(0)\in D_l}\left(\mathbb{E}\left\{\varphi(x_i(\Delta t),v_i(\Delta t))\Big|x_1(0),v_1(0),\dots,x_n(0),v_n(0)\right\}\right)^2\\
&= \mathbb{E}\left(\mathbb{E}\left\{\langle\varphi,\mu_l^{(n)}(\Delta t)\rangle\Big|x_1(0),v_1(0),\dots,x_n(0),v_n(0)\right\}\right)^2+R^{(n)}\\
&= \mathbb{E}\left(\langle\varphi,\mu_l^{(n)}(0)\rangle+\Delta t\,\mathcal{B}_l(\varphi,\mu_l^{(n)}(0))\right)^2+R^{(n)}\,, \qquad (3.304)
\end{aligned}$$

where $R^{(n)}$ tends to zero since φ is bounded. Lemma A.4 and (3.301) imply

$$\langle\varphi,\mu_l^{(n)}(0)\rangle\to\langle\varphi,F_l(0)\rangle \qquad \text{in probability} \qquad (3.305)$$

and

$$\mathcal{B}_l(\varphi,\mu_l^{(n)}(0))\to\mathcal{B}_l(\varphi,F_l(0)) \quad \text{in probability,} \qquad (3.306)$$

as a consequence of Lemma A.7. Moreover, one obtains

$$\left|\mathcal{B}_l(\varphi, \mu_l^{(n)}(0))\right| \leq \frac{2\,||\varphi||_\infty}{|D_l|} \sup_{v,w\in\mathbb{R}^3} \int_{\mathcal{S}^2} B(v,w,e)\,de\,. \tag{3.307}$$

Using (3.305)-(3.307) and applying Lemma A.6, one derives from (3.303) and (3.304) that

$$\lim_{n\to\infty} \mathbb{E}\,\langle \varphi, \mu_l^{(n)}(\Delta t)\rangle = \langle \varphi, F_l(0)\rangle + \Delta t\,\mathcal{B}_l(\varphi, F_l(0)) \tag{3.308}$$

and

$$\lim_{n\to\infty} \mathbb{E}\,\langle \varphi, \mu_l^{(n)}(\Delta t)\rangle^2 = \Big\{\langle \varphi, F_l(0)\rangle + \Delta t\,\mathcal{B}_l(\varphi, F_l(0))\Big\}^2. \tag{3.309}$$

According to (3.302), (3.308) and (3.309), one more application of Lemma A.6 implies

$$\langle \varphi, \mu_l^{(n)}(\Delta t)\rangle \to \langle \varphi, F_l(\Delta t)\rangle \quad \text{in probability.}$$

Thus, the assertion follows from Lemma A.4. ∎

Note that convergence for the collision process follows from Theorem 3.49 and Corollary A.5, since $F(t, \partial D_l \times \mathbb{R}^3) = 0$ for $t = 0, \Delta t$ (cf. (3.299)).

Nanbu's original method suffered from certain deficiencies (quadratic effort in the number of particles, conservation of momentum and energy only on average). Later it was considerably improved (cf. [7], [165], [8]) so that it did successfully work in applications like the reentry problem (cf. [150], [153], [151], [11]). Convergence for the Nanbu scheme and its modifications was studied in [8] (spatially homogeneous case) and [12] (spatially inhomogeneous case). We note that one step of the argument is not completely convincing. The key result states: if there is weak convergence at time zero, then there is weak convergence with probability one at time Δt (cf. [8, Lemma 2, p.48], [12, Lemma 6.1, p.61]). However, in order to obtain convergence at all time steps, the type of convergence at time zero must be reproduced at time Δt. But assuming only weak convergence with probability one at time zero seems to be not enough for the proof, which uses the central limit theorem.

3.5.5 Approximation order

The stochastic algorithms for the Boltzmann equation depend on three main approximation parameters – the number of particles n (cf. Remark 3.5), the splitting time step Δt (cf. (3.17)) and the cell size Δx (cf. (3.58)). There are recommendations based on physical insight and computational experience: the time step should be kept $\sim 1/4$ of the local mean collision time, the cell size should be kept $\sim 1/3$ of the local mean free path, and the number of particles per cell should be at least 20. However, the order of convergence with respect

to these parameters is an important issue, both from a theoretical and a practical point of view.

The order with respect to the number of particles n has been studied in the context of general Markov processes in [149], [72], [148]. These results can be applied to the numerical algorithms giving the order $1/n$. Situations, where the number of particles is variable (e.g., if inflow and outflow are to be considered), have not yet been covered by theoretical results. However, the same order of convergence would be expected, as well as in the stationary case (cf. remarks at the end of Section 2.3.3).

After taking the limit with respect to n, an equation is obtained that contains the remaining two approximation parameters (cf. Section 3.1.3). In [12], studying convergence of the Nanbu scheme, the authors showed that the approximation error with respect to the time step Δt and to the maximum cell diameter Δx is at least of first order, provided that the solution of the Boltzmann equation satisfies certain regularity assumptions. The approximation error with respect to the time step of the standard DSMC scheme has drawn the attention of several authors. Second order was proved by Bogomolov [35] in 1988. This result had been widely accepted (cf. [51, p.290]). However, in 1998 Ohwada [155] noticed a mistake in Bogomolov's derivation and concluded that the time step error is of first order. We reproduce these results here. Using the magic of functional analysis, the derivation becomes rather straightforward.

Consider the equation

$$\frac{d}{dt} f(t) = \mathcal{A} f(t) + Q(f(t), f(t)) , \qquad f(0) = f_0 , \tag{3.310}$$

where $\mathcal{A}$ is the generator of a Markov process and Q is a bilinear operator.

Lemma 3.50. *The solution of equation*

$$\frac{d}{dt} g(t) = \mathcal{A} g(t) + b(t) , \qquad g(0) = g_0 ,$$

has the probabilistic representation

$$g(t) = \mathcal{P}(t)\, g_0 + \int_0^t \mathcal{P}(t-s)\, b(s)\, ds ,$$

where the semi-group $\mathcal{P}(t)$ satisfies

$$\frac{d}{dt} \mathcal{P}(t) = \mathcal{A} \mathcal{P}(t) , \qquad \mathcal{P}(0) = I .$$

Example 3.51. In the Boltzmann case (with no boundary conditions) we use

$$\mathcal{A} \varphi(x,v) = -\big(v, \nabla_x\big)\, \varphi(x,v) , \qquad \mathcal{P}(t)\, \varphi(x,v) = \varphi(x - t\, v, v) \tag{3.311}$$

and

$$Q(\varphi,\psi)(x,v) = \tag{3.312}$$
$$\frac{1}{2}\int_{\mathbb{R}^3} dw \int_{\mathcal{S}^2} de\, B(v,w,e)\Big[\varphi(x,v'(v,w,e))\,\psi(x,w'(v,w,e)) +$$
$$\psi(x,v'(v,w,e))\,\varphi(x,w'(v,w,e)) - \varphi(x,v)\,\psi(x,w) - \psi(x,v)\,\varphi(x,w)\Big]$$

or

$$Q(\varphi,\psi)(x,v) = \frac{1}{2}\int_{\mathbb{R}^3} dy \int_{\mathbb{R}^3} dw \int_{\mathcal{S}^2} de\, h(x,y)\,B(v,w,e)\times$$
$$\Big[\varphi(x,v'(v,w,e))\,\psi(y,w'(v,w,e)) +$$
$$\psi(x,v'(v,w,e))\,\varphi(y,w'(v,w,e)) - \varphi(x,v)\,\psi(y,w) - \psi(x,v)\,\varphi(y,w)\Big],$$

in the mollified case. ■

Using Lemma 3.50 one obtains from (3.310)

$$f(t) = \mathcal{P}(t)\,f_0 + \int_0^t \mathcal{P}(t-s)\,Q(f(s),f(s))\,ds\,.$$

Note that

$$\frac{d}{dt}\,\mathcal{P}(t)\,Q(f_0,f_0) = \mathcal{A}\,\mathcal{P}(t)\,Q(f_0,f_0)$$

and

$$\frac{d}{ds}\,\mathcal{P}(t-s)\,Q(f(s),f(s)) =$$
$$-\mathcal{A}\,\mathcal{P}(t-s)\,Q(f(s),f(s)) + 2\,\mathcal{P}(t-s)\,Q(f'(s),f(s))\,.$$

Taylor expansions give

$$f(t) = \mathcal{P}(t)\,f_0 + t\,\mathcal{P}(t)\,Q(f_0,f_0) + \frac{t^2}{2}\,\frac{d}{ds}\,\mathcal{P}(t-s)\,Q(f(s),f(s))\Big|_{s=0} + O(t^3)$$
$$= \mathcal{P}(t)\,f_0 + t\,Q(f_0,f_0) + t^2\,\mathcal{A}\,Q(f_0,f_0) +$$
$$\frac{t^2}{2}\Big[-\mathcal{A}\,Q(f_0,f_0) + 2\,Q(\mathcal{A}\,f_0 + Q(f_0,f_0),f_0)\Big] + O(t^3)$$
$$= \mathcal{P}(t)\,f_0 + t\,Q(f_0,f_0) +$$
$$\frac{t^2}{2}\,\mathcal{A}\,Q(f_0,f_0) + t^2\,Q(\mathcal{A}\,f_0,f_0) + t^2\,Q(Q(f_0,f_0),f_0) + O(t^3)\,.$$

For the standard DSMC procedure,

$$\frac{d}{dt}\,f^{(1)}(t) = \mathcal{A}\,f^{(1)}(t)\,, \qquad f^{(1)}(0) = f_0\,,$$
$$\frac{d}{dt}\,f_\tau^{(2)}(t) = Q(f_\tau^{(2)}(t),f_\tau^{(2)}(t))\,, \qquad f_\tau^{(2)}(0) = f^{(1)}(\tau)\,,$$

one obtains

$$
\begin{aligned}
f_\tau^{(2)}(\tau) &= \mathcal{P}(\tau)\, f_0 + \int_0^\tau Q(f_\tau^{(2)}(t), f_\tau^{(2)}(t))\, dt \\
&= \mathcal{P}(\tau)\, f_0 + \tau\, Q(f_\tau^{(2)}(0), f_\tau^{(2)}(0)) + \frac{\tau^2}{2}\, \frac{d}{dt}\, Q(f_\tau^{(2)}(t), f_\tau^{(2)}(t))\Big|_{t=0} + O(\tau^3) \\
&= \mathcal{P}(\tau)\, f_0 + \tau\, Q(\mathcal{P}(\tau)\, f_0, \mathcal{P}(\tau)\, f_0) + \tau^2\, Q(\frac{d}{dt}\, f_\tau^{(2)}(t)\Big|_{t=0}, f_\tau^{(2)}(0)) + O(\tau^3) \\
&= \mathcal{P}(\tau)\, f_0 + \tau\, Q(f_0, f_0) + 2\,\tau^2\, Q(\mathcal{A}\, f_0, f_0) + \tau^2\, Q(Q(f_0, f_0), f_0) + O(\tau^3)
\end{aligned}
$$

and

$$
\begin{aligned}
\mathrm{Error}_{\mathrm{DSMC}}(\tau) &= f(\tau) - f_\tau^{(2)}(\tau) \\
&= \frac{\tau^2}{2}\, \mathcal{A}\, Q(f_0, f_0) - \tau^2\, Q(\mathcal{A}\, f_0, f_0) + O(\tau^3)\,. \qquad (3.313)
\end{aligned}
$$

For the Nanbu procedure,

$$
\tilde{f}_\tau^{(2)}(t) = f^{(1)}(\tau) + t\, Q(f^{(1)}(\tau), f^{(1)}(\tau))\,, \qquad (3.314)
$$

one obtains

$$
\tilde{f}_\tau^{(2)}(\tau) = \mathcal{P}(\tau)\, f_0 + \tau\, Q(f_0, f_0) + 2\,\tau^2\, Q(\mathcal{A}\, f_0, f_0) + O(\tau^3) \qquad (3.315)
$$

and

$$
\begin{aligned}
\mathrm{Error}_{\mathrm{Nanbu}}(\tau) &= f(\tau) - \tilde{f}_\tau^{(2)}(\tau) \\
&= \mathrm{Error}_{\mathrm{DSMC}}(\tau) + \tau^2\, Q(Q(f_0, f_0), f_0) + O(\tau^3)\,. \qquad (3.316)
\end{aligned}
$$

Note that for the collision step

$$
\frac{d}{dt}\, g(t) = Q(g(t), g(t))\,, \qquad g(0) = g_0\,,
$$

one obtains

$$
g(t) = g_0 + t\, Q(g_0, g_0) + t^2\, Q(Q(g_0, g_0), g_0) + O(t^3)\,.
$$

According to (3.314), the collision step is resolved only up to first order in the Nanbu procedure, while it is solved exactly in standard DSMC. If the collision step was resolved up to second order, i.e. (instead of (3.314))

$$
\tilde{f}_\tau^{(2)}(t) = f^{(1)}(\tau) + t\, Q(f^{(1)}(\tau), f^{(1)}(\tau)) + t^2\, Q(Q(f^{(1)}(\tau), f^{(1)}(\tau)), f^{(1)}(\tau))\,,
$$

then one would obtain (instead of (3.315))

$$
\begin{aligned}
&\tilde{f}_\tau^{(2)}(\tau) = \\
&\quad \mathcal{P}(\tau)\, f_0 + \tau\, Q(f_0, f_0) + 2\,\tau^2\, Q(\mathcal{A}\, f_0, f_0) + \tau^2\, Q(Q(f_0, f_0), f_0) + O(\tau^3)
\end{aligned}
$$

and (instead of (3.316))

$$\mathrm{Error}_{\mathrm{Nanbu-mod}}(\tau) = f(\tau) - \tilde{f}_\tau^{(2)}(\tau) = \mathrm{Error}_{\mathrm{DSMC}}(\tau) + O(\tau^3)\,.$$

For Ohwada's modification,

$$\begin{aligned}
&\frac{d}{dt}\,\bar{f}_\tau^{(2)}(t) = Q(\bar{f}_\tau^{(2)}(t), \bar{f}_\tau^{(2)}(t))\,, \qquad \bar{f}_\tau^{(2)}(0) = f^{(1)}(\tau/2)\,,\\
&\frac{d}{dt}\,f_\tau^{(3)}(t) = \mathcal{A}\,f_\tau^{(3)}(t)\,, \qquad f_\tau^{(3)}(0) = \bar{f}_\tau^{(2)}(\tau)\,,
\end{aligned}$$

one obtains

$$\mathrm{Error}_{\mathrm{Ohwada}}(\tau) = f(\tau) - f_\tau^{(3)}(\tau/2) = O(\tau^3)\,.$$

This modification is a generalization of Strang's splitting method, as studied in [31], [32].

Consider the DSMC-error (3.313) in the special case (3.311), (3.312). The first term in (3.313) takes the form

$$\begin{aligned}
\mathcal{A}\,Q(g,g)(x,v) &= -(v,\nabla_x)\int_{\mathbb{R}^3} dw \int_{\mathcal{S}^2} de\, B(v,w,e)\times\\
&\quad\Big[g(x,v'(v,w,e))\,g(x,w'(v,w,e)) - g(x,v)\,g(x,w)\Big]\\
&= \int_{\mathbb{R}^3} dw \int_{\mathcal{S}^2} deB(v,w,e)\Big\{\Big[-(v,\nabla_x)\,g(x,v'(v,w,e))\Big]g(x,w'(v,w,e))\\
&\qquad +g(x,v'(v,w,e))\Big[-(v,\nabla_x)\,g(x,w'(v,w,e))\Big]\\
&\qquad -\Big[-(v,\nabla_x)\,g(x,v)\Big]g(x,w) - g(x,v)\Big[-(v,\nabla_x)\,g(x,w)\Big]\Big\}.
\end{aligned}$$

The second term in (3.313) takes the form

$$\begin{aligned}
Q(\mathcal{A}\,g,g)(x,v) &= \frac{1}{2}\int_{\mathbb{R}^3} dw \int_{\mathcal{S}^2} de\, B(v,w,e)\times\\
&\Big\{\Big[-(v'(v,w,e),\nabla_x)\,g(x,v'(v,w,e))\Big]g(x,w'(v,w,e))\\
&\qquad +g(x,v'(v,w,e))\Big[-(w'(v,w,e),\nabla_x)\,g(x,w'(v,w,e))\Big]\\
&\qquad -\Big[-(v,\nabla_x)\,g(x,v)\Big]g(x,w) - g(x,v)\Big[-(w,\nabla_x)\,g(x,w)\Big]\Big\}.
\end{aligned}$$

Putting terms together one obtains

$$\mathrm{Error}_{\mathrm{DSMC}}(\tau,x,v) = O(\tau^3) - \tau^2\,\frac{1}{2}\int_{\mathbb{R}^3} dw \int_{S^2} de\, B(v,w,e)\times$$
$$\Big\{\Big[(v-v'(v,w,e),\nabla_x)\, f_0(x,v'(v,w,e))\Big] f_0(x,w'(v,w,e)) +$$
$$f_0(x,v'(v,w,e))\Big[(v-w'(v,w,e),\nabla_x)\, f_0(x,w'(v,w,e))\Big] -$$
$$\Big[(v-v,\nabla_x)\, f_0(x,v)\Big] f_0(x,w) - f_0(x,v)\Big[(v-w,\nabla_x)\, f_0(x,w)\Big]\Big\}.$$

This expression is identical to formula (14) in [155], when the notation there is appropriately interpreted. Bogomolov's mistake was to identify the two second order terms in (3.313), that is

$$\mathcal{A}\,Q(g,g) = 2\,Q(\mathcal{A}\,g,g)\,.$$

Without any doubt, Ohwada's modification guarantees second order. However, what about standard DSMC splitting? This procedure has been extensively used in engineering context, and no problems with time step approximation have occurred. Moreover, theoretical derivations based on physical arguments predicted second order with respect to both cell size [2] and time step [75]. Partly these predictions were confirmed quantitatively by numerical experiments in [68].

An observation related to this problem was published in [169]. The authors reported that steady state DSMC results for the stress tensor and the heat flux are considerably improved by measuring the quantities twice - before and after the collision step. Obviously, preserved quantities (density, total momentum, energy) are not affected by this procedure. In [80] it was noted that the modification from [169] is a variant of Strang's splitting leading to second order convergence. Extending results from [156], examples illustrating first order behavior of standard DSMC were given. It was also pointed out that DSMC results for stress tensor and heat flux show second order behavior, if these quantities are measured as fluxes through a surface during the free flow step (as in [68]) and not as cell averages. This clarified the situation to a large extent.

As it can be seen from the above derivation, the Nanbu scheme has a worse time step behavior than standard DSMC. Therefore attempts to introduce recollisions in the Nanbu-Babovsky scheme (cf. [51, p.309], [190]) would improve the time step accuracy to the level of standard DSMC.

3.5.6 Further references

Stochastic modeling procedures related to the Leontovich-Kac-process were studied in [15], [16], [13], [14], [111], [99], [90]. A numerical approach using branching processes was developed in [58], [57]. Algorithms for the stationary Boltzmann equation were introduced in [34], [182]. A numerical technique

based on Wild sums (cf. [208]) was studied in [158], [159], [160]. Low discrepancy sequences were introduced instead of sequences of random numbers in some parts of the Nanbu-Babovsky procedure, later called finite pointset method (cf. [152], [150]). Further studies concerning low discrepancy sequences in the context of the Boltzmann equation were performed in [118], [119], [120]. Stochastic algorithms for generalized Boltzmann equations, including multicomponent gases and chemical reactions, were studied, e.g., in [55], [129]. An "information preservation method" (cf. [62], [191] and references therein) has been developed for low Mach number flows occurring in micro-electromechanical systems (MEMS). DSMC modifications related to dense gases have been introduced (cf. [1], [65], [139], [67], [69]). DSMC algorithms for the Uehling-Uhlenbeck-Boltzmann equation related to ideal quantum gases have been studied (cf. [70] and references therein).

4

Numerical experiments

In this chapter we present results of numerical experiments performed with the algorithms from Chapter 3.

In Sections 4.1, 4.2, 4.3, 4.4 we consider the spatially homogeneous Boltzmann equation

$$\frac{\partial}{\partial t} f(t,v) = \int\limits_{\mathbb{R}^3} \int\limits_{\mathcal{S}^2} B(v,w,e)\Big(f(t,v')f(t,w') - f(t,v)f(t,w)\Big)\,de\,dw \tag{4.1}$$

with the initial condition

$$f(0,v) = f_0(v)\,, \qquad v \in \mathbb{R}^3\,. \tag{4.2}$$

The post-collision velocities v', w' are defined in (1.6). We mostly use the particularly simple model of pseudo-Maxwell molecules with isotropic scattering

$$B(v,w,e) = \frac{1}{4\,\pi}\,. \tag{4.3}$$

This model is very important for validating the algorithms, since quite a bit of analytical information is available. Some experiments are performed for the hard sphere model

$$B(v,w,e) = \frac{1}{4\,\pi}\,|v-w|\,, \tag{4.4}$$

where no non-trivial explicit formulas for functionals of the solution are known. Note that the density

$$\varrho(t) = \int\limits_{\mathbb{R}^3} f(t,v)\,dv = \int\limits_{\mathbb{R}^3} f_0(v)\,dv = \varrho\,, \tag{4.5}$$

the bulk velocity

$$V(t) = \frac{1}{\varrho} \int\limits_{\mathbb{R}^3} v\, f(t,v)\, dv = \frac{1}{\varrho} \int\limits_{\mathbb{R}^3} v\, f_0(v)\, dv = V \tag{4.6}$$

and the temperature (cf. (1.46), (1.44))

$$\begin{aligned} T(t) &= \frac{m}{3\,k\,\varrho} \int\limits_{\mathbb{R}^3} |v - V|^2\, f(t,v)\, dv \\ &= \frac{m}{3\,k\,\varrho} \left(\int\limits_{\mathbb{R}^3} |v|^2\, f_0(v)\, dv - \varrho\, |V|^2 \right) = T \end{aligned} \tag{4.7}$$

are conserved quantities. We put

$$\varrho = 1\,, \qquad m = 1\,, \qquad k = 1$$

and study the relaxation of the distribution function to the final Maxwell distribution, i.e.

$$\lim_{t \to \infty} f(t,v) = M_{V,T}(v)\,,$$

where the parameters V and T are determined by the initial distribution f_0. First we consider the moments

$$M(t) = \int\limits_{\mathbb{R}^3} v v^{\mathsf{T}}\, f(t,v)\, dv\,, \tag{4.8a}$$

$$r(t) = \int\limits_{\mathbb{R}^3} v |v|^2\, f(t,v)\, dv\,, \tag{4.8b}$$

$$s(t) = \int\limits_{\mathbb{R}^3} |v|^4\, f(t,v)\, dv\,. \tag{4.8c}$$

We also study the criterion of local thermal equilibrium (1.91), which takes the form

$$Crit(t) = \frac{1}{T} \left(\frac{1}{2}\, ||\tau(t)||_F^2 + \frac{2}{5\,T}\, |q(t)|^2 + \frac{1}{120\,T^2}\, \gamma^2(t) \right)^{1/2}, \tag{4.9}$$

where (cf. (1.43), (1.45), (1.47), (1.90), (1.89))

$$\tau(t) = \int\limits_{\mathbb{R}^3} (v - V)(v - V)^{\mathsf{T}}\, f(t,v)\, dv - T\, I\,, \tag{4.10a}$$

$$q(t) = \frac{1}{2} \int\limits_{\mathbb{R}^3} (v - V) |v - V|^2\, f(t,v)\, dv\,, \tag{4.10b}$$

$$\gamma(t) = \int\limits_{\mathbb{R}^3} |v - V|^4\, f(t,v)\, dv - 15\, T^2\,. \tag{4.10c}$$

The quantities (4.10a)-(4.10c) can be expressed in terms of the moments (4.8a)-(4.8c). Finally, we consider tail functionals of the form

$$\mathrm{Tail}(R,t) = \int\limits_{|v|\geq R} f(t,v)\,dv\,, \qquad R \geq 0\,, \tag{4.11}$$

describing the portion of particles outside some ball. In the calculations we use a confidence level of $p = 0.999$ (cf. Section 3.1.4). Other basic parameters are

$$\nu^{(n)}(0) = n\,, \qquad \nu^{(n)}_{max} = 4\,n\,, \qquad g^{(n)}_{max} = \frac{2}{n}\,, \qquad \kappa = 1\,.$$

In Section 4.5 we study a spatially one-dimensional shock wave problem. Such problems can be solved with remarkably high accuracy using stochastic numerical methods. In Section 4.6 we consider a spatially two-dimensional model problem. Here low density regions of the flow are of special interest to illustrate some of the new features of the stochastic weighted particle method. In these spatially inhomogeneous situations we use the hard sphere model (cf. (1.95), (1.93))

$$B(v,w,e) = \frac{1}{4\sqrt{2}\,\pi\,\mathrm{Kn}}\,|v-w|\,. \tag{4.12}$$

4.1 Maxwellian initial state

In this section we consider the spatially homogeneous Boltzmann equation (4.1). The most simple test example is obtained if the initial distribution is a normalized Maxwell distribution, i.e. $f_0 = M_{0,1}$ in (4.2). Since the function

$$f(t,v) = f_0(v)\,, \qquad t \geq 0\,,$$

solves the equation, all moments and other functionals of the solution remain constant in time.

First we study the case of pseudo-Maxwell molecules (4.3). We use the SWPM algorithm with the unbiased mass preserving reduction procedure from Example 3.45. We illustrate that SWPM with weighted particles leads to a much better (more "uniform") resolution of the velocity space than DSMC using particles with constant weights. Due to this more uniform approximation of the velocity space, we are able to compute very small functionals, or "rare events", with a relatively low number of particles. As a model of such functionals we consider tail functionals (4.11). According to (A.12), these functionals take the form

$$\mathrm{Tail}(R,t) = \mathrm{Tail}(R,0) = 1 - \mathrm{erf}\Big(\frac{R}{\sqrt{2}}\Big) + \frac{2\,R}{\sqrt{\pi}}\,\exp\Big(-\frac{R^2}{2}\Big). \tag{4.13}$$

Finally we show that similar results (uniform resolution of the velocity space) are obtained in the case of hard sphere molecules (4.4).

4.1.1 Uniform approximation of the velocity space

Here we generate one ensemble of particles by the SWPM algorithm with $n = 1024$ on the time interval $[0, 16]$ and illustrate how the particles occupy a bigger and bigger part of the velocity space during the time.

The left plot of Fig. 4.1 shows the projections of the three-dimensional velocities of the particles at $t = 0$ into the plane $v_1 \times v_2$, while the right plot shows the "final" picture for $\nu^{(n)}(16) = 1234$ particles (after 64 reductions). Having almost the same number of particles, the new system is rather different from the initial one. Now only half of all particles is responsible for the resolution of the "main stream" within the ball $|v| \le 3$ while the second half of particles is more or less uniformly distributed within the much bigger ball $|v| \le 6$. Thus the new system of particles can be successfully used for the estimation of very rare events, e.g. for the tail functionals (4.11). The 4th and the 64th reductions of particles are illustrated in Figs. 4.2-4.3. It is important that the "useful" but small particles living in the tails are not destroyed during the reduction. Thus the system of particles uniformly occupies bigger and bigger part of the velocity space during the collisions until the weights of the most distant particles become too small to be useful. Such particles will be removed by the next reduction with a high probability.

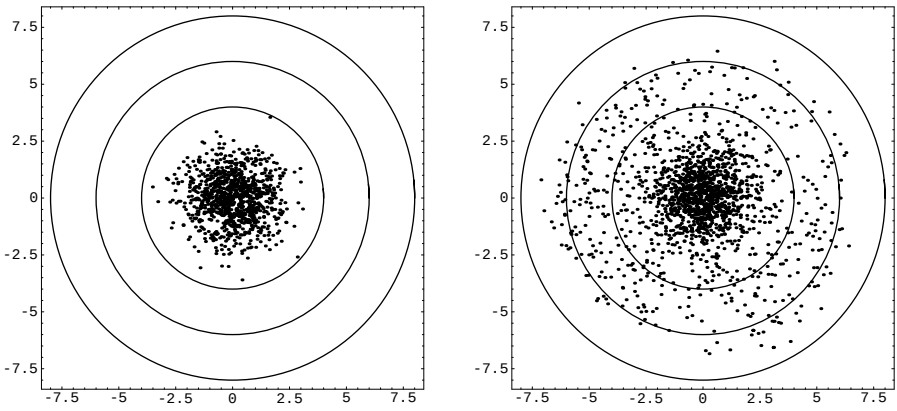

Fig. 4.1. Initial and "final" distributions of SWPM particles

4.1.2 Stability of moments

Here we illustrate the stability of the SWPM algorithm, which preserves only the mass of the system. We start with $n = 16\,384$ particles. The left plot of Fig. 4.4 shows the norm of the bulk velocity $|V(t)|$ on the time interval $[0, 64]$ in order to demonstrate the long time behavior of the system. The right plot

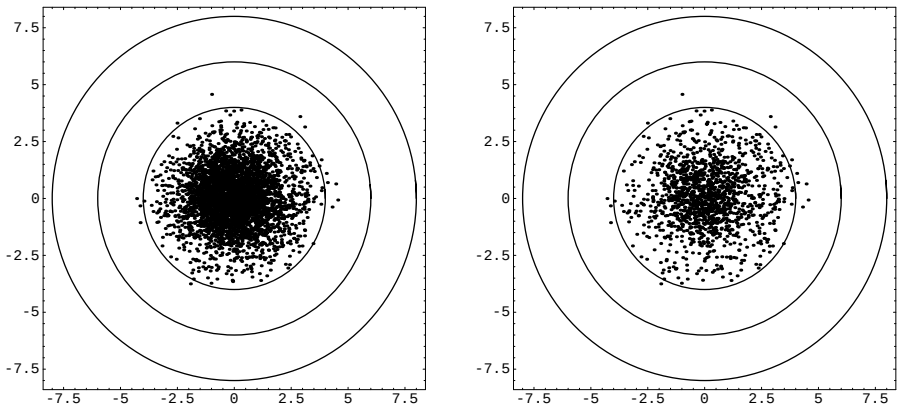

Fig. 4.2. 4th reduction of particles, pseudo-Maxwell molecules

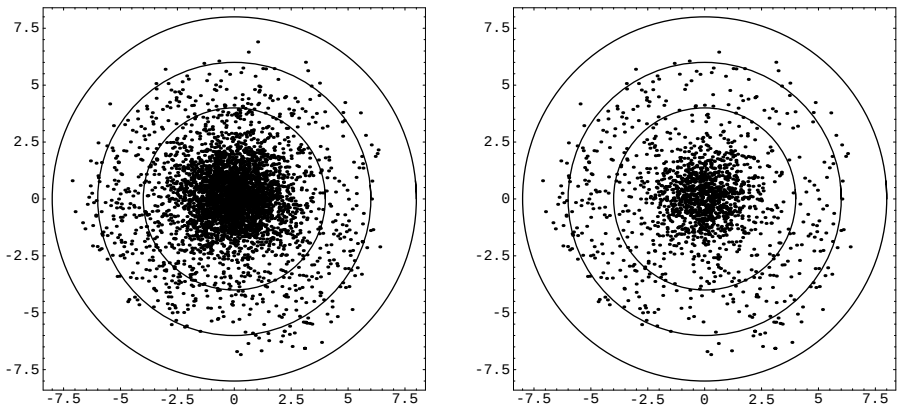

Fig. 4.3. 64th reduction of particles, pseudo-Maxwell molecules

shows the temperature $T(t)$. These curves were obtained using $N = 128$ independent ensembles.

There are errors in the bulk velocity and in the temperature due to non-conservative stochastic reduction of particles. But the deviation from the correct constant value is small. However, it is always necessary to control this deviation.

4.1.3 Tail functionals

Here we provide the results of numerical computations of the tails (4.13) with different values of the radius R,

$$\mathrm{Tail}(4,t) = 0.113398\ldots\cdot 10^{-2}\,, \tag{4.14a}$$

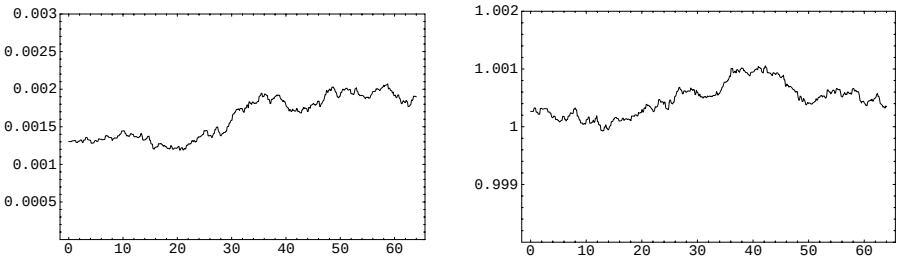

Fig. 4.4. Long time behavior of $|V(t)|$ and $T(t)$

$$\mathrm{Tail}(5,t) = 0.154404\ldots \cdot 10^{-4}\,, \tag{4.14b}$$

$$\mathrm{Tail}(6,t) = 0.748837\ldots \cdot 10^{-7}\,, \tag{4.14c}$$

$$\mathrm{Tail}(7,t) = 0.130445\ldots \cdot 10^{-9}\,. \tag{4.14d}$$

The number of particles in DSMC is $n = 65\,536$, while SWPM starts with $n = 16\,384$ particles. The computational time is then similar for both algorithms. Averages are taken over $N = 4\,096$ independent ensembles. Simulations are performed on the time interval $[0, 16]$.

We observe that at the begin of the simulation the width of the confidence intervals is better for DSMC due to the higher number of particles. The number of particles forming the tail remains almost constant for DSMC. The corresponding number increases for SWPM leading to smaller confidence intervals. In the figures confidence intervals obtained using DSMC are shown by thin solid lines, while confidence intervals obtained using SWPM are shown by thin dotted lines. The analytical values for the tails (4.14a)-(4.14d) are displayed by thick solid lines. In the figures showing the average numbers of particles forming the tails, the left plots corresponds to DSMC and the right plots to SWPM.

In the case $R = 4$, the tail formed using SWPM contains a rather large number of particles compared to DSMC (Fig. 4.6). The accuracy of both methods is similar (Fig. 4.5) because many of these particles are not responsible for resolving this tail, their weights are too small. However, many of them play an important role in resolving the smaller tails.

The resolution of the second tail ($R = 5$) becomes better for SWPM after some time. The width of the DSMC confidence intervals is almost two times larger (Fig. 4.7). Thus the results of SWPM can be reached using four times more independent ensembles and therefore four times more computational time. Thus we can say that SWPM is four times "faster" computing this tail with similar accuracy. Fig. 4.8 shows the corresponding number of particles in the second tail.

This tendency continues also for the tail with $R = 6$. Now the width of the DSMC confidence intervals is four-five times larger (Fig. 4.9). Thus SWPM can be considered 16-25 times "faster" computing this tail with similar

accuracy. The number of particles in this tail for SWPM seems to be still increasing (Fig. 4.10). This means that the forming of this tail has not yet been finished.

Fig. 4.11 shows the results obtained using SWPM for the tail with $R = 7$. There are no stable DSMC results for this very small tail. Even if the tail is still not formed on this time interval and the number of particles for SWPM is still rapidly growing (Fig. 4.12) the analytical value of this functional is reached with considerable accuracy.

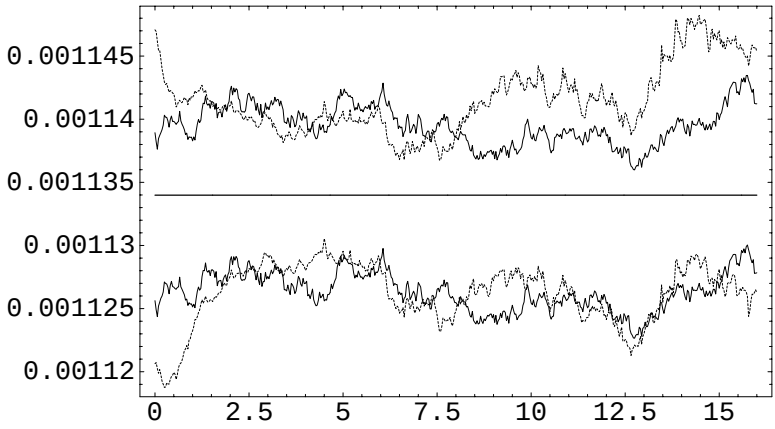

Fig. 4.5. Tail functional for $R = 4$

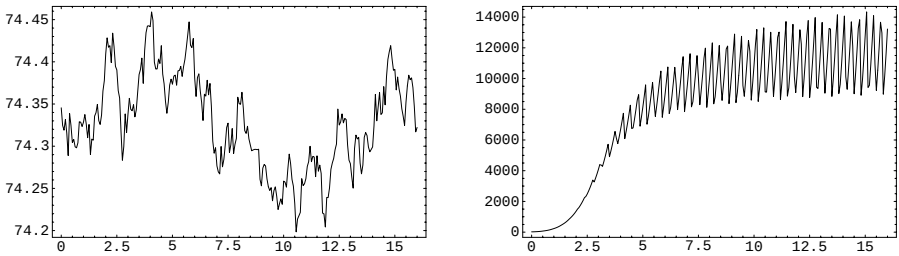

Fig. 4.6. Number of particles in the tail for $R = 4$

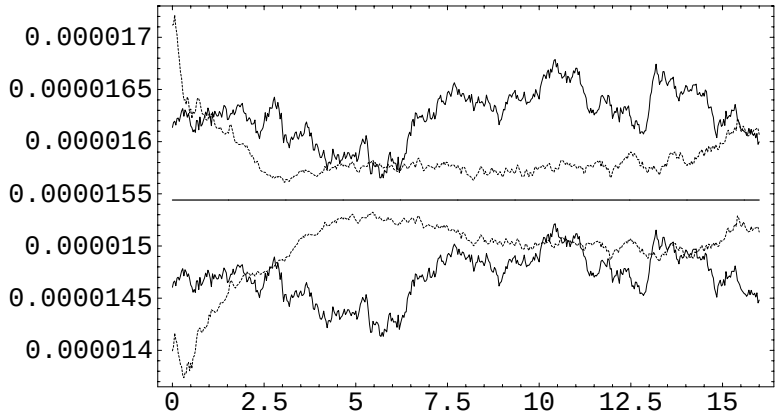

Fig. 4.7. Tail functional for $R = 5$

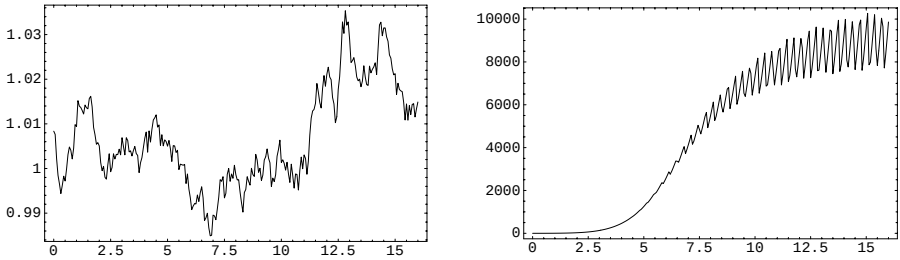

Fig. 4.8. Number of particles in the tail for $R = 5$

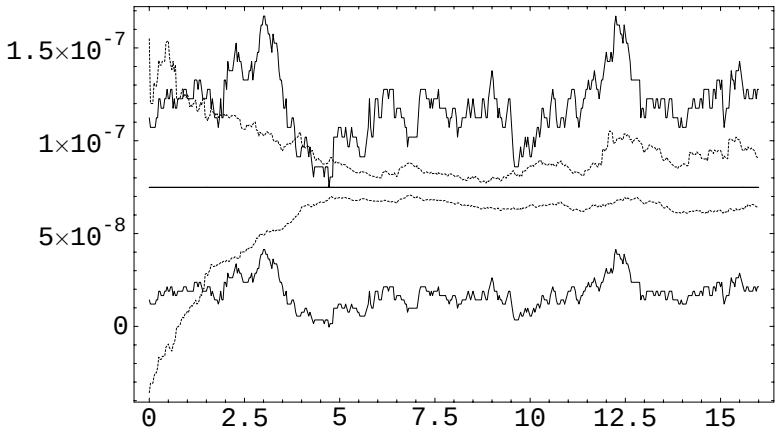

Fig. 4.9. Tail functional for $R = 6$

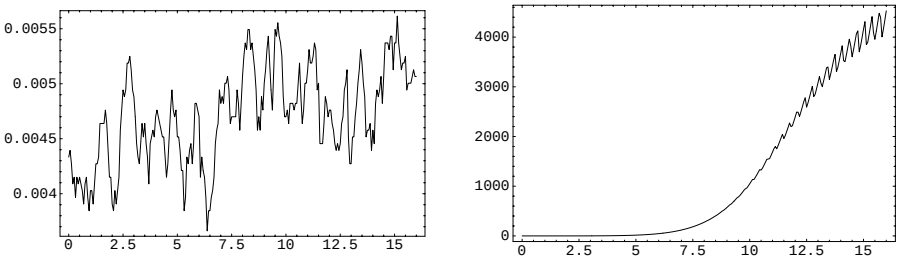

Fig. 4.10. Number of particles in the tail for $R = 6$

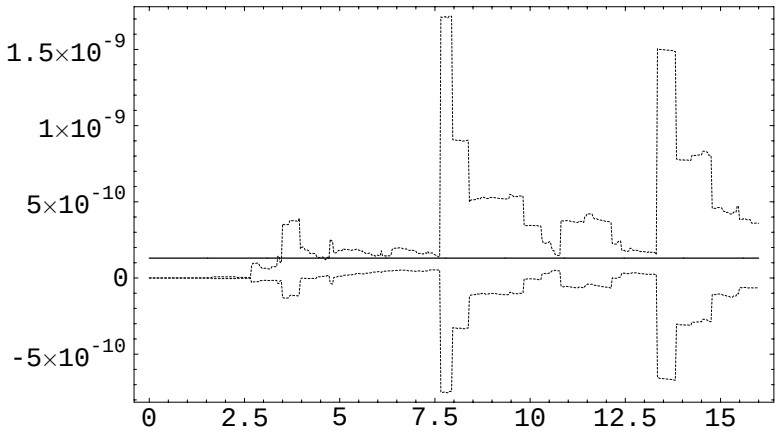

Fig. 4.11. Tail functional for $R = 7$

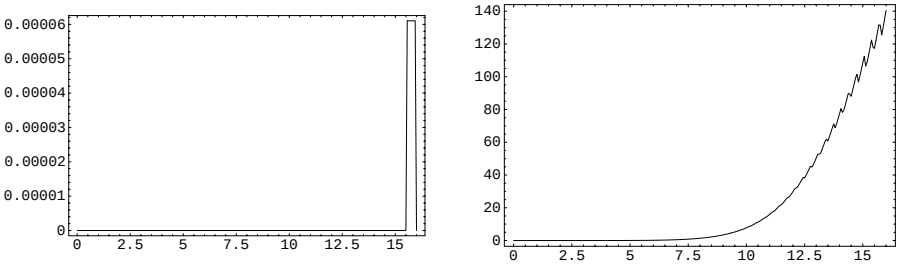

Fig. 4.12. Number of particles in the tail for $R = 7$

Considering the longer time interval $[0, 32]$ we see that the number of SWPM particles stops growing. The corresponding curves are shown in Fig. 4.13 for $R = 6$ (left plot) and $R = 7$ (right plot).

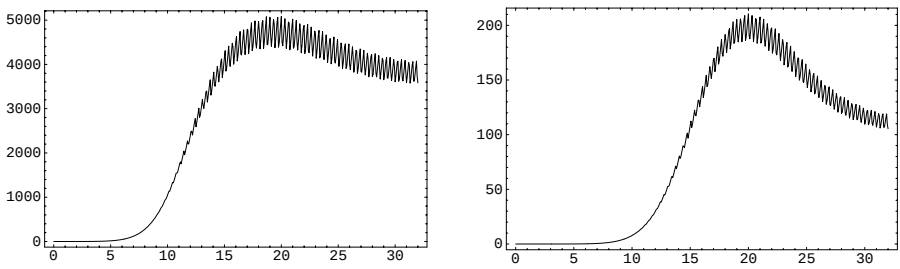

Fig. 4.13. Number of SWPM particles in the tails for $R = 6, 7$

4.1.4 Hard sphere model

Here we consider the case of hard sphere molecules (4.4) and illustrate the "uniform" approximation of the velocity space using the SWPM algorithm. We generate one ensemble of particles with $n = 1024$ on the time interval $[0, 16]$.

The systems of particles before and after the 4th and the 64th reductions are illustrated in Figs. 4.14, 4.15. The behavior of the particle system is

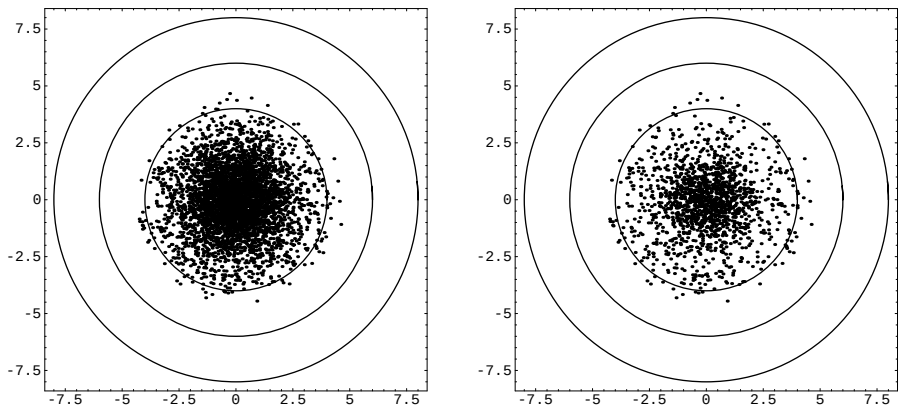

Fig. 4.14. 4th reduction of particles, hard sphere model

similar to the case of pseudo-Maxwell molecules. The particles occupy bigger and bigger parts of the velocity space during the simulation. The reductions keep the "useful" particles in the tail.

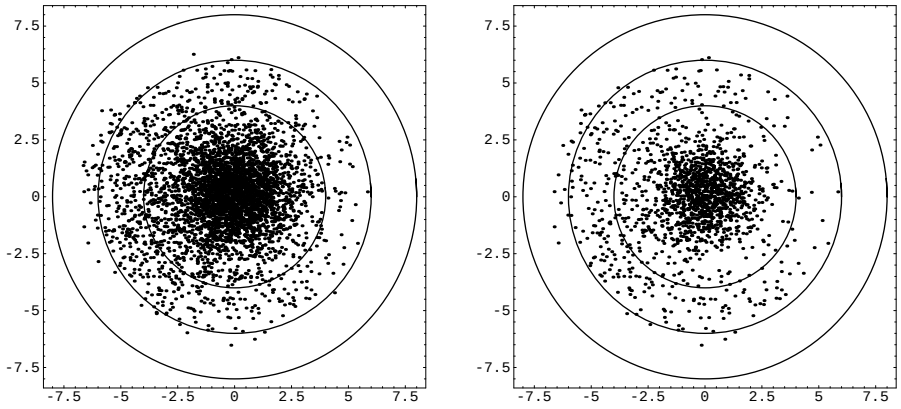

Fig. 4.15. 64th reduction of particles, hard sphere model

4.2 Relaxation of a mixture of two Maxwellians

In this section we consider the spatially homogeneous Boltzmann equation (4.1) with the initial distribution

$$f_0(v) = \alpha M_{V_1,T_1}(v) + (1-\alpha) M_{V_2,T_2}(v)\,, \qquad 0 \le \alpha \le 1\,, \tag{4.15}$$

which is a mixture of two Maxwell distributions. Fig. 4.16 shows a two-

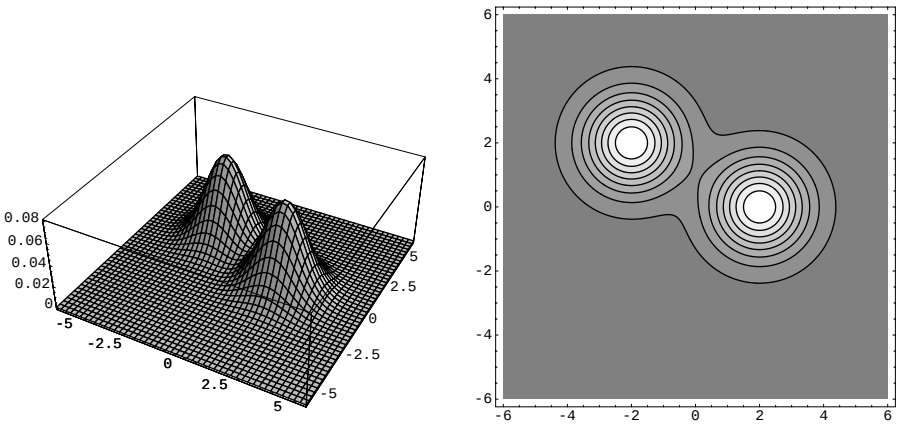

Fig. 4.16. Initial distribution $\tilde{f}_0(v_1, v_2)$

dimensional plot of the function

$$\tilde{f}_0(v_1, v_2) = \int_{-\infty}^{\infty} f_0(v_1, v_2, v_3)\, dv_3$$

as well as its contours for the set of parameters

$$V_1 = (-2, 2, 0)\,, \quad V_2 = (2, 0, 0)\,, \quad T_1 = T_2 = 1\,, \quad \alpha = 1/2\,. \tag{4.16}$$

We first consider the case of pseudo-Maxwell molecules (4.3). Using the analytic formulas from Section A.2, we study the convergence behavior of DSMC and SWPM (with two different reduction procedures) with respect to the number of particles. Then we study the approximation of tail functionals (4.11). According to (A.11), the initial and the asymptotic values of these functionals are known, while analytical information about the time relaxation is not available. Finally we show that similar results (convergence with respect to the number of particles) are obtained in the case of hard sphere molecules (4.4).

Note that (cf. (A.7a)-(A.7c))

$$V = \alpha V_1 + (1-\alpha) V_2\,, \tag{4.17a}$$

$$T = \alpha T_1 + (1-\alpha) T_2 + \frac{1}{3}\alpha(1-\alpha)|V_1 - V_2|^2\,, \tag{4.17b}$$

$$M_0 = \alpha\Big(T_1\, I + V_1 V_1^{\mathsf{T}}\Big) + (1-\alpha)\Big(T_2\, I + V_2 V_2^{\mathsf{T}}\Big)\,, \tag{4.17c}$$

$$r_0 = \alpha\Big(5T_1 + |V_1|^2\Big) V_1 + (1-\alpha)\Big(5T_2 + |V_2|^2\Big) V_2\,, \tag{4.17d}$$

$$\begin{aligned} s_0 = {} & \alpha\Big(|V_1|^4 + 15\, T_1^2 + 10\, T_1\, |V_1|^2\Big) + \\ & (1-\alpha)\Big(|V_2|^4 + 15\, T_2^2 + 10\, T_2\, |V_2|^2\Big), \end{aligned} \tag{4.17e}$$

where M_0, r_0, s_0 are the initial values of the moments (4.8a)-(4.8c). Considering the parameters (4.16), we obtain from (4.17a)-(4.17e)

$$\begin{gathered} V = \begin{pmatrix} 0 \\ 1 \\ 0 \end{pmatrix}, \qquad T = \frac{8}{3}\,, \qquad M_0 = \begin{pmatrix} 5 & -2 & 0 \\ -2 & 3 & 0 \\ 0 & 0 & 1 \end{pmatrix}, \\ r_0 = \begin{pmatrix} -4 \\ 13 \\ 0 \end{pmatrix}, \qquad s_0 = 115 \end{gathered} \tag{4.18}$$

and from (A.18a)-(A.18c)

$$M(t) = \frac{1}{3}\begin{pmatrix} 8 & 0 & 0 \\ 0 & 11 & 0 \\ 0 & 0 & 8 \end{pmatrix} + \frac{1}{3}\begin{pmatrix} 7 & -6 & 0 \\ -6 & -2 & 0 \\ 0 & 0 & -5 \end{pmatrix} e^{-t/2}\,, \tag{4.19a}$$

$$r(t) = \frac{1}{3}\begin{pmatrix} 0 \\ 43 \\ 0 \end{pmatrix} - \frac{1}{3}\begin{pmatrix} 12 \\ 4 \\ 0 \end{pmatrix} e^{-t/2}\,, \tag{4.19b}$$

$$s(t) = \frac{403}{3} - 25\, e^{-t/3} + \frac{25}{3}\, e^{-t} - \frac{8}{3}\, e^{-t/2}\,. \tag{4.19c}$$

Moreover, one obtains from (4.18) and (A.22)-(A.24)

$$\tau(t) = \frac{1}{3}\begin{pmatrix} 7 & -6 & 0 \\ -6 & -2 & 0 \\ 0 & 0 & -5 \end{pmatrix} e^{-t/2}\,, \qquad q(t) = 0\,, \qquad \gamma(t) = -25\,e^{-t/3} + \frac{25}{3}e^{-t}$$

so that the function (4.9) takes the form

$$Crit(t) = \frac{5}{256}\Big(30\,e^{-2t} - 180\,e^{-4t/3} + 3072\,e^{-t} + 270\,e^{-2t/3}\Big)^{1/2}\,. \tag{4.20}$$

4.2.1 Convergence of DSMC

Here we demonstrate the convergence of the DSMC method with respect to the number of particles n on some time interval $[0, t_{max}]$. For a given functional Ψ, the maximal error is defined as

$$E_{max}(\Psi) = \max_{0\le k\le K} |\Psi(t_k) - \eta(t_k)|\,, \tag{4.21}$$

where

$$t_k = k\Delta t\,, \quad k = 0, \ldots, K\,, \quad \Delta t = \frac{t_{max}}{K} \tag{4.22}$$

and K denotes the number of observation points. The "asymptotic" error is defined as

$$E_\infty(\Psi) = |\Psi(t_{max}) - \eta(t_{max})|\,. \tag{4.23}$$

The quantity η in (4.21), (4.23) denotes the value of the functional calculated by the algorithm and averaged over N independent runs (cf. (3.23)). We use the parameters

$$N = 2^{20} = 1\,048\,576\,, \qquad t_{max} = 16\,. \tag{4.24}$$

The thick solid lines in Fig. 4.17 correspond to the analytical solution (4.19a) for M_{11}. The pairs of thin solid lines represent the confidence intervals (3.25) for $n = 16$ and $n = 64$ (from above). The left plot shows the results on the time interval $[0, 1]$ illustrating that the initial condition is well approximated for both values of n. The right plot shows the results on the time interval $[4, 16]$ clearly indicating that the "asymptotic" error for $n = 64$ is four times smaller than for $n = 16$. Thus the convergence order of the systematic error (3.24) $O(n^{-1})$ can be seen. On the other hand, the thickness of the confidence intervals representing the stochastic error (fluctuations) behaves as $O(n^{-1/2})$. This behavior is perfectly shown in Table 4.1. The numerical values of the errors (4.21) and (4.23) are displayed, respectively, in the second and fourth columns. The sixth column shows the maximal thickness of the confidence interval (CI). The third, fifth and seventh columns of this table

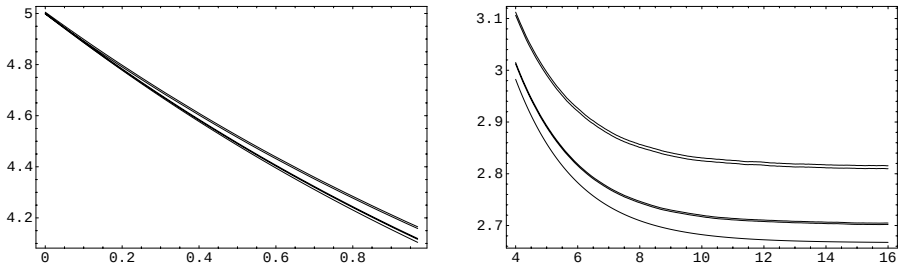

Fig. 4.17. Exact curve $M_{11}(t)$ and confidence intervals for $n = 16, 64$

Table 4.1. Numerical convergence of M_{11}, DSMC

n	$E_{max}(M_{11})$	CF	$E_\infty(M_{11})$	CF	$CI(M_{11})$	CF
16	0.147 E-00	-	0.143 E-00	-	0.338 E-02	-
32	0.728 E-01	2.02	0.720 E-01	2.01	0.238 E-02	1.42
64	0.369 E-01	1.97	0.359 E-01	2.01	0.169 E-02	1.41
128	0.189 E-01	1.95	0.183 E-01	1.96	0.119 E-02	1.42
256	0.959 E-02	1.97	0.920 E-02	1.99	0.853 E-03	1.41

show the "convergence factors", i.e. the quotients between the errors in two consecutive lines of the previous columns. Note that the asymptotic value of this moment (cf. (4.19a)) is $(M_\infty)_{11} = 8/3$. Thus the relative error for $n = 256$ is only 0.35% .

Analogous results for the second component of the energy flux vector r_2 are presented in Fig. 4.18 and Table 4.2. Note that the asymptotic value of this moment (cf. (4.19b)) is $(r_\infty)_2 = 43/3$. Thus the relative error for $n = 256$ is only 0.06% .

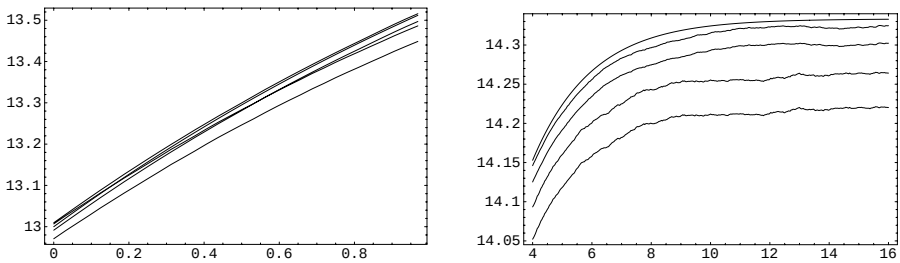

Fig. 4.18. Exact curve $r_2(t)$ and confidence intervals for $n = 16, 64$

Results for the fourth moment s (4.17d) are presented in Fig. 4.19 and Table 4.3. Note that the asymptotic value of this moment (cf. (4.19c)) is $s_\infty = 403/3$. Thus the relative error for $n = 256$ is only 0.8% .

Table 4.2. Numerical convergence of r_2, DSMC

n	$E_{max}(r_2)$	CF	$E_\infty(r_2)$	CF	$CI(r_2)$	CF
16	0.980 E-01	-	0.907 E-01	-	0.220 E-02	-
32	0.480 E-01	2.04	0.429 E-01	2.11	0.157 E-02	1.40
64	0.238 E-01	2.02	0.194 E-01	2.21	0.112 E-02	1.40
128	0.134 E-01	1.78	0.115 E-01	1.69	0.793 E-02	1.41
256	0.553 E-02	2.43	0.296 E-02	3.89	0.562 E-03	1.41

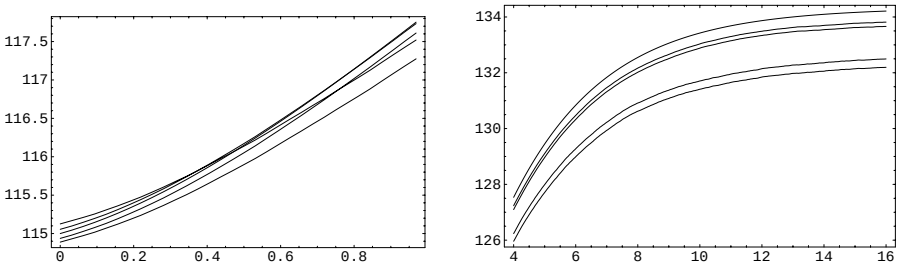

Fig. 4.19. Exact curve $s(t)$ and confidence intervals for $n = 16, 64$

Table 4.3. Numerical convergence of s, DSMC

n	$E_{max}(s)$	CF	$E_\infty(s)$	CF	$CI(s)$	CF
16	0.189 E+01	-	0.186 E+01	-	0.150 E-00	-
32	0.992 E-00	1.90	0.991 E-00	1.88	0.107 E-00	1.40
64	0.480 E-00	2.07	0.473 E-00	2.10	0.766 E-01	1.40
128	0.244 E-00	1.97	0.237 E-00	2.00	0.543 E-01	1.41
256	0.120 E-00	2.03	0.108 E-00	1.91	0.385 E-01	1.41

The time relaxation of the criterion of local thermal equilibrium (4.20) is displayed in Fig. 4.20, which illustrates the dependence of the criterion on the number of particles. The left plot shows the relaxation of the numerical values for $n = 16$ and for $n = 32$ (thin solid lines) on the time interval $[0, 16]$ as well as the analytical solution given in (4.22) (thick solid line). The right plot shows the "convergence" for $n = 16, 32, 64, 128$ and 256 (thin solid lines, from above) to the analytical solution (thick line) on the time interval $[8, 16]$.

4.2.2 Convergence of SWPM

Here we study the convergence of the SWPM method with respect to the initial number of particles n on some time interval $[0, t_{max}]$. We consider the sets of parameters (4.16) and (4.24), in analogy with the previous section.

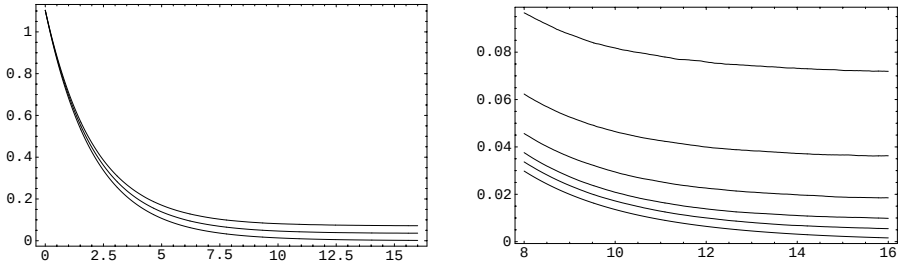

Fig. 4.20. Criterion of local thermal equilibrium

Unbiased mass preserving reduction procedure

First we consider SWPM with the reduction measure from Example 3.45. The time behavior of the number of particles for $n = 256$ is illustrated in Fig. 4.21. The decreasing amplitude of particle number fluctuations is due to different time points the reductions took place for different independent ensembles.

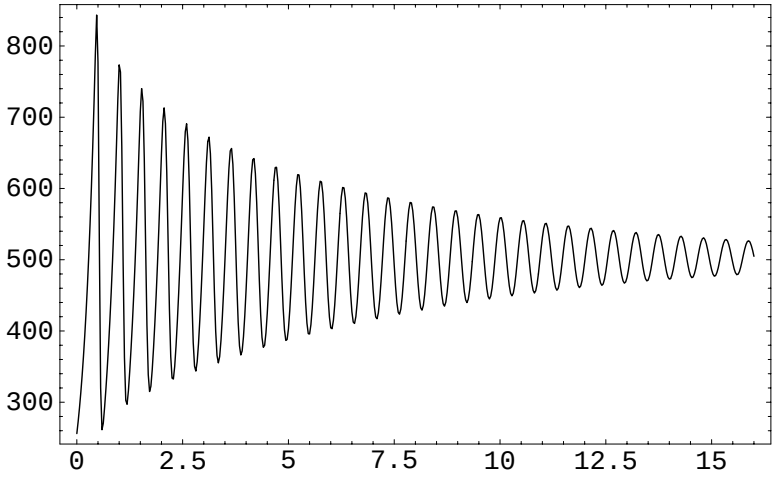

Fig. 4.21. Number of SWPM particles for $n = 256$

The results, which are optically indistinguishable from those obtained using DSMC, are presented in Tables 4.4-4.6.

Mass, momentum and energy preserving reduction procedure

Now we solve the same problem using SWPM with the reduction measure from Example 3.46 (with $k(i) = 3$ and uniform σ_{red}). The results are presented in Tables 4.7-4.9.

Table 4.4. Numerical convergence of M_{11}, SWPM, stochastic reduction

n	$E_{max}(M_{11})$	CF	$E_{\infty}(M_{11})$	CF	$CI(M_{11})$	CF
16	0.149 E-00	-	0.149 E-00	-	0.630 E-02	-
32	0.724 E-01	2.04	0.717 E-01	2.08	0.412 E-02	1.53
64	0.362 E-01	2.00	0.348 E-01	2.06	0.264 E-02	1.56
128	0.185 E-01	1.96	0.184 E-01	1.89	0.167 E-02	1.58
256	0.970 E-02	1.91	0.928 E-02	1.98	0.105 E-02	1.59

Table 4.5. Numerical convergence of r_2, SWPM, stochastic reduction

n	$E_{max}(r_2)$	CF	$E_{\infty}(r_2)$	CF	$CI(r_2)$	CF
16	0.889 E-01	-	0.869 E-01	-	0.612 E-01	-
32	0.522 E-01	1.70	0.515 E-01	1.69	0.391 E-01	1.57
64	0.239 E-01	2.18	0.199 E-01	2.59	0.244 E-01	1.60
128	0.150 E-01	1.59	0.106 E-01	1.88	0.152 E-01	1.61
256	0.799 E-02	1.88	0.378 E-02	2.80	0.959 E-02	1.58

Table 4.6. Numerical convergence of s, SWPM, stochastic reduction

n	$E_{max}(s)$	CF	$E_{\infty}(s)$	CF	$CI(s)$	CF
16	0.222 E+02	-	0.222 E+02	-	0.682 E-00	-
32	0.125 E+02	1.78	0.125 E+02	1.78	0.418 E-00	1.63
64	0.572 E+01	2.18	0.572 E+01	2.18	0.252 E-00	1.66
128	0.233 E+01	2.45	0.233 E+01	2.45	0.154 E-00	1.64
256	0.932 E-00	2.50	0.932 E-00	2.50	0.961 E-00	1.60

Table 4.7. Numerical convergence of M_{11}, SWPM, deterministic reduction

n	$E_{max}(M_{11})$	CF	$E_{\infty}(M_{11})$	CF	$CI(M_{11})$	CF
16	0.146 E-00	-	0.145 E-00	-	0.331 E-02	-
32	0.727 E-01	2.01	0.727 E-01	1.99	0.234 E-02	1.41
64	0.499 E-01	1.46	0.361 E-01	2.01	0.165 E-02	1.40
128	0.383 E-01	1.30	0.186 E-01	1.94	0.117 E-02	1.41
256	0.143 E-01	2.68	0.916 E-02	2.03	0.828 E-03	1.41

Table 4.8. Numerical convergence of r_2, SWPM, deterministic reduction

n	$E_{max}(r_2)$	CF	$E_{\infty}(r_2)$	CF	$CI(r_2)$	CF
16	0.856 E-01	-	0.833 E-01	-	0.212 E-01	-
32	0.344 E-01	2.49	0.343 E-01	2.42	0.147 E-01	1.44
64	0.288 E-01	1.20	0.201 E-01	1.71	0.102 E-01	1.44
128	0.230 E-01	1.25	0.115 E-01	1.75	0.722 E-02	1.41
256	0.109 E-01	2.11	0.776 E-02	1.48	0.509 E-02	1.42

Table 4.9. Numerical convergence of s, SWPM, deterministic reduction

n	$E_{max}(s)$	CF	$E_\infty(s)$	CF	$CI(s)$	CF
64	0.156 E+02	-	0.156 E+02	-	0.645E-01	-
128	0.127 E+02	1.22	0.127 E+02	1.22	0.463E-01	1.39
256	0.861 E+01	1.48	0.861 E+01	1.48	0.335E-01	1.38
1048576	0.400 E-01	-	0.228 E-01	-	-	-

SWPM with deterministic reduction shows less stable convergence for the usual moments and unstable behavior for the moment s for small number of particles ($n = 16, 32$). However, increasing the number of particles (see last row of Table 4.9) leads to a convergent procedure even for this high moment.

4.2.3 Tail functionals

Here we study the time relaxation of tail functionals (4.11) and compare the DSMC and SWPM algorithms. The parameters of the initial distribution (4.15) are

$$V_1 = (96, 0, 0)\,, \quad V_2 = (-32/3, 0, 0)\,, \quad T_1 = T_2 = 1\,, \quad \alpha = 1/10$$

so that, according to (4.17a), (4.17b),

$$V = (0, 0, 0)\,, \qquad T = 1027/3\,.$$

The asymptotic value of the tail functional takes the form (cf. (A.12))

$$\mathrm{Tail}(R, \infty) = 1 - \mathrm{erf}\Big(\frac{R}{\sqrt{2\,T}}\Big) + \frac{2\,R}{\sqrt{\pi\,T}}\,\exp\Big(-\frac{R^2}{2\,T}\Big).$$

In particular, one obtains

$$\begin{aligned}
\mathrm{Tail}(100, \infty) &= 0.202177\ldots \cdot 10^{-5}\,,\\
\mathrm{Tail}(110, \infty) &= 0.102966\ldots \cdot 10^{-6}\,,\\
\mathrm{Tail}(120, \infty) &= 0.388809\ldots \cdot 10^{-8}\,,\\
\mathrm{Tail}(130, \infty) &= 0.108962\ldots \cdot 10^{-9}\,.
\end{aligned}$$

The number of particles for DSMC is $n = 65\,536$. The initial number of particles for SWPM (with stochastic reduction) is $n = 16\,384$. The number of independent ensembles is $N = 32\,768$ for DSMC and $N = 16\,384$ for SWPM. For these choices the computational time for SWPM is approximately 2/3 of that for DSMC. Simulations are performed on the time interval $[0, 32]$.

The highly oscillating number of SWPM particles is shown in Fig. 4.22. The average number of particles is close to $40\,000$. The time relaxation for $\mathrm{Tail}(100, t)$ (obtained using both DSMC and SWPM) is shown in Fig. 4.23.

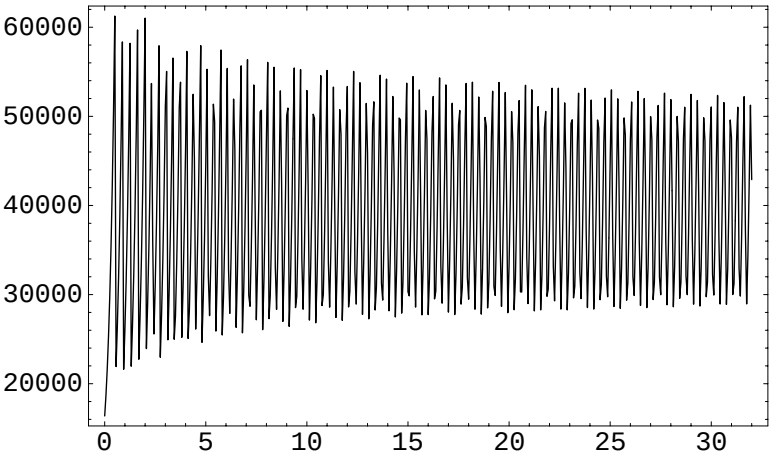

Fig. 4.22. Number of SWPM particles with $n = 16\,384$

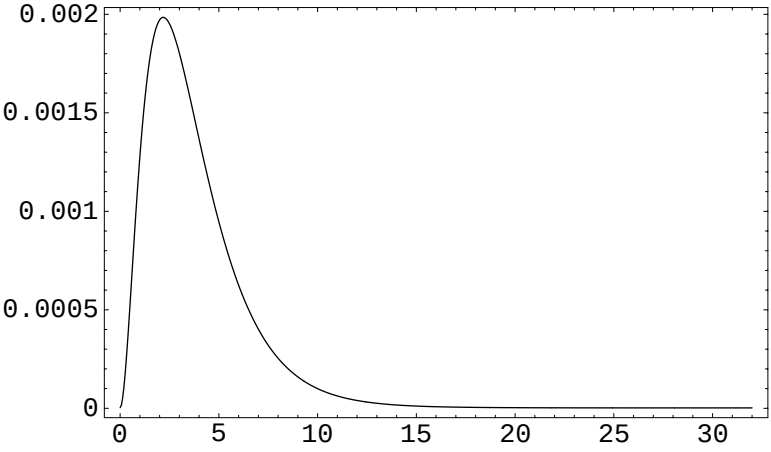

Fig. 4.23. Tail functional $\mathrm{Tail}(100, t)$

In the following figures confidence intervals obtained using DSMC are shown by thin solid lines, while confidence intervals obtained using SWPM are shown by thin dotted lines. The analytical asymptotic values for the tails (4.14a)-(4.14d) are displayed by thick solid lines. In the figures showing the average numbers of particles forming the tails, the left plots corresponds to DSMC and the right plots to SWPM. Note that the tail functionals are shown on the time interval $[16, 32]$ to illustrate the relaxation to the known asymptotic values, while the number particles is plotted for the whole time interval $[0, 32]$.

We see in Fig. 4.24 that the width of the confidence intervals is similar for DSMC and for SWPM for the first tail functional with $R = 100$. Fig. 4.25 shows that both methods have only few particles forming the tail at the beginning of the simulation. Then SWPM produces much more particles in the tail and keeps them during the reductions while the corresponding number for DSMC just follows the functional to compute (cf. Fig. 4.23). Note that the tail formed using SWPM contains a rather large number of particles compared to DSMC. The accuracy is similar because many of these particles are not responsible for resolving this tail, their weights are too small. Many of them play an important role resolving the tails for larger values of R.

As we see in Fig. 4.26 the resolution of the second tail ($R = 110$) is already better for SWPM. The results of SWPM can be reached by DSMC using three-four times more computational time. Thus we can say that SWPM is three-four times "faster" computing this tail with similar accuracy. Fig. 4.27 shows the corresponding numbers of particles in the second tail.

This tendency continues also for the tail with $R = 120$ as shown in Fig. 4.28. Now the width of the DSMC confidence intervals is about three times larger. Thus SWPM can be considered about ten times faster computing this tail with similar accuracy. The number of SWPM particles in this tail shown in Fig. 4.29 is now decreasing in time. However it is still rather big.

Figs. 4.30 and 4.31 show the results obtained using SWPM for the tail with $R = 130$. There are no stable DSMC results for this very small tail, while SWPM still reproduces the asymptotic analytical value.

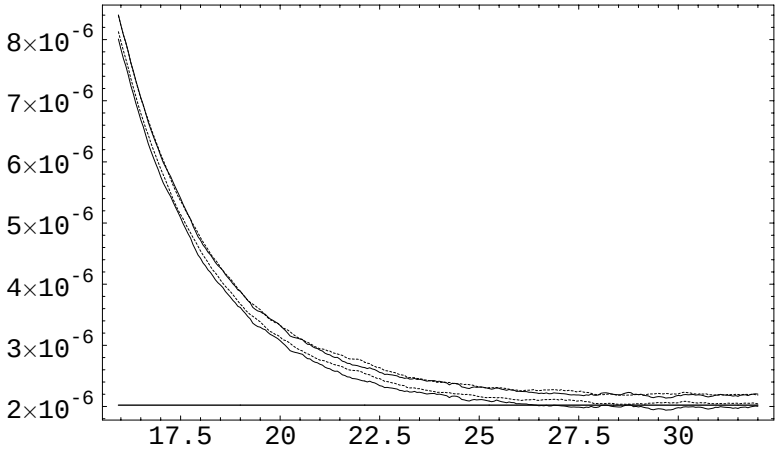

Fig. 4.24. Tail functional for $R = 100$

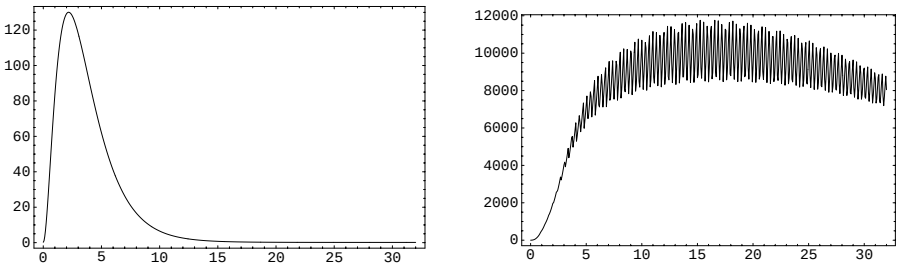

Fig. 4.25. Number of particles in the tail for $R = 100$

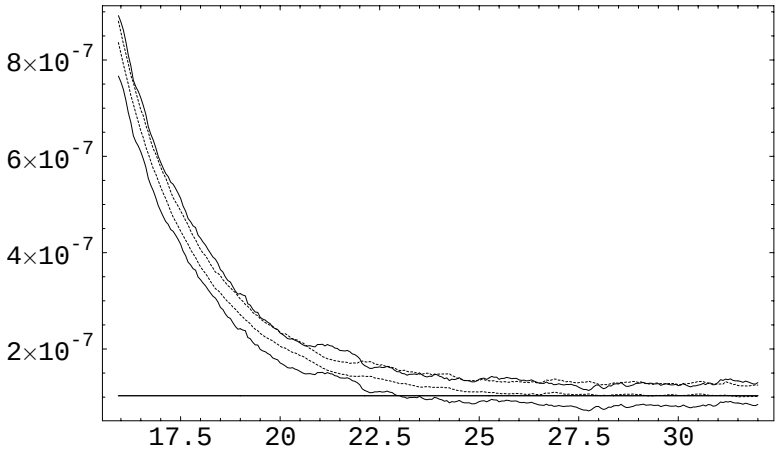

Fig. 4.26. Tail functional for $R = 110$

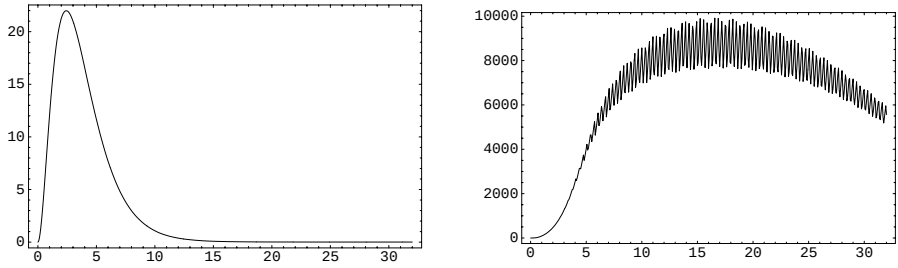

Fig. 4.27. Number of particles in the tail for $R = 110$

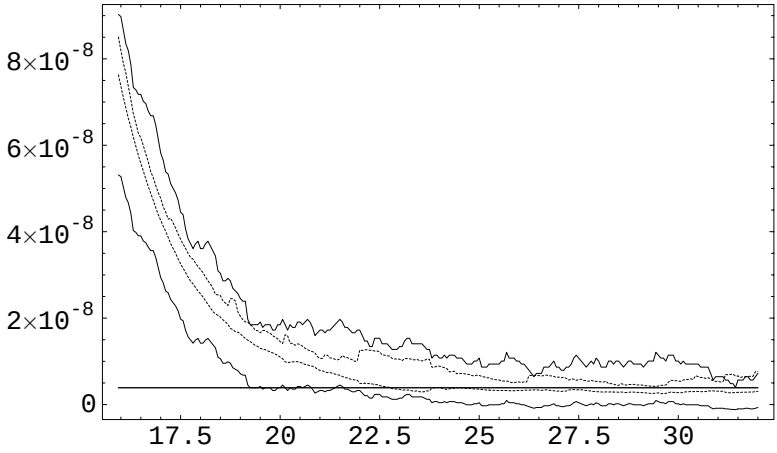

Fig. 4.28. Tail functional for $R = 120$

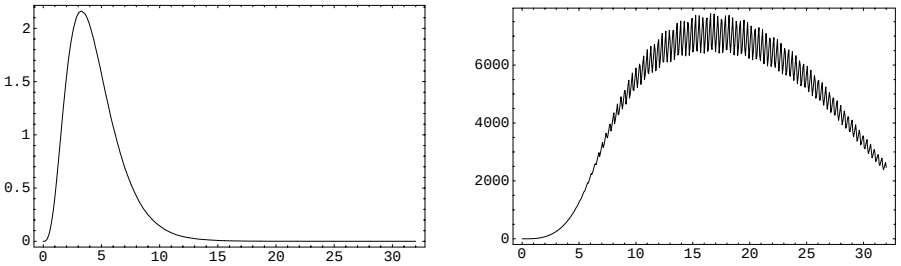

Fig. 4.29. Number of particles in the tail for $R = 120$

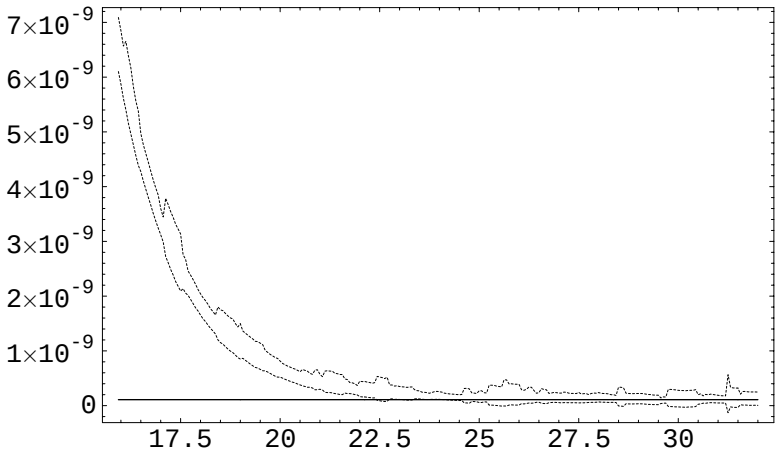

Fig. 4.30. Tail functional for $R = 130$

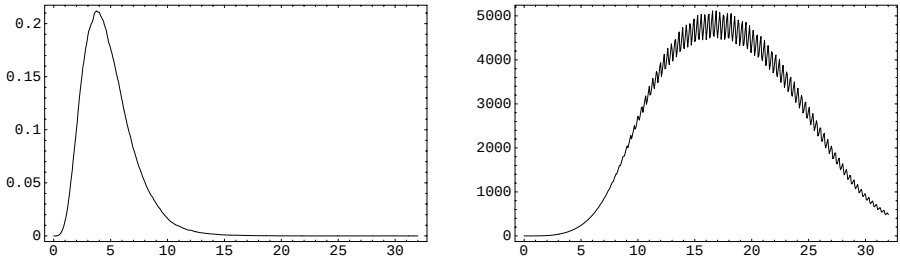

Fig. 4.31. Number of particles in the tail for $R = 130$

4.2.4 Hard sphere model

Here we consider the case of hard sphere molecules (4.4) and study convergence of DSMC and SWPM with respect to the number of particles. Since exact time relaxation curves are not available, we illustrate the "convergence" plotting the DSMC curves for $n = 16,\ 64,\ 256$ and $N = 65\,536$ independent ensembles. The SWPM results are optically indistinguishable from those obtained by DSMC. Simulations are performed on the time interval $[0, 4]$.

Results are given for the second moments $M_{11}(t), M_{12}(t), M_{22}(t), M_{33}(t)$ in Figs. 4.32, 4.33, for the third moments $r_1(t), r_2(t)$ in Fig. 4.34 and for the fourth moment $s(t)$ in Fig. 4.35. Note that the asymptotic values of all these moments are identical to those given in (4.18), (4.19a)-(4.19c) for pseudo-Maxwell molecules.

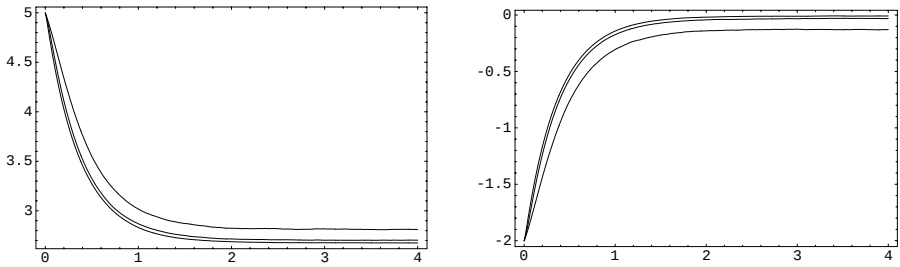

Fig. 4.32. Time relaxation of the moments $M_{11}(t), M_{12}(t)$ for $n = 16, 64, 256$

Fig. 4.36 shows the whole number of collisions as well as the number of fictitious collisions for both DSMC (left plot) and SWPM (right plot) methods. Note that fictitious collisions will necessarily appear for DSMC too, if the model of interaction is different from pseudo-Maxwell molecules. The number of particles for DSMC is $n = 256$. The initial number of particles for SWPM (with stochastic reduction) is $n = 64$. Note that the number of SWPM collisions is significantly bigger than the number of DSMC collisions due to the complicated collision procedure involving more fictitious collisions.

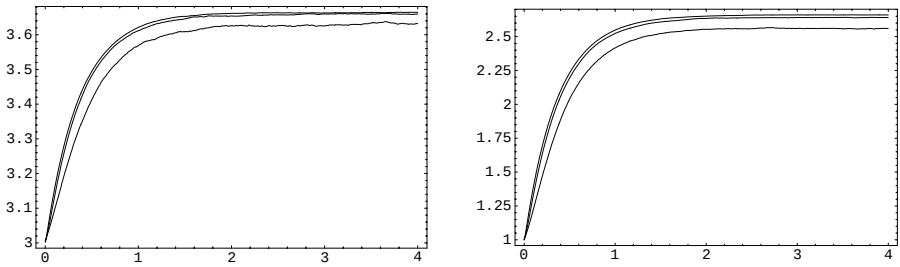

Fig. 4.33. Time relaxation of the moments $M_{22}(t), M_{33}(t)$ for $n = 16, 64, 256$

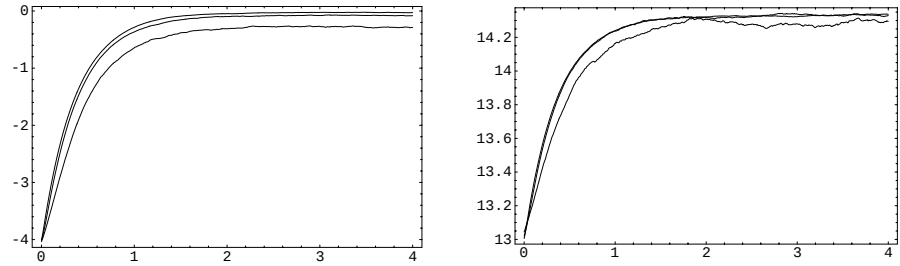

Fig. 4.34. Time relaxation of the moments $r_1(t), r_2(t)$ for $n = 16, 64, 256$

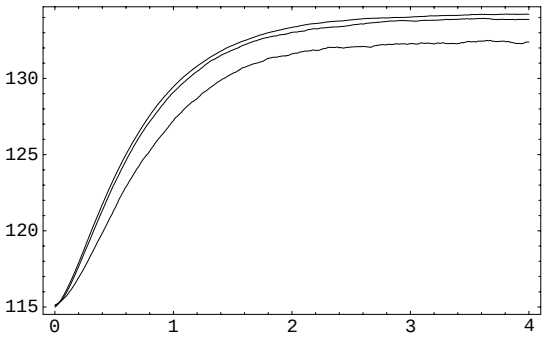

Fig. 4.35. Time relaxation of the moment $s(t)$ for $n = 16, 64, 256$

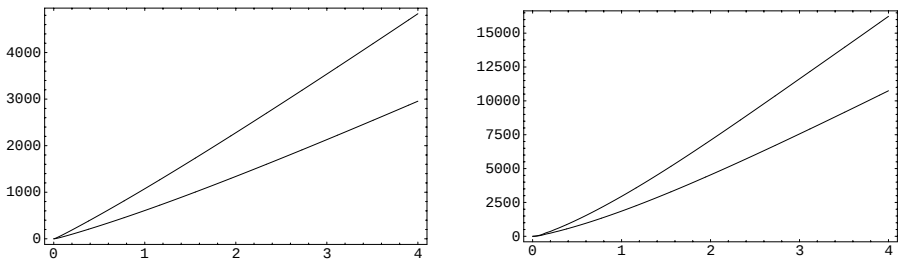

Fig. 4.36. The number of collisions for DSMC and SWPM

4.3 BKW solution of the Boltzmann equation

In this section we consider the BKW solution (A.35) of the spatially homogeneous Boltzmann equation (4.1) with the collision kernel (4.3). Taking into account that (cf. (A.32))

$$\alpha = \frac{1}{4} \int_0^\pi \sin^3 \theta \, d\theta = \frac{1}{3}$$

and choosing the set of parameters (cf. (A.36))

$$\beta_0 = 2/3 \,, \qquad \varrho = 1 \,, \qquad T = 1 \,,$$

one obtains

$$f(t,v) = \frac{1}{(2\,\pi)^{3/2}} \left(\beta(t)+1\right)^{3/2} \left(1 + \beta(t)\Big(\frac{\beta(t)+1}{2}|v|^2 - \frac{3}{2}\Big)\right) e^{-\frac{\beta(t)+1}{2}|v|^2} \,,$$

where (cf. (A.34))

$$\beta(t) = \frac{2\,e^{-t/6}}{5 - 2\,e^{-t/6}} \,.$$

Fig. 4.37 shows a two-dimensional plot of the function

$$\tilde{f}_0(v_1,v_2) = \int_{-\infty}^{\infty} f_0(v_1,v_2,v_3)\,dv_3 = \frac{5}{18\,\pi}\Big(1 + \frac{5}{6}(v_1^2+v_2^2)\Big) e^{-\frac{5}{6}(v_1^2+v_2^2)}$$

and its contours.

We study the time relaxation of the functionals (cf. (A.37))

$$\int_{\mathbb{R}^3} |v|\, f(t,v)\,dv = \left(\frac{2}{\pi}\right)^{1/2} \frac{\beta(t)+2}{(\beta(t)+1)^{1/2}} \,, \tag{4.26a}$$

$$\int_{\mathbb{R}^3} |v|^3\, f(t,v)\,dv = 4\left(\frac{2}{\pi}\right)^{1/2} \frac{3\beta(t)+2}{(\beta(t)+1)^{3/2}} \,, \tag{4.26b}$$

$$\int_{\mathbb{R}^3} |v|^{10}\, f(t,v)\,dv = 10\,395\,\frac{5\beta(t)+1}{(\beta(t)+1)^5} \,. \tag{4.26c}$$

According to (A.38), the function (4.9) representing the criterion of local equilibrium takes the form

$$Crit(t) = \frac{\sqrt{30}}{25}\, e^{-t/3} \,. \tag{4.27}$$

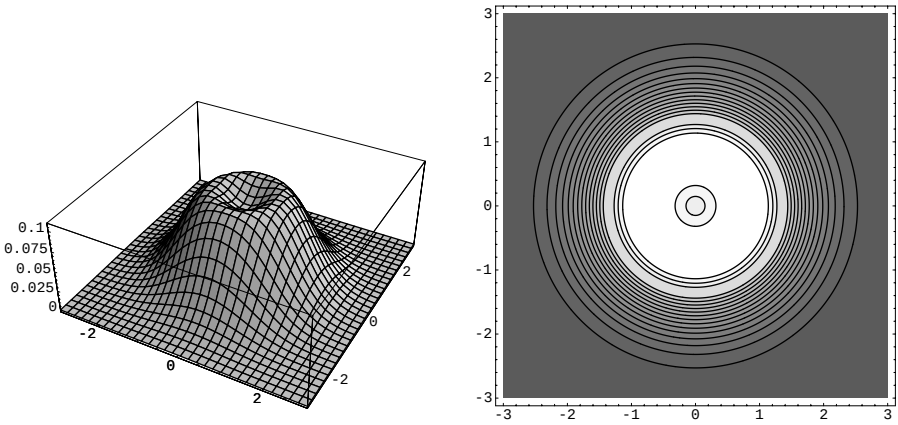

Fig. 4.37. Initial distribution $\tilde{f}_0(v_1, v_2)$

Finally we consider tail functionals (4.11) (cf. (A.39))

$$\mathrm{Tail}(R,t) = 1 - \mathrm{erf}\Big(\sqrt{\frac{\beta(t)+1}{2}}\,R\Big) + \frac{2}{\sqrt{\pi}}\sqrt{\frac{\beta(t)+1}{2}}R\Big(1+\beta(t)R^2\frac{\beta(t)+1}{2}\Big)\exp\Big(-\frac{\beta(t)+1}{2}\,R^2\Big). \tag{4.28}$$

4.3.1 Convergence of moments

Here we demonstrate convergence of the DSMC algorithm for the power functionals (4.26a)-(4.26c). In Figs. 4.38-4.40 the analytical curves are represented by thick solid lines, while the thin solid lines show the curves of the numerical solutions for $n = 16, 64, 256$. The results were obtained generating $N = 2048$ independent ensembles. Note that the numerical solutions obtained for $n = 256$ in Figs. 4.38, 4.39 are optically almost identical to the analytical solutions. The numerical solution obtained using $n = 256$ particles in Fig. 4.40 is of the good quality even for the very high tenth moment.

The analytical (cf. (4.27)) and numerical time relaxation of the criterion of the local thermal equilibrium for the same setting of parameters is shown in Fig. 4.41. It should be pointed out that the numerical computation of this complicated functional involving third and fourth moments is quite stable even for rather small numbers of particles. This fact is of interest when having in mind spatially non-homogeneous computations, where the number of particles per spatial cell can not be as big as in spatially homogeneous case.

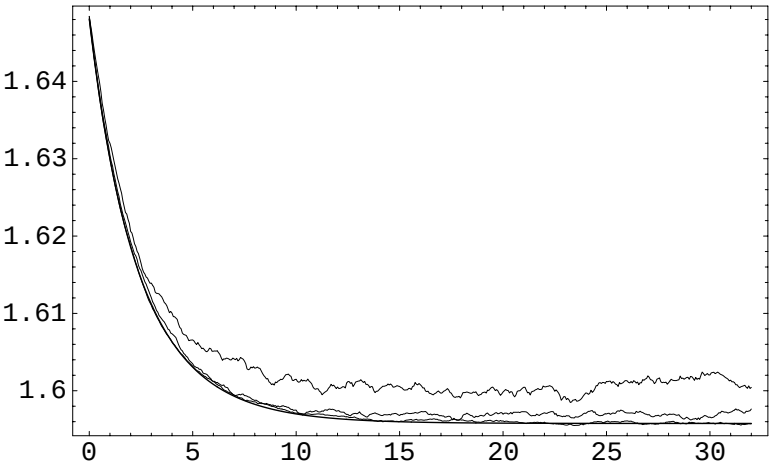

Fig. 4.38. Power functional (4.26a)

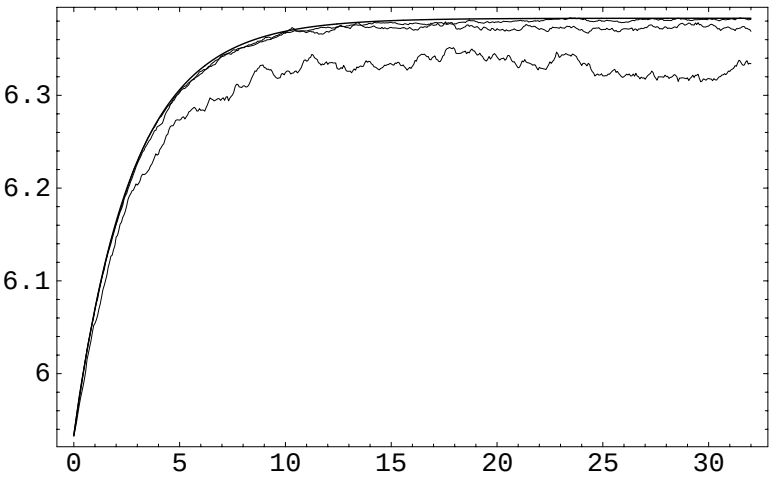

Fig. 4.39. Power functional (4.26b)

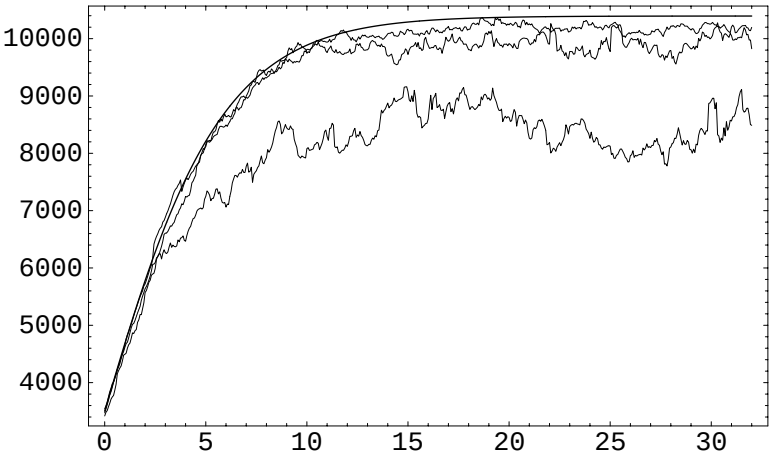

Fig. 4.40. Power functional (4.26c)

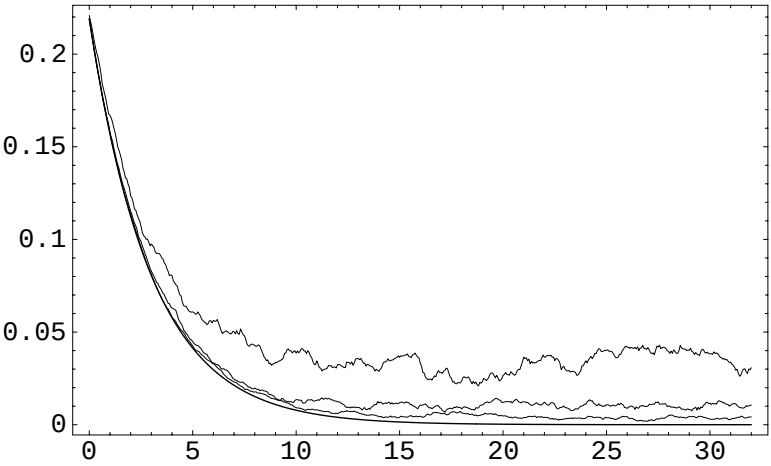

Fig. 4.41. Criterion of the local thermal equilibrium (4.27)

4.3.2 Tail functionals

Here we study the time relaxation of the tail functional (4.28) on the time interval $[0, 32]$ using both DSMC and SWPM algorithms. The number of particles for DSMC is $n = 65\,536$. SWPM (with the stochastic reduction algorithm from Example 3.45) is started using $n = 16\,384$ particles. The number of independent ensembles is $N = 16\,384$. The computational time is similar for both methods.

In the figures confidence intervals obtained using DSMC are shown by thin solid lines, while confidence intervals obtained using SWPM are shown by thin dotted lines. The analytical curves of the tails (4.28) are displayed by thick solid lines. In the figures showing the average numbers of particles forming the tails, the left plots corresponds to DSMC and the right plots to SWPM.

Since the tail for $R = 4$ is computed with high accuracy using both methods the different lines in Fig. 4.42 are optically indistinguishable. As we see in Fig. 4.43 the tail formed using SWPM contains a rather large number of particles compared to DSMC. The accuracy is similar because many of these particles are not useful for resolving this tail, their weights are too small. Many of them play an important role resolving tails with larger values of R.

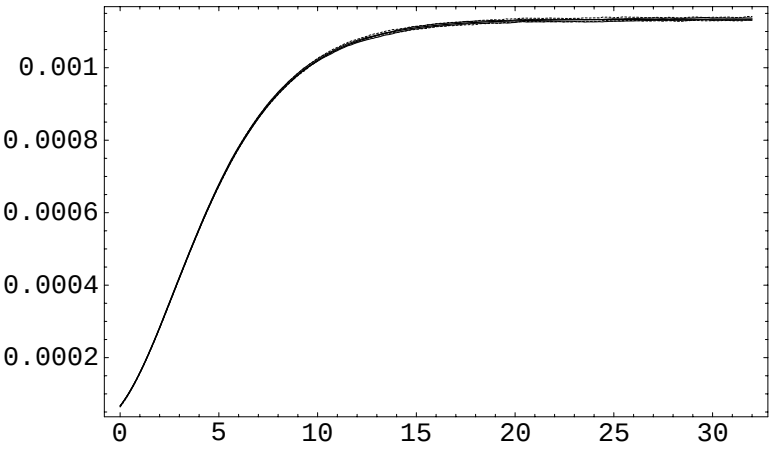

Fig. 4.42. Tail functional (4.28) for $R = 4$

The resolution of the tail with $R = 5$ is already better for SWPM as shown in Fig. 4.44. In other words, SWPM is two-three times "faster" computing this tail with similar accuracy. Fig. 4.45 displays the corresponding numbers of particles.

This tendency continues for the tail with $R = 6$ as shown in Fig. 4.46. Now the width of the DSMC confidence intervals is about three times larger.

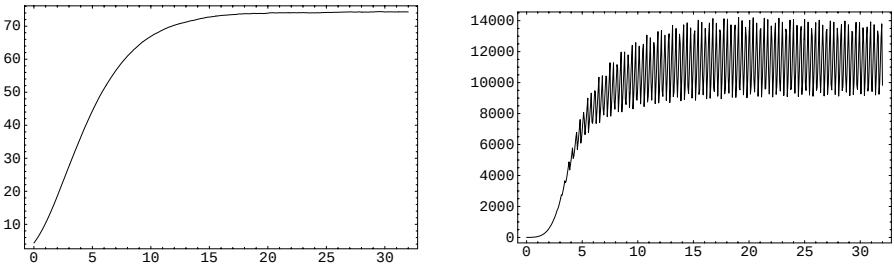

Fig. 4.43. Number of particles in the tail for $R = 4$

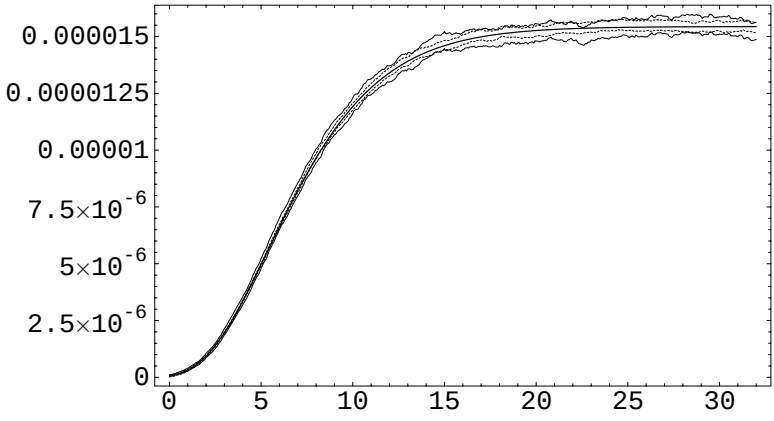

Fig. 4.44. Tail functional (4.28) for $R = 5$

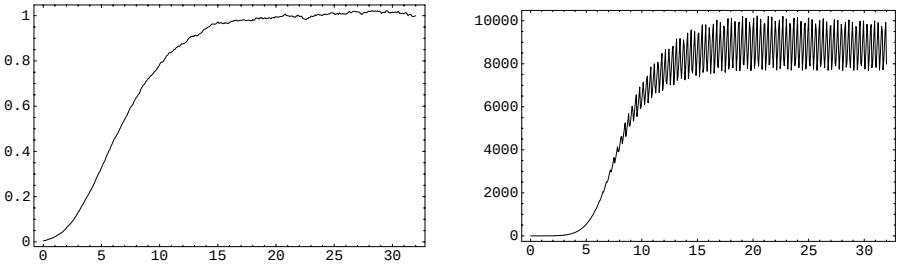

Fig. 4.45. Number of particles in the tail for $R = 5$

Thus SWPM can be considered about nine times "faster" computing this tail with similar accuracy. The number of particles in this tail for DSMC is now very small as shown in Fig. 4.47, while the number of SWPM particles is quite stable apart from the regular fluctuations due to reductions.

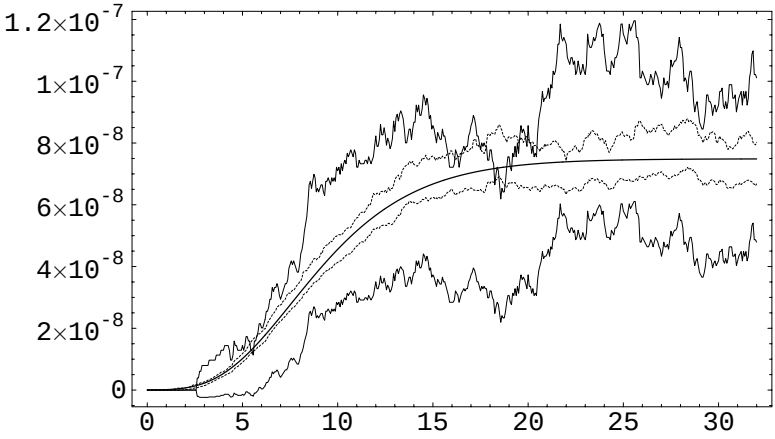

Fig. 4.46. Tail functional (4.28) for $R = 6$

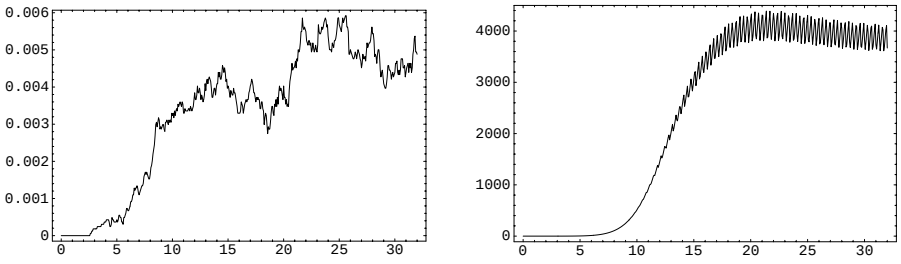

Fig. 4.47. Number of particles in the tail for $R = 6$

Figs. 4.48 and 4.49 show the results obtained using SWPM for the tail with $R = 7$. There are no stable DSMC results for this very small tail, while SWPM reproduces the analytical curve on the whole time interval.

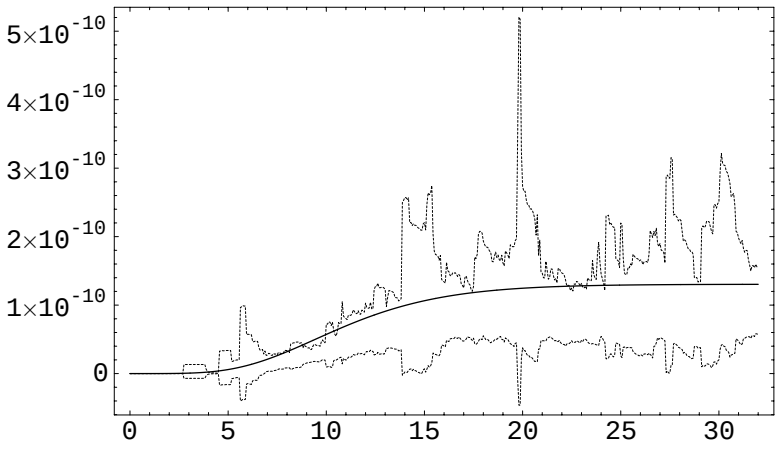

Fig. 4.48. Tail functional (4.28) for $R = 7$

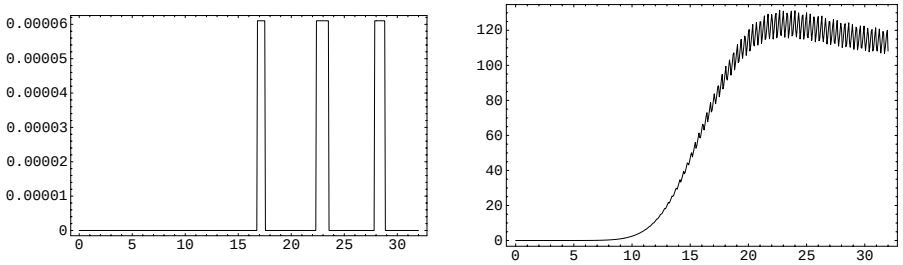

Fig. 4.49. Number of particles in the tail for $R = 7$

4.4 Eternal solution of the Boltzmann equation

In this section we consider the spatially homogeneous Boltzmann equation (4.1) with the collision kernel (4.3). According to results obtained in [30], [28], [29], two solutions can be expressed in an almost explicit form. The first solution is

$$f(t,v) = \frac{8}{(2\,\pi)^{5/2}}\,\beta^3(t)\int\limits_0^\infty \frac{s^3}{(1+s^2)^2}\,e^{-s^2\beta^2(t)\,|v|^2/2}\,ds \tag{4.29}$$

with

$$\beta(t) = e^{-t/3}\,. \tag{4.30}$$

A two-dimensional plot of the function

$$\tilde{f}_0(v_1,v_2) = \int\limits_{-\infty}^{\infty} f_0(v_1,v_2,v_3)\,dv_3 = \frac{2}{\pi^2}\int\limits_0^\infty \frac{s^2}{(1+s^2)^2}e^{-s^2(v_1^2+v_2^2)}\,ds$$

as well as its contours are shown in Fig. 4.50.

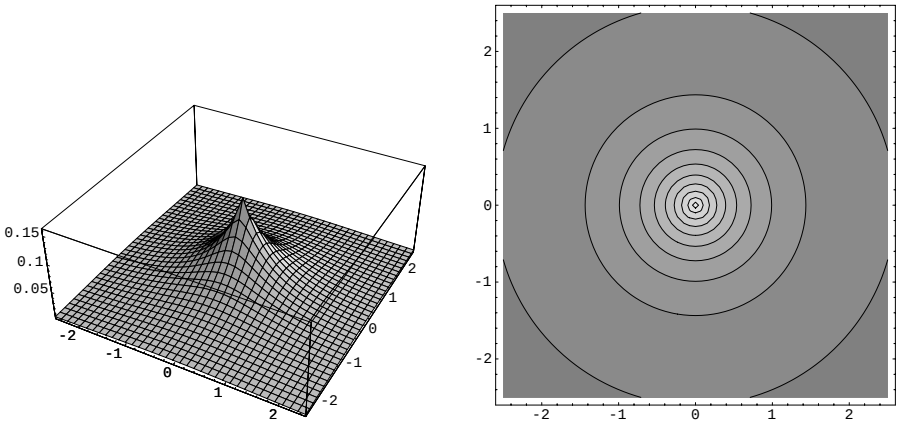

Fig. 4.50. Initial distribution $\tilde{f}_0(v_1, v_2)$

Power functionals of the solution (4.29) can be computed analytically (partly using some computer algebra). One obtains

$$\int\limits_{\mathbb{R}^3} |v|^\alpha f(t,v)dv = C_\alpha e^{\alpha\, t/3}\,, \qquad 0 \le \alpha < 1\,, \tag{4.31}$$

where

$$C_\alpha = \frac{2(1+\alpha)}{\pi^{1/2}}\, \Gamma\left(\frac{3+\alpha}{2}\right) 2^{\alpha/2} \frac{1}{\cos\left(\alpha\,\pi/2\right)}\,.$$

Note that the solution (4.29) has no physical moments. In particular, the momentum

$$\int\limits_{\mathbb{R}^3} v\, f(t,v)dv = 0$$

exists only as a Cauchy principal value integral.

The second solution has the form

$$f(t,v) = \frac{3\sqrt{3}}{(2\,\pi)^{5/2}}\, \beta^3(t) \int\limits_0^\infty \frac{(2+s)s^{9/2}}{(1+s+s^2)^2}\, e^{-s^3\beta^2(t)\,|v|^2/2}\, ds \tag{4.32}$$

with

$$\beta(t) = e^{-3t/4}\,.$$

Power functionals can be obtained in a more or less closed form also for the solution (4.32), but the corresponding expressions contain generalized hypergeometric functions so that these functionals are less convenient for numerical purposes.

4.4.1 Power functionals

The function

$$\int_{\mathbb{R}^3} |v|^{1/2} f(t,v)\,dv = \frac{6}{2^{1/4}\,\pi^{1/2}}\,\Gamma\Big(\frac{7}{4}\Big)\,e^{t/6} \tag{4.33}$$

is used for numerical tests. The most interesting thing with this function is that it is unbounded in time. Since every DSMC simulation conserves energy (which increases with increasing number of particles and independent ensembles), the numerical curves for the power functional (4.31) can not follow the analytic solution (4.33) to infinity. Thus they will converge to some constant value depending on the number of particles and on the number of independent ensembles. We illustrate this behavior in Fig. 4.51, where the analytic curve (4.33) is presented with the thick solid line, while three thin solid lines show the numerical approximations obtained for $n = 4\,096$, $16\,384$ and $262\,144$ particles and $N = 8$ independent ensembles on the time interval $[0, 64]$. It can be clearly seen that for larger values of n the curves follow the exact solution for longer time and converge to a larger value.

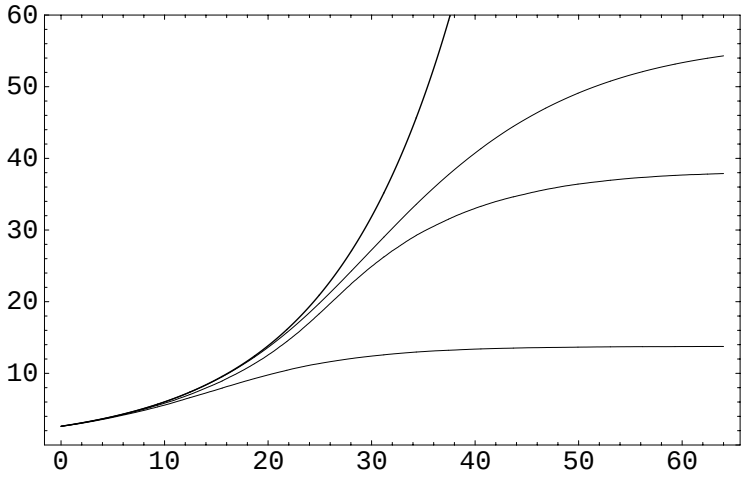

Fig. 4.51. Power functional (4.33)

4.4.2 Tail functionals

Tail functionals (4.11) of the eternal solution (4.29) can be expressed in the form (cf. (4.30))

$$\mathrm{Tail}(R,t) = 1 - \frac{4}{\pi}\int_0^\infty \frac{\mathrm{erf}(\beta(t)\,R\,s/\sqrt{2}\,)}{(1+s^2)^2}\,ds + \frac{2^{5/2}}{\pi^{3/2}}\,\beta(t)\,R\int_0^\infty \frac{s}{(1+s^2)^2}\,e^{-\beta(t)^2\,R^2\,s^2/2}\,ds\,. \tag{4.34}$$

The main feature of these tails is that they tend to 1 in time for all $R > 0$. This follows from the fact that $\lim_{t\to\infty}\beta(t) = 0$. Thus the whole mass of the system moves to infinity. The relaxation of the tails (4.34) on the time interval $[0, 16]$ is illustrated in Fig. 4.52 for the parameters $R = 4, 8$ and 16.

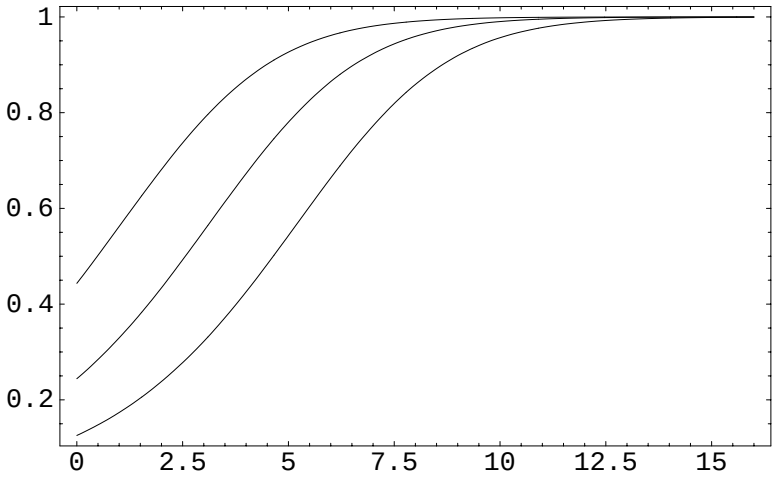

Fig. 4.52. Tail functionals (4.34) for $R = 4, 8$ and 16

4.5 A spatially one-dimensional example

In this section we deal with the shock wave problem on the real axis. We consider the spatially one-dimensional Boltzmann equation

$$v_1\,\frac{\partial}{\partial x} f(x,v) = Q(f,f)(x,v)\,, \qquad x \in \mathbb{R}\,, \quad v \in \mathbb{R}^3\,, \tag{4.35}$$

where the notation

$$Q(f,f)(x,v) = \int\limits_{\mathbb{R}^3}\int\limits_{\mathcal{S}^2} B(v,w,e)\Big(f(x,v')f(x,w') - f(x,v)f(x,w)\Big)\,de\,dw \tag{4.36}$$

is used and the post-collision velocities are defined in (1.6). Since the domain in the physical space is unbounded one has to impose some additional conditions at infinity on the distribution function. We assume

$$\lim_{x\to-\infty} f(x,v) = f_{M_-}(v)\,, \qquad \lim_{x\to\infty} f(x,v) = f_{M_+}(v)\,, \tag{4.37}$$

where

$$f_{M_\pm}(v) = \frac{\varrho_\pm}{(2\pi\,T_\pm)^{3/2}} \exp\left(-\frac{|v-u_\pm e_1|^2}{2\,T_\pm}\right), \qquad v\in\mathbb{R}^3\,. \tag{4.38}$$

The parameters $\varrho_\pm, T_\pm$ and $u_\pm$ are positive numbers, while $e_1 = (1,0,0)^\mathsf{T}$ is the first canonical unit vector.

4.5.1 Properties of the shock wave problem

Here we collect some properties of the steady state problem (4.35). The moment equations (1.67) take the form

$$\frac{d}{dx}\Big(\varrho\,u\Big) = 0\,, \tag{4.39a}$$

$$\frac{d}{dx}\Big(p_{11} + \varrho\,u^2\Big) = 0\,, \tag{4.39b}$$

$$\frac{d}{dx}\left(q_1 + p_{11}\,u + \varrho\left(e + \frac{1}{2}u^2\right)u\right) = 0\,, \tag{4.39c}$$

where ϱ is the density, u is the first component of the bulk velocity, p_{11} is the first component of the stress tensor, e is the internal energy and q_1 is the first component of the heat flux vector. Thus the quantities in parentheses in (4.39a)-(4.39c) are some constants

$$\varrho(x)\,u(x) = c_1\,, \tag{4.40a}$$

$$p_{11}(x) + \varrho(x)\,u^2(x) = c_2\,, \tag{4.40b}$$

$$q_1(x) + p_{11}(x)\,u(x) + \varrho(x)\Big(e(x) + \frac{1}{2}u^2(x)\Big)u(x) = c_3\,. \tag{4.40c}$$

If $x\to\pm\infty$ then the gas tends to the equilibrium state corresponding to the conditions (4.37) so that

$$\lim_{x\to\pm\infty} \varrho(x) = \varrho_\pm\,,$$
$$\lim_{x\to\pm\infty} u(x) = u_\pm\,,$$

$$\lim_{x\to\pm\infty} p_{11}(x) = \varrho_\pm T_\pm\,,$$
$$\lim_{x\to\pm\infty} q_1(x) = 0\,,$$
$$\lim_{x\to\pm\infty} e(x) = \frac{3}{2}T_\pm\,.$$

Here the relations $p(x) = \varrho(x)\,T(x)$ and $T(x) = 2/3\,e(x)$ have been used. The parameters of the Maxwell distributions (4.38) are therefore related to each other as

$$c_1 = \varrho_-\,u_- = \varrho_+\,u_+\,, \tag{4.41a}$$
$$c_2 = \varrho_-\Big(T_- + u_-^2\Big) = \varrho_+\Big(T_+ + u_+^2\Big)\,, \tag{4.41b}$$
$$c_3 = \varrho_- u_-\Big(\frac{5}{2}\,T_- + \frac{1}{2}u_-^2\Big) = \varrho_+ u_+\Big(\frac{5}{2}\,T_+ + \frac{1}{2}u_+^2\Big)\,. \tag{4.41c}$$

These are the **Rankine-Hugoniot conditions** for shock waves in an ideal compressible fluid.

Introducing the Mach number (cf. (1.49))

$$M(x) = \frac{u(x)}{\sqrt{\frac{5}{3}\,T(x)}}\,, \qquad M_\pm = \frac{u_\pm}{\sqrt{\frac{5}{3}\,T_\pm}}$$

we can rewrite the quantities u_-, ϱ_+, u_+, T_+ and M_+ in terms of the quantities ϱ_-, M_- and T_- as

$$u_- = M_-\sqrt{\frac{5}{3}\,T_-}\,, \tag{4.42a}$$
$$\varrho_+ = \frac{4\,M_-^2}{3 + M_-^2}\,\varrho_-\,, \tag{4.42b}$$
$$u_+ = \frac{3 + M_-^2}{4\,M_-^2}u_-\,, \tag{4.42c}$$
$$T_+ = \frac{5\,M_-^4 + 14\,M_-^2 - 3}{16\,M_-^2}T_-\,, \tag{4.42d}$$
$$M_+ = \frac{3 + M_-^2}{\sqrt{5\,M_-^4 + 14\,M_-^2 - 3}}\,. \tag{4.42e}$$

The formulas (4.42a)–(4.42e) allow us the construction of different shock waves for numerical purposes.

One of the interesting features of the shock wave problem is the temperature overshoot downstream. To explain this phenomenon we consider the longitudinal temperature defined as

$$T_\parallel(x) = \frac{p_{11}(x)}{\varrho(x)}\,,$$

where the component p_{11} of the stress tensor P is given by

$$p_{11}(x) = \int_{\mathbb{R}^3} (v_1 - u(x))^2 f(x,v)\, dv\,.$$

Using the relations (4.40b), (4.40a) we rewrite the longitudinal temperature in the form

$$T_\parallel(x) = \frac{c_2}{\varrho(x)} - u^2(x) = \frac{c_2}{\varrho(x)} - \frac{c_1^2}{\varrho^2(x)}\,.$$

The constants c_1 and c_2 are related to the upstream values ϱ_-, T_- and M_- as (cf. (4.42a))

$$c_1 = \varrho_-\, M_- \sqrt{\frac{5}{3}\, T_-}\,, \qquad c_2 = \varrho_-\, T_- + \varrho_-\, M_-^2\, \frac{5}{3}\, T_-\,.$$

Thus we get

$$T_\parallel(x) = \frac{T_-}{3}\left((3 + 5\, M_-^2)\Big(\frac{\varrho_-}{\varrho(x)}\Big) - 5 M_-^2 \Big(\frac{\varrho_-}{\varrho(x)}\Big)^2 \right)\,.$$

The function $T_\parallel$ can be considered as a quadratic function of the variable $z = \varrho_-/\varrho$ and achieves its maximum

$$T_\parallel^* = \frac{\Big(3 + 5\, M_-^2\Big)^2}{60\, M_-^2}\, T_- \tag{4.43}$$

at

$$z^* = \frac{\varrho_-}{\varrho^*} = \frac{3 + 5\, M_-^2}{10\, M_-^2}\,.$$

This maximum will be reached only if the condition $\varrho_- < \varrho^* < \varrho_+$ or equivalently (cf. (4.42b))

$$1 < \frac{10\, M_-^2}{3 + 5\, M_-^2} < \frac{4\, M_-^2}{3 + M_-^2}$$

is fulfilled. Thus the condition for the temperature overshoot of the longitudinal temperature is

$$M_- > \sqrt{\frac{9}{5}}\,. \tag{4.44}$$

The overshoot itself can be expressed using (4.42d) and (4.43) as

$$\frac{T_\parallel^*}{T_+} = \frac{4\left(3 + 5\, M_-^2\right)^2}{75\, M_-^4 + 210\, M_-^2 - 45} > 1 \quad \text{for} \quad M_- > \sqrt{\frac{9}{5}}\,.$$

Note that the maximal value of the longitudinal temperature given in (4.43) is known analytically while the position x^* of this maximum with respect to the space coordinate x

$$x^* \,:\, \varrho(x^*) = \varrho^* = \varrho_- \frac{10\, M_-^2}{3 + 5\, M_-^2} \tag{4.45}$$

can be determined only numerically.

4.5.2 Mott-Smith model

Here we describe the Mott-Smith ansatz for the distribution function f as an $x-$dependent convex combination of the two given Maxwellians,

$$\begin{gathered} f_{MS}(x,v) = a(x)\, f_{M_-}(v) + (1 - a(x))\, f_{M_+}(v)\,, \\ 0 \le a(x) \le 1\,, \quad x \in \mathbb{R}\,. \end{gathered} \tag{4.46}$$

The function f_{MS} can not satisfy the Boltzmann equation (4.35). Thus the residuum

$$R_{MS}(x,v) = v_1 \frac{\partial}{\partial x} f_{MS}(x,v) - Q(f_{MS}, f_{MS})(x,v)$$

is not identical to zero. The main idea of the Mott-Smith approach was to multiply the residuum R_{MS} by a test function φ, integrate the result over the whole velocity space $\mathbb{R}^3$ and then set the result of the integration to zero, i.e.

$$\int\limits_{\mathbb{R}^3} R_{MS}(x,v)\, \varphi(v)\, dv = 0\,. \tag{4.47}$$

Thus the Mott-Smith ansatz is a very simple example of what we call now Galerkin-Petrov solution of an operator equation. Using the special form of the function f_{MS} defined in (4.46) we can easily derive from (4.47) the ordinary differential equation for the function a

$$\frac{d\,a}{d\,x} = \beta\, a(1-a)\,, \qquad x \in \mathbb{R}\,. \tag{4.48}$$

The constant β in (4.48) is defined as

$$\beta = 2\, \frac{\displaystyle\int\limits_{\mathbb{R}^3} Q(f_{M_-}, f_{M_+})\, \varphi(v)\, dv}{\displaystyle\int\limits_{\mathbb{R}^3} v_1 \Big(f_{M_-}(v) - f_{M_+}(v) \Big)\, \varphi(v)\, dv} \tag{4.49}$$

provided that the denominator does not vanish. Equation (4.48) can be solved immediately giving

$$a(x) = \frac{e^{\beta(x-x_0)}}{1+e^{\beta(x-x_0)}}\,, \qquad x \in \mathbb{R}\,.$$

This solution automatically fulfils the conditions for the function a at $\pm\infty$ for all negative values of the constant β

$$\lim_{x\to-\infty} a(x) = 1\,, \qquad \lim_{x\to+\infty} a(x) = 0\,.$$

Thus the integration constant x_0 which defines the "center" of the Mott-Smith shock

$$f_{MS}(x_0, v) = \frac{1}{2}\, f_{M_-}(v) + \frac{1}{2}\, f_{M_+}(v)$$

can not be determined from the conditions at infinity. The calculation of the constant β, which is responsible for the "thickness" of the Mott-Smith shock, in a closed form is technically impossible even for very simple test functions φ (except the case of pseudo-Maxwell molecules). Thus it is more convenient to consider the Mott-Smith ansatz as the following two-parametric ($\beta < 0\,,\ x_0 \in \mathbb{R}$) family

$$f_{MS}(x, v) = \frac{e^{\beta(x-x_0)}}{1+e^{\beta(x-x_0)}}\, f_{M_-}(v) + \frac{1}{1+e^{\beta(x-x_0)}}\, f_{M_+}(v)\,. \tag{4.50}$$

Note that this distribution function does not really depend on three components of the velocity v. If we switch to the polar coordinates (r, φ) in the plane $v_2 \times v_3$ we obtain

$$\begin{aligned} f_{MS}(x, v_1, r) = a(x)\frac{\varrho_-}{(2\pi\, T_-)^{3/2}} \exp\left(-\frac{(v_1-u_-)^2+r^2}{2\,T_-}\right) + \\ (1-a(x))\frac{\varrho_+}{(2\pi\, T_+)^{3/2}} \exp\left(-\frac{(v_1-u_+)^2+r^2}{2\,T_+}\right). \end{aligned}$$

We discuss now some properties of the distribution function f_{MS}. From the analytic expression (4.50) we compute the main physical quantities of this distribution. The density is

$$\varrho_{MS}(x) = \int\limits_{\mathbb{R}^3} f_{MS}(x, v)\, dv = a(x)\, \varrho_- + (1-a(x))\, \varrho_+\,. \tag{4.51}$$

Computing the first component of the momentum

$$\varrho_{MS}(x) u_{MS}(x) = \int\limits_{\mathbb{R}^3} v_1\, f_{MS}(x, v)\, dv = a(x)\, \varrho_- u_- + (1-a(x))\, \varrho_+ u_+ = c_1$$

we can see that this is constant, i.e. equation (4.40a) is fulfilled. For the first component of the stress tensor we obtain with (4.41b) the expression

$$\big(p_{11}\big)_{MS}(x) = \int\limits_{\mathbb{R}^3} (v_1 - u_{MS}(x))^2 \, f_{MS}(x,v)\, dv = a(x)\varrho_-\big(T_- + u_-^2\big) + (1 - a(x))\varrho_+\big(T_+ + u_+^2\big) - \varrho_{MS}(x)u_{MS}^2(x) = c_2 - \varrho_{MS}(x)u_{MS}^2(x)\,.$$

Thus equation (4.40b) is also fulfilled. Now we are able to compute an expression for the Mott-Smith temperature

$$\begin{aligned} T_{MS}(x) &= \frac{1}{3\,\varrho_{MS}(x)}\Big(\int\limits_{\mathbb{R}^3} \Big|v - u_{MS}(x)(1,0,0)^{\mathsf{T}}\Big|^2 \, f_{MS}(x,v)\, dv\Big) \\ &= \frac{1}{3\,\varrho_{MS}(x)}\Big(\big(p_{11}\big)_{MS}(x) - 2\,a(x)\varrho_- T_- + 2\,(1 - a(x))\varrho_+ T_+\Big)\,. \end{aligned}$$

Computing the first component of the heat flux vector and using the property (4.41c) we can see that also equation (4.40c) is fulfilled,

$$\begin{aligned} \big(q_1\big)_{MS}(x) &= \frac{1}{2}\int\limits_{\mathbb{R}^3} \Big|v - u_{MS}(x)(1,0,0)^{\mathsf{T}}\Big|^2 \, (v_1 - u_{MS}(x))\, f_{MS}(x,v)\, dv = \\ &\quad a(x)\varrho_- u_-\Big(\frac{5}{2}T_- + \frac{1}{2}u_-^2\Big) + (1 - a(x))\varrho_+ u_+\Big(\frac{5}{2}T_+ + \frac{1}{2}u_+^2\Big) - \\ &\quad \big(p_{11}\big)_{MS}(x)\, u_{MS}(x) - \varrho_{MS}(x)u_{MS}(x)\Big(\frac{3}{2}T_{MS}(x) + \frac{1}{2}u_{MS}^2(x)\Big) \\ &= c_3 - \big(p_{11}\big)_{MS}(x)\, u_{MS}(x) - \varrho_{MS}(x)u_{MS}(x)\Big(\frac{3}{2}T_{MS}(x) + \frac{1}{2}u_{MS}^2(x)\Big)\,. \end{aligned}$$

Thus the physical quantities of the Mott-Smith distribution fulfil the same system of algebraic equations as the solution of the Boltzmann equation. However the system (4.40a)–(4.40c) of three equations contains five unknown functions ϱ, u, p_{11}, T and q_1. As we will see later the physical quantities of the Mott-Smith distribution will differ from those obtained solving the Boltzmann equation (4.35) numerically.

Since the physical quantities of the Mott-Smith distribution function fulfil the same equations, we deduce the same property for the longitudinal temperature $T_{\parallel,MS}$. Its maximal value is identical to those of the Boltzmann equation (cf. (4.43)

$$T^*_{\parallel,MS} = \frac{\Big(3 + 5\,M_-^2\Big)^2}{60\,M_-^2}\,T_-\,.$$

However the position of this maximal value can now be computed analytically as

$$x^* = x_0 + \beta\,\ln\Big(\frac{2\,M_-^2(5\,M_-^2 - 9)}{(M_-^2 + 3)(5\,M_-^2 - 3)}\Big),$$

using the formulas for the density (4.51) and for the position of the maximum (4.45). Note that the maximum of the longitudinal temperature occurs only if $M_-^2 > 9/5$ (cf. (4.44)).

The formula for the density (4.51) allows us the exact computation of the thickness of the shock using the definition

$$L_{s,MS} = \frac{\varrho_+ - \varrho_-}{\max\, \varrho'_{MS}(x)}\,. \tag{4.52}$$

We obtain that the density reaches its maximal slope at $x = x_0$ and the corresponding thickness of the shock is

$$L_{s,MS} = 4\,\frac{\varrho_+ - \varrho_-}{\beta}\,.$$

Thus the parameter β is directly responsible for the thickness of the shock in the Mott-Smith model. Later we will determine both parameters x_0 and β using numerical results for the value L_s obtained from the stochastic simulation of the Boltzmann equation.

Another interesting property of the Mott-Smith distribution function (4.50) is the following. Let

$$S_3 = \left\{ v \in \mathbb{R}^3 \;:\; f_{M_-}(v) = f_{M_+}(v) \right\} \subset \mathbb{R}^3$$

denote the set of such velocities for which both upstream and downstream Maxwell distributions are equal. This set is a sphere

$$(v_1 - u^*)^2 + v_2^2 + v_3^2 = R^2$$

with

$$u^* = \frac{T_+ u_- - T_- u_+}{T_+ - T_-}$$

and

$$R^2 = \frac{T_+ T_-}{T_+ - T_-}\left(\ln\left(\frac{\varrho_-}{\varrho_+}\right)^2 \left(\frac{T_+}{T_-}\right)^3 + \frac{(u_+ - u_-)^2}{T_+ - T_-} \right).$$

The distribution function (4.50) is constant with respect to the variable x on the sphere S_3 , i.e.

$$f_{MS}(x,v) = a(x) f_{M_-}(v) + (1 - a(x)) f_{M_+}(v) = f_{M_-}(v) = f_{M_+}(v)\,, \quad v \in S_3\,.$$

The one-dimensional distribution functions for the Mott-Smith model

$$\begin{aligned} f^{(1)}_{MS}(x, v_1) &= \int_{-\infty}^{\infty}\int_{-\infty}^{\infty} f_{MS}(x,v)\, dv_2\, dv_3 \\ &= a(x)\frac{\varrho_-}{(2\pi\, T_-)^{1/2}} \exp\left(-\frac{(v_1 - u_-)^2}{2\, T_-} \right) + \\ &\quad (1 - a(x))\frac{\varrho_+}{(2\pi\, T_+)^{1/2}} \exp\left(-\frac{(v_1 - u_+)^2}{2\, T_+} \right) \end{aligned} \tag{4.53}$$

have two common points (for different x) at

$$v_1^{\pm} = u^* \pm R\,. \tag{4.54}$$

4.5.3 DSMC calculations

Since stochastic numerical algorithms for the Boltzmann equation are genuine time-dependent methods, we start this subsection rewriting the steady state problem (4.35) on the whole real axis as a time-dependent problem on a finite interval,

$$\frac{\partial}{\partial t} f + v_1 \frac{\partial}{\partial x} f = Q(f,f)\,, \qquad t > 0\,, \quad 0 < x < L\,, \quad v \in \mathbb{R}^3\,,$$

where $L > 0$ is the first "discretization parameter". The conditions at infinity (4.37) are now transformed into inflow boundary conditions (cf. (1.36)) on the ends of the interval $[0, L]$,

$$f(t,0,v) = f_{M_-}(v)\,, \qquad f(t,L,v) = f_{M_+}(v)\,.$$

We now need also an initial condition for $t = 0$. This can be chosen in an artificial way, in order to reach the steady state solution fast. The choice

$$f(0,x,v) = \begin{cases} f_{M_-}(v)\,, & 0 \le x \le L/2\,, \\ f_{M_+}(v)\,, & L/2 < x \le L\,, \end{cases}$$

is very convenient for numerical tests. For the parameters

$$\varrho_- = 1\,, \quad T_- = 3\,, \quad M_- = 3\,, \tag{4.55}$$

one obtains according to (4.42a)–(4.42e)

$$u_- = 3\sqrt{5}\,,\ \varrho_+ = 3\,,\ T_+ = 11\,,\ M_+ = \sqrt{33}/11\,,\ u_+ = \sqrt{5}\,. \tag{4.56}$$

We use the value $L = 2$ for the interval length and the Knudsen number $\mathrm{Kn} = 0.05$. The discretization parameters of the problem are

$$\begin{aligned} &n_x = 1\,024\,, \qquad \Delta x = L/n_x = 0.1953125 \cdot 10^{-2}\,, \\ &\Delta t = 0.291155 \cdot 10^{-3}\,. \end{aligned} \tag{4.57}$$

The time discretization parameter Δt is chosen on such a way that a particle in in the undisturbed gas upstream having the typical velocity $v = u_-$ will cross exactly one spatial cell during the time interval Δt. We initially use 8 192 particles per spatial cell to resolve the density $\varrho_- = 1$ in the undisturbed gas upstream. Thus the total number of particles in the computational domain was about $1.6 \cdot 10^7$. After formation of the shock 4 096 time averaging steps were realised in order to reduce the stochastic fluctuations.

In Fig. 4.53 the density ϱ and the first component u of the bulk velocity are presented. In Fig. 4.54 we show the profiles of the first component p_{11} of the stress tensor as well as of the pressure $p = \varrho T$. In Fig. 4.55 the profiles of the temperature T and of the Mach number are drawn. Finally, Fig. 4.56 shows the first component q_1 of the heat flux vector and the criterion of local thermal equilibrium $Crit$ computed corresponding to (1.91).

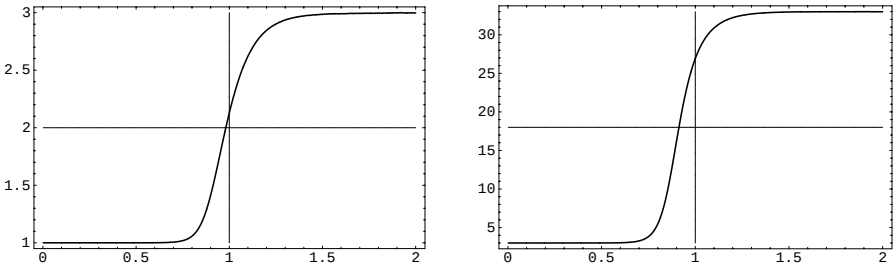

Fig. 4.53. ϱ and u

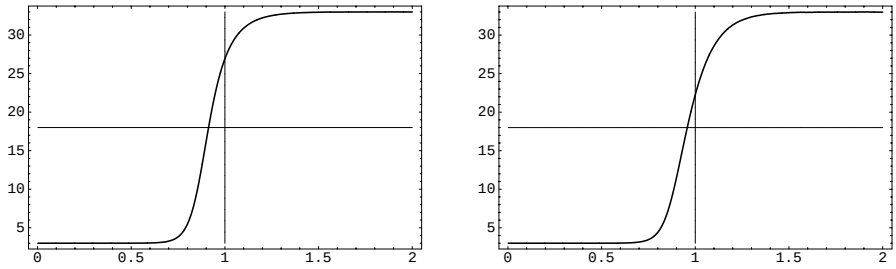

Fig. 4.54. p_{11} and p

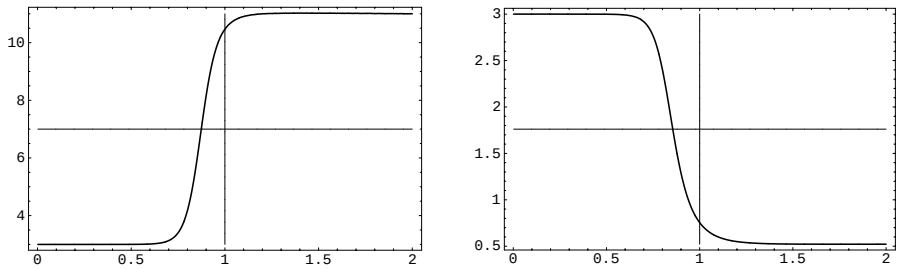

Fig. 4.55. T and Mach number

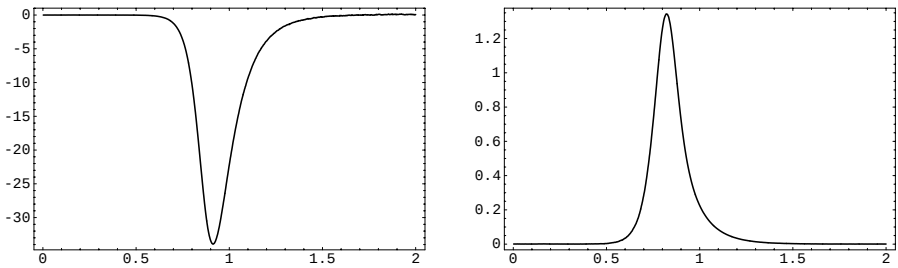

Fig. 4.56. q_1 and $Crit$

Overshoot of the temperature

We consider the same set of parameters of the Maxwell distributions f_{M_-} and f_{M_+} as in (4.55), (4.56) and the same discretization parameters as in (4.57). The maximal value of the longitudinal temperature $T_\parallel^*$ defined in (4.43) takes the form

$$T_\parallel^* = \frac{\left(3 + 5\,M_-^2\right)^2}{60\,M_-^2}\,T_- = \frac{64}{5} = 12.8$$

while its value at the right end of the interval $[0, L]$ is $T_\parallel(L) = 11$.

In Fig. 4.57 the thin horizontal lines represent the value of $T_\parallel^* = 12.8$ and the value at the end of the interval $T_\parallel(L) = 11$. Because of the overshoot of the longitudinal temperature $T_\parallel$ the temperature T presented on the left plot of Fig. 4.55 has also an overshoot. This can be clearly seen in Fig. 4.58, where we zoom the figure plotting the temperature on the interval $[L/2, L]$. Again the thin line represents the temperature value at the end of the interval $[0, L]$ which is $T(L) = 11$.

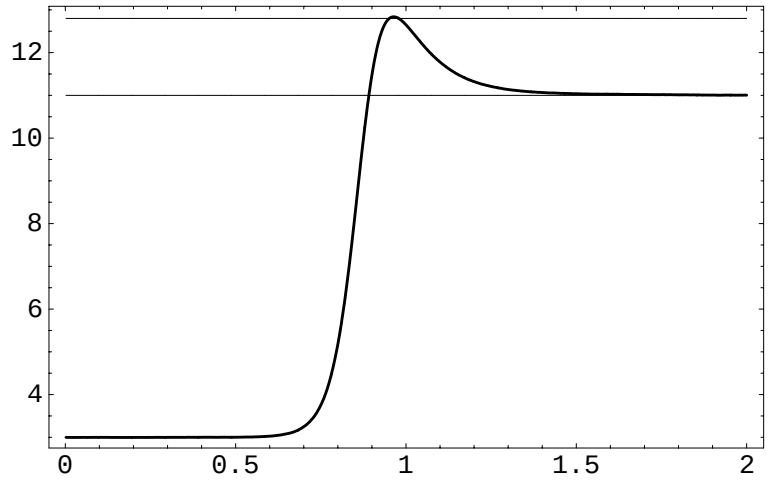

Fig. 4.57. Overshoot of the longitudinal temperature $T_\parallel$

4.5.4 Comparison with the Mott-Smith model

Using the numerical data for the density (cf. left plot Fig. 4.53) we are able to compute the numerical thickness of the shock which is defined as

$$L_s = \frac{\varrho_+ - \varrho_-}{\max\,\varrho'(x)}\,,$$

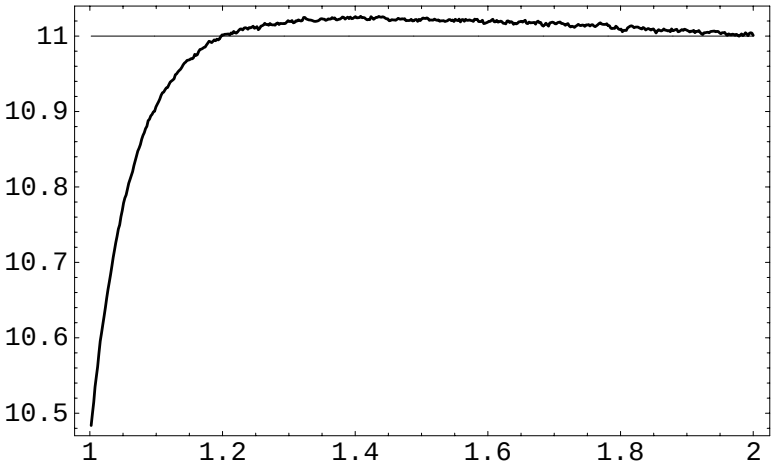

Fig. 4.58. Overshoot of the temperature T

where the maximum is taken over all $0 \leq x \leq L$. If we use the central differences to approximate the derivative of the density

$$\varrho_{x,i} = \frac{\varrho_{i+1} - \varrho_{i-1}}{2\,\Delta x}\,, \qquad i = 2, \ldots, n_x - 1\,,$$

then we can determine the maximum of the $\varrho'(x)$ numerically. The profile of the $\varrho_{x,i}$ is shown in Fig. 4.59.

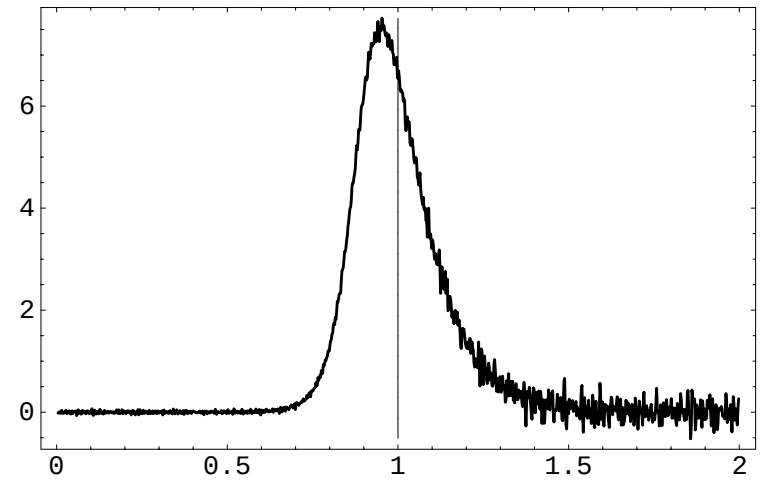

Fig. 4.59. Derivative of the density $\varrho'(x)$

Using the numerical data, we obtain $\max \varrho'(x^*) = 7.72529\ldots$ at the position $x_0 = 0.94921\ldots$ and $L_s = 0.25888\ldots$ for the thickness of the shock. These quantities allow us to determine the parameters in the Mott-Smith model (4.50). Thus the center of the shock is x_0 and the parameter β are defined from the position an the thickness of the shock in the Mott-Smith model as it was shown in (4.52). Thus we obtain

$$x_0 = 0.97949\ldots, \qquad \beta = -15.45058\ldots \tag{4.58}$$

and now we are able to compare the physical quantities obtained numerically with those from the Mott-Smith model. We illustrate the difference between the numerical solution (thick lines) and the Mott-Smith model (thin lines) for the main physical quantities in Figs. 4.60 and 4.61.

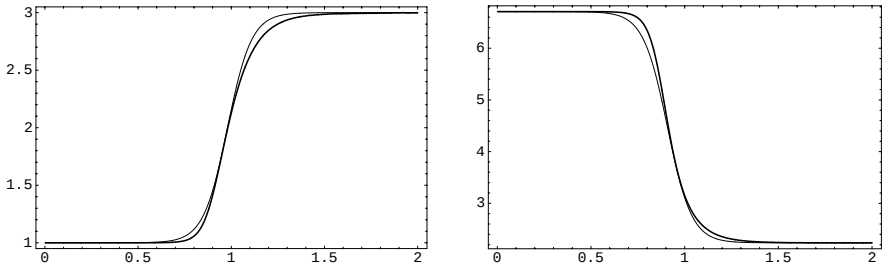

Fig. 4.60. ϱ and u

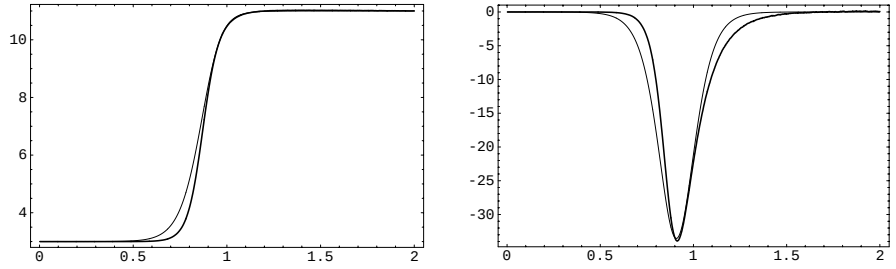

Fig. 4.61. T and $q1$

Fig. 4.62 shows the profile of both numerical and Mott-Smith longitudinal temperature $T_{\|}$. Thus the numerical results fit quite well to the Mott-Smith model. However the temperature T does not form an overshoot for the Mott-Smith model as it can be seen in Fig. 4.63.

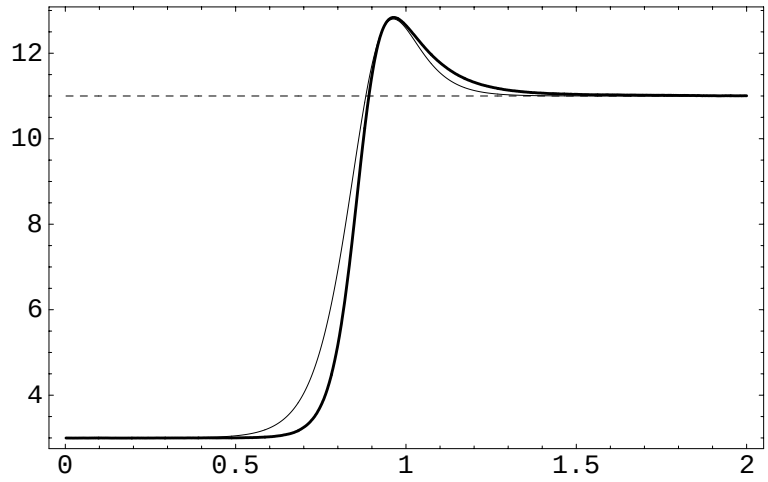

Fig. 4.62. Longitudinal temperature $T_{\|}$

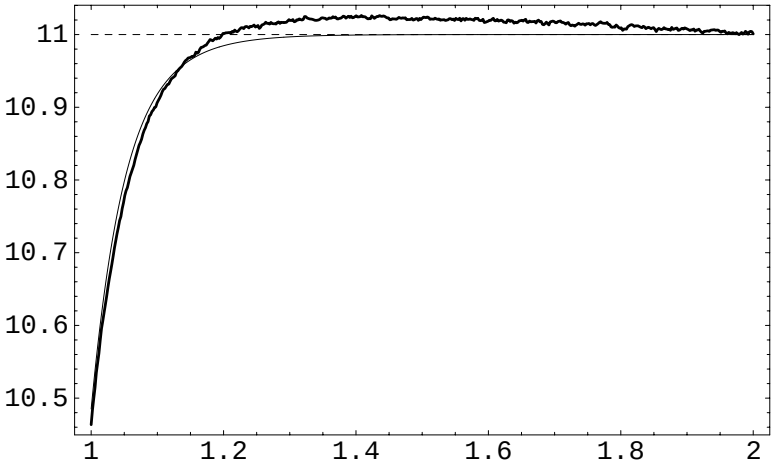

Fig. 4.63. Temperature T

4.5.5 Histograms

Here we compare the numerical histograms of the distribution function computed during the simulation at various positions x with the analytical Mott-Smith distribution $f_{MS}^{(1)}$ (cf. (4.53)). We choose 40 equidistant points x_i on the interval $[0.64, 1.42]$ across the shock and compute the one-dimensional histograms of the distribution function f using 1024 equidistant subintervals of the interval $[-10.5, 19.5]$ for the first component v_1 of the velocity v. Figs. 4.64–4.66 display the corresponding histograms (thick lines) as well as the one-dimensional Mott-Smith distribution (4.53) with parameters (4.58).

Fig. 4.64 shows the nearly undisturbed upstream Maxwell distribution f_{M_-} on the left plot, while the right plot shows the downstream Maxwell distribution f_{M_+} . In Figs. 4.65, 4.66 we show how the distribution function passes the shock. We observe quite good agreement between the numerical data and Mott-Smith distribution. The Mott-Smith distribution passes the shock a bit "faster" then the numerical solution.

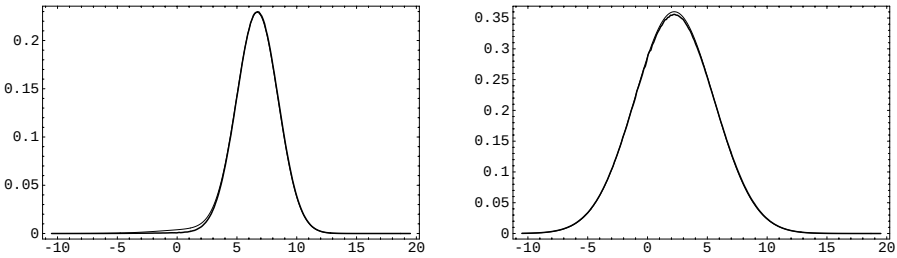

Fig. 4.64. Numerical and the Mott-Smith distribution at $x = 0.7$ and $x = 1.4$

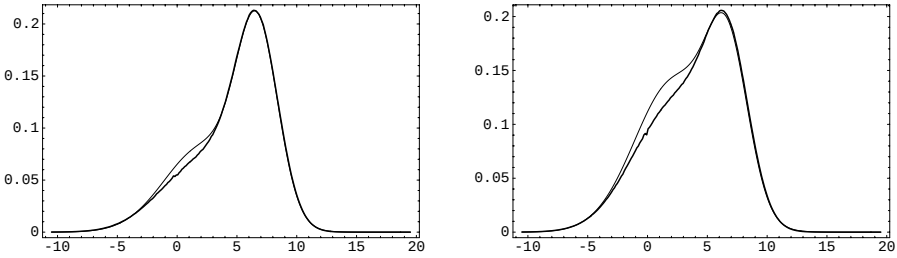

Fig. 4.65. Numerical and the Mott-Smith distribution at $x = 0.9$ and $x = 0.95$

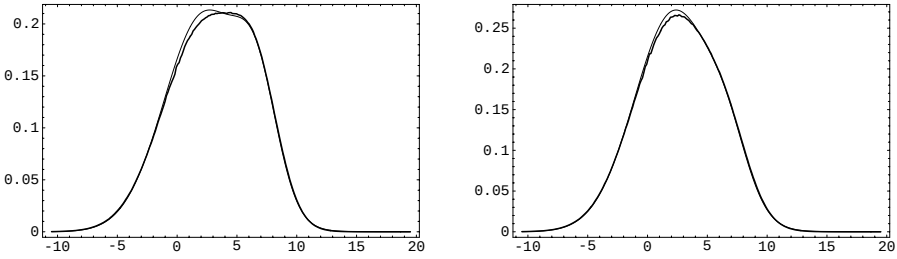

Fig. 4.66. Numerical and the Mott-Smith distribution at $x = 1.0$ and $x = 1.05$

If we perform three-dimensional plots of both distribution functions then it is hard to see any difference as shown in Figs. 4.67 and 4.68. The contour plots show again that the Mott-Smith distribution crosses the shock faster then the numerical distribution. It indicates that the parameter β for the Mott-Smith model as chosen in (4.58) is probably too big.

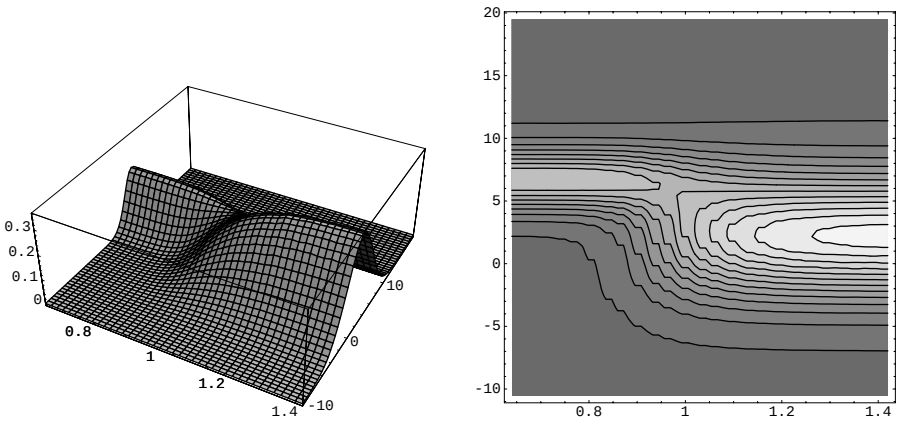

Fig. 4.67. Numerical distribution for $x \in [0.64, 1.42]$ and $v_1 \in [-10.5, 19.5]$

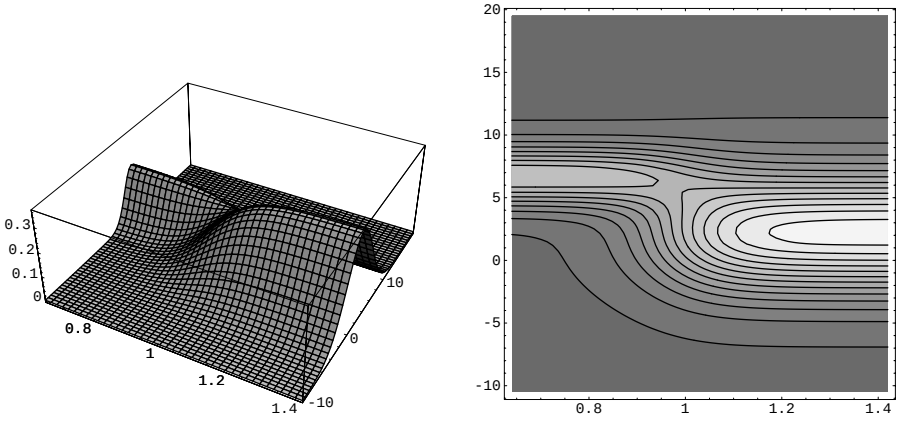

Fig. 4.68. Mott-Smith distribution for $x \in [0.64, 1.42]$ and $v_1 \in [-10.5, 19.5]$

Finally we illustrate the common points of the one-dimensional distributions for different x. In Fig. 4.69 we show five numerical curves for $x = 0.7, 0.9, 1.0, 1.1$ and $x = 1.4$. All numerical curves have two common points at

$$v_1^- = 5.814556\ldots, \qquad v_1^+ = 10.955953\ldots .$$

This fact was theoretically predicted for the Mott-Smith model (cf. (4.54)). The corresponding curves for the Mott-Smith model are shown in Fig. 4.70.

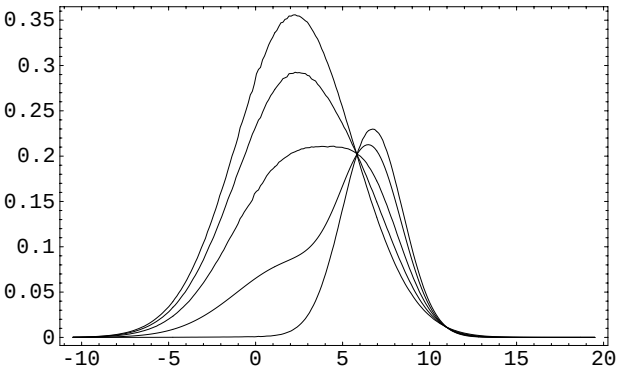

Fig. 4.69. Numerical curves for different x

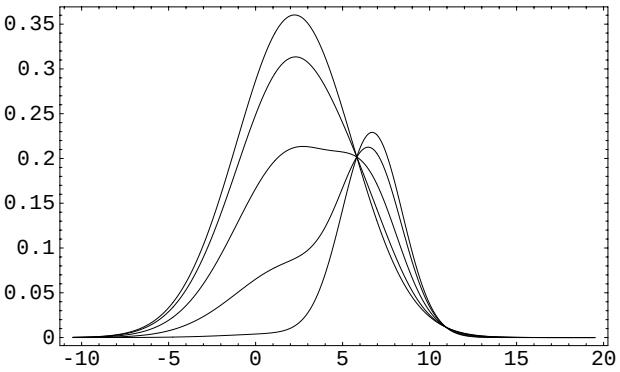

Fig. 4.70. Mott-Smith curves for different x

4.5.6 Bibliographic remarks

Concerning the classical shock wave problem in a rarefied monatomic perfect gas on the real axis we refer to [50]. The interesting feature of the temperature overshoot is explained in [209]. The Mott-Smith ansatz originates from [141]. In this paper the test function in (4.47), (4.49) was chosen in the form $\varphi(v) = v_1^2$. Definition (4.52) goes back to [142].

4.6 A spatially two-dimensional example

In this section we deal with some steady state problems for the spatially two-dimensional Boltzmann equation

$$v_1 \frac{\partial}{\partial x_1} f + v_2 \frac{\partial}{\partial x_2} f = \int\limits_{\mathbb{R}^3} \int\limits_{\mathcal{S}^2} B(v, w, e) \Big(f(t, x, v') f(t, x, w') - f(t, x, v) f(t, x, w) \Big) de \, dw \,, \tag{4.59}$$

where $x \in D$ and $v \in \mathbb{R}^3$. The computational domain is a trapezoid

$$D = \{ x = (x_1, x_2) \,, \quad 0 < x_1 < a \,, \quad 0 < x_2 < b + x_1 \tan(\alpha) \}$$

as shown in Fig. 4.71 for the parameters

$$a = 2.0 \,, \quad b = 0.4 \,, \quad \alpha = \arctan(0.2) \,. \tag{4.60}$$

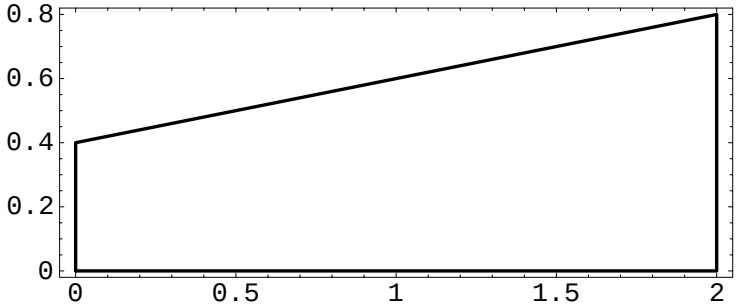

Fig. 4.71. Computational domain D

Boundary conditions are defined separately for each of the four straight pieces

$$\partial D = \Gamma_l \cup \Gamma_b \cup \Gamma_r \cup \Gamma_t$$

denoting the left, bottom, right and top parts of the boundary, respectively. The corresponding unit inward normal vectors are

$$n_l = \begin{pmatrix} 1 \\ 0 \\ 0 \end{pmatrix} \,, \; n_b = \begin{pmatrix} 0 \\ 1 \\ 0 \end{pmatrix} \,, \; n_r = \begin{pmatrix} -1 \\ 0 \\ 0 \end{pmatrix} \,, \; n_t = \begin{pmatrix} -\sin(\alpha) \\ \cos(\alpha) \\ 0 \end{pmatrix} \,.$$

The bottom part represents the axis of symmetry, so we use specular reflection (1.37) there, i.e.

$$f(x,v) = f(x, v - 2\,(v, n(x))\,n(x))\,, \qquad x \in \Gamma_b\,, \quad v_2 > 0\,.$$

On the right part we are modeling outflow (particles are permanently absorbed), i.e.

$$f(x,v) = 0\,, \qquad x \in \Gamma_r\,, \quad v_1 < 0\,.$$

On the left part there is an incoming flux of particles prescribed according to the boundary condition (1.36), i.e.

$$f(x,v) = f_{in}(x,v) = M_{in}(v)\,, \qquad x \in \Gamma_l\,, \quad v_1 > 0\,,$$

with an inflow Maxwellian

$$M_{in}(v) = \frac{\varrho_{in}}{(2\pi T_{in})^{3/2}} \exp\left(-\frac{|v - V_{in}|^2}{2T_{in}}\right). \tag{4.61}$$

The boundary condition on the top part Γ_t is defined in two different ways. First we assume absorption of particles. Considering the collisionless case, we find explicit expressions for certain functionals of the solution. These formulas are used for validating the algorithms. Applying both DSMC and SWPM to the problem of simulating rare events, we illustrate the new opportunities achieved by the introduction of variable weights for the approximation of the inflow boundary condition. Then we show that similar results are obtained in the case with collisions, where no analytic results are available. Finally we consider diffuse reflection on the top part of the boundary and study the influence of the hot wall on the flow.

In the numerical experiments we assume

$$\varrho_{in} = 1\,, \qquad T_{in} = 10$$

and consider the inflow velocity in the form (cf. (1.48), (1.49) with $m = 1$ and $k = 1$)

$$V_{in} = \mathrm{Mach}\,\sqrt{\gamma\,T_{in}} \begin{pmatrix} 1 \\ 0 \\ 0 \end{pmatrix}. \tag{4.62}$$

The computations were performed on the uniform spatial 240×96 cells grid covering the rectangle $(0.0, 2.0) \times (0.0, 0.8)$. The time step was chosen so that a typical particle moves over one cell. On average, there were 200 DSMC-particles per cell. The corresponding number was 50 for SWPM. The stochastic reduction algorithm from Example 3.45 was applied during the collision simulation step, when the number of particles reached 200. For this choice, the computational time for SWPM was about one half of the DSMC time. Unless indicated otherwise, the results were obtained using 1000 averaging steps after reaching the steady state.

4.6.1 Explicit formulas in the collisionless case

Here we consider equation (4.59) in the collisionless case, i.e when the Knudsen number in (4.12) is $\mathrm{Kn} = \infty$. We assume absorption of particles on the top part of the boundary and remove the axis of symmetry by doubling the computational domain.

This setup is equivalent to the steady state problem for the free flow equation

$$\big(v, \mathrm{grad}_x f\big) = 0\,, \qquad x \in D\,, \quad v \in \mathbb{R}^3\,, \tag{4.63}$$

with the boundary condition

$$f(x,v) = f_{in}(x,v)\,, \qquad x \in \partial D\,, \quad v_1 > 0\,, \tag{4.64}$$

where

$$D = \{x \in \mathbb{R}^3\,,\ x_1 > 0\}\,, \qquad \partial D = \{x \in \mathbb{R}^3\,,\ x_1 = 0\}$$

and the inflow function is defined as (cf. (4.61))

$$f_{in}(x,v) = \begin{cases} M_{in}(v)\,, & x_1 = 0\,, \quad -b \le x_2 \le b\,, \\ 0\,, & \text{otherwise.} \end{cases} \tag{4.65}$$

The solution of the boundary value problem (4.63), (4.64) is given by the formula

$$f(x,v) = f_{in}(x + t\,v, v)\,, \qquad x_1 > 0\,, \quad v_1 > 0\,, \tag{4.66}$$

where

$$t = t(x,v) = -\frac{x_1}{v_1} \tag{4.67}$$

is chosen such that $x + t\,v \in \partial D$.

Now we compute a functional of the solution (4.66), namely the spatial density. Using (4.65) and (4.67) we obtain

$$\begin{aligned} \varrho(x) &= \int\limits_{\mathbb{R}^3} f(x,v)\,dv \qquad\qquad (4.68) \\ &= \int\limits_{\mathbb{R}_+(x)} M_{in}(v) dv = \int\limits_0^\infty dv_1 \int\limits_{\frac{x_2-b}{x_1}\,v_1}^{\frac{x_2+b}{x_1}\,v_1} dv_2 \int\limits_{-\infty}^{\infty} M_{in}(v)\,dv_3\,, \end{aligned}$$

where

$$\mathbb{R}_+(x) = \Big\{v \in \mathbb{R}^3\,, \quad v_1 > 0\,, \quad -b \le x_2 - \frac{x_1}{v_1}\,v_2 \le b\Big\}.$$

Assuming

$$V_{in} = (V, 0, 0)^{\mathsf{T}} \tag{4.69}$$

and using the substitutions $v_1 = \sqrt{2\,T_{in}}\,z_1$, $v_2 = \sqrt{2\,T_{in}}\,z_2$, we conclude from (4.68) that (cf. (A.3))

$$\begin{aligned}
\varrho(x) &= \frac{\varrho_{in}}{2\pi\,T_{in}} \int_0^\infty \exp\left(-\frac{(v_1 - V)^2}{2\,T_{in}}\right) \int_{\frac{x_2-b}{x_1}\,v_1}^{\frac{x_2+b}{x_1}\,v_1} \exp\left(-\frac{v_2^2}{2\,T_{in}}\right) dv_2\, dv_1 \\
&= \frac{\varrho_{in}}{\pi} \int_0^\infty \exp\left(-\left(z_1 - \frac{V}{\sqrt{2\,T_{in}}}\right)^2\right) \int_{\frac{x_2-b}{x_1}\,z_1}^{\frac{x_2+b}{x_1}\,z_1} \exp\left(-z_2^2\right) dz_2\, dz_1\,, \qquad (4.70) \\
&= \frac{\varrho_{in}}{2\sqrt{\pi}} \int_0^\infty \exp\left(-(z - \frac{V}{\sqrt{2\,T_{in}}})^2\right) \left(\operatorname{erf}\left(\frac{x_2+b}{x_1}\,z\right) - \operatorname{erf}\left(\frac{x_2-b}{x_1}\,z\right)\right) dz\,.
\end{aligned}$$

Note that the density is a symmetric function with respect to the plane $x_2 = 0$.

Further simplification is possible if the inflow mean velocity is zero, i.e. $V = 0$ in (4.69). In this case we use

$$\int_0^\infty \exp\left(-z^2\right) \operatorname{erf}(yz)\, dz = \frac{1}{\sqrt{\pi}}\, \arctan y$$

and obtain

$$\varrho(x) = \frac{\varrho_{in}}{2\,\pi} \left(\arctan \frac{x_2 + b}{x_1} - \arctan \frac{x_2 - b}{x_1}\right) .$$

Here we assume absorption of particles on the top part of the boundary and consider the collisionless case $\mathrm{Kn} = \infty$, where the analytical solution (4.70) is available. We calculate the density along the vertical straight line

$$x = \begin{pmatrix} 1 \\ 0.005 \\ 0 \end{pmatrix} + \lambda \begin{pmatrix} 0 \\ 1 \\ 0 \end{pmatrix}, \qquad 0 \le \lambda \le 0.99\,. \tag{4.71}$$

The parameter α in (4.60) is increased appropriately so that the line (4.71) is contained in the computational domain. Note the upper and right boundaries do not influence the flow.

The generation of SWPM particles at the inflow boundary Γ_l is performed according to Example 3.8 with the choice (3.57). We use $\kappa_{in} = 1$ so that the inflow intensity does not change compared to DSMC. Choosing $\tau > 1$ we are

able to place artificially more particles in the tail region of the prescribed distribution function. The parameter $c_{in} \in [0,1]$ controls the proportion of such particles. We use $c_{in} = 0.5$ and $\tau = 8$ in the subsequent SWPM simulations. The initial condition is vacuum, i.e. the computational domain is empty at the beginning.

Mach number 5

First we choose the inflow Mach number in (4.62) equal to 5.0. Fig. 4.72 shows the analytic expression for the density (4.70) (thick dashed line) and the confidence bands (thin lines) of the numerical solutions obtained with DSMC (left plot) and SWPM (right plot) on the interval $x_2 \in [0.005, 0.6]$. We see very good agreement of the numerical solutions in the "high" density region for both methods. In Fig. 4.73 we show the same values in the "low" density region $x_2 \in [0.88, 0.995]$. Here we can see that the results obtained using DSMC are reasonable but the confidence bands of SWPM are better. Thus some reduction of the variance is achieved using weighted particles. The relative accuracy (i.e. the quotient of the thickness of the confidence bands and of the exact solution) is presented in Fig. 4.74. Thus the DSMC scheme is slightly better in the "high" density region and SWPM accuracy becomes much higher in the "low" density region, i.e. for $x_2 > 0.8$.

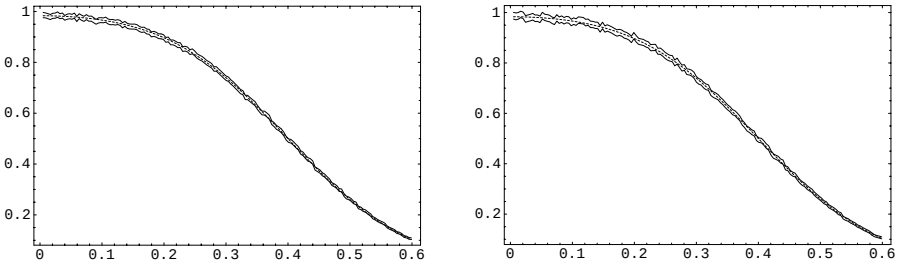

Fig. 4.72. "High" density region, Mach = 5.0

Mach number 7

Now we choose the inflow Mach number equal to 7.0. Fig. 4.75 shows the analytic expression for the density (4.70) (thick dashed line) and the confidence bands (thin lines) of the numerical solutions obtained with DSMC (left plot) and SWPM (right plot) on the interval $x_2 \in [0.005, 0.6]$. Very good agreement of the numerical solutions can be seen in the "high" density region. Fig. 4.76 illustrates the same values in the "low" density region $x_2 \in [0.88, 0.995]$. Here we see only some fluctuations obtained using DSMC while the confidence

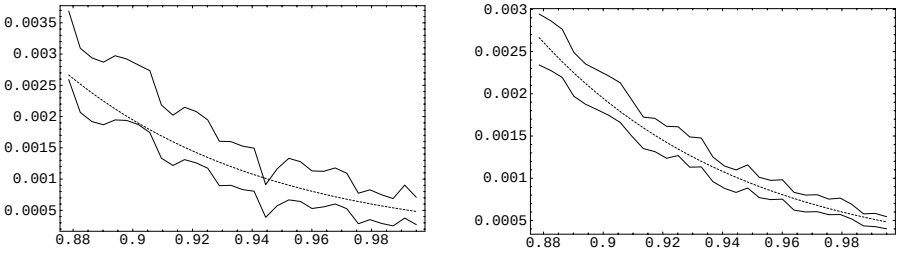

Fig. 4.73. "Low" density region, Mach = 5.0

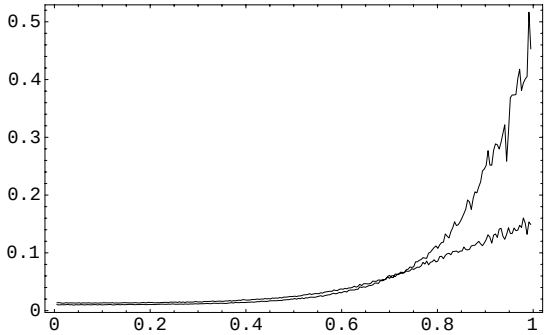

Fig. 4.74. The relative accuracy, Mach = 5.0

bands for SWPM are still good. Thus an enormous reduction of the variance is achieved using weighted particles. The relative accuracy is presented in Fig. 4.77. Note that the plot is restricted to the interval $x_2 \in [0.005, 0.8]$ because the DSMC results do not allow one a stable computation of the confidence bands behind this point. Thus the DSMC scheme is again slightly better in the "high" density region, while it becomes unacceptable for $x_2 > 0.8$.

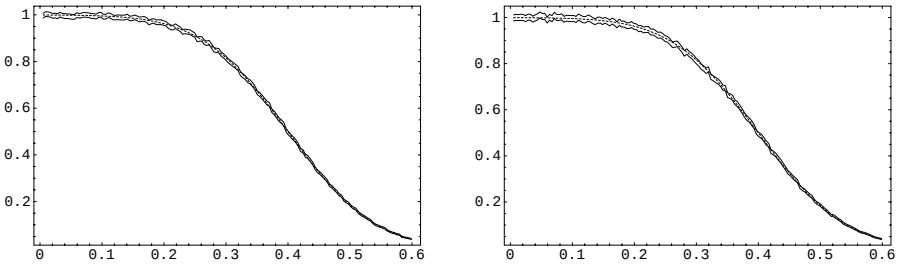

Fig. 4.75. "High" density region, Mach = 7.0

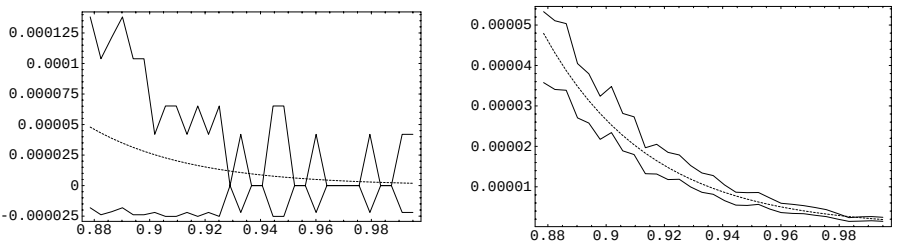

Fig. 4.76. "Low" density region, Mach = 7.0

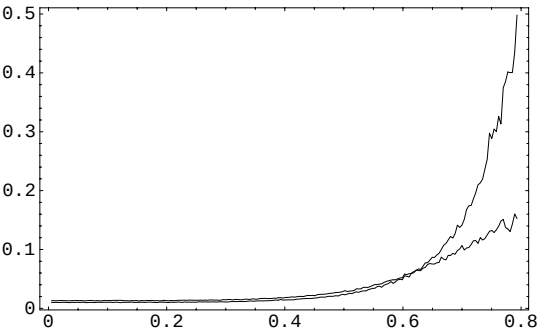

Fig. 4.77. The relative accuracy, Mach = 7.0

Mach number 10

Finally we choose the inflow Mach number equal to 10.0. Fig. 4.78 shows the analytic expression for the density (4.70) (thick dashed line) and the confidence bands (thin lines) of the numerical solutions on the interval $x_2 \in [0.005, 0.6]$. The DSMC results (left plot) were obtained using 10 000 smoothing steps while the SWPM results (right plot) were obtained using 1 000 smoothing steps. We see very good agreement of the numerical and the analytic solution in the "high" density region. Fig. 4.79 illustrates the same values in the "low" density region $x_2 \in [0.88, 0.995]$ but only for SWPM. The DSMC results were identical to zero there. The confidence band of SWPM is still rather good. The relative accuracy is presented in the Fig. 4.80. The plot is restricted to the interval $x_2 \in [0.005, 0.7]$ because the DSMC error reaches the 100% level at 0.7. There are no stable DSMC results behind this point and the computation of the confidence bands is not possible. Thus we have illustrated how an extremely low density can be resolved using weighted particles.

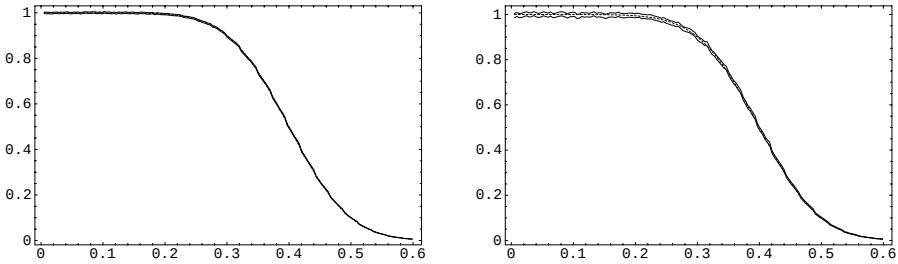

Fig. 4.78. "High" density region, Mach = 10.0

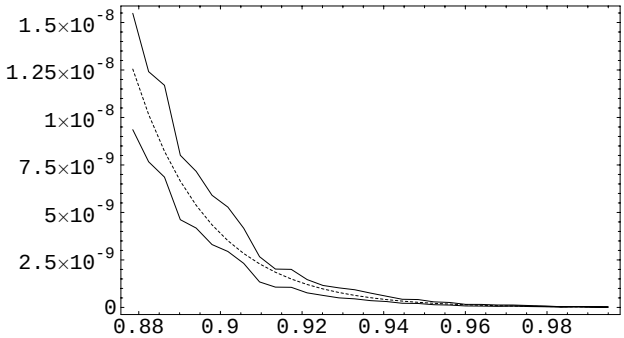

Fig. 4.79. "Low" density region, Mach = 10.0

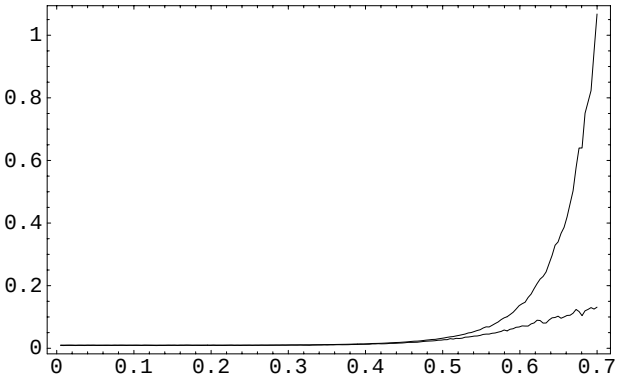

Fig. 4.80. The relative accuracy, Mach = 10.0

4.6.2 Case with collisions

Here we assume absorption of particles on the top part of the boundary and consider the Knudsen number $\mathrm{Kn} = 0.05$. In this case there is no analytic information available. In Fig. 4.81 we show the density profile on the whole interval $x_2 \in [0.005, 0.995]$. Here the thick dashed line represents the course of the analytic solution (4.70) (i.e. the situation for $\mathrm{Kn} = \infty$) while the thin lines represent the confidence bands obtained using DSMC. These results correspond to the rather low inflow Mach number $\mathrm{Mach} = 1.0$ to make the deviation from the collisionless case visible. The difference becomes smaller for higher Mach numbers.

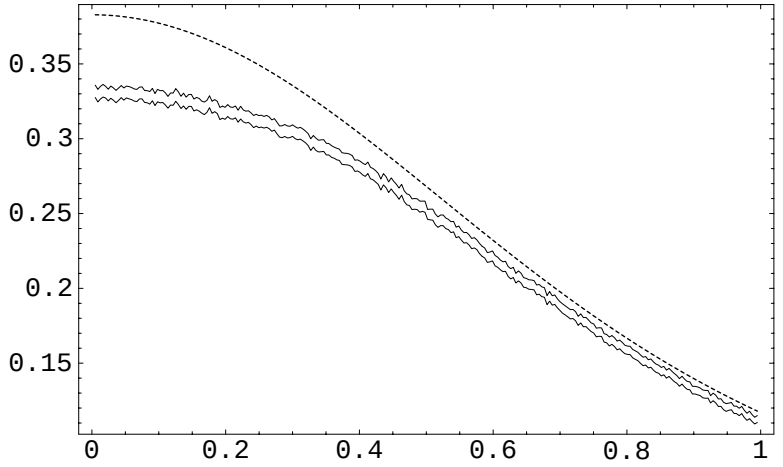

Fig. 4.81. The course of the density, Mach = 1.0

It is clear that collisions reduce the effect of artificial particles generated according to the auxiliary stream. On their way these particles collide and change their velocities so that not all of them will reach the desired region of low density. However, for a high Mach number, there is still considerable efficiency gain achieved by SWPM as the following examples show.

Mach number 7

First we choose the inflow Mach number in (4.62) equal to 7.0. Fig. 4.82 shows the confidence bands for DSMC (thin lines) and SWPM (thick lines). The left plot shows the situation in the "high" density region $x_2 \in [0.005, 0.6]$. The low density region $x_2 \in [0.88, 0.995]$ is presented in the right plot. Thus we see a considerable advantage of SWPM when computing small functionals.

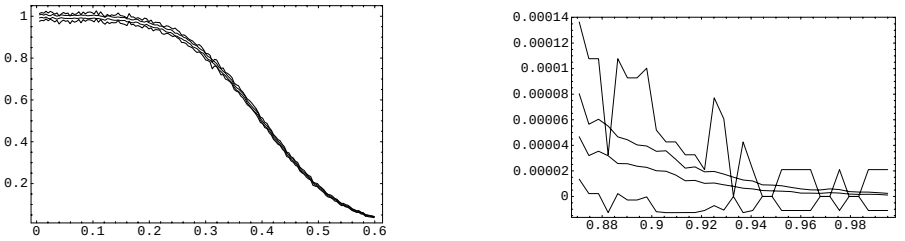

Fig. 4.82. The course of the density, Mach = 7

Mach number 10

Now we choose the inflow Mach number equal to 10.0 . In this case no stable results in the low density region $x_2 \in [0.88, 0.95]$ could be obtained using DSMC, even with 10 times more computational time compared with SWPM. In this sense the situation is similar to the collisionless case. The numerical results for SWPM are shown in Fig. 4.83. The empirical mean value of the density is represented with a thick dashed line while the thin lines correspond to the confidence bands. The left plot shows the situation in the "high" density region $x_2 \in [0.005, 0.6]$. The low density region $x_2 \in [0.88, 0.995]$ is presented in the right plot. The results obtained using SWPM are not as good as in the collisionless case (there are some considerable fluctuations). However the small values of the density are resolved.

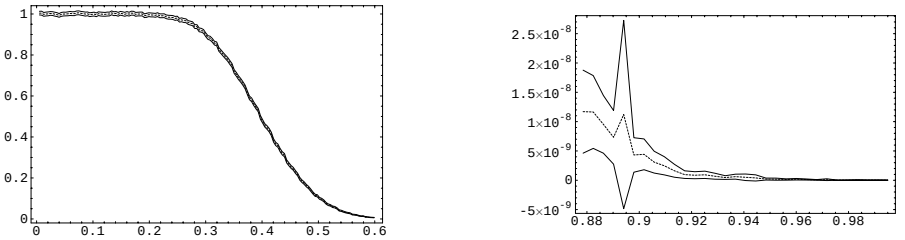

Fig. 4.83. The course of the density, Mach = 10

4.6.3 Influence of a hot wall

Here we assume diffuse reflection (1.38) of particles on the top part of the boundary, with a boundary Maxwellian

$$M_{\Gamma_t}(v) = \frac{1}{2\pi\,(T_t)^2} \exp\left(-\frac{|v|^2}{2\,T_t}\right)$$

having constant temperature $T_t = 300.0$. The inflow Mach number in (4.62) is chosen equal to 5.0. The number of averaging time steps after reaching the "steady-state" situation was 10 000.

We first consider the collisionless case. Figs. 4.84-4.87 show on the left the contour plots of the density, of the Mach number, of the temperature and of the criteria of the local thermal equilibrium while the right plots show the absolute values of these quantities plotted along the axis of symmetry $x_2 = 0$. The picture of the flow changes if we consider the Knudsen number $\mathrm{Kn} = 0.05$. The corresponding results are shown in Figs. 4.88–4.91. Now the influence of the hot top on the flow values at the left boundary is almost negligible. Instead there is a clear maximum of the density in the middle of the domain. In the same region the temperature reaches its maximum.

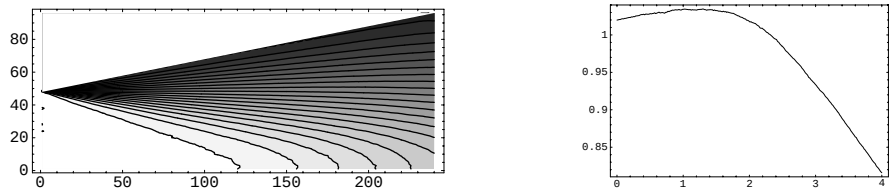

Fig. 4.84. Density, $\mathrm{Kn} = \infty$

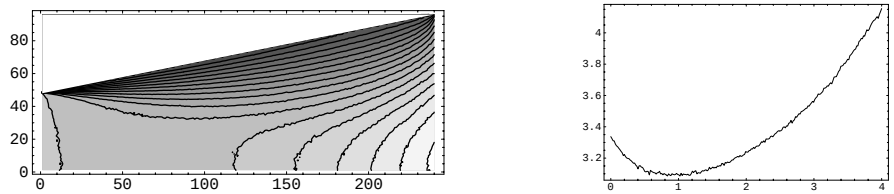

Fig. 4.85. Mach number, $\mathrm{Kn} = \infty$

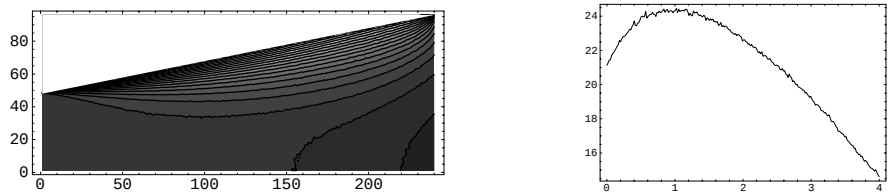

Fig. 4.86. Temperature, $\mathrm{Kn} = \infty$

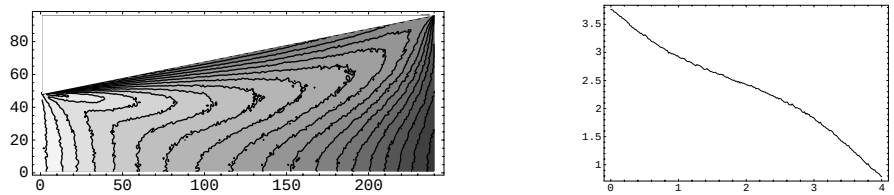

Fig. 4.87. Criteria of local thermal equilibrium, Kn = ∞

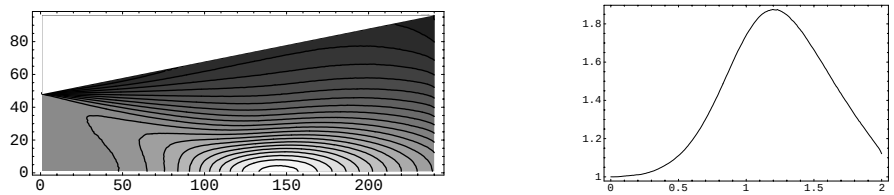

Fig. 4.88. Density, Kn = 0.05

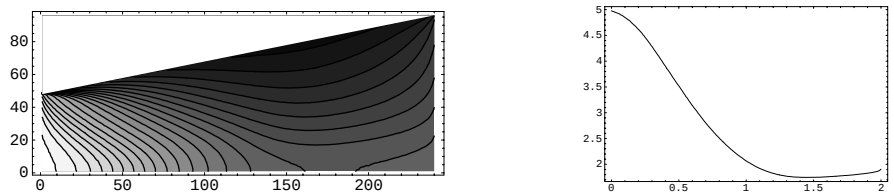

Fig. 4.89. Mach number, Kn = 0.05

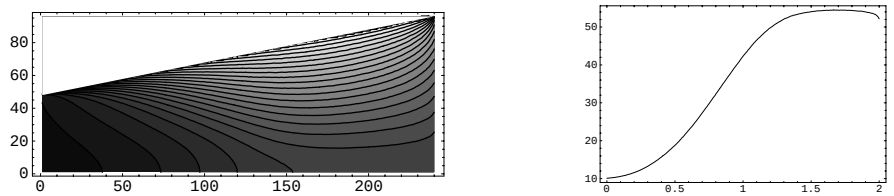

Fig. 4.90. Temperature, Kn = 0.05

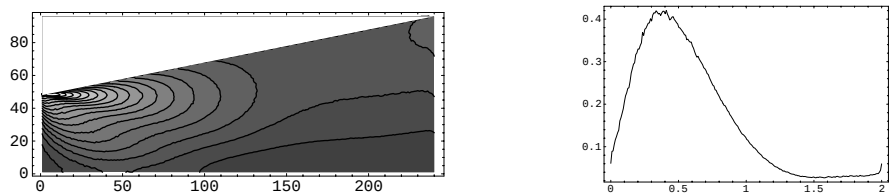

Fig. 4.91. Criteria of local thermal equilibrium, Kn = 0.05

4.6.4 Bibliographic remarks

The example considered in this section was motivated by the problem of supersonic molecular beam skimmers first studied in [22]. Further investigations related to this problem can be found in [39]. The geometry of Fig. 4.71 was considered in [181]. Though the example is extremely simplified, the results obtained so far are just a preliminary step.

A

Auxiliary results

A.1 Properties of the Maxwell distribution

Here we collect some analytic formulas for functionals of the Maxwell distribution. These functionals are expressed in terms of the following functions. The **gamma function** is defined as

$$\Gamma(s) = \int_0^\infty x^{s-1}\, e^{-x}\, dx\,, \qquad s > 0\,, \tag{A.1}$$

and has the properties

$$\begin{aligned} &\Gamma(s) = (s-1)\,\Gamma(s-1)\,, \quad s > 1\,, \\ &\Gamma(1) = 1\,, \quad \Gamma(0.5) = \sqrt{\pi}\,. \end{aligned} \tag{A.2}$$

The **error function** is defined as

$$\begin{aligned} \mathrm{erf}(y) &= \frac{2}{\sqrt{\pi}} \int_0^y \exp(-z^2)\, dz\,, \qquad y \geq 0\,, \\ \mathrm{erf}(y) &= -\mathrm{erf}(-y)\,, \qquad y < 0\,. \end{aligned} \tag{A.3}$$

It satisfies $\mathrm{erf}(\infty) = 1$.

Lemma A.1. *For any $\alpha > -3$, the following holds*

$$G(\alpha) := \int_{\mathbb{R}^3} |v|^\alpha\, M_{0,1}(v)\, dv = \frac{2^{\frac{\alpha+2}{2}}}{\sqrt{\pi}}\, \Gamma\left(\frac{\alpha+3}{2}\right). \tag{A.4}$$

If $\alpha = 2n$, $n = 1, 2, \dots$, then (A.4) takes the form

$$G(2n) = \frac{2^{n+1}}{\sqrt{\pi}}\, \frac{2n+1}{2}\, \cdots\, \frac{1}{2}\, \Gamma\left(\frac{1}{2}\right) = \prod_{l=0}^{n-1} (3 + 2\,l)\,.$$

In particular, one obtains

$$G(2) = 3\,, \qquad G(4) = 15\,, \qquad G(6) = 105\,, \qquad G(8) = 945\,. \tag{A.5}$$

Proof. Switching to spherical coordinates and using the substitution $r = \sqrt{2x}$, one obtains

$$\begin{aligned} G(\alpha) &= \int_0^\infty r^\alpha \, \frac{1}{(2\pi)^{3/2}} \, \exp(-r^2/2) \, r^2 \, (4\pi) \, dr \\ &= 2^{-\frac{3}{2}+2+\frac{\alpha+2}{2}-\frac{1}{2}} \, \pi^{-\frac{3}{2}+1} \int_0^\infty x^{\frac{\alpha+1}{2}} \, e^{-x} \, dx \end{aligned}$$

so that (A.4) follows from (A.1). ∎

Further moments of the Maxwell distribution are

$$\int_{\mathbb{R}^3} |v|^\alpha \, M_{0,T}(v) \, dv = T^{\alpha/2} \, G(\alpha) \,, \tag{A.6}$$

and

$$\int_{\mathbb{R}^3} v v^\mathsf{T} \, M_{V,T}(v) \, dv = T \, I + V V^\mathsf{T} \,, \tag{A.7a}$$

$$\int_{\mathbb{R}^3} v |v|^2 \, M_{V,T}(v) \, dv = (5T + |V|^2) V \,, \tag{A.7b}$$

$$\int_{\mathbb{R}^3} |v|^4 \, M_{V,T}(v) \, dv = |V|^4 + 15 \, T^2 + 10 \, T \, |V|^2 \,. \tag{A.7c}$$

Lemma A.2. *For any $e \in \mathcal{S}^2$, the following holds*

$$\begin{aligned} &\int_{(v,e)>0} M_{V,T}(v) \, (v,e) \, dv = \\ &\sqrt{\frac{T}{2\pi}} \, \exp\left(-\frac{(V,e)^2}{2\,T} \right) + \frac{(V,e)}{2} \left[1 + \operatorname{erf}\left(\frac{(V,e)}{\sqrt{2\,T}} \right) \right] . \end{aligned} \tag{A.8}$$

If $(V,e) = 0$, then (A.8) takes the form

$$\int_{(v,e)>0} M_{V,T}(v) \, (v,e) \, dv = \sqrt{\frac{T}{2\pi}}$$

and the appropriate normalization factor is

$$\frac{1}{(2\pi T)^{3/2}} \, \sqrt{\frac{2\pi}{T}} = \frac{1}{2\pi T^2} \,.$$

Proof. Using the substitution

$$v = V + \sqrt{2\,T} \, \tilde{v} \,, \qquad dv = (2\,T)^{3/2} d\tilde{v}$$

as well as a rotation of the coordinate system such that e becomes the first basis vector, one obtains

$$\int\limits_{(v,e)>0} M_{V,T}(v)\,(v,e)\,dv = \frac{\sqrt{2\,T}}{\pi^{3/2}} \int\limits_{(\tilde v,e)>-a} \Big[a + (\tilde v,e)\Big] \exp(-|\tilde v|^2) d\tilde v$$

$$= \frac{\sqrt{2\,T}}{\pi^{3/2}} \int\limits_{\xi_1>-a} (a+\xi_1) \exp(-\xi_1^2) d\xi_1 \int\limits_{\mathbb{R}^2} \exp(-\xi_2^2-\xi_3^2) d\xi_2\, d\xi_3 \qquad \text{(A.9)}$$

$$= \sqrt{\frac{2\,T}{\pi}} \int\limits_{-\infty}^{a} (a-z)\, \exp(-z^2)\, dz\,, \qquad \text{where} \quad a = \frac{(V,e)}{\sqrt{2\,T}}\,.$$

Since

$$\int\limits_{-\infty}^{y} (a-z)\, \exp(-z^2)\, dz = a\,\frac{\sqrt{\pi}}{2}\Big[1+\operatorname{erf}(y)\Big] + \frac{1}{2}\,\exp(-y^2)\,, \qquad \text{(A.10)}$$

for any $y \le a$, assertion (A.8) follows from (A.9). ∎

Finally, tails of the Maxwell distribution take the form (cf. (A.3))

$$\operatorname{Tail}_{V,T}(U,R) := \int\limits_{|v-U|\ge R} M_{V,T}(v)\, dv \qquad \text{(A.11)}$$

$$= 1 + \frac{1}{2}\left(\operatorname{erf}\Big(\frac{a-b}{\sqrt{2}}\Big) - \operatorname{erf}\Big(\frac{a+b}{\sqrt{2}}\Big)\right) + \frac{1}{\sqrt{2\,\pi}\,a}\left(\exp\Big(-\frac{(a-b)^2}{2}\Big) - \exp\Big(-\frac{(a+b)^2}{2}\Big)\right),$$

where

$$a = \frac{|V-U|}{\sqrt{T}}\,, \qquad b = \frac{R}{\sqrt{T}}\,.$$

If the tail functional is centered, i.e. $U = V$, then one obtains

$$\operatorname{Tail}_{V,T}(V,R) = \lim_{U\to V} \operatorname{Tail}_{V,T}(U,R) = 1 - \operatorname{erf}\Big(\frac{b}{\sqrt{2}}\Big) + \frac{2}{\sqrt{\pi}}\, b\, \exp\Big(-\frac{b^2}{2}\Big)\,. \qquad \text{(A.12)}$$

A.2 Exact relaxation of moments

Here we consider the spatially homogeneous Boltzmann equation (4.1) with constant collision kernel (4.3). Following the paper [33], we find analytic expressions for the relaxation of the moments (4.8a)-(4.8c) of the solution. We use the notations (4.5)-(4.7) and assume $\varrho = 1$.

Lemma A.3. *The moments (4.8a)-(4.8c) satisfy the system of ordinary differential equations (cf. (1.89))*

$$\frac{d}{dt}\,M(t) = -\frac{1}{2}\,M(t) + \frac{1}{2}\Big(T\,I + VV^{\mathsf{T}}\Big)\,, \tag{A.13a}$$

$$\frac{d}{dt}\,r(t) = -\frac{1}{3}\,r(t) + \frac{2}{3}\Big(3\,T + |V|^2\Big)V - \frac{1}{3}\,M(t)V\,, \tag{A.13b}$$

$$\frac{d}{dt}\,s(t) = -\frac{1}{3}\,s(t) + \frac{2}{3}\Big(3T + |V|^2\Big)^2 - \frac{1}{3}\,||M(t)||_F^2\,. \tag{A.13c}$$

Proof. The derivation uses the weak form of the Boltzmann collision integral (cf. Lemma 1.11)

$$\int\limits_{\mathbb{R}^3} g(v)\,Q(f,f)(v)\,dv = \tag{A.14}$$
$$\frac{1}{2}\int\limits_{\mathbb{R}^3}\int\limits_{\mathbb{R}^3} f(v)f(w)\frac{1}{4\pi}\int\limits_{\mathcal{S}^2}\Big(g(v') + g(w') - g(v) - g(w)\Big)\,de\,dw\,dv\,,$$

where $Q(f,f)(v)$ denotes the right-hand side of equation (4.1) and v', w' are the post-collision velocities (1.6). First we consider the test function $g(v) = vv^{\mathsf{T}}$. Using the property

$$\frac{1}{4\pi}\int\limits_{\mathcal{S}^2} ee^{\mathsf{T}}\,de = \frac{1}{3}\,I$$

we compute the average over the unit sphere in (A.14) and obtain

$$\frac{1}{4\pi}\int\limits_{\mathcal{S}^2}\Big(v'(v')^{\mathsf{T}} + w'(w')^{\mathsf{T}} - vv^{\mathsf{T}} - ww^{\mathsf{T}}\Big)\,de =$$
$$-\frac{1}{2}\Big(vv^{\mathsf{T}} + ww^{\mathsf{T}} + vw^{\mathsf{T}} + wv^{\mathsf{T}}\Big) + \frac{1}{6}\Big(|v|^2 + |w|^2 - 2(v,w)\Big)\,I\,.$$

The conservation property

$$\int\limits_{\mathbb{R}^3} |v|^2 f(t,v)\,dv = 3\,T + |V|^2$$

implies then

$$\int\limits_{\mathbb{R}^3} vv^{\mathsf{T}} Q(f,f)(v)\,dv = -\frac{1}{2}M(t) + \frac{1}{2}\Big(T\,I + VV^{\mathsf{T}}\Big)\,. \tag{A.15}$$

Averaging $g(v) = v|v|^2$ over the unit sphere leads to

$$\frac{1}{4\pi}\int\limits_{\mathcal{S}^2}\Big(v'|v'|^2+w'|w'|^2-v|v|^2-w|w|^2\Big)\,de=$$
$$-\frac{1}{3}\Big(v|v|^2+w|w|^2+(v,w)(v+w)\Big)+\frac{2}{3}\Big(v|w|^2+w|v|^2\Big)$$

and

$$\int\limits_{\mathbb{R}^3} v|v|^2Q(f,f)(v)\,dv=-\frac{1}{3}r(t)+\frac{2}{3}\Big(3\,T+|V|^2\Big)\,V-\frac{1}{3}M(t)V\,. \tag{A.16}$$

Finally, using the test function $g(v)=|v|^4$ gives

$$\frac{1}{4\pi}\int\limits_{\mathcal{S}^2}\Big(|v'|^4+|w'|^4-|v|^4-|w|^4\Big)\,de=$$
$$-\frac{1}{3}\Big(|v|^4+|w|^4+2(v,w)^2\Big)+\frac{4}{3}\,|v|^2|w|^2$$

and

$$\int\limits_{\mathbb{R}^3}|v|^4Q(f,f)(v)\,dv=-\frac{1}{3}s(t)+\frac{2}{3}\Big(3\,T+|V|^2\Big)^2-\frac{1}{3}||M(t)||_F^2\,. \tag{A.17}$$

The assertion follows from the Boltzmann equation and the properties (A.15)-(A.17). ∎

The linear system (A.13a)-(A.13c) can be solved explicitly and the solution takes the form

$$M(t)=M_0\,e^{-t/2}+\Big(T\,I+VV^{\mathsf{T}}\Big)\Big(1-e^{-t/2}\Big)\,, \tag{A.18a}$$
$$r(t)=r_0\,e^{-t/3}+\Big(5\,T+|V|^2\Big)\,V\,\Big(1-e^{-t/3}\Big) \tag{A.18b}$$
$$+2\Big(M_0-VV^{\mathsf{T}}-T\,I\Big)\,V\,\Big(e^{-t/2}-e^{-t/3}\Big)\,,$$
$$s(t)=s_0\,e^{-t/3}+\Big(|V|^4+15\,T^2+10\,T\,|V|^2\Big)\Big(1-e^{-t/3}\Big) \tag{A.18c}$$
$$+\frac{1}{2}\Big(||M_0||_F^2-3\,T^2+|V|^4-2(M_0V,V)\Big)\Big(e^{-t}-e^{-t/3}\Big)$$
$$+4\,\Big((M_0V,V)-|V|^4-T\,|V|^2\Big)\Big(e^{-t/2}-e^{-t/3}\Big),$$

where

$$M_0=\int\limits_{\mathbb{R}^3}vv^{\mathsf{T}}\,f_0(v)\,dv\,,\qquad r_0=\int\limits_{\mathbb{R}^3}v|v|^2\,f_0(v)\,dv\,,\qquad s_0=\int\limits_{\mathbb{R}^3}|v|^4\,f_0(v)\,dv$$

are the corresponding moments of the initial distribution f_0 of the Boltzmann equation. Formulas (A.18a)-(A.18c) are extremely useful for numerical tests

because they provide the explicit time evolution of moments of the solution of the Boltzmann equation for any initial condition. Furthermore, they allow us to obtain an analytic expression for the function (4.9) representing a criterion for thermal local equilibrium. The terms (4.10a)-(4.10c) satisfy

$$\tau(t) = M(t) - \Big(VV^{\mathsf{T}} + T\,I\Big)\,, \tag{A.19}$$

$$\begin{aligned} q(t) &= \frac{1}{2}\Big(r(t) - 2\,M(t)V + |V|^2\,V - 3\,T\,V\Big) \\ &= \frac{1}{2}\Big(r(t) - (5\,T + |V|^2)\,V\Big) - \tau(t)\,V \end{aligned} \tag{A.20}$$

and

$$\begin{aligned} \gamma(t) &= \int\limits_{\mathbb{R}^3} |v-V|^2\,|v|^2\,f(t,v)\,dv - 3\,T\,|V|^2 - 4\,\big(q(t),V\big) - 15\,T^2 \\ &= s(t) - 2\,\big(r(t),V\big) + |V|^2\Big(3\,T + |V|^2\Big) - 3\,T\,|V|^2 - 4\,\big(q(t),V\big) - 15\,T^2 \\ &= s(t) - \Big(|V|^4 + 15\,T^2 + 10\,T\,|V|^2\Big) - 4\,\big(\tau(t)V,V\big) - 8\,\big(q(t),V\big)\,. \end{aligned} \tag{A.21}$$

Note that $w\,\big(v,V\big) = w\,v^{\mathsf{T}}\,V$ and $|v-V|^2 = |v|^2 - |V|^2 - 2\big(v-V,V\big)$. According to (A.18a)-(A.18c), we conclude from (A.19)-(A.21) that

$$\tau(t) = \Big(M_0 - VV^{\mathsf{T}} - T\,I\Big)e^{-t/2}\,, \tag{A.22}$$

$$\begin{aligned} q(t) &= \frac{1}{2}\Big(r_0 - (5\,T + |V|^2)V\Big)e^{-t/3} + \\ &\quad \Big(M_0 - VV^{\mathsf{T}} - T\,I\Big)\,V\,\Big(e^{-t/2} - e^{-t/3}\Big) - \Big(M_0 - VV^{\mathsf{T}} - T\,I\Big)V\,e^{-t/2} \\ &= \frac{1}{2}\Big(r_0 - 2\,M_0V + (|V|^2 - 3\,T)\,V\Big)e^{-t/3} \end{aligned} \tag{A.23}$$

and

$$\begin{aligned} \gamma(t) &= \Big(s_0 - |V|^4 - 15\,T^2 - 10\,T\,|V|^2\Big)e^{-t/3} + \\ &\quad \frac{1}{2}\Big(||M_0||_F^2 - 3\,T^2 + |V|^4 - 2\,\big(M_0V,V\big)\Big)\Big(e^{-t} - e^{-t/3}\Big) + \\ &\quad 4\,\Big(\big(M_0V,V\big) - |V|^4 - T\,|V|^2\Big)\Big(e^{-t/2} - e^{-t/3}\Big) - \\ &\quad 4\Big(\big(M_0V,V\big) - |V|^4 - T\,|V|^2\Big)e^{-t/2} - \\ &\quad 4\Big(\big(r_0,V\big) - 2\,\big(M_0V,V\big) + (|V|^2 - 3\,T)\,|V|^2\Big)e^{-t/3} \\ &= \frac{1}{2}\Big(2\,s_0 - 3\,|V|^4 - 27\,T^2 + 12\,T\,|V|^2 - ||M_0||_F^2 + \end{aligned}$$

$$10\,(M_0V,V) - 8\,(r_0,V)\Big)e^{-t/3} + \tag{A.24}$$
$$\frac{1}{2}\Big(||M_0||_F^2 - 3\,T^2 + |V|^4 - 2\,(M_0V,V)\Big)e^{-t}\,.$$

A.3 Properties of the BKW solution

Here we consider the spatially homogeneous Boltzmann equation (4.1) with the collision kernel

$$B(v,w,e) = \tilde{B}(\cos(\theta))\,, \qquad \cos(\theta) = \frac{(v-w,e)}{|v-w|}\,,$$

where

$$\int\limits_{\mathcal{S}^2} \tilde{B}\left(\frac{(v-w,e)}{|v-w|}\right) de < \infty\,,$$

and study the famous exact solution found by Bobylev [27] and Krook and Wu [115]. We look for a solution in the form

$$f(t,v) = \big(a + b|v|^2\big)e^{-c|v|^2}, \tag{A.25}$$

where the parameters a, b and c are functions of the time variable t. Since the bulk velocity satisfies $V(t) = 0$ by symmetry, there are only two conserved physical quantities of the solution (A.25), namely the density $\varrho(t)$ and the temperature $T(t)$. This fact provides two equations for the unknown parameters a, b, c. Using the substitution $\sqrt{2c}\,w = w'$ one obtains (cf. (A.4), (A.5))

$$\int\limits_{\mathbb{R}^3} e^{-c|w|^2} dw = \frac{1}{(2c)^{3/2}}\,(2\pi)^{3/2}\,G(0) = \pi^{3/2}\frac{1}{c^{3/2}}\,,$$
$$\int\limits_{\mathbb{R}^3} |w|^2 e^{-c|w|^2} dw = \frac{1}{(2c)^{5/2}}\,(2\pi)^{3/2}\,G(2) = \frac{3\pi^{3/2}}{2}\frac{1}{c^{5/2}}\,,$$
$$\int\limits_{\mathbb{R}^3} |w|^4 e^{-c|w|^2} dw = \frac{1}{(2c)^{7/2}}\,(2\pi)^{3/2}\,G(4) = \frac{15\pi^{3/2}}{4}\frac{1}{c^{7/2}}$$

so that

$$\varrho(t) = \int\limits_{\mathbb{R}^3} f(t,v)\,dv = \frac{\pi^{3/2}}{2}\frac{2ac+3b}{c^{5/2}} = \varrho \tag{A.27}$$

and

$$3\varrho\, T(t) = \int\limits_{\mathbb{R}^3} |v|^2\, f(t,v)\, dv = \frac{\pi^{3/2}}{4}\, \frac{2ac + 5b}{c^{7/2}} = 3\varrho\, T\,. \tag{A.28}$$

Using (A.27) and (A.28), we express the functions a and b in terms of ϱ, T and c,

$$a = \frac{1}{\pi^{3/2}}\, \varrho\, c^{3/2}(5/2 - 3Tc)\,, \qquad b = \frac{1}{\pi^{3/2}}\, \varrho\, c^{5/2}(2Tc - 1)\,, \tag{A.29}$$

so that the function (A.25) takes the form

$$f(t,v) = \frac{\varrho}{\pi^{3/2}} \Big(2T|v|^2 c^{7/2} - (3T + |v|^2) c^{5/2} + 5/2 c^{3/2} \Big) e^{-c|v|^2}\,. \tag{A.30}$$

Next we use the Boltzmann equation (4.1) to determine the remaining parameter c. The time derivative of the function (A.30) is

$$\frac{\partial}{\partial t} f = \frac{\varrho}{\pi^{3/2}} c^{1/2}(1 - 2Tc) \Big(c^2|v|^4 - 5c|v|^2 + 15/4 \Big) e^{-c|v|^2}\, \frac{dc}{dt}\,. \tag{A.31}$$

We denote the right-hand side of equation (4.1) by $Q(f,f)$ and compute this collision integral for the function (A.25). First, using conservation of energy during a collision, we get

$$f(v')f(w') - f(v)f(w) = b^2 \big(|v'|^2 |w'|^2 - |v|^2 |w|^2 \big) e^{-c\left(|v|^2 + |w|^2\right)}\,.$$

Then, with the substitutions

$$U = \frac{1}{2}\big(v + w\big)\,, \qquad u = v - w\,,$$

we obtain

$$|v'|^2|w'|^2 - |v|^2|w|^2 = \big(U,u\big)^2 - |u|^2 \big(U,e\big)^2 = \big(U,u\big)^2 - |u|^2 U^{\mathsf{T}} e e^{\mathsf{T}} U\,.$$

Thus the integral over the unit sphere leads to

$$e^{-c\left(|v|^2 + |w|^2\right)} \int\limits_{\mathcal{S}^2} \tilde{B}\left(\frac{(u,e)}{|u|} \right) \Big(\big(U,u\big)^2 - |u|^2 U^{\mathsf{T}} e e^{\mathsf{T}} U \Big)\, de\,.$$

This integral can be computed using spherical coordinates related to the direction of the vector u. The result is

$$\begin{aligned} &\alpha\, e^{-c\left(|v|^2 + |w|^2\right)} \Big(3\big(U,u\big)^2 - |u|^2 |U|^2 \Big) = \\ &\frac{\alpha}{2}\, e^{-c\left(|v|^2 + |w|^2\right)} \Big(|v|^4 + |w|^4 - 4|v|^2|w|^2 + 2v^{\mathsf{T}}\, w w^{\mathsf{T}}\, v \Big), \end{aligned}$$

where

$$\alpha = \pi \int_0^\pi \tilde{B}(\cos\theta) \sin^3\theta \, d\theta \,. \tag{A.32}$$

Integrating the last expression with respect to w over $\mathbb{R}^3$ we get the final result

$$Q(f,f) = b^2 \frac{\alpha}{2} \pi^{3/2} \frac{1}{c^{7/2}} \Big(c^2 |v|^4 - 5c|v|^2 + 15/4 \Big) e^{-c|v|^2} \,. \tag{A.33}$$

Equating (A.31) and (A.33) and using (A.29), one obtains the differential equation for the function c

$$\frac{dc}{dt} = -\frac{\alpha}{2} \, \varrho \, (2Tc - 1) \, c \,.$$

Using the substitution $2Tc - 1 = \beta$ we get

$$\frac{d\beta}{dt} = -\frac{\alpha}{2} \, \varrho \, \beta \, (\beta + 1)$$

and finally

$$\beta(t) = \frac{\beta_0 \, e^{-\alpha \, \varrho \, t/2}}{1 + \beta_0 \, (1 - e^{-\alpha \, \varrho \, t/2})} \,, \tag{A.34}$$

where β_0 denotes the initial value for the function β and α is defined in (A.32). Putting $c = (\beta + 1)/(2T)$ into (A.30) we obtain

$$f(t,v) = \tag{A.35}$$
$$\frac{\varrho}{(2\pi T)^{3/2}} (\beta(t) + 1)^{3/2} \left(1 + \beta(t) \Big(\frac{\beta(t) + 1}{2T} |v|^2 - \frac{3}{2} \Big) \right) e^{-\frac{\beta(t)+1}{2T} |v|^2} \,.$$

This solution is non-negative for

$$0 \le \beta_0 \le 2/3 \,. \tag{A.36}$$

In the following we derive explicit expressions for certain functionals of the solution (A.35), which are useful for numerical tests. We assume $\varrho = 1$. Introducing the notation $T_\beta = T/(\beta + 1)$ and taking into account (A.6) and (A.4), one obtains

$$\begin{aligned}
&\int_{\mathbb{R}^3} |v|^\alpha \, f(t,v) \, dv = \\
&\qquad \left(1 - \frac{3}{2} \, \beta \right) \int_{\mathbb{R}^3} |v|^\alpha \, M_{0,T_\beta}(v) \, dv + \frac{\beta}{2T_\beta} \int_{\mathbb{R}^3} |v|^{\alpha+2} \, M_{0,T_\beta}(v) \, dv \\
&= \left(1 - \frac{3}{2} \, \beta \right) T_\beta^{\frac{\alpha}{2}} \, \frac{2^{\frac{\alpha+2}{2}}}{\sqrt{\pi}} \, \Gamma\left(\frac{\alpha+3}{2} \right) + \frac{\beta}{2T_\beta} \, T_\beta^{\frac{\alpha+2}{2}} \, \frac{2^{\frac{\alpha+4}{2}}}{\sqrt{\pi}} \, \Gamma\left(\frac{\alpha+5}{2} \right) \\
&= \frac{1}{\sqrt{\pi}} \, (2\,T_\beta)^{\frac{\alpha}{2}} \, \Gamma\left(\frac{\alpha+3}{2} \right) \Big(2 - 3\beta + \beta(\alpha+3) \Big) .
\end{aligned}$$

Thus, power functionals of the solution (A.35) take the form

$$\int\limits_{\mathbb{R}^3} |v|^\alpha f(t,v)\,dv = \frac{1}{\sqrt{\pi}}\,(2\,T)^{\alpha/2}\,\Gamma\Big(\frac{\alpha+3}{2}\Big)\frac{\alpha\,\beta+2}{(\beta+1)^{\alpha/2}}\,,$$

where $\alpha > -3$ and $\beta = \beta(t)$ is defined in (A.34). If $\alpha = m \in \mathbb{N}$ then one obtains using (A.2)

$$\int\limits_{\mathbb{R}^3} |v|^m f(t,v)\,dv = \begin{cases} \frac{1}{\sqrt{\pi}}\,(k+1)!\,\Big(\frac{\beta+1}{2\,T}\Big)^{-m/2}\big(m\,\beta+2\big), & m = 2\,k+1\,, \\ \big(2\,k+1\big)!!\,\Big(\frac{\beta+1}{T}\Big)^{-k}\big(k\,\beta+1\big), & m = 2\,k\,. \end{cases} \tag{A.37}$$

Furthermore, we derive an analytic expression for the function (4.9) representing a criterion of local thermal equilibrium. Since by symmetry (cf. (4.8a)-(4.8c)) $V = 0\,,\ M(t) = T\,I\,,\ r(t) = 0$ and according to (A.37)

$$s(t) = \int\limits_{\mathbb{R}^3} |v|^4 f(t,v)\,dv = 15\,T^2\,\frac{2\beta+1}{(\beta+1)^2}\,,$$

the terms (4.10a)-(4.10c) satisfy

$$\tau(t) = 0\,, \quad q(t) = 0\,, \quad \gamma(t) = -15\,T^2\left(\frac{\beta}{\beta+1}\right)^2$$

so that the function (4.9) takes the form

$$Crit(t) = \sqrt{\frac{15}{8}}\left(\frac{\beta}{\beta+1}\right)^2. \tag{A.38}$$

Finally, tail functionals (4.11) of the solution (A.35) take the form (cf. (A.3)),

$$\mathrm{Tail}(R,t) = \tag{A.39}$$
$$1 + \frac{2}{\sqrt{\pi}}\sqrt{\frac{\beta+1}{2\,T}}R\Big(1+\beta R^2\frac{\beta+1}{2\,T}\Big)\exp\Big(-\frac{\beta+1}{2\,T}\,R^2\Big) - \mathrm{erf}\Big(\sqrt{\frac{\beta+1}{2\,T}}\,R\Big).$$

A.4 Convergence of random measures

Here we collect some convergence properties of random measures. We consider the space $Z = D \times \mathbb{R}^3$ and the metric ϱ_L defined in (3.153). Let $\nu^{(n)}$ be a sequence of random measures such that

$$\nu^{(n)}(Z) \le C \quad \text{a.s.} \tag{A.40}$$

and ν be a deterministic finite measure on Z.

Lemma A.4. *The following conditions are equivalent:*

(i) $\lim\limits_{n\to\infty} \mathbb{E}\,\varrho_L(\nu^{(n)},\nu) = 0$

(ii) $\varrho_L(\nu^{(n)},\nu) \to 0$ *in probability*

(iii) $\langle\varphi,\nu^{(n)}\rangle \to \langle\varphi,\nu\rangle$ *in probability,*
for any continuous bounded function φ

(iv) $\langle\varphi,\nu^{(n)}\rangle \to \langle\varphi,\nu\rangle$ *in probability,*
for any measurable bounded function φ *such that* $\nu(\mathcal{D}(\varphi)) = 0$,

where $\mathcal{D}(\varphi)$ *denotes the set of discontinuity points of the function* φ.

Lemma A.4 was proved in [204, Cor. 3.5].

Corollary A.5 *Let the measure* ν *be absolutely continuous with respect to Lebesgue measure. Then the following conditions are equivalent:*

(i) $\varrho_L(\nu^{(n)},\nu) \to 0$ *in probability*

(ii) $\varrho_L(\nu_l^{(n)},\nu_l) \to 0$ *in probability,* $\forall\, l = 1,\dots,l_c$,

where $\nu_l^{(n)}, \nu_l$ *denote the restrictions of the measures* $\nu^{(n)}, \nu$ *to the sets* $D_l \times \mathbb{R}^3$ *(cf. (3.58)).*

Lemma A.6. *Let* ξ_n *be a sequence of random variables. If*

$$\lim_{n\to\infty} \mathbb{E}\,\xi_n = a \in (-\infty,\infty) \quad \textit{and} \quad \lim_{n\to\infty} \operatorname{Var}\xi_n = 0 \tag{A.41}$$

then

$$\xi_n \to a \quad \textit{in probability.} \tag{A.42}$$

If

$$\sup_n |\xi_n| \le c < \infty \quad \textit{a.s.}$$

then (A.42) implies (A.41).

Proof. The first assertion follows from

$$\begin{aligned}\operatorname{Prob}(|\xi_n - a| \ge \varepsilon) &\le \operatorname{Prob}(|\xi_n - \mathbb{E}\,\xi_n| + |\mathbb{E}\,\xi_n - a| \ge \varepsilon)\\ &\le \operatorname{Prob}(|\xi_n - \mathbb{E}\,\xi_n| \ge \varepsilon/2) \le \frac{2\operatorname{Var}\xi_n}{\varepsilon},\end{aligned}$$

where $\varepsilon > 0$ is arbitrary and n is sufficiently large. The estimates

$$|\mathbb{E}\,\xi_n - a| \le \mathbb{E}\,|\xi_n - a| \le (a+c)\operatorname{Prob}(|\xi_n - a| > \varepsilon) + \varepsilon$$

and

$$\begin{aligned}\operatorname{Var}\xi_n &= \mathbb{E}\,(\xi_n - a)^2 - (\mathbb{E}\,\xi_n - a)^2\\ &\le (a+c)^2\operatorname{Prob}(|\xi_n - a| > \varepsilon) + \varepsilon^2 - (\mathbb{E}\,\xi_n - a)^2\end{aligned}$$

imply the second assertion. ∎

Lemma A.7. *Let the measure ν be absolutely continuous with respect to Lebesgue measure. If*

$$\varrho_L(\nu^{(n)}, \nu) \to 0 \quad \textit{in probability} \tag{A.43}$$

then

$$\int_Z \int_Z \Phi(z, z_1)\, \nu^{(n)}(dz)\, \nu^{(n)}(dz_1) \to \int_Z \int_Z \Phi(z, z_1)\, \nu(dz)\, \nu(dz_1) \quad \textit{in probability,}$$

for any continuous bounded function Φ.

Proof. Consider a step function

$$\Phi_N(z, z_1) = \sum_{i=1}^{k_N} c_{N,i} \chi_{A_{N,i}}(z)\, \chi_{B_{N,i}}(z_1)\,,$$

where $N \geq 1$, $k_N \geq 1$ and $A_{N,i}, B_{N,i}$ are rectangles in Z. Denote

$$a^{(n)} = \left| \int_Z \int_Z \Phi(z, z_1)\, \nu^{(n)}(dz)\, \nu^{(n)}(dz_1) - \int_Z \int_Z \Phi(z, z_1)\, \nu(dz)\, \nu(dz_1) \right|$$

and

$$b^{(n)}_{R,N} = \left| \int_{Z_R} \int_{Z_R} \Phi_N(z, z_1)\, \nu^{(n)}(dz)\, \nu^{(n)}(dz_1) - \int_{Z_R} \int_{Z_R} \Phi_N(z, z_1)\, \nu(dz)\, \nu(dz_1) \right|,$$

where

$$Z_R = \{z \in Z \,:\, |z| \leq R\}\,, \qquad R > 0\,.$$

Using (A.43), (A.40), absolute continuity of ν, Lemma A.4 and Lemma A.6, one obtains

$$\lim_{n \to \infty} \mathbb{E}\, b^{(n)}_{R,N} = 0\,, \qquad \forall\, R, N\,, \tag{A.44}$$

and $\nu(Z) \leq C$. The triangle inequality implies

$$a^{(n)} \leq \left| \int_Z \int_Z \Phi(z, z_1)\, \nu^{(n)}(dz)\, \nu^{(n)}(dz_1) - \int_{Z_R} \int_{Z_R} \Phi(z, z_1)\, \nu^{(n)}(dz)\, \nu^{(n)}(dz_1) \right| + \left| \int_{Z_R} \int_{Z_R} \Phi(z, z_1)\, \nu^{(n)}(dz)\, \nu^{(n)}(dz_1) - \right.$$

$$\int_{Z_R}\int_{Z_R} \Phi_N(z,z_1)\,\nu^{(n)}(dz)\,\nu^{(n)}(dz_1)\Big| + b_{R,N}^{(n)} +$$
$$\left|\int_{Z_R}\int_{Z_R} \Phi_N(z,z_1)\,\nu(dz)\,\nu(dz_1) - \int_{Z_R}\int_{Z_R} \Phi(z,z_1)\,\nu(dz)\,\nu(dz_1)\right| +$$
$$\left|\int_{Z_R}\int_{Z_R} \Phi(z,z_1)\,\nu(dz)\,\nu(dz_1) - \int_{Z}\int_{Z} \Phi(z,z_1)\,\nu(dz)\,\nu(dz_1)\right|$$
$$\le 2\,C\,||\Phi||_\infty\,\nu^{(n)}(Z\setminus Z_R) + C^2 \sup_{(z,z_1)\in Z_R\times Z_R} |\Phi(z,z_1)-\Phi_N(z,z_1)| + b_{R,N}^{(n)} +$$
$$C^2 \sup_{(z,z_1)\in Z_R\times Z_R} |\Phi(z,z_1)-\Phi_N(z,z_1)| + 2\,C\,||\Phi||_\infty\,\nu(Z\setminus Z_R)\,, \qquad \text{(A.45)}$$

for any R and N. Consider the measures $\bar\nu^{(n)}$ defined as

$$\bar\nu^{(n)}(B) = \mathbb{E}\,\nu^{(n)}(B)\,, \qquad B\in\mathcal{B}(Z)\,,$$

and note that $\langle\varphi,\bar\nu^{(n)}\rangle = \mathbb{E}\,\langle\varphi,\nu^{(n)}\rangle$. Using (A.40), (A.43), Lemma A.4 and Lemma A.6, one obtains that the measures $\bar\nu^{(n)}$ converge weakly to the measure ν. Tightness implies that, for any $\varepsilon>0$, there exists R such that

$$\sup_n \bar\nu^{(n)}(Z\setminus Z_R)\le\varepsilon \quad\text{and}\quad \nu(Z\setminus Z_R)\le\varepsilon\,. \qquad \text{(A.46)}$$

For given ε and R, there exists a step function Φ_N such that

$$\sup_{(z,z_1)\in Z_R\times Z_R} |\Phi(z,z_1)-\Phi_N(z,z_1)|\le\varepsilon\,, \qquad \text{(A.47)}$$

since Φ is continuous. Using (A.46) and (A.47) one obtains from (A.45) that

$$\mathbb{E}\,a^{(n)} \le 4\,C\,||\Phi||_\infty\,\varepsilon + 2\,C^2\varepsilon + \mathbb{E}\,b_{R,N}^{(n)}$$

and, according to (A.44),

$$\limsup_{n\to\infty} \mathbb{E}\,a^{(n)} \le 4\,C\,||\Phi||_\infty\,\varepsilon + 2\,C^2\varepsilon\,, \qquad \forall\,\varepsilon>0\,,$$

so that the assertion follows. ∎

A.5 Existence of solutions

Existence results for the spatially homogeneous or the mollified Boltzmann equation can be found in [4], [48, Ch. VIII.2]. For completeness, we reproduce a version adapted to our purpose (cf. Remark 3.26).

Theorem A.8. *Let the mollifying function h and the collision kernel B satisfy (3.149) and f_0 be such that*

$$f_0(x,v)\ge 0 \qquad \text{(A.48)}$$

and

$$||f_0||_1 = \int_D \int_{\mathbb{R}^3} f_0(x,v)\, dv\, dx < \infty\,. \tag{A.49}$$

Then there exists a unique solution in $L^1(D \times \mathbb{R}^3)$ *of the equation*

$$\frac{\partial}{\partial t} f(t,x,v) = \int_D \int_{\mathbb{R}^3} \int_{\mathcal{S}^2} h(x,y)\, B(v,w,e) \times \Big[f(t,x,v')\, f(t,y,w') - f(t,x,v)\, f(t,y,w) \Big] de\, dw\, dy \tag{A.50}$$

with the initial condition

$$f(0,x,v) = f_0(x,v)\,. \tag{A.51}$$

This solution satisfies

$$f(t,x,v) \geq 0\,, \qquad t \geq 0\,, \tag{A.52}$$

and

$$\int_D \int_{\mathbb{R}^3} f(t,x,v)\, dv\, dx = \int_D \int_{\mathbb{R}^3} f_0(x,v)\, dv\, dx\,. \tag{A.53}$$

If, in addition,

$$\int_D \int_{\mathbb{R}^3} |v|^2\, f_0(x,v)\, dv\, dx < \infty \tag{A.54}$$

then

$$\int_D \int_{\mathbb{R}^3} |v|^2\, f(t,x,v)\, dv\, dx = \int_D \int_{\mathbb{R}^3} |v|^2\, f_0(x,v)\, dv\, dx\,. \tag{A.55}$$

Remark A.9. The corresponding measure-valued function

$$F(t, dx, dv) = f(t,x,v)\, dx\, dv$$

solves the weak equation (3.168). ■

Introduce the operators

$$Q_1(f)(x,v) = \int_D \int_{\mathbb{R}^3} \int_{\mathcal{S}^2} h(x,y)\, B(v,w,e)\, f(y,w)\, de\, dw\, dy$$

and

$$Q_2(f,g)(x,v) = \int_D \int_{\mathbb{R}^3} \int_{\mathcal{S}^2} h(x,y)\, B(v,w,e)\, f(x,v')\, g(y,w')\, de\, dw\, dy\,,$$

where $f, g \in L^1(D \times \mathbb{R}^3)$. Equation (A.50), (A.51) takes the form

$$\frac{d}{dt} f(t) = Q(f(t), f(t)) , \qquad f(0) = f_0 , \tag{A.56}$$

where

$$Q(f, g) = Q_2(f, g) - f\, Q_1(g) . \tag{A.57}$$

Using properties of the mollifying function h, the collision kernel B and the collision transformation v', w', one obtains (cf. Lemma 1.3 and (1.55))

$$\int_D \int_{\mathbb{R}^3} Q_2(f, g)(x, v)\, dv\, dx = \int_D \int_{\mathbb{R}^3} f(x, v)\, Q_1(g)(x, v)\, dv\, dx \tag{A.58}$$

and

$$\begin{aligned} \int_D \int_{\mathbb{R}^3} |v|^2\, Q_2(f, f)(x, v)\, dv\, dx &= \frac{1}{2} \int_D \int_{\mathbb{R}^3} \int_D \int_{\mathbb{R}^3} \int_{\mathcal{S}^2} \\ &\quad \Big[|v'|^2 + |w'|^2 \Big] h(x, y)\, B(v, w, e)\, f(x, v)\, f(y, w)\, de\, dw\, dy\, dv\, dx \\ &= \int_D \int_{\mathbb{R}^3} |v|^2\, f(x, v)\, Q_1(f)(x, v)\, dv\, dx , \end{aligned} \tag{A.59}$$

for non-negative f, g. Assumption (3.149) implies

$$|Q_1(f)(x, v)| \le C_b\, ||f||_1 \tag{A.60}$$

so that

$$||Q_2(f, g)||_1 \le C_b\, ||f||_1\, ||g||_1 \tag{A.61}$$

and

$$\int_D \int_{\mathbb{R}^3} |v|^2\, Q_2(f, f)(x, v)\, dv\, dx \le C_b\, ||f||_1 \int_D \int_{\mathbb{R}^3} |v|^2\, f(x, v)\, dv\, dx , \tag{A.62}$$

according to (A.58) and (A.59).

Lemma A.10. *Consider the iteration scheme*

$$\begin{aligned} f^{n+1}(t) &= \exp(-c\, t\, ||f_0||_1)\, f_0 \; + \int_0^t \exp(-c\, (t - s)\, ||f_0||_1) \times \\ &\qquad \Big(Q_2(f^n(s), f^n(s)) + f^n(s) \Big[c\, ||f^n(s)||_1 - Q_1(f^n(s)) \Big] \Big)\, ds , \\ f^0(t) &= 0 , \qquad t \ge 0 , \qquad n = 0, 1, 2, \dots , \qquad c \ge C_b , \end{aligned} \tag{A.63}$$

where f_0 satisfies (A.48), (A.49). Then, for any $n = 1, 2, \dots$ and $t \ge 0$,

$$f^n(t, x, v) \ge f^{n-1}(t, x, v) \ge 0 , \tag{A.64}$$

$$||f^n(t)||_1 \le ||f_0||_1 \tag{A.65}$$

and

$$\int_D \int_{\mathbb{R}^3} |v|^2\, f^n(t, x, v)\, dv\, dx \le \int_D \int_{\mathbb{R}^3} |v|^2\, f_0(x, v)\, dv\, dx . \tag{A.66}$$

Proof. Properties (A.64)-(A.66) are fulfilled for $n = 1$, according to definition (A.63). Assume these properties hold for some $n \geq 1$. Using (A.64),

$$Q_2(f^n(s), f^n(s)) \geq Q_2(f^{n-1}(s), f^{n-1}(s))$$

and (cf. (A.60))

$$\begin{aligned} c\,||f^n(s)||_1 - Q_1(f^n(s)) &= c\,||f^n(s) - f^{n-1}(s)||_1 - \\ &\quad Q_1(f^n(s) - f^{n-1}(s)) + c\,||f^{n-1}(s)||_1 - Q_1(f^{n-1}(s)) \\ &\geq c\,||f^{n-1}(s)||_1 - Q_1(f^{n-1}(s))\,, \end{aligned}$$

one obtains

$$f^{n+1}(t, x, v) \geq f^n(t, x, v)\,. \tag{A.67}$$

According to (A.58), definition (A.63) implies

$$\begin{aligned} &||f^{n+1}(t)||_1 = \\ &\exp(-c\,t\,||f_0||_1)\,||f_0||_1 + c\int_0^t \exp(-c\,(t-s)\,||f_0||_1)\,||f^n(s)||_1^2\,ds\,. \end{aligned} \tag{A.68}$$

Using (A.65) one obtains

$$\begin{aligned} &||f^{n+1}(t)||_1 \leq \\ &\exp(-c\,t\,||f_0||_1)\,||f_0||_1 + c\,||f_0||_1^2 \int_0^t \exp(-c\,(t-s)\,||f_0||_1)\,ds = ||f_0||_1\,. \end{aligned} \tag{A.69}$$

Finally, (A.63), (A.59), (A.65) and (A.66) imply

$$\begin{aligned} &\int_D \int_{\mathbb{R}^3} |v|^2\, f^{n+1}(t, x, v)\,dv\,dx \leq \exp(-c\,t\,||f_0||_1) \int_D \int_{\mathbb{R}^3} |v|^2\, f_0(x, v)\,dv\,dx + \\ &\qquad c\,||f_0||_1 \int_D \int_{\mathbb{R}^3} |v|^2\, f_0(x, v)\,dv\,dx \int_0^t \exp(-c\,(t-s)\,||f_0||_1)\,ds \\ &= \int_D \int_{\mathbb{R}^3} |v|^2\, f_0(x, v)\,dv\,dx\,. \end{aligned} \tag{A.70}$$

Thus, taking into account (A.67), (A.69) and (A.70), the assertions follow by induction. ∎

Proof of Theorem A.8. By Lemma A.10 and the monotone convergence theorem there exists

$$f(t) = \lim_{n\to\infty} f^n(t) \qquad \text{in } L^1(D \times \mathbb{R}^3)\,, \qquad t \geq 0\,.$$

By continuity of the operators (cf. (A.60), (A.61)), this limit $f(t)$ satisfies (cf. (A.63))

$$f(t) = \exp(-c\,t\,||f_0||_1)\,f_0 + \int_0^t \exp(-c\,(t-s)\,||f_0||_1)\left(Q_2(f(s),f(s)) + f(s)\Big[c\,||f(s)||_1 - Q_1(f(s))\Big]\right) ds \tag{A.71}$$

and $\beta(t) := ||f(t)||_1$ satisfies (cf. (A.68))

$$\beta(t) = \exp(-c\,t\,||f_0||_1)\,||f_0||_1 + c\int_0^t \exp(-c\,(t-s)\,||f_0||_1)\,\beta(s)^2\,ds\,. \tag{A.72}$$

Note that $\beta_0(t) := ||f_0||_1$ is the unique solution of equation (A.72). Thus, equation (A.71) takes the form

$$f(t) = \exp(-c\,t\,||f_0||_1)\,f_0 + \int_0^t \exp(-c\,(t-s)\,||f_0||_1)\left(Q_2(f(s),f(s)) + f(s)\Big[c\,||f_0||_1 - Q_1(f(s))\Big]\right) ds\,. \tag{A.73}$$

A differentiation in (A.73) implies that $f(t)$ satisfies (A.56). Moreover, (A.52) and (A.53) are fulfilled.

Using (A.66) and the monotone convergence theorem, one obtains

$$\int_D \int_{\mathbb{R}^3} |v|^2\,f(t,x,v)\,dv\,dx \le \int_D \int_{\mathbb{R}^3} |v|^2\,f_0(x,v)\,dv\,dx\,. \tag{A.74}$$

Finally, it follows from (A.59) that (cf. (A.60)-(A.62), (A.54))

$$\int_D \int_{\mathbb{R}^3} |v|^2\,Q(f,f)(x,v)\,dv\,dx = 0\,,$$

and (A.56) implies equality in (A.74) so that (A.55) holds.

Uniqueness follows from the local Lipschitz property of the operator (A.57) (cf. (A.60), (A.61)),

$$||Q(f,f) - Q(g,g)||_1 \le C_b\,||f-g||_1\Big[||f||_1 + ||g||_1\Big].$$

This completes the proof. ∎

B

Modeling of distributions

Here we collect some material concerning the generation of samples from a given distribution. In particular, we describe all procedures used in the numerical experiments of Chapter 4. Alternative (sometimes more efficient) algorithms can be found in Monte Carlo textbooks.

B.1 General techniques

B.1.1 Acceptance-rejection method

Consider some measurable space (X, μ) and two functions f and F on X satisfying the majorant condition

$$0 \le f(x) \le F(x)\,, \qquad \forall x \in X\,. \tag{B.1}$$

Assume that

$$\int_X f(x)\,\mu(dx) > 0 \quad \text{and} \quad \int_X F(x)\,\mu(dx) < \infty\,.$$

Let a random variable ξ be defined by the following procedure:

1. Generate a random variable η with the probability density
$$P(x) = \frac{F(x)}{\int_X F(x)\,\mu(dx)}\,. \tag{B.2}$$
2. Generate independently a random variable u uniformly distributed on $[0, 1]$.
3. If the acceptance condition
$$u \le \frac{f(\eta)}{F(\eta)} \tag{B.3}$$
is satisfied, then $\xi = \eta$ and stop. Otherwise, go to 1.

Then the random variable ξ has the probability density

$$p(x) = \frac{f(x)}{\int_X f(x)\,\mu(dx)}\,.$$

The acceptance rate is

$$\frac{\int_X f(x)\,\mu(dx)}{\int_X F(x)\,\mu(dx)}\,.$$

B.1.2 Transformation method

Consider a random variable ξ with values in an open set $G \subset \mathbb{R}^d$ and density p_ξ. Define the random variable

$$\eta = \Phi^{-1}(\xi)\,, \tag{B.4}$$

where $\Phi : G_1 \to G$ is some diffeomorphism and $G_1 \subset \mathbb{R}^d$. One obtains

$$\begin{aligned}\mathbb{E}\, f(\eta) = \mathbb{E}\, f(\Phi^{-1}(\xi)) &= \int_G f(\Phi^{-1}(x))\, p_\xi(x)\, dx \\ &= \int_{G_1} f(y)\, p_\xi(\Phi(y))\, |\det \Phi'(y)|\, dy\,,\end{aligned}$$

where Φ' denotes the Jacobian matrix and f is some test function. Consequently, the random variable (B.4) has the density

$$p_\eta(y) = p_\xi(\Phi(y))\, |\det(\Phi'(y)|\,. \tag{B.5}$$

Samples of ξ can be obtained by first generating η and then transforming the result into $\xi = \Phi(\eta)$.

Analogous arguments apply to the parametrization of ξ by spherical coordinates.

A simple particular case is (for strictly positive densities)

$$\Phi = F_\xi^{-1} : (0,1) \to \mathbb{R}\,,$$

where F_ξ denotes the distribution function of the random variable ξ. The density (B.5) takes the form

$$p_\eta(y) = p_\xi(F_\xi^{-1}(y))\, \frac{1}{F_\xi'(F_\xi^{-1}(y))} = 1\,.$$

Thus, samples of ξ are obtained as

$$\xi = F_\xi^{-1}(\eta)\,,$$

where η is uniformly distributed on $[0,1]$.

B.1.3 Composition method

Consider some probability space (Y, ν) and a family of probability measures

$$\mu_y(dx)\,, \qquad y \in Y\,,$$

on some measurable space X. Let a random variable ξ be defined by the following procedure:

1. Generate a random variable η with values in Y according to ν.
2. Generate ξ according to μ_η.

Then the random variable ξ has the distribution

$$P(dx) = \int_Y \mu_y(dx)\,\nu(dy)\,. \tag{B.6}$$

B.2 Uniform distribution on the unit sphere

Here we generate a random variable ξ according to the probability density

$$p_\xi(e) = \frac{1}{4\,\pi}\,, \qquad e \in \mathcal{S}^2\,.$$

We apply the transformation method (cf. Section B.1.2).

Switching to spherical coordinates

$$e = e(\varphi, \theta) = \begin{pmatrix} \cos\varphi\,\sin\theta \\ \sin\varphi\,\sin\theta \\ \cos\theta \end{pmatrix}, \qquad 0 \le \varphi < 2\pi\,, \quad 0 \le \theta \le \pi\,, \tag{B.7}$$

one obtains

$$p_\eta(\varphi, \theta) = \frac{1}{4\,\pi}\,\sin\theta\,.$$

The components φ and θ of the random variable η are independent so that it remains to solve the equations

$$\frac{1}{2\,\pi}\int_0^{\varphi^*} d\varphi = r_1\,, \qquad \frac{1}{2}\int_0^{\theta^*} \sin\theta\,d\theta\; = r_2\,,$$

where r_1 and r_2 are random numbers uniformly distributed on $(0, 1)$. One obtains

$$\varphi^* = 2\pi\,r_1\,, \qquad \cos\theta^* = 1 - 2\,r_2$$

and, according to (B.7),

$$\xi = e(\varphi^*, \theta^*)\,. \tag{B.8}$$

Algorithm B.1 *Uniform distribution on the unit sphere*

`UniSphere`(r_1, r_2)

`1. Compute:`

$$\varphi^* = 2\pi\, r_1$$

`2. Compute:`

$$\cos\theta^* = 1 - 2\, r_2$$

`3. Compute:`

$$\sin\theta^* = \sqrt{1 - (\cos\theta^*)^2}$$

`4. Final result:` `(B.8)`

B.3 Directed distribution on the unit sphere

Here we generate a random variable ξ according to the probability density

$$p_\xi(e) = \frac{1}{2\,\pi}\,|(u, e)|\,, \qquad e \in \mathcal{S}^2\,,$$

where $u \in \mathcal{S}^2$ is some parameter. We apply the transformation method (cf. Section B.1.2).

First we construct an orthogonal matrix $Q(u)$ such that

$$Q(u)'\,u = (0, 0, 1)\,,$$

where Q' denotes the transposed matrix. Note that the matrices

$$A_1(\psi) = \begin{pmatrix} 1 & 0 & 0 \\ 0 & \cos\psi & -\sin\psi \\ 0 & \sin\psi & \cos\psi \end{pmatrix} \qquad A_2(\psi) = \begin{pmatrix} \cos\psi & 0 & \sin\psi \\ 0 & 1 & 0 \\ -\sin\psi & 0 & \cos\psi \end{pmatrix}$$

$$A_3(\psi) = \begin{pmatrix} \cos\psi & -\sin\psi & 0 \\ \sin\psi & \cos\psi & 0 \\ 0 & 0 & 1 \end{pmatrix}$$

perform rotations over an angle ψ around the first, second and third basis vectors, respectively. Let u be given in spherical coordinates as

$$u = \Big(\cos\varphi_u\,\sin\theta_u\,,\,\sin\varphi_u\,\sin\theta_u\,,\,\cos(\theta_u)\Big).$$

Then one obtains

$$A_3(-\varphi_u)\,u = \tilde{u} = (\sin\theta_u, 0, \cos\theta_u)\,, \qquad A_2(-\theta_u)\,\tilde{u} = (0, 0, 1)$$

so that $Q(u)' = A_2(-\theta_u)\,A_3(-\varphi_u)$ and

$$Q(u) = A_3(\varphi_u)\, A_2(\theta_u) = \begin{pmatrix} \cos\varphi_u \cos\theta_u & -\sin\varphi_u & \cos\varphi_u \sin\theta_u \\ \sin\varphi_u \cos\theta_u & \cos\varphi_u & \sin\varphi_u \sin\theta_u \\ -\sin\theta_u & 0 & \cos\theta_u \end{pmatrix}. \tag{B.9}$$

If $\sin\theta_u = 0$ then φ_u is not uniquely determined and it is convenient to put $\varphi_u = 0$.

Using the substitution (cf. (B.7))

$$e = Q(u)\, e(\varphi, \theta)\,, \qquad 0 \le \varphi < 2\pi\,, \quad 0 \le \theta \le \pi\,, \tag{B.10}$$

which corresponds to a rotation and a transition to spherical coordinates, one obtains

$$\begin{aligned} p_\eta(\varphi, \theta) &= \frac{1}{2\,\pi}\, |(u, Q(u)\, e(\varphi, \theta))|\, \sin\theta \\ &= \frac{1}{2\,\pi}\, |(Q(u)'u, e(\varphi, \theta))|\, \sin\theta = \frac{1}{2\,\pi}\, |\cos\theta|\, \sin\theta\,. \end{aligned}$$

Note that the uniform surface measure on the unit sphere is invariant with respect to rotations. The components φ and θ of the random variable η are independent so that it remains to solve the equations

$$\frac{1}{2\,\pi} \int_0^{\varphi^*} d\varphi = r_1\,, \qquad \int_0^{\theta^*} |\cos\theta|\, \sin\theta\, d\theta\, = r_2\,,$$

where r_1 and r_2 are random numbers uniformly distributed on $(0, 1)$. One obtains

$$\varphi^* = 2\pi\, r_1\,, \qquad \cos\theta^* = \begin{cases} \sqrt{1 - 2\, r_2} & \text{if} \quad r_2 \le 1/2\,, \\ -\sqrt{2\, r_2 - 1} & \text{if} \quad r_2 > 1/2\,, \end{cases}$$

and, according to (B.10),

$$\xi = Q(u)\, e(\varphi^*, \theta^*)\,. \tag{B.11}$$

Algorithm B.2 *Directed distribution on the unit sphere*

`DirectUniSphere(`r_1, r_2, u`)`

`1. Compute:`

$$\varphi^* = 2\pi\, r_1$$

`2. if` $r_2 \le 1/2$ `then set`

$$\cos\theta^* = \sqrt{1 - 2\, r_2}$$

`else set`

$$\cos\theta^* = -\sqrt{2\, r_2 - 1}$$

`3. Compute:`

$$\sin\theta^* = \sqrt{1-(\cos\theta^*)^2}$$

`4. If` $u=(0,0,1)$ `or` $u=(0,0,-1)$, `i.e.` $\sin\theta_u = 0$, `then set`

$$\varphi_u = 0$$

`else compute`

$$\cos\theta_u = u_3\,, \quad \sin\theta_u = \sqrt{1-\cos^2\theta_u}\,,$$
$$\cos\varphi_u = u_1/\sin\theta_u\,, \quad \sin\varphi_u = u_2/\sin\theta_u$$

`5. Final result:` `(B.11)`

B.4 Maxwell distribution

Here we generate a random variable ξ according to the probability density

$$p_\xi(v) = M_{V,T}(v)\,, \qquad v\in\mathbb{R}^3\,. \tag{B.12}$$

We apply the transformation method (cf. Section B.1.2).

Using the substitution

$$v = V + \sqrt{T}\,w\,, \qquad dv = T^{3/2}\,dw \tag{B.13}$$

and switching to the spherical coordinates

$$w = r\,e\,, \qquad 0\le r<\infty\,, \quad e\in\mathcal{S}^2\,, \qquad dw = r^2\,dr\,de \tag{B.14}$$

one obtains

$$p_\eta(r,e) = \frac{1}{(2\pi)^{3/2}}\,r^2\,\exp\left(-\frac{r^2}{2}\right).$$

The components r and e of the random variable η are independent. Since the vector e is uniformly distributed on the unit sphere, we define

$$e^* = \texttt{UniSphere}(\mathtt{r}_1,\mathtt{r}_2)$$

and it remains to solve the equation

$$F(r^*) := \int_0^{r^*} r^2\,\exp(-r^2/2)\,dr = \sqrt{\frac{\pi}{2}}\,r_3\,, \tag{B.15}$$

where r_1, r_2 and r_3 are random numbers uniformly distributed on $(0,1)$. According to (B.13), (B.14), one obtains

$$\xi = V + \sqrt{T}\, r^*\, e^* \,. \tag{B.16}$$

The nonlinear equation (B.15) is solved using the Newton method. Integrating by parts we express the function F in the form (see Fig. B.1)

$$F(z) = -z\, \exp(-z^2/2) + \sqrt{\frac{\pi}{2}}\, \mathrm{erf}\Big(\frac{z}{\sqrt{2}}\Big). \tag{B.17}$$

The first two derivatives are

$$F'(z) = z^2 \exp(-z^2/2)\,, \qquad F''(z) = z\,(2 - z^2) \exp(-z^2/2)\,.$$

Convergence of the Newton iterations does not occur automatically for all

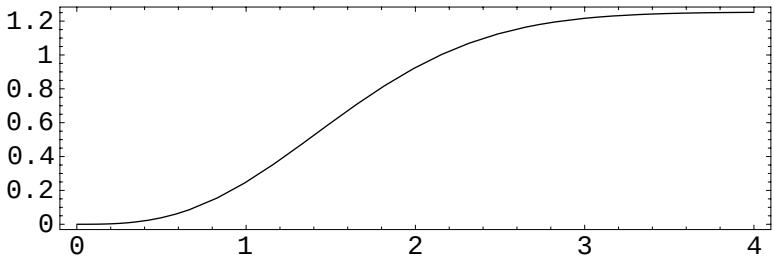

Fig. B.1. The function (B.17)

possible initial guesses r_0 , or can be slow. The reason for this is the inflection point at $\sqrt{2}$. However, using $z_0 = \sqrt{2}$ as the initial guess, $3 - 4$ iterations are usually enough to get 8 digits of the solution correct and $4 - 5$ iterations to reach the double precision accuracy of a computer.

Algorithm B.3 *Maxwell distribution*

`Maxwell(`r_1, r_2, r_3, V, T`)`

`1. Compute`

$$e^* = \texttt{UniSphere}(r_1, r_2)$$

`2. Initial guess:`

$$z_0 = \sqrt{2}$$

`3. Newton iterations for` $k = 0, 1, \ldots$

`3.1 Error:`

$$E_k = -z_k \exp(-z_k^2/2) + \sqrt{\frac{\pi}{2}} \left(\mathrm{erf}\Big(\frac{z_k}{\sqrt{2}}\Big) - r_3 \right)$$

`3.2 New guess:`

$$z_{k+1} = z_k - \frac{E_k}{z_k^2 \exp(-z_k^2/2)}$$

3.3 Stopping criterion:

$$|E_k| \le 10^{-8}$$

3.4 Solution:

$$r^* = z_{k+1}$$

4. Final result: (B.16)

B.5 Directed half-space Maxwell distribution

Here we generate a random variable ξ according to the probability density

$$p_\xi(v) = \frac{1}{m_a(a)}\, \chi_{\{(v,u)>0\}}(v)\, M_{V,T}(v)\, (v,u)\,, \qquad v \in \mathbb{R}^3\,,$$

where $u \in \mathcal{S}^2$ is some parameter and (cf. (A.8))

$$m_a(z) = \sqrt{\frac{T}{2}} \left(a\,[1 + \mathrm{erf}(z)] + \frac{1}{\sqrt{\pi}}\, \exp(-z^2) \right), \qquad z \le a\,, \tag{B.18}$$

with the notation

$$a = \frac{(V,u)}{\sqrt{2\,T}}\,.$$

We apply the transformation method (cf. Section B.1.2).

Consider the orthogonal matrix $Q(u)$ defined in (B.9), which performs a rotation such that $Q(u)'u = (0,0,1)$. Using the substitutions

$$v = V + \sqrt{2\,T}\, Q(u)\, w\,, \qquad dv = (2\,T)^{3/2}\, dw\,, \tag{B.19}$$

and

$$\begin{aligned} &w_1 = r\, \cos\varphi\,, \qquad w_2 = r\, \sin\varphi\,, \qquad w_3 = -z\,, \\ &r \ge 0\,, \quad \varphi \in [0, 2\pi)\,, \quad z \in \mathbb{R}\,, \qquad dw = r\, dr\, d\varphi\, dz\,, \end{aligned} \tag{B.20}$$

and taking into account that

$$(V + \sqrt{2\,T}\, Q(u)\, w, u) = \sqrt{2\,T}\, (a + (Q(u)\, w, u)) = \sqrt{2\,T}\, (a - z)\,,$$

one obtains

$$\begin{aligned} p_\eta(r,\varphi,z) &= \frac{1}{m_a(a)}\, \chi_{\{(v,u)>0\}}(V + \sqrt{2\,T}\, Q(u)\, w) \times \\ &\quad M_{V,T}(V + \sqrt{2\,T}\, Q(u)\, w)\, (V + \sqrt{2\,T}\, Q(u)\, w, u)\, (2\,T)^{3/2} \\ &= \frac{\sqrt{2\,T}}{m_a(a)\, \pi^{3/2}}\, \chi_{(-\infty,a)}(z)\, (a - z)\, \exp(-z^2)\, r\, \exp(-r^2)\,. \end{aligned}$$

The components r, φ and z of the random variable η are independent so that it remains to solve the equations

$$2\int_0^{r^*} r\,\exp(-r^2)\,dr = 1-\exp(-(r^*)^2) = r_1\,, \qquad \frac{1}{2\,\pi}\int_0^{\varphi^*} d\varphi = r_2$$

and (cf. (B.18), (A.10))

$$\frac{1}{m_a(a)}\sqrt{\frac{2\,T}{\pi}}\int_{-\infty}^{z^*}\chi_{(-\infty,a)}(z)\,(a-z)\exp(-z^2)\,dz = \frac{m_a(z^*)}{m_a(a)} = r_3\,, \qquad \text{(B.21)}$$

where r_1, r_2 and r_3 are random numbers uniformly distributed on $(0,1)$. One obtains

$$r^* = \sqrt{-\ln(r_1)}\,, \qquad \varphi^* = 2\pi\,r_2$$

and, according to (B.19), (B.20),

$$\xi = V + \sqrt{2\,T}\,Q(u)\begin{pmatrix} r^*\,\cos\varphi^* \\ r^*\,\sin\varphi^* \\ -z^* \end{pmatrix}. \qquad \text{(B.22)}$$

The nonlinear equation (B.21) is solved using the Newton method. The function $m_a(z)/m_a(a)$ is shown in Fig. B.2 for $a = 1$. It has an inflection point at $z = (a-\sqrt{a^2+2})/2$. This value is a good initial guess for the Newton method. Usually, $4-6$ iterations are needed to reach double precision accuracy 10^{-15}.

In the special case $a = 0$ equation (B.21) is immediately solved by

$$z^* = \sqrt{-\ln(r_3)}\,.$$

Algorithm B.4 *Directed half-space Maxwell distribution*

`HSMaxwell`(r_1, r_2, r_3, V, T, u)

`1. Compute:`

$$r^* = \sqrt{-\ln(r_1)}$$

`2. Compute:`

$$\varphi^* = 2\,\pi\,r_2$$

`3. Compute:`

$$a = \frac{(V,u)}{\sqrt{2\,T}}$$

`4. Initial guess:`

$$z_0 = (a-\sqrt{a^2+2})/2$$

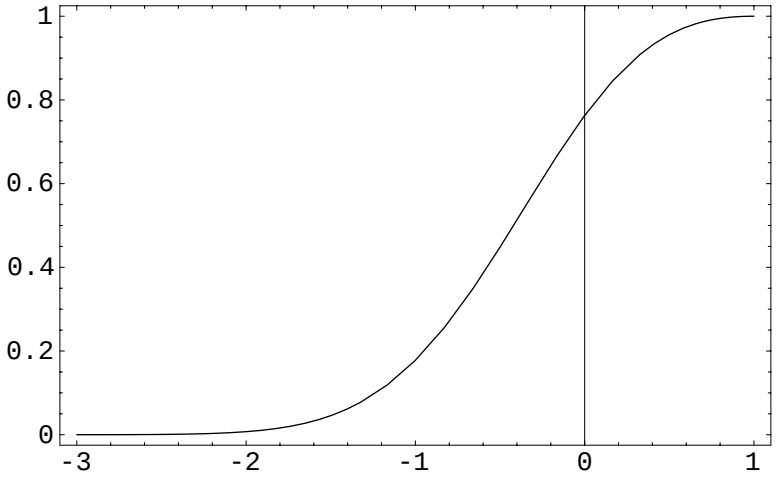

Fig. B.2. The function $m_1(z)/m_1(1)$ (cf. (B.18))

5. Newton iterations for $k = 0, 1, \ldots$

5.1 Error:

$$E_k = m_a(z_k)/m_a(a) - r_3$$

5.2 New guess:

$$z_{k+1} = z_k - \frac{m_a(a)\,\sqrt{\pi}\,E_k}{\sqrt{2\,T}\,(a - z_k)\exp(-z_k^2)}$$

5.3 Stopping criterion:

$$|E_k| \le 10^{-8}$$

5.4 Solution:

$$z^* = z_{k+1}$$

6. If $u = (0, 0, 1)$ or $u = (0, 0, -1)$, i.e. $\sin\theta_u = 0$, then set

$$\varphi_u = 0$$

else compute

$$\cos\theta_u = u_3\,, \quad \sin\theta_u = \sqrt{1 - \cos^2\theta_u}\,,$$
$$\cos\varphi_u = u_1/\sin\theta_u\,, \quad \sin\varphi_u = u_2/\sin\theta_u$$

7. Final result: (B.22)

B.6 Initial distribution of the BKW solution

Here we generate a random variable ξ according to the probability density (cf. (A.35))

$$p_\xi(v) = \left(\frac{\beta+1}{2\,\pi\,T}\right)^{3/2} \left[1+\beta\Big(\frac{\beta+1}{2T}\,|v|^2 - \frac{3}{2}\Big)\right] \exp\Big(-\frac{\beta+1}{2T}\,|v|^2\Big), \quad v \in \mathbb{R}^3\,,$$

where $\beta \in [0, 2/3]$ and $T > 0$ are some parameters. We apply the transformation method (cf. Section B.1.2).

Using the substitution

$$v = \left(\frac{\beta+1}{T}\right)^{-1/2} w\,, \qquad dv = \left(\frac{\beta+1}{T}\right)^{-3/2} dw \tag{B.23}$$

and switching to spherical coordinates

$$w = r\,e\,, \qquad 0 \le r < \infty\,, \quad e \in \mathcal{S}^2\,, \qquad dw = r^2\,dr\,de \tag{B.24}$$

one obtains

$$p_\eta(r,e) = \frac{1}{(2\,\pi)^{3/2}}\,r^2\left(1+\beta\Big(\frac{1}{2}\,r^2 - \frac{3}{2}\Big)\right)\exp(-r^2/2)\,.$$

The components r and e of the random variable η are independent. Since the vector e is uniformly distributed on the unit sphere, we define

$$e^* = \texttt{UniSphere}(\texttt{r}_1, \texttt{r}_2)$$

and it remains to solve the equation

$$F(r^*) := \int_0^{r^*} r^2\left(1+\beta\Big(\frac{1}{2}r^2 - \frac{3}{2}\Big)\right)\exp\Big(-r^2/2\Big)\,dr = \sqrt{\frac{\pi}{2}}\;r_3\,, \tag{B.25}$$

where r_1, r_2 and r_3 denote random numbers uniformly distributed on $(0,1)$. According to (B.23), (B.24), one obtains

$$\xi = \left(\frac{\beta+1}{T}\right)^{-1/2} r^*\,e^*\,. \tag{B.26}$$

The nonlinear equation (B.25) is solved using the Newton method. Integrating by parts we express the function F in the form (see Fig. B.3)

$$F(z) = -\left(z + \frac{\beta}{2}z^3\right)\exp\Big(-z^2/2\Big) + \sqrt{\frac{\pi}{2}}\;\mathrm{erf}\Big(\frac{z}{\sqrt{2}}\Big). \tag{B.27}$$

The first two derivatives are

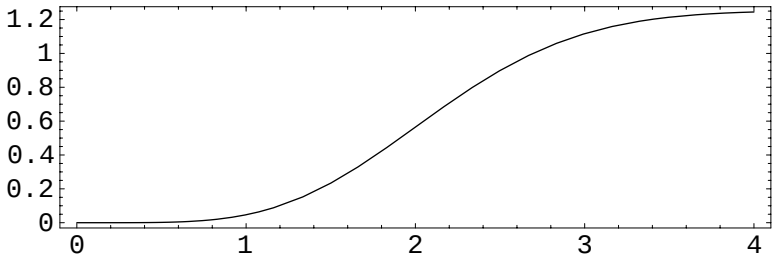

Fig. B.3. The function (B.27) for $\beta = 2/3$

$$F'(z) = z^2 \left(1 + \beta\Big(\frac{1}{2}z^2 - \frac{3}{2}\Big)\right) \exp\Big(-z^2/2\Big),$$
$$F''(z) = -\frac{1}{2}\, z \left(\beta\, z^4 - (7\beta - 2)z^2 - 2(2 - 3\beta)\right) \exp\Big(-z^2/2\Big).$$

Convergence of the Newton iterations is optimal if we start at the inflection point

$$z_0 = \sqrt{\frac{7\beta - 2 + \sqrt{25\beta^2 - 12\beta + 4}}{2\beta}}\ . \tag{B.28}$$

Algorithm B.5 *BKW solution*

`IniBKW`$(r_1, r_2, r_3, V, \beta, T)$

`1. Compute`

$$e^* = \texttt{UniSphere}(\mathtt{r}_2, \mathtt{r}_3)$$

`2. Initial guess:` (B.28)

`3. Newton iterations for` $k = 0, 1, \ldots$

`3.1 Error:`

$$E_k = -\left(z_k + \frac{\beta}{2} z_k^3\right) \exp\Big(-z_k^2/2\Big) + \sqrt{\frac{\pi}{2}}\, \left(\mathrm{erf}\Big(\frac{z_k}{\sqrt{2}}\Big) - r_3\right)$$

`3.2 New guess:`

$$z_{k+1} = z_k - \frac{E_k}{z_k^2 \left(1 + \beta\Big(\frac{1}{2}z_k^2 - \frac{3}{2}\Big)\right) \exp\Big(-z_k^2/2\Big)}$$

`3.3 Stopping criterion:`

$$|E_k| \le 10^{-8}$$

`3.4 Solution:`

$$r^* = z_{k+1}$$

`4. Final result:` (B.26)

B.7 Initial distribution of the eternal solution

Here we generate a random variable ξ according to the probability density (cf. (4.29))

$$p_\xi(v) = \frac{8}{(2\,\pi)^{5/2}} \int\limits_0^\infty \frac{s^3}{(1+s^2)^2}\, e^{-s^2\,|v|^2/2}\, ds\,, \qquad v \in \mathbb{R}^3\,. \tag{B.29}$$

We apply the composition method (cf. Section B.1.3).

The density (B.29) has the form (B.6) with $X = \mathbb{R}^3$, $Y = (0,\infty)$,

$$\nu(ds) = \frac{4}{\pi}\, \frac{1}{(1+s^2)^2}\, ds$$

and

$$\mu_s(dv) = \frac{s^3}{(2\,\pi)^{3/2}}\, e^{-s^2\,|v|^2/2}\, dv\,, \qquad s \in Y\,.$$

Thus one obtains

$$\xi = \texttt{Maxwell}(r_1, r_2, r_3, (0,0,0), (s^*)^{-2})\,, \tag{B.30}$$

where s^* is the solution of the equation

$$F(s^*) := \int\limits_0^{s^*} \frac{2}{(1+s^2)^2}\, ds = \frac{\pi}{2}\, r_4 \tag{B.31}$$

and r_1, r_2, r_3, r_4 are random numbers uniformly distributed on $(0,1)$.

The nonlinear equation (B.31) is solved using the Newton method. The function F, which takes the form

$$F(s) = \frac{s}{1+s^2} + \arctan\, s\,, \tag{B.32}$$

is shown in Fig. B.4. The first derivative is

$$F'(s) = \frac{2}{(1+s^2)^2}$$

so that there is an inflection point at $s_0 = 0$.

Algorithm B.6 *Eternal solution*

`Eternal`(r_1, r_2, r_3, r_4)

`1. Initial guess:`

$$s_0 = 0$$

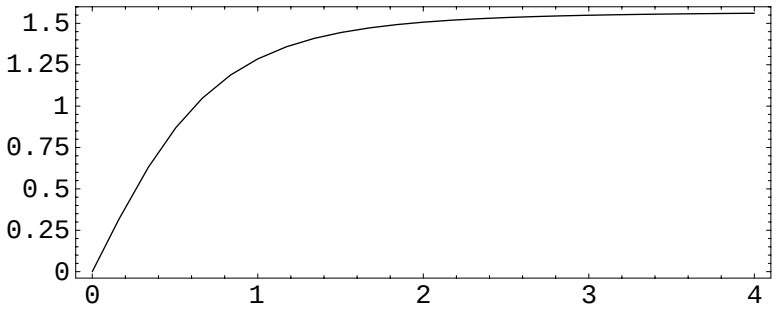

Fig. B.4. The function (B.32)

2. Newton iterations for $k = 0, 1, \ldots$

2.1 Error:

$$E_k = \frac{s_k}{1 + s_k^2} + \arctan\, s_k - \frac{\pi}{2}\, r_4$$

2.2 New guess:

$$s_{k+1} = s_k - \frac{(1 + s_k^2)^2}{2} E_k$$

2.3 Stopping criteria:

$$|E_k| \leq 10^{-8}$$

2.4 Solution:

$$s^* = s_{k+1}$$

3. Final result: (B.30)

References

1. F. J. Alexander, A. L. Garcia, and B. J. Alder. A consistent Boltzmann algorithm. *Phys. Rev. Lett.*, 74(26):5212–5215, 1995.
2. F. J. Alexander, A. L. Garcia, and B. J. Alder. Cell size dependence of transport coefficients in stochastic particle algorithms. *Phys. Fluids*, 10(6):1540–1542, 1998.
3. H. L. Anderson. Scientific uses of the MANIAC. *J. Statist. Phys.*, 43(5-6):731–748, 1986.
4. L. Arkeryd. On the Boltzmann equation. Part I. Existence. *Arch. Rational Mech. Anal.*, 45:1–16, 1972.
5. A. A. Arsenev. Approximation of the solution of the Boltzmann equation by solutions of Ito stochastic differential equations. *Zh. Vychisl. Mat. i Mat. Fiz.*, 27(3):400–410, 1987. In Russian.
6. A. A. Arsenev. Approximation of the Boltzmann equation by stochastic equations. *Zh. Vychisl. Mat. i Mat. Fiz.*, 28(4):560–567, 1988. In Russian.
7. H. Babovsky. On a simulation scheme for the Boltzmann equation. *Math. Methods Appl. Sci.*, 8:223–233, 1986.
8. H. Babovsky. A convergence proof for Nanbu's Boltzmann simulation scheme. *European J. Mech. B Fluids*, 8(1):41–55, 1989.
9. H. Babovsky. Time averages of simulation schemes as approximations to stationary kinetic equations. *European J. Mech. B Fluids*, 11(2):199–212, 1992.
10. H. Babovsky. Monte Carlo simulation schemes for steady kinetic equations. *Transport Theory Statist. Phys.*, 23(1-3):249–264, 1994.
11. H. Babovsky. *Die Boltzmann-Gleichung: Modellbildung–Numerik–Anwendungen.* B. G. Teubner, Stuttgart, 1998.
12. H. Babovsky and R. Illner. A convergence proof for Nanbu's simulation method for the full Boltzmann equation. *SIAM J. Numer. Anal.*, 26(1):45–65, 1989.
13. O. M. Belotserkovskij, A. I. Erofeev, and V. E. Yanitskij. A nonstationary method for direct statistical simulation of rarefied gas flows. *Zh. Vychisl. Mat. i Mat. Fiz.*, 20(5):1174–1204, 1980. In Russian.
14. O. M. Belotserkovskij, A. I. Erofeev, and V. E. Yanitskij. Direct statistical modelling of problems in aero-gas dynamics. *Adv. in Mech.*, 5(3/4):11–40, 1982. In Russian.
15. O. M. Belotserkovskij and V. E. Yanitskij. Statistical particle in cell method for problems in rarefied gas dynamics. I. Construction of the method. *Zh. Vychisl. Mat. i Mat. Fiz.*, 15(5):1195–1209, 1975. In Russian.

16. O. M. Belotserkovskij and V. E. Yanitskij. Statistical particle in cell method for problems in rarefied gas dynamics. II. Numerical aspects of the method. *Zh. Vychisl. Mat. i Mat. Fiz.*, 15:1553–1567, 1975. In Russian.
17. P. H. Bézandry, R. Ferland, G. Giroux, and J.-C. Roberge. Une approche probabiliste de résolution d'équations non linéaires. In *Measure-valued processes, stochastic partial differential equations, and interacting systems (Montreal, PQ, 1992)*, volume 5 of *CRM Proc. Lecture Notes*, pages 17–33. Amer. Math. Soc., Providence, RI, 1994.
18. P. H. Bezandry, X. Fernique, and G. Giroux. A functional central limit theorem for a nonequilibrium model of interacting particles with unbounded intensity. *J. Statist. Phys.*, 72(1/2):329–353, 1993.
19. G. A. Bird. Approach to translational equilibrium in a rigid sphere gas. *Phys. Fluids*, 6:1518–1519, 1963.
20. G. A. Bird. Shock wave structure in a rigid sphere gas. In J.H. de Leeuw, editor, *Rarefied Gas Dynamics*, volume 1, pages 216–222. Academic Press, New York, 1965.
21. G. A. Bird. *Molecular Gas Dynamics*. Clarendon Press, Oxford, 1976.
22. G. A. Bird. Transition regime behavior of supersonic beam skimmers. *Phys. Fluids*, 19(10):1486–1491, 1976.
23. G. A. Bird. Monte–Carlo simulation in an engineering context. In S. Fisher, editor, *Proc. of the 12th International Symposium on Rarefied Gas Dynamics (Charlottesville, 1980)*, volume 74 of *Progress in Astronautics and Aeronautics*, pages 239–255. AIAA, New York, 1981.
24. G. A. Bird. Perception of numerical methods in rarefied gas dynamics. *Progr. Astronaut. Aeronaut.*, 118:211–226, 1989.
25. G. A. Bird. *Molecular Gas Dynamics and the Direct Simulation of Gas Flows*. Clarendon Press, Oxford, 1994.
26. G. A. Bird. Forty years of DSMC, and now? In T. J. Bartel and M. A. Gallis, editors, *Rarefied Gas Dynamics, 22nd International Symposium, Sydney, Australia, 9-14 July 2000*, volume 585 of *AIP Conference Proceedings*, pages 372–380. AIP Publishing Center, New York, 2001.
27. A. V. Bobylev. Exact solutions of the Boltzmann equation. *Dokl. Akad. Nauk SSSR*, 225(6):1296–1299, 1975. In Russian.
28. A. V. Bobylev and C. Cercignani. Exact eternal solutions of the Boltzmann equation. *J. Statist. Phys.*, 106(5-6):1019–1038, 2002.
29. A. V. Bobylev and C. Cercignani. The inverse Laplace transform of some analytic functions with an application to the eternal solutions of the Boltzmann equation. *Appl. Math. Lett.*, 15(7):807–813, 2002.
30. A. V. Bobylev and C. Cercignani. Moment equations for a granular material in a thermal bath. *J. Statist. Phys.*, 106(3-4):547–567, 2002.
31. A. V. Bobylev and T. Ohwada. On the generalization of Strang's splitting scheme. *Riv. Mat. Univ. Parma (6)*, 2*:235–243, 1999.
32. A. V. Bobylev and T. Ohwada. The error of the splitting scheme for solving evolutionary equations. *Appl. Math. Lett.*, 14(1):45–48, 2001.
33. A. V. Bobylev and S. Rjasanow. Numerical solution of the Boltzmann equation using a fully conservative difference scheme based on the fast Fourier transform. *Transport Theory Statist. Phys.*, 29(3-5):289–310, 2000.
34. A. V. Bobylev and J. Struckmeier. Numerical simulation of the stationary one-dimensional Boltzmann equation by particle methods. *European J. Mech. B Fluids*, 15(1):103–118, 1996.

35. S. V. Bogomolov. Convergence of the method of summary approximation for the Boltzmann equation. *Zh. Vychisl. Mat. i Mat. Fiz.*, 28(1):119–126, 1988. In Russian.
36. L. Boltzmann. Weitere Studien über das Wärmegleichgewicht unter Gasmolekülen. *Sitzungsber. Akad. Wiss. Wien*, 66:275–370, 1872.
37. J.-F. Bourgat, P. Le Tallec, B. Perthame, and Y. Qiu. Coupling Boltzmann and Euler equations without overlapping. In *Domain decomposition methods in science and engineering (Como, 1992)*, pages 377–398. Amer. Math. Soc., Providence, RI, 1994.
38. I. Boyd, G. Chen, and G. Candler. Predicting Failure of the Continuum Fluid Equations. *AIAA*, 94:2352, 1994.
39. I. D. Boyd. Conservative species weighting scheme for the direct simulation Monte Carlo method. *J. of Thermophysics and Heat Transfer*, 10(4):579–585, 1996.
40. G. Brasseur and S. Solomon. *Aeronomy of the Middle Atmosphere*. D. Reidel Publishing Company, Dordrecht, 1984.
41. N. P. Buslenko, D. I. Golenko, Yu. A. Shreider, I. M. Sobol, and V. G. Sragovich. *The Monte Carlo method. The method of statistical trials*. International Series of Monographs in Pure and Applied Mathematics, Vol. 87. Pergamon Press, Oxford, 1966.
42. N. P. Buslenko, D. I. Golenko, I. M. Sobol, V. G. Sragovich, and Ju. A. Shreider. *Metod statisticheskikh ispytanii (Metod Monte-Karlo)*. Gosudarstv. Izdat. Fiz.-Mat. Lit., Moscow, 1962. (Russian) [The method of statistical testing (The Monte Carlo method)] English translation: [41].
43. N. P. Buslenko and Ju. A. Shreider. *Metod statisticheskikh ispytanii (Monte-Karlo) i ego realizatsiya na tsifrovykh vychislitelnykh mashinakh*. Biblioteka Prikladnogo Analiza i Vyčislitelnoĭ Matematiki. Gosudarstv. Izdat. Fiz-Mat. Lit., Moscow, 1961. (Russian) [The Monte-Carlo method and how it is carried out on digital computers].
44. S. Caprino and M. Pulvirenti. A cluster expansion approach to a one–dimensional Boltzmann equation: a validity result. *Comm. Math. Phys.*, 166:603–631, 1995.
45. S. Caprino, M. Pulvirenti, and W. Wagner. Stationary particle systems approximating stationary solutions to the Boltzmann equation. *SIAM J. Math. Anal.*, 29(4):913–934, 1998.
46. C. Cercignani. On the master equation in the space inhomogeneous case. In *Théories cinétiques classiques et relativistes, Colloques Internationaux C.N.R.S. 236 (Paris 1974)*, pages 209–221, 1975.
47. C. Cercignani. The Grad limit for a system of soft spheres. *Comm. Pure Appl. Math.*, 36(4):479–494, 1983.
48. C. Cercignani. *The Boltzmann Equation and its Applications*. Springer, New York, 1988.
49. C. Cercignani. *Ludwig Boltzmann. The Man who Trusted Atoms*. Oxford University Press, Oxford, 1998.
50. C. Cercignani. *Rarefied Gas Dynamics. From Basic Concepts to Actual Calculations*. Cambridge Texts in Applied Mathematics. Cambridge University Press, 2000.
51. C. Cercignani, R. Illner, and M. Pulvirenti. *The Mathematical Theory of Dilute Gases*. Springer, New York, 1994.

52. E. G. D. Cohen, W. Fiszdon, and A. Palczewski, editors. *Fundamental problems in statistical mechanics. IV*. Ossolineum, Wrocław, 1978. Proceedings of the Fourth International Summer School in Statistical Mechanics, held in Jadwisin, September 14–24, 1977.
53. M. H. A. Davis. Piecewise–deterministic Markov processes: A general class of non–diffusion stochastic models. *J. Roy. Statist. Soc. Ser. B*, 46(3):353–388, 1984.
54. M. H. A. Davis. *Markov Models and Optimization*. Chapman & Hall, London, 1993.
55. S. M. Deshpande. The statistical particle–in–cell method for multicomponent gases. *Zh. Vychisl. Mat. i Mat. Fiz.*, 23(1):170–177, 1983.
56. S. M. Ermakov. *Metod Monte-Karlo i smezhnye voprosy*. Nauka, Moscow, 1971. (Russian) [The Monte Carlo method and related problems].
57. S. M. Ermakov and N. M. Moskaleva. Branching processes and the Boltzmann equation. Numerical aspects. *Vestnik Leningrad Univ. Ser. 1*, 3:38–43, 1987. In Russian.
58. S. M. Ermakov, V. V. Nekrutkin, and A. S. Sipin. *Sluchainye protsessy dlya resheniya klassicheskikh uravnenii matematicheskoi fiziki*. Nauka, Moscow, 1984. English translation: [59].
59. S. M. Ermakov, V. V. Nekrutkin, and A. S. Sipin. *Random Processes for Classical Equations of Mathematical Physics*, volume 34 of *Mathematics and its Applications (Soviet Series)*. Kluwer Academic Publishers Group, Dordrecht, 1989.
60. M. H. Ernst. Exact solutions of the nonlinear Boltzmann and related kinetic equations. In *Nonequilibrium phenomena. I. The Boltzmann equation*, pages 51–119. North–Holland, 1983.
61. S. N. Ethier and T. G. Kurtz. *Markov Processes, Characterization and Convergence*. Wiley, New York, 1986.
62. J. Fan and C. Shen. Statistical simulation of low-speed rarefied gas flows. *J. Comput. Phys.*, 167:393–412, 2001.
63. W. Feller. Zur Theorie der stochastischen Prozesse. *Math. Ann.*, 113:113–160, 1937.
64. R. Ferland, X. Fernique, and G. Giroux. Compactness of the fluctuations associated with some generalized nonlinear Boltzmann equations. *Can. J. Math.*, 44(6):1192–1205, 1992.
65. A. Frezzotti. A particle scheme for the numerical solution of the Enskog equation. *Phys. Fluids*, 9(5):1329–1335, 1997.
66. T. Funaki. Construction of stochastic processes associated with the Boltzmann equation and its applications. In K. Ito and T. Hida, editors, *Stochastic processes and their applications*, volume 1203 of *Lecture Notes in Mathematics*, pages 51–65. Springer, Berlin/Heidelberg, 1986.
67. A. L. Garcia and W. Wagner. The limiting kinetic equation of the consistent Boltzmann algorithm for dense gases. *J. Statist. Phys.*, 101(5-6):1065–1086, 2000.
68. A. L. Garcia and W. Wagner. Time step truncation error in direct simulation Monte Carlo. *Phys. Fluids*, 12(10):2621–2633, 2000.
69. A. L. Garcia and W. Wagner. Some new properties of the kinetic equation for the Consistent Boltzmann Algorithm. *Transport Theory Statist. Phys.*, 31(4-6):579–594, 2002.

70. A. L. Garcia and W. Wagner. Direct simulation Monte Carlo method for the Uehling-Uhlenbeck-Boltzmann equation. *Physical Review E*, 68(056703):1–11, 2003.
71. D. I. Golenko. *Modelirovanie i statisticheskii analiz psevdosluchainykh chisel na elektronnykh vychislitelnykh mashinakh*. Izdat. "Nauka", Moscow, 1965. (Russian) [Simulation and statistical analysis of pseudo-random numbers on electronic computing machines].
72. C. Graham and S. Méléard. Stochastic particle approximations for generalized Boltzmann models and convergence estimates. *Ann. Probab.*, 25(1):115–132, 1997.
73. F. A. Grünbaum. Propagation of chaos for the Boltzmann equation. *Arch. Rational Mech. Anal.*, 42(5):323–345, 1971.
74. M. Günther, P. Le Tallec, J. P. Perlat, and J. Struckmeier. Numerical modeling of gas flows in the transition between rarefied and continuum regimes. In *Numerical flow simulation, I (Marseille, 1997)*, pages 222–241. Vieweg, Braunschweig, 1998.
75. N. G. Hadjiconstantinou. Analysis of discretization in direct simulation Monte Carlo. *Phys. Fluids*, 12(10):2634–2638, 2000.
76. J. H. Halton. A retrospective and prospective survey of the Monte Carlo method. *SIAM Rev.*, 12:1–63, 1970.
77. J. M. Hammersley and D. C. Handscomb. *Monte Carlo methods*. Methuen & Co. Ltd., London, 1965.
78. H. A. Hassan and D. B. Hash. A generalized hard-sphere model for Monte Carlo simulations. *Phys. Fluids A*, 5 : 738–744, 1993.
79. J. K. Haviland and M. L. Lavin. Application of the Monte Carlo method to heat transfer in a rarefied gas. *Phys. Fluids*, 5(11):1399–1405, 1962.
80. T. Hokazono, S. Kobayashi, T. Ohsawa, and T. Ohwada. On the time step error of the DSMC. In A. D. Ketsdever and E. P. Muntz, editors, *Rarefied Gas Dynamics*, pages 390–397. AIP Publishing Center, New York, 2003.
81. J. Horowitz and R. L. Karandikar. Martingale problems associated with the Boltzmann equation. In *Seminar on Stochastic Processes, 1989*, volume 18 of *Progress in Probability*, pages 75–122. Birkhäuser, Boston/Basel/Berlin, 1990.
82. K. Huang. *Statistical mechanics*. John Wiley & Sons Inc., New York, second edition, 1987.
83. R. Illner and H. Neunzert. On simulation methods for the Boltzmann equation. *Transport Theory Statist. Phys.*, 16(2&3):141–154, 1987.
84. R. Illner and S. Rjasanow. Random discrete velocity models: Possible bridges between the Boltzmann equation, discrete velocity models and particle simulation? In V. C. Boffi, F. Bampi, and G. Toscani, editors, *Nonlinear kinetic theory and mathematical aspects of hyperbolic systems*, pages 152–158. World Scientific, Singapore, 1992.
85. R. Illner and S. Rjasanow. Numerical solution of the Boltzmann equation by random discrete velocity models. *European J. Mech. B Fluids*, 13(2):197–210, 1994.
86. R. Illner and W. Wagner. A random discrete velocity model and approximation of the Boltzmann equation. *J. Statist. Phys.*, 70(3/4):773–792, 1993.
87. R. Illner and W. Wagner. Random discrete velocity models and approximation of the Boltzmann equation. Conservation of momentum and energy. *Transport Theory Statist. Phys.*, 23(1–3):27–38, 1994.

88. M. S. Ivanov and S. V. Rogasinsky. Theoretical analysis of traditional and modern schemes of the DSMC method. In A. E. Beylich, editor, *Proc. of the 17th International Symposium on Rarefied Gas Dynamics*, pages 629–642, Aachen, 1990.
89. M. S. Ivanov and S. V. Rogazinskij. Comparative analysis of algorithms of the direct statistical modeling method in rarefied gas dynamics. *Zh. Vychisl. Mat. i Mat. Fiz.*, 28(7):1058–1070, 1988. In Russian.
90. M. S. Ivanov and S. V. Rogazinskij. Efficient schemes for direct statistical modeling of rarefied gas flows. *Mat. Model.*, 1(7):130–145, 1989. In Russian.
91. M. Kac. Foundations of kinetic theory. In *Third Berkeley Symposium on Mathematical Statistics and Probability Theory*, volume 3, pages 171–197, 1956.
92. M. Kac. *Some Stochastic Problems in Physics and Mathematics.* Magnolia Petroleum Co., 1956.
93. M. Kac. *Probability and Related Topics in Physical Sciences.* Interscience, London, 1959.
94. M. Kac. *Veroyatnost' i smezhnye voprosy v fizike.* Mir, Moscow, 1965. Russian translation of [93].
95. M. Kac. *Neskol'ko veroyatnostnykh zadach fiziki i matematiki.* Nauka, Moscow, 1967. Russian translation of the Polish edition of [92].
96. M. Kac. Some probabilistic aspects of the Boltzmann equation. *Acta Phys. Austriaca*, Suppl. X:379–400, 1973.
97. M. Kac. Nonlinear dynamics and inverse problems. In *Fundamental problems in statistical mechanics, IV (Proc. Fourth Internat. Summer School, Jadwisin, 1977)*, pages 199–222. Ossolineum, Wrocław, 1978.
98. M. Kac and J. Logan. Fluctuations. In *Fluctuation Phenomena*, volume VII of *Studies in Statistical Mechanics*, pages 1–60. North-Holland, 1979.
99. A. I. Khisamutdinov. A simulation method for statistical modeling of rarefied gases. *Dokl. Akad. Nauk SSSR*, 291(6):1300–1304, 1986. In Russian.
100. R. Kirsch. Die Boltzmann-Gleichung für energieabhängige Verteilungsfunktionen. Diplomarbeit, Universität des Saarlandes, 1999.
101. A. Klar. Convergence of alternating domain decomposition schemes for kinetic and aerodynamic equations. *Math. Methods Appl. Sci.*, 18(8):649–670, 1995.
102. A. Klar. Domain decomposition for kinetic problems with nonequilibrium states. *European J. Mech. B Fluids*, 15(2):203–216, 1996.
103. A. Klar. Asymptotic analysis and coupling conditions for kinetic and hydrodynamic equations. *Comput. Math. Appl.*, 35(1-2):127–137, 1998.
104. Yu. L. Klimontovich. Kinetic theory of fluctuations in gases and plasma. In *Fundamental problems in statistical mechanics, IV (Proc. Fourth Internat. Summer School, Jadwisin, 1977)*, pages 265–309. Ossolineum, Wrocław, 1978.
105. Yu. L. Klimontovich. Dissipative equations for many-particle distribution functions. *Uspekhi Fiz. Nauk*, 139(4):689–700, 1983. In Russian.
106. Yu. L. Klimontovich. *Statistical theory of open systems. Vol. 1*, volume 67 of *Fundamental Theories of Physics.* Kluwer Academic Publishers Group, Dordrecht, 1995.
107. M. Knudsen. *Kinetic Theory of Gases.* Methuen, London, 1952.
108. A. Kolmogoroff. Über die analytischen Methoden in der Wahrscheinlichkeitsrechnung. *Math. Ann.*, 104:415–458, 1931.
109. A. Kolmogoroff and M. Leontowitsch. Zur Berechnung der mittleren Brownschen Fläche. *Physik. Zeitschr. d. Sowjetunion*, 4:1–13, 1933.

110. A. N. Kolmogoroff. *Grundbegriffe der Wahrscheinlichkeitsrechnung*. Springer, Berlin, 1933.
111. Yu. N. Kondyurin. A statistical approach to the solution of the Boltzmann equation. *Zh. Vychisl. Mat. i Mat. Fiz.*, 26(10):1527–1534, 1986. In Russian.
112. K. Koura. Null–collision technique in the direct–simulation Monte Carlo method. *Phys. Fluids*, 29(11):3509–3511, 1986.
113. K. Koura and H. Matsumoto. Variable soft sphere molecular model for inverse-power-law or Lennard-Jones potential. *Phys. Fluids A*, 3 : 2459–2465, 1991.
114. K. Koura and H. Matsumoto. Variable soft sphere molecular model for air species. *Phys. Fluids A*, 4 : 1083–1085, 1992.
115. M. Krook and T. T. Wu. Exact solutions of the Boltzmann equation. *Phys. Fluids*, 20(10):1589–1595, 1977.
116. M. Lachowicz and M. Pulvirenti. A stochastic system of particles modelling the Euler equation. *Arch. Rational Mech. Anal.*, 109(1):81–93, 1990.
117. P. Le Tallec and F. Mallinger. Coupling Boltzmann and Navier-Stokes equations by half fluxes. *J. Comput. Phys.*, 136(1):51–67, 1997.
118. C. Lécot. A direct simulation Monte Carlo scheme and uniformly distributed sequences for solving the Boltzmann equation. *Computing*, 41(1/2):41–57, 1989.
119. C. Lécot. Low discrepancy sequences for solving the Boltzmann equation. *J. Comput. Appl. Math.*, 25(2):237–249, 1989.
120. C. Lécot. A quasi-Monte Carlo method for the Boltzmann equation. *Math. Comp.*, 56(194):621–644, 1991.
121. M. A. Leontovich. Basic equations of the kinetic gas theory from the point of view of the theory of random processes. *Zhurnal Teoret. Ehksper. Fiziki*, 5(3-4):211–231, 1935. In Russian.
122. M. Leontowitsch. Zur Statistik der kontinuierlichen Systeme und des zeitlichen Verlaufes der physikalischen Vorgänge. *Physik. Zeitschr. d. Sowjetunion*, 3:35–63, 1933.
123. H. W. Liepmann, R. Narasimha, and M. T. Chahine. Structure of a plane shock layer. *Phys. Fluids*, 5:1313, 1962.
124. J. Logan and M. Kac. Fluctuations and the Boltzmann equation. *Phys. Rev. A*, 13(1):458–470, 1976.
125. A. V. Lukshin. A stochastic method for solving the Boltzmann equation for a gas with an arbitrary interaction law. *Differentsial'nye Uravneniya*, 23(11):2001–2004, 1987. In Russian.
126. A. V. Lukshin. Stochastic algorithms of the mathematical theory of the spatially inhomogeneous Boltzmann equation. *Mat. Model.*, 1(7):146–159, 1989. In Russian.
127. A. V. Lukshin and S. N. Smirnov. On a stochastic method for solving the Boltzmann equation. *Zh. Vychisl. Mat. i Mat. Fiz.*, 28(2):293–297, 1988. In Russian.
128. A. V. Lukshin and S. N. Smirnov. An efficient stochastic algorithm for solving the Boltzmann equation. *Zh. Vychisl. Mat. i Mat. Fiz.*, 29(1):118–124, 1989. In Russian.
129. A. V. Lukshin and I. E. Yuferov. Stochastic algorithms for solving the spatially homogeneous Boltzmann equation for gas mixtures. *Mat. Model.*, 1(2):151–160, 1989. In Russian.
130. I. Matheis and W. Wagner. Convergence of the stochastic weighted particle method for the Boltzmann equation. *SIAM J. Sci. Comput.*, 24(5):1589–1609, 2003.

131. M. J. McEwan and L. F. Phillips. *The Chemistry of the Atmosphere*. Edward Arnold (Publishers) Ltd., London, 1975.
132. H. P. McKean. Speed of approach to equilibrium for Kac's caricature of a Maxwellian gas. *Arch. Rational Mech. Anal.*, 21:343–367, 1966.
133. H. P. McKean. An exponential formula for solving Boltzmann's equation for a Maxwellian gas. *J. Combin. Theory*, 2:358–382, 1967.
134. H. P. McKean. Fluctuations in the kinetic theory of gases. *Comm. Pure Appl. Math.*, 28(4):435–455, 1975.
135. J. Meixner. Zur Thermodynamik irreversibler Prozesse. *Z. Phys. Chem.*, 53 B:253, 1941.
136. S. Meleard. Stochastic approximations of the solution of a full Boltzmann equation with small initial data. *ESAIM Probab. Statist.*, 2:23–40 (electronic), 1998.
137. N. Metropolis and S. Ulam. The Monte Carlo method. *J. Amer. Statist. Assoc.*, 44:335–341, 1949.
138. G. A. Mikhailov and S. V. Rogazinskii. Weighted Monte Carlo methods for the approximate solution of the nonlinear Boltzmann equation. *Sibirsk. Mat. Zh.*, 43(3):620–628, 2002. In Russian.
139. J. M. Montanero and A. Santos. Simulation of the Enskog equation *á la* Bird. *Phys. Fluids*, 9:2057–2060, 1997.
140. D. Morgenstern. Analytical studies related to the Maxwell–Boltzmann equation. *J. Rational Mech. Anal.*, 4:533–555, 1955.
141. H. Mott-Smith. The solution of the Boltzmann equation for a shock wave. *Phys. Rev.*, 82:885–892, 1951.
142. C. Muckenfuss. Some aspects of shock structure according to the bimodal model. *Phys. Fluids*, 5(11):1325–1336, 1962.
143. H. Murata. Propagation of chaos for Boltzmann-like equations of noncutoff–type in the plane. *Hiroshima Math. J.*, 7:479–515, 1977.
144. K. Nanbu. Direct simulation scheme derived from the Boltzmann equation. I. Monocomponent gases. *J. Phys. Soc. Japan*, 49(5):2042–2049, 1980.
145. K. Nanbu. Interrelations between various direct simulation methods for solving the Boltzmann equation. *J. Phys. Soc. Japan*, 52(10):3382–3388, 1983.
146. K. Nanbu. Theoretical basis of the direct simulation Monte Carlo method. In V. Boffi and C. Cercignani, editors, *Rarefied Gas Dynamics*, volume 1, pages 369–383. Teubner, Stuttgart, 1986.
147. K. Nanbu. Weighted particles in Coulomb collision simulations based on the theory of a cumulative scattering angle. *J. Comput. Phys.*, 145:639–654, 1998.
148. V. Nekrutkin and N. Tur. Asymptotic expansions and estimators with small bias for Nanbu processes. *Monte Carlo Methods Appl.*, 3(1):1–35, 1997.
149. V. V. Nekrutkin and N. I. Tur. On the justification of a scheme of direct modelling of flows of rarefied gases. *Zh. Vychisl. Mat. i Mat. Fiz.*, 29(9):1380–1392, 1989. In Russian.
150. H. Neunzert, F. Gropengiesser, and J. Struckmeier. Computational methods for the Boltzmann equation. In *Applied and industrial mathematics (Venice, 1989)*, volume 56 of *Math. Appl.*, pages 111–140. Kluwer Acad. Publ., Dordrecht, 1991.
151. H. Neunzert, A. Klar, and J. Struckmeier. Particle methods: theory and applications. In *ICIAM 95 (Hamburg, 1995)*, pages 281–306. Akademie Verlag, Berlin, 1996.

152. H. Neunzert and J. Struckmeier. The finite pointset method for hypersonic flows in the rarefied gas regime. In *Advances in hypersonics, Vol. 3 (Colorado Springs, CO, 1989; Aachen, 1990)*, pages 342–370. Birkhäuser Boston, Boston, MA, 1992.
153. H. Neunzert and J. Struckmeier. Particle methods for the Boltzmann equation. In *Acta Numerica 1995*, pages 417–457. Cambridge University Press, Cambridge, 1995.
154. A. Nordsieck, W. E. Lamb, Jr., and G. E. Uhlenbeck. On the theory of cosmic–ray showers. I. The furry model and the fluctuation problem. *Physica*, 7(4):344–360, 1940.
155. T. Ohwada. Higher order approximation methods for the Boltzmann equation. *J. Comput. Phys.*, 139:1–14, 1998.
156. T. Ohwada. Higher order time integration of spatially nonhomogeneous Boltzmann equation: deterministic and stochastic computations. *Transport Theory Statist. Phys.*, 29(3-5):495–508, 2000.
157. G. C. Papanicolaou. Asymptotic analysis of transport processes. *Bull. Amer. Math. Soc.*, 81(2):330–392, 1975.
158. L. Pareschi and R. E. Caflisch. An implicit Monte Carlo method for rarefied gas dynamics. I. The space homogeneous case. *J. Comput. Phys.*, 154(1):90–116, 1999.
159. L. Pareschi and G. Russo. Time relaxed Monte Carlo methods for the Boltzmann equation. *SIAM J. Sci. Comput.*, 23(4):1253–1273, 2001.
160. L. Pareschi and B. Wennberg. A recursive Monte Carlo method for the Boltzmann equation in the Maxwellian case. *Monte Carlo Methods Appl.*, 7(3-4):349–357, 2001.
161. G. Pichon. Sur la propagation du chaos moléculaire. *C. R. Acad. Sci. Paris Sér. A*, 274:1667–1670, 1972.
162. G. Pichon. Chaos moléculaire et équation de Boltzmann. *C. R. Acad. Sci. Paris Sér. A*, 276:583–585, 1973.
163. G. Pichon. Chaos moléculaire et équation de Boltzmann. *J. Math. Pures Appl.*, 53(2):183–195, 1974.
164. G. Pichon. Chaos moléculaire et équation de Boltzmann. In *Théories cinétiques classiques et relativistes, Colloques Internationaux C.N.R.S. 236 (Paris 1974)*, pages 195–207, 1975.
165. H. Ploss. On simulation methods for solving the Boltzmann equation. *Computing*, 38:101–115, 1987.
166. A. Ya. Povzner. On the Boltzmann equation in kinetic gas theory. *Matem. Sb.*, 58(1):65–86, 1962. In Russian.
167. M. Pulvirenti, W. Wagner, and M. B. Zavelani Rossi. Convergence of particle schemes for the Boltzmann equation. *European J. Mech. B Fluids*, 13(3):339–351, 1994.
168. P. Quell. Nonlinear stability of entropy flux splitting schemes on bounded domains. *IMA J. Numer. Anal.*, 20(3):441–459, 2000.
169. A. K. Rebrov and P. A. Skovorodko. An improved sampling procedure in DSMC method. In C. Shen, editor, *Rarefied Gas Dynamics*, pages 215–220. Peking University Press, Beijing, 1997.
170. F. Rezakhanlou. Kinetic limits for a class of interacting particle systems. *Probab. Theory Related Fields*, 104(1):97–146, 1996.
171. F. Rezakhanlou. Propagation of chaos for particle systems associated with discrete Boltzmann equation. *Stochastic Process. Appl.*, 64(1):55–72, 1996.

172. F. Rezakhanlou. A stochastic model associated with Enskog equation and its kinetic limit. *Comm. Math. Phys.*, 232(2):327–375, 2003.
173. F. Rezakhanlou and J. E. Tarver. Boltzmann-Grad limit for a particle system in continuum. *Ann. Inst. H. Poincaré Probab. Statist.*, 33(6):753–796, 1997.
174. *Rarefied Gas Dynamics, Proceedings of the 23rd International Symposium (Whistler, Canada, 20-25 July 2002), eds. Ketsdever, A. D. and Muntz, E. P.*, volume 663 of *AIP Conference Proceedings*, AIP Publishing Center, New York, 2003.
175. *Rarefied gas dynamics: Proceedings of the First International Symposium (Nice, France, 1958)*, International Series on Aeronautical Sciences and Space Flight, Division IX, Vol. 3, Pergamon Press, New York, 1960.
176. S. Rjasanow, T. Schreiber, and W. Wagner. Reduction of the number of particles in the stochastic weighted particle method for the Boltzmann equation. *J. Comput. Phys.*, 145(1):382–405, 1998.
177. S. Rjasanow and W. Wagner. A stochastic weighted particle method for the Boltzmann equation. *J. Comput. Phys.*, 124(2):243–253, 1996.
178. S. Rjasanow and W. Wagner. A generalized collision mechanism for stochastic particle schemes approximating Boltzmann-type equations. *Comput. Math. Appl.*, 35(1/2):165–178, 1998.
179. S. Rjasanow and W. Wagner. On time counting procedures in the DSMC method for rarefied gases. *Math. Comput. Simulation*, 48(2):153–178, 1998.
180. S. Rjasanow and W. Wagner. A temperature time counter scheme for the Boltzmann equation. *SIAM J. Numer. Anal.*, 37(6):1800–1819, 2000.
181. S. Rjasanow and W. Wagner. Simulation of rare events by the stochastic weighted particle method for the Boltzmann equation. *Math. Comput. Modelling*, 33(8-9):907–926, 2001.
182. S. V. Rogasinsky. Solution of stationary boundary value problems for the Boltzmann equation by the Monte Carlo method. *Monte Carlo Methods Appl.*, 5(3):263–280, 1999.
183. M. Schreiner. Weighted particles in the finite pointset method. *Transport Theory Statist. Phys.*, 22(6):793–817, 1993.
184. A. J. F. Siegert. On the approach to statistical equlibrium. *Phys. Rev.*, 76(11):1708–1714, 1949.
185. A. V. Skorokhod. *Stokhasticheskie uravneniya dlya slozhnykh sistem.* Nauka, Moscow, 1983. English translation: [186].
186. A. V. Skorokhod. *Stochastic Equations for Complex Systems*, volume 13 of *Mathematics and its Applications (Soviet Series).* D. Reidel Publishing Co., Dordrecht, 1988.
187. S. N. Smirnov. On the justification of a stochastic method for solving the Boltzmann equation. *Zh. Vychisl. Mat. i Mat. Fiz.*, 29(2):270–276, 1989. In Russian.
188. I. M. Sobol. *Chislennye metody Monte-Karlo.* Izdat. "Nauka", Moscow, 1973. (Russian) [Numerical Monte Carlo methods].
189. J. Spanier and E. M. Gelbard. *Monte Carlo principles and neutron transport problems.* Addison-Wesley Publishing Co., Reading, Mass.-London-Don Mills, Ont., 1969.
190. J. Struckmeier and K. Steiner. A comparison of simulation methods for rarefied gas flows. *Phys. Fluids*, 7(11):2876–2885, 1995.
191. Q. Sun and I.D. Boyd. A direct simulation method for subsonic, microscale gas flows. *J. Comput. Phys.*, 179:400–425, 2002.

192. A.-S. Sznitman. Équations de type de Boltzmann, spatialement homogènes. *C. R. Acad. Sci. Paris Sér. I Math.*, 295:363–366, 1982.
193. A. S. Sznitman. Équations de type de Boltzmann, spatialement homogènes. *Z. Wahrsch. Verw. Gebiete*, 66(4):559–592, 1984.
194. A. S. Sznitman. Topics in propagation of chaos. In *Lecture Notes in Mathematics*, volume 1464, pages 165–251. Springer, Berlin, 1991.
195. H. Tanaka. On Markov processes corresponding to the Boltzmann equation of Maxwellian gas. In *Lecture Notes in Mathematics*, volume 330, pages 478–489. Springer, Berlin, 1973.
196. H. Tanaka. Probabilistic treatment of the Boltzmann equation of Maxwellian molecules. *Z. Wahrsch. Verw. Gebiete*, 46(1):67–105, 1978.
197. H. Tanaka. Some probabilistic problems in the spatially homogeneous Boltzmann equation. In G. Kallianpur, editor, *Theory and Applications of Random Fields*, volume 49 of *Lecture Notes in Control and Inform. Sci.*, pages 258–267, Springer, Berlin, 1983.
198. C. J. Thompson. The contributions of Mark Kac to mathematical physics. *Ann. Probab.*, 14(4):1129–1138, 1986.
199. S. Tiwari. Coupling of the Boltzmann and Euler equations with automatic domain decomposition. *J. Comput. Phys.*, 144(2):710–726, 1998.
200. S. Tiwari and A. Klar. An adaptive domain decomposition procedure for Boltzmann and Euler equations. *J. Comput. Appl. Math.*, 90(2):223–237, 1998.
201. S. Tiwari and S. Rjasanow. Sobolev norm as a criterion of local thermal equilibrium. *European J. Mech. B Fluids*, 16(6):863–876, 1997.
202. H. F. Trotter and J. W. Tukey. Conditional Monte Carlo for normal samples. In *Symposium on Monte Carlo methods, University of Florida, 1954*, pages 64–79. John Wiley and Sons, Inc., New York, 1956.
203. K. Uchiyama. Fluctuations in population dynamics. In M. Kimura, G. Kallianpur, and T. Hida, editors, *Stochastic Methods in Biology*, volume 70 of *Lecture Notes in Biomathematics*, pages 222–229, Springer, Berlin, 1987.
204. W. Wagner. A convergence proof for Bird's direct simulation Monte Carlo method for the Boltzmann equation. *J. Statist. Phys.*, 66(3/4):1011–1044, 1992.
205. W. Wagner. A stochastic particle system associated with the spatially inhomogeneous Boltzmann equation. *Transport Theory Statist. Phys.*, 23(4):455–477, 1994.
206. W. Wagner. Stochastic systems of particles with weights and approximation of the Boltzmann equation. The Markov process in the spatially homogeneous case. *Stochastic Anal. Appl.*, 12(5):639–659, 1994.
207. W. Wagner. A functional law of large numbers for Boltzmann type stochastic particle systems. *Stochastic Anal. Appl.*, 14(5):591–636, 1996.
208. E. Wild. On Boltzmann's equation in the kinetic theory of gases. *Proc. Cambridge Philos. Soc.*, 47:602–609, 1951.
209. S.-M. Yen. Temperature overshoot in shock waves. *Phys. Fluids*, 9(7):1417–1418, 1966.

Index

acceptance-rejection method 229
approximation order 140

BKW solution 217
Boltzmann equation 1
  linear 47
  mollified 47
  scaled 30
  spatially homogeneous 19
boundary conditions 71
  diffuse reflection 11
  inflow 11, 47, 74
  Maxwell boundary condition 48
  specular reflection 11
bounded Lipschitz metric 99

cell structure 78
collision integral 4, 5
collision invariant 18
collision kernel 4
collision transformation 2–4
composition method 231
confidence interval 70
criterion of local equilibrium 28
cross section
  differential 4
  total 9

degrees of freedom 53

empirical mean value 70
empirical measure 41, 102
error function 211
eternal solution 178

Euler equations 24
exit time 34

fictitious collisions 80
fluxes 12
free flow 33

gamma function 211

H-functional 19
heat flux vector 14

ideal gas law 13
impact parameter 2
interaction distance 9
interaction models
  hard interactions 10
  hard sphere molecules 8
  Maxwell molecules 10
  pseudo-Maxwell molecules 10
  soft interactions 10
  variable hard sphere model 10

jump time 35
jump types
  annihilation jumps 37, 49
  collision jumps 36, 48
  creation jumps 37, 49
  reduction jumps 99
  reflection jumps 38, 49
  scattering jumps 37, 49

Knudsen number 29
Kolmogorov's forward equation 55

Mach number 14
majorants 82
master equation 57
Maxwell distribution IX, 1
mean free path 14
mean molecule velocity 14
Monte Carlo method 132
Mott-Smith model 185

Navier-Stokes equations 24
number density 13

pressure tensor 13
propagation of chaos 57

Rankine-Hugoniot conditions 183
reduction measure 99, 119

scalar pressure 13
scattering angle 2
specific heat ratio 14
speed of sound 14
statistical error 70
stream velocity 13
systematic error 70

temperature 13
time counting procedures 132
time step 68
transformation method 230
transition measure 35

variance reduction 134

waiting time 80